UILU-ENG-86-2009

ENGINEERING STUDIES
RAL RESEARCH SERIES NO. 527

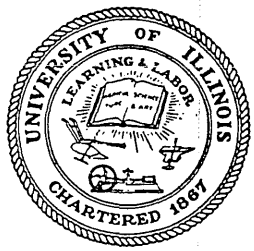

ISSN: 0069-4274

PRELIMINARY REPORT ON SEISMIC TESTING OF A FULL-SCALE SIX-STORY STEEL BUILDING

By
DOUGLAS A. FOUTCH
SUBHASH C. GOEL
CHARLES W. ROEDER

A Report on Research Projects
Sponsored by
THE NATIONAL SCIENCE FOUNDATION
U.S./Japan Cooperative Earthquake Research Program Utilizing Large Size Testing Facilities
Research Grants CEE 83-12656, CEE 82-06200, ECE 85-11315, CEE 82-07521, ECE 84-15419, and CEE 83-00684

UNIVERSITY OF ILLINOIS
AT URBANA-CHAMPAIGN
URBANA, ILLINOIS
NOVEMBER 1986

Preliminary Report on Seismic Testing of a Full-Scale Six-Story Steel Building

by

Douglas A. Foutch
University of Illinois at Urbana-Champaign

Charles W. Roeder
University of Washington at Seattle

Subhash C. Goel
University of Michigan at Ann Arbor

November, 1986

50272-101

REPORT DOCUMENTATION PAGE	1. REPORT NO.	2.	3. Recipient's Accession No.

4. Title and Subtitle

Preliminary Report on Seismic Testing of a Full-Scale Six-Story Steel Building

5. Report Date
November 1986

6.

7. Author(s)
D. A. Foutch, C. W. Roeder, and S. C. Goel

8. Performing Organization Rept. No.

9. Performing Organization Name and Address

Univ. of Illinois
208 N. Romine St.
Urbana, IL 61801

Univ. of Washington
233-B More Hall FX10
Seattle, WA 98195

Univ. of Michigan
Ann Arbor, MI 48105

10. Project/Task/Work Unit No.

11. Contract(C) or Grant(G) No.
(C) CEE-8206208, CEE-8312656
(G) ECE-8511315, CEE-8207512
CEE-8306684, ECE-8415419

12. Sponsoring Organization Name and Address

National Science Foundation

13. Type of Report & Period Covered

14.

15. Supplementary Notes

16. Abstract (Limit: 200 words)

A full-scale six-story steel building was constructed and tested as part of the U.S./Japan Cooperative Earthquake Research Program Utilizing Large Size Testing Facilities. The program was jointly funded by the Ministry of Construction of Japan and the United States National Science Foundation. The overall objective of the program is to improve seismic safety in practice and to determine the relationships among full-scale tests, small-scale tests, component tests and analytical studies.

The full-scale building was 15m square in plan and measured 22.38m from the test floor to the top of the roof girders. It was tested as a concentric braced frame; repaired and tested as an eccentric braced frame; tested as a moment frame; and finally, tested with cladding and other nonstructural elements installed. The tests were conducted using the pseudodynamic testing technique which simulated actual seismic loadings. This preliminary report describes the full-scale building and the testing program and presents preliminary results and conclusions.

17. Document Analysis a. Descriptors

Natural Hazards, Steel Buildings: Earthquake Response, Full-Scale Test, Inelastic Behavior, Seismic Design

b. Identifiers/Open-Ended Terms

c. COSATI Field/Group

18. Availability Statement	19. Security Class (This Report) UNCLASSIFIED	21. No. of Pages 181
	20. Security Class (This Page) UNCLASSIFIED	22. Price

(See ANSI-Z39.18) *See Instructions on Reverse*

OPTIONAL FORM 272 (4-77)
(Formerly NTIS-35)
Department of Commerce

ACKNOWLEDGEMENTS

This research program was funded by the United States National Science Foundation and the Japanese Government Ministry of Construction under the auspices of the United States Cooperative Program on Natural Resources. A number of separate grants to U.S. investigators were provided by NSF under the guidance of Dr. S. C. Liu and Dr. John B. Scalzi and the authors gratefully acknowledge this support. The authors served in Japan as U.S. observers for this test program and they are participating in a coordinated effort to analyze the results of the full-scale tests. This work is funded under grants CEE 82-06200, CEE 83-12656 and ECE 85-11315 to the University of Illinois at Urbana-Champaign, CEE 82-07521 and ECE 84-15419 to the University Washington and CEE 83-00684 to the University of Michigan. The conclusions and opinions expressed in this report are those of the authors and do not necessarily represent those of the sponsors.

The authors spent a combined total of nearly two years in Tsukuba, Japan at the Building Research Institute (BRI). The success of the project and the enjoyment that the authors experienced while in Japan is due primarily to the energetic leadership provided by Dr. H. Yamanouchi of BRI and to the openness and generosity of him and his co-workers, Dr. M. Midorikawa and Dr. Y. Nishiyama. The authors also wish to greatly acknowledge the assistance, support and friendship of Professor M. Watabe of Tokyo Metropolitan University (formerly at BRI).

Assistance was provided by Mr. C. Chang and Mr. S. Adeel in preparing the figures for this report. Preparation of the manuscript was done by Ms. M. Kadenko. These efforts are gratefully acknowledged.

TABLE OF CONTENTS

CHAPTER Page

LIST OF TABLES

LIST OF FIGURES

CHAPTER 1

INTRODUCTION

On May 18, 1982, the National Science Foundation (NSF) of the United States and the Ministry of Construction (MOC) of Japan under the auspices of the United States-Japan Cooperative Program on Natural Resources (UJNR) entered into an agreement to cooperate in research on the seismic behavior of steel buildings. The program was called the U.S./Japan Cooperative Earthquake Research Program Utilizing Large-Size Testing Facilities. The overall objective of the program is to improve seismic safety in practice through studies to determine the relationships among full-scale tests, small-scale tests, component tests and analytical studies. The program consists of experimental and analytical studies carried out by investigators in the U.S. and Japan. The centerpiece of the program is a full-scale six-story steel test structure that was constructed and tested in the Large Size Structures Laboratory of the Building Research Institute (BRI) operated by the MOC in Tsukuba, Japan.

The purpose of this preliminary report is to describe the test program for the full-scale structure and to present a summary of the preliminary experimental and analytical results from the four phases of the test program. More detailed studies of the data collected during these tests and additional analytical studies are currently underway and will be reported in future publications.

The program is managed by the Joint Technical Coordinating Committee (JTCC). The Technical Coordinator is R. D. Hanson (University of Michigan) who serves as chairman of the JTCC and who has managed the

program through a grant from the National Science Foundation to the University of Michigan. The JTCC is composed of principal investigators of supporting research projects and of special consultants. The members are V. V. Bertero (UC Berkeley), H. J. Degenkolb (Henry J. Degenkolb and Associates), D. A. Foutch (University of Illinois at Urbana-Champaign), S. C. Goel (University of Michigan), R. G. Johnston (Brandow Johnston and Associates), H. Krawinkler (Stanford University), L. W. Lu (Lehigh University), S. A. Mahin (UC Berkeley), E. P. Popov (UC Berkeley), C. W. Roeder (University of Washington at Seattle), R. L. Sharpe (EDAC), and M. L. Wang (UC Berkeley). A similar group was formed in Japan with M. Watabe (Tokyo Metropolitan University, formerly BRI) as the Technical Coordinator. The Japanese JTCC was composed of researchers from government and private research institutes and from universities. The construction and testing of the full-scale test specimen was conducted under the supervision of H. Yamanouchi with the help of M. Midorikawa and Y. Nishiyama of BRI. Each of the authors of this report participated in the test program in Tsukuba, Japan for an extended period of time. The cumulative total of time spent was about 18 months and covered the period from just prior to the beginning of construction to the completion of Phase II.

The test program for the full-scale building was divided into four phases. The test building was designed, constructed and tested as a concentric braced frame for Phase I. After completion of Phase I, the concentric braces were removed, the building was repaired and eccentric braces were installed for the Phase II tests. At the end of Phase II, the eccentric braces were removed and the moment frames were tested for

Phase III. For Phase IV nonstructural walls and cladding were installed on the building and an additional series of tests were performed.

This report includes a description of the design and construction of the test structure. The test program and instrumentation are summarized, and the preliminary analytical and experimental results are presented with preliminary conclusions for Phase I and Phase II. Results from Phases III and IV are described in less detail.

CHAPTER 2

DESIGN AND CONSTRUCTION OF THE BUILDING

2.1 Design of the Six Story Building

The design of the test structure was a major accomplishment of the JTCC since seismic design practice is quite different in the United States and Japan. Every effort was made to obtain a structure which was consistent with both the U.S. [1] and Japanese [2] design codes and professional practice, but some compromises were necessary. The goal of the test was to generate displacements large enough to ascertain the strength, ductility and failure mechanisms of the alternate structural systems. Interstory drifts of approximately 2% were thought to be adequate to this purpose, but capacity limitations of the test apparatus applied further constraints upon the design.

The building was designed as a six-story structure with a general floor plan as shown in Fig. 2.1. It was 15m (49.2 ft) square in plan with two 7.5m (24.6 ft) bays in each direction. It measured 22.38m (73.4 ft) from the test floor to the top of the roof girders. The structure consisted of three frames (A, B, C) parallel to the direction of loading and three frames (1, 2, 3) perpendicular to the loading direction. The dimensions shown are column centerline dimensions. However, the slab overhung the Frames A and C centerlines by 0.5m (1.64 ft). Member sizes are given in Tables 2.1, 2.2 and 2.3. The beams and columns used A36 steel, but A500 Grade B was used in the braces.

Frame B was the primary lateral load carrying element for the Phase I and Phase II tests, since it contained the brace elements, and it

provided the bulk of the strength and stiffness of the structure. Figure 2.2a shows an elevation view of the B Frame for the Phase I tests and Figs. 2.2b-2.2d show details of the braced bay of this frame. The vertical dimensions are to the top of the steel girder at any floor level. The floor level notation and the story designations are also shown. Note that the top of the foundation (Z1) is 0.88m (2.89 ft) above the test floor (Z0). Concentric K-bracing was provided in the south (1-2) bay at every story of the Phase I specimen. In addition, a moment connection was provided at every girder-to-column connection in this frame. It is not typical practice in the U.S. to provide girder-to-column moment connections in braced frames although it is common practice in Japan. An elevation of Frames A and C is shown in Fig. 2.3, and the elevation of Frames 1 and 3 is shown in Fig. 2.4. Rigid moment resisting connections were used throughout Frames A and C and typical connection details are shown in Fig. 2.5. Frames 1, 2 and 3 employed simple beam to column connections, and cross bracing was provided in all bays of the outside frames (Frames 1 and 3). The cross bracing provided lateral stability for the building in the transverse direction and greatly increased the structure's torsional stiffness. This insured that accidental twisting deformation of the floor would be minimized. Frames 1, 2 and 3 had simple girder-to-column connections at all locations.

The beams and girders were designed for composite action under gravity loads. The concrete slab was lightweight concrete with a 165mm (6.5 inch) maximum thickness, and it was placed over a 75mm (3 inch) deep ribbed metal deck. The ribs of the metal deck were oriented in the

east-west direction. Reinforcing bars, 6mm (.25 inch) in diameter and 100mm (4 inches) on center were placed in both directions. Shear connectors, which were 19mm or 22mm (.75 inch or .875 inch) in diameter and 130mm (5.75 inch) in length, were attached with the size and spacings shown in Tables 2.2 and 2.3. Additional shear connectors were placed midway between these on the segment of the G2 girder of the B frame that would later serve as the shear link of the Phase II structure.

The foundation consisted of built-up steel column footings under each column. These were bolted to the floor using high strength prestressing rods. In addition, built-up steel grade beams were provided for the B frame. These were bolted to the floor and welded to the column footings. A plan view of the foundation is shown in Fig. 2.6.

The members were selected using the usual allowable stress design procedures [3]. Total dead loads of $4.3^{KN}/m^2$ (90 psf), $3.6^{KN}/m^2$ (75 psf), and $1.4^{KN}/m^2$ (30 psf) were used for the floor, roof and exterior wall areas, respectively. The dead load for the floor and roof areas included were $2.8^{KN}/m^2$ (60 psf) for slabs and beams and $1.8^{KN}/m^2$ (37 psf) for girders. The seismic design resulted in a total base shear capacity of .197 W where W was the weight of the building considered for the seismic design. The total weight, W, excluded the live load, since it is not commonly considered in seismic design, and the weight of walls and partitions since they were not present during the test. The inclusion of this additional dead weight in the seismic design would have resulted in a structure too strong to be suitably damaged with the actuators available at the test facility. The total base shear was equivalent to UBC design base shear of .113 W where the braced bay was

designed for 125% of the design shear and the moment frames were designed for an additional 50% of the UBC value. This is larger than required by UBC for the building to be considered as a dual system. This was done to help reconcile the difference in the design requirements in the U.S. and Japan. The seismic design codes are very different for the U.S. and Japan. Japanese practice generally results in larger base shears than used in the U.S., and so the seismic design loads would be consistent with design loads required for the test structure on firm ground in the U.S. or soft soil in Japan. The distribution of load between frames is also different in the U.S. and Japan as reflected in the above description.

Typical connection details for the test structure are illustrated in Fig. 2.5. Several of these details are different from those currently used in the U.S. The square-tube braces of Phase I structure were welded directly to the girders using full penetration welds as shown in Figs. 2.5b and 2.5e. Column splices were made using full penetration groove welds for the flanges, and web plates that were temporarily bolted and then welded to the web as shown in Fig. 2.5a. Shear connectors were not always welded through the metal deck as commonly done in this country. Instead a special gap or trough in the deck was employed as shown in Fig. 2.5c. Finally, an unusual beam splice was employed at the junction of the beam to the Phase I braces as shown in Fig. 2.5e.

After completion of the Phase I testing, the concentric K-braces were removed from the south bay of Frame B, and for Phase II testing eccentric K-braces [4] were installed in the north bay of this frame. The elevation view for Frame B for Phase II is shown in Fig. 2.7 and a

typical detail of a shear link shown in Fig. 2.5f. The beam and column sizes were unchanged for this phase of the research, although the brace sizes were designed as shown in Table 2.3. The braces were again tubular members, but the brace connections employed gusset plates which are more typical of U.S. practices as shown in Fig. 2.5f, and web stiffeners were required as illustrated in the sketch.

Since the beam and column sizes were chosen for the Phase I testing, the total design base shear is different for the Phase II test. The design base shear should be the same (approx .056 W) for the moment frames, and it should be approximately .066 W for the eccentrically braced frame. This suggests that the total seismic design load for Phase II is approximately 62% of that used for Phase I. Lateral support details for Phase II were similar to those used for Phase I, and additional web stiffeners were required as shown in Figs. 2.7 and 2.5f.

2.2 Construction of the Building

The construction of the test building began on December 1, 1982, with the placement of the first column footing on the test floor of the Large Size Structure Laboratory and ended on February 5, 1983, when the last floor slab was cast. The construction was completed in 51 work days. The construction of the building was done by the Shimizu Construction Company and fabrication was done in the shop of Tomoe Gumi Fabrication Company.

Each steel column footing on the A and C line was square in plan and was bolted to the test floor using eight threaded high strength steel rods. Each footing on the B line was rectangular in plan and was bolted

to the test floor using fourteen rods. Steel base girders were also provided on the B line as an added precaution since the B frame was expected to carry much higher shear during the tests than the A and C frames. Each of the two girders was first bolted to the test floor using 10 threaded rods and then was welded to the column footings. The top flange and web welds were full penetration groove welds. The bottom flange welds were partial penetration groove welds because of the difficulty of placing backing plates at these locations.

The steel framework was erected in three units each consisting of two stories. The general sequence for erecting each 2-story unit was the same. The two halves of the braced bay (1-2 bay) of the B Frame were spliced together in the horizontal position. This was done on the parking lot just outside of the laboratory door as shown in Fig. 2.8. The splice line was at the centerline of the bay. This resulted in the unusual splice details shown in Figs. 4e and 2.9. This bay was then lifted and bolted into position using temporary erection bolts and then guyed for stability. Fig. 2.10a shows workers using a chain-pull to align the brace ends for temporary connection. The temporary connection is shown in Fig. 2.10b. The remaining members of the unit were then erected and guyed (Fig. 2.11), but tightening of the bolts was only done using a spud wrench. When the steel framework for all six stories was in place, final tightening of the high strength bolts using long-handled wrenches (as shown in Fig. 2.12) began at the bottom and proceeded upward at approximately one floor per day. The field welding generally followed the bolt tightening at each level by one or two days. A temporary and final column splice are shown in Fig. 2.13. All field welds were

inspected using the ultrasonic testing method, and all welds were acceptable by Japanese welding society standards.

Special care was taken to determine the "as built" dimensions of the building. The departures from a vertical line of the column centerlines at each floor level are shown in Figs. 2.14-2.16. These were determined by hanging a plumb line from the top story and using the center point of the column at the footing level as the reference point. The departures were measured from the plumb line. The departures from a straight line for each brace are shown in Fig. 2.17. The x departures are out of the plane of the frame and y departures are in-plane. The departures were measured perpendicular to the brace centerline.

The floors were made of reinforced lightweight concrete on formed metal deck. The decking is Kawatsu-Kenzai QL 99-1.6 which is equivalent to H. H. Robertson's QL-99. The thickness of the deck was 1.6mm (0.063 in). The nominal slab thickness was 90mm (3.54 in) and 165mm (6.50 in) at the ribs. The ribs ran parallel to the 1, 2 and 3 frames. The reinforcing was deformed bar mats of 6mm (0.24 in) diameter bars on a 100mm (3.94 in) grid with a nominal minimum cover of 29mm (1.14 in). Each mat measured 2m x 4m (6.56 ft x 13.12 ft). In the region of the edge loading beams 10mm (0.39 in) diameter bars were used in the mats. This region is marked "S2" on Fig. 2.1. Steel studs, 22mm (0.87 in) diameter by 130mm (5.12 in) length, were welded to each girder in the A and C frames in a double row with a 300mm (11.81 in) pitch; to each girder in the B frame in a single row with a 150mm (5.91 in) pitch; and to each floor beam and subbeam, in a single row with a 300mm (11.81 in) pitch. A typical section through the floor is shown in Fig. 2.5c.

The placement of the formed metal deck began at the second floor level (Z2) and proceeded upward. The metal deck was placed in position and secured using puddle welds. Steel studs (22mm diameter) were then arc welded through the deck to the floor beams and to the girders of the A and C Frames. Construction photographs of the deck placement are shown in Figs. 2.18 and 2.19. They were welded directly to the girders on lines B, 1, 2 and 3. Mats of reinforcing steel were placed on chairs to ensure a cover of 29mm (0.24 in). The lightweight concrete slabs at the Z2, Z4, and Z6 were placed on the first day of casting and those at the Z3, Z5, and ZR levels were placed on the second day.

The actual slab thickness was measured at several points along the edge and at three interior points for each floor. The interior points were measured where holes in the floor were provided for the instrumentation to pass through. One of these was at the center (B2) column and the other two were located on the centerline of the braced bay and 400mm (15.75 in) on either side of the B frameline. The edge measurements were all within 1mm (0.04 in) of the design values so these are not reported. The measured values at the interior points are given in Table 2.4. Where two values are given it was possible to measure at a rib and at the minimum depth. The wire mesh reinforcing was not perfectly flat, so the actual position of the reinforcing could not be measured precisely. Each mat was bowed in the middle and was placed with the bow up. The elevation of the reinforcing varied by about 10mm (0.39 in). This departure from the correct position probably was reduced somewhat when the concrete was cast.

2.3 Material Properties

The material specified for the W shapes used in the structure was U.S. grade A36. This is equivalent to the Japanese grade SS41 which has a nominal yield stress of 234 N/mm^2 (34.1 ksi). Three coupons were taken from the flange and three from the web of each different size of W shape. A 50mm (1.97 in) gage length was used for all coupon tests except for those from the flange of the W 12x136 where a 100mm (3.94 in) gage length was used. The elongation at fracture was measured between punch points on a 200mm (7.87 in) gage. The average strain rate during testing was about 5% per minute. The average values of material properties for the flange coupons for each member size are given in Table 2.5. Typical stress-strain curves are shown in Figs. 2.20 and 2.21.

The average yield stress of all of the flange specimens was 282 N/mm^2 (40.9 ksi) with a coefficient of variation of 0.06. The average yield stress of the web specimens was 318 N/mm^2 (46.07 ksi) with a coefficient of variation of 0.31. For the individual samples for each member size, the variation in yield stress for the three flange coupons was very small, usually less then 2%.

The brace members were cold formed square-shape tubes of ASTM A500 B steel with a specified minimum yield stress of 317 N/mm^2 (46 ksi). One coupon from each of the three sides that were not welded for each tube size was tested. The averages from the three coupon tests for each tube size are given in Table 2.6. The average yield stress of all brace coupons was 401 N/mm^2 (58.2 ksi) with a coefficient of variation of 0.05. A typical stress-strain curves is shown in Fig. 2.22.

The specified compressive strength of the lightweight concrete was 21 N/mm^2 (3000 psi). Two 10cm x 10cm x 20cm (3.94 in x 3.94 in x 7.87 in) cylinders were tested from those cast as each floor-slab was cast. These were field cured and tested approximately 28 days after casting. The average for the two cylinders tested for each floor are given in Table 2.7.

Three samples from the D6 wire mesh and three from the D10 wire mesh were tested. The following average properties were determined for the D6 reinforcing: σ_y, 398 N/mm^2 (57.7 ksi); σ_u, 544 N/mm^2 (78.95 ksi); ε_u, 11.4%. The following values were determined for the D10 reinforcing: σ_y, 244 N/mm^2 (35.4 ksi); σ_u, 508 N/mm^2 (73.7 ksi); ε_u, 17.5%.

CHAPTER 3

TEST PROCEDURE AND INSTRUMENTATION

3.1 Test Facility and Instrumentation

The tests were conducted in the Large Size Structures Laboratory of BRI. This is perhaps the largest and most advanced structural testing laboratory in the world. The central reaction wall is 6.6m (21.7 ft) by 20m (65.6 ft) in plan and stands 25m (82 ft) high. Simultaneous testing on both sides of the reaction wall is possible. A schematic of a test specimen and the reaction wall on the strong floor is shown in Fig. 3.1.

The 6 story test building was built on the strong floor south of the reaction wall. Eight servo-controlled actuators attached to the reaction wall were used to load the structure. The loads were applied through rigid loading beams installed at the edge of each floor. The points of application of the force were at the midpoint of the 1-2 and the 2-3 bays. The roof level had two actuators with a capacity of $\pm$ 100 metric ton (220 kips) and $\pm$ 1m ($\pm$ 39.4 in) displacement. The 2nd, 3rd, 4th and 5th floors were loaded with a single actuator with 100 metric ton (220 kips) load capacity and $\pm$ 500mm ($\pm$ 19.7 in) displacement capacity, and the 6th floor level had 2 of these shorter stroke actuators.

Two types of data were measured and stored. The first type was that used for conducting the pseudo-dynamic tests which included the measured actuator forces and the floor displacements and the computed velocities and accelerations. The test procedure is described below. These data will be used to study the gross load-deflection relationships of the building. They will also be used to study the performance of the

pseudo-dynamic testing method. The second type was the member strain and displacement data that were measured with strain gages and linear voltage displacement transducers (LVDT's). These data will be used to study moment-rotation relationships for beams, load-deflection relationships for braces, panel zone behavior and many other phenomena including the determination of the distribution of the total story shear between the column and bracing members at different levels of damage. About 1000 channels of this second type of data were collected for each test. This data included:

1. Groups of 4 strain gages were attached near the mid-height (two above mid-height on opposite flanges and two below) of each column in each story in Frames A and B. This data was used to determine axial force, bending moments, and shears in the columns. Additional strain gages were placed at the top and bottom of each of these columns to detect inelastic behavior in potential hinging regions.
2. Similar strain gage patterns were attached to the girders in Frames A and B and transverse girders in Frame 2.
3. Load cells and elongation potentiometers were attached to the braces in Frame B. This permitted determination of the force-deflection behavior of each brace. A drawing of the load cell that was fabricated and installed in each brace of the Phase I structure is shown in Fig. 3.2 with the specific dimensions given in Table 3.1.

4. Displacement transducers were attached in parallel and criss-cross groups to determine plastic rotations near the connections and shear deformation of panel zones.
5. Strain gages were attached to the cross bracing in Frames 1 and 2 so that the forces in these members could be estimated.
6. Strain gages were attached to deck reinforcement and the metal decking at the Z3 level to evaluate the deck strains and composite action.
7. Applied loads and deflections were measured at each floor level, and additional deflections were measured at critical locations such as the center of the girder in the Phase I braced bay or the ends of the eccentric link in the Phase II test.
8. Additional strain gages were attached to study local effects such as buckling of braces or forces developed in lateral bracing elements.

3.2 Pseudo-dynamic Test Method

The seismic tests of the building were conducted using the computer on-line actuator (COLA) test facility of BRI. This type of testing has been most commonly referred to in the literature as pseudodynamic testing. For the COLA test method, the structure is interfaced with the computer through the actuators and the displacement transducers in such a way that the response of the building to a given earthquake can be closely simulated [4,5].

Consider the equations of motion of the test building:

$$\mathbf{m}\underline{a} + \mathbf{c}\underline{v} + \underline{\mathbf{r}}(x) = \mathbf{m}\mathbf{b}\underline{ag} \tag{1}$$

where $\mathbf{m}$ and $\mathbf{c}$ = the mass and damping matrices

$\mathbf{r}(x)$ = structure restoring force vector

$\underline{a}$ and $\underline{v}$ = acceleration and velocity vectors

$\underline{ag}$ = ground acceleration vector

$\underline{\mathbf{b}}$ = ground acceleration transformation matrix.

In a standard nonlinear analysis the restoring force vector, $\mathbf{r}(x)$, would be computed using a finite element or structural analysis program. Thus, the validity of the results is highly dependent on ability of the program to model material and structural behavior. This is the most difficult and unreliable element to estimate in Eq. 1 because most analytical structural models are highly idealized and can't be expected to correctly model the complex joint behavior, construction flaws, unknown material properties and geometric irregularities that would be characteristic in a real building. Indeed, this is why we must conduct experiments in the first place.

During a pseudodynamic test, the restoring force vector is measured as feedback from the structure. Actually, the test is conducted in a step-by-step fashion in the same manner as a nonlinear analysis would be done. At each step in the process the restoring force vector is measured and the next ground acceleration is input. Equation 1 is solved for the next values of $\underline{a}$, $\underline{v}$ and $\underline{x}$. The actuators then push or pull on the structure to conform to the calculated values of $\underline{x}$. The process is repeated until the end of the earthquake is reached or until the

structure collapses. Thus, the COLA procedure is actually an experimental analysis.

The advantages of pseudodynamic testing are as follows: (1) much larger specimens may be tested than can be accommodated on currently available shake tables; (2) since the inertial effects are partially included, the correct failure mechanism may be obtained for complex structures which is not necessarily the case for normal static testing; (3) the test is conducted slowly so that the damage patterns may be visually inspected. One disadvantage of the method is that, since the test is conducted slowly, strain rate effects are not present as they would be for a shake table test. This is particularly important for brittle structures, but it could also affect the behavior of structures that are ductile. Thus, it is possible that the failure mechanism is different under slowly applied loads. Another drawback is that errors in measurements propagate through the test and can sometimes grow with time. This was encountered during the early stages of this test program and will be discussed later. Some good references are available on the pseudodynamic test method [5,6]. A picture of the control room and one of the actuators in place is shown in Fig. 3.3 and Fig. 3.4, respectively.

CHAPTER 4

PHASE I - SEISMIC TESTING OF THE CONCENTRIC BRACED BUILDING

4.1 Overview of Phase I

The concentric braced building was described in detail in Chapter 2 and was shown in Figs. 2.1-2.5. The primary objectives of the test program were to determine the strength, ductility, energy absorbing capacity and failure mechanism for the structure. Correlation studies are also of interest to determine the accuracy of analytical predictions of the building's behavior. To achieve these objectives, some preliminary studies and three levels of seismic testing were undertaken and completed.

4.2 Preliminary Studies

Linear and nonlinear analyses of very detailed models of the concentric braced building were conducted using several combinations of input ground motion and damping levels. The analyses were done to ensure that the parameters used for the pseudo-dynamic tests would result in actuator forces and story displacements that would cause the desired level of damage in the structure (approximately 2% story drift) but that would not exceed the force or displacement capacity of any actuator. Several different earthquakes scaled to 400 gal ($\approx$0.4g), 450 gal or 500 gal peak acceleration were considered in conjunction with different levels of damping. In addition, several different analytical structural models were used. These ranged from simple "stick" models where centerline dimensions and nominal material properties were used to ones

that included panel zone deformation, P-Δ effects and measured material properties. A great deal of effort was spent on this by the Japanese researchers. This is understandable since a very small safety margin was used. A maximum force of 85 tons and a maximum displacement of 425mm were all that would be allowed based on the analysis. One can imagine the technical and political difficulties that would have arisen had the test needed to be stopped in mid-course because an actuator capacity had been exceeded.

The analytical results also indicated where damage would be concentrated so that the instrumentation could be placed at locations where the most damage was expected. Figures 4.1-4.4 show some typical results for the various models for the Miyagi-ken Oki accelerogram scaled to 500 gal (500 cm/sec^2 ≈ 0.5g) acceleration. These figures from Ref. [7] indicate that the inclusion of panel zone deformations into the analysis had a very significant effect on the results. The analysis indicated that the story displacements (and therefore the damage) would be greatest at the third story and that significant damage would also occur in the lower two stories as well. Therefore, the instrumentation was concentrated in the lowest three stories. It is interesting to note that some preliminary studies done in the U.S. indicated that the fifth story would suffer the greatest damage. Consequently, the initial instrumentation plans called for a heavy concentration of instruments at this level which was relatively undamaged during the tests.

Vibration tests were performed on the structure before and after each major test of the research program and after any repair or modification. These results indicated the damping of the structure and

the frequencies or periods of the first several modes. In addition, comparison of these values showed how damage or repair affected the structural properties. Table 4.1 summarizes some of these measured values. Static unit load tests were also performed before each major test. This data was used to estimate the initial stiffness for the structure prior to the next pseudodynamic test.

Based on the preliminary studies the earthquake record chosen as input for COLA tests was the Miyagi-ken Oki accelerogram shown in Fig. 4.5 with the peak acceleration scaled to an appropriate value. Also shown in Fig. 4.5 are the accelerograms used in Phase II and Phase III. Three pseudodynamic tests were conducted: the "Elastic" tests with 65 gal (about 6.5% g) peak acceleration, the "Moderate" test with 250 gal peak acceleration and the "Final" test with 500 gal peak acceleration. The multiple test levels were chosen because they provide a wide range of information concerning the structural behavior, and they are consistent with the usual multi-level seismic design approach. Mathematical damping values of 0.5%, 0.5% and 2.0% of critical were used for the first three modes of vibration, respectively, for each test. These correspond roughly to those measured during forced vibration tests of the building.

4.3 Elastic Tests

Two preliminary earthquake tests were conducted at the 65 gal level to check out and evaluate the loading system, the instrumentation system and the various parameters used in the test algorithms.

These revealed that an instability was present in the COLA system. This resulted from the algorithm that was used in the BRI facility. The

calculated displacements were only approached but not reached for each time step. This systematic error generated something like negative damping in the system that caused spurious response in the highest mode. As a result the mathematical damping was increased to 90% in the highest three modes and a small "overshoot" was added to the calculated displacements. This latter adjustment had the effect of adding about 1.6% damping to the first two modes. Therefore, the effective damping during the Elastic test was about 2% in the lowest three modes and 90% in the highest three. The Elastic test was then run. This generated approximately design level forces in the building. All of the members remained elastic as expected. The maximum roof displacement was 4.0cm. The floor displacement generated during the test are shown in Fig. 4.6 and the story shear vs. story displacement for the first two stories are shown in Fig. 4.7.

4.4 Moderate Test

The Moderate test was conducted next. The objective of this test was to generate a large enough response that brace buckling would be initiated at some locations. Further, this test should simulate the behavior of the structure during a moderate level earthquake which could occur at infrequent intervals during the life of the structure. The moderate test also provides important information concerning the relationship between the observed damage to the structure and its gross load deformation behavior. Plots of the displacement response of the floors are shown in Fig. 4.8. The shear force-displacement relationships are shown in Fig. 4.9-4.11.

At the end of the Moderate test, a small amount of structural damage was observable. Figure 4.12 is a graphical summary of this observed damage after completion of the Moderate tests. Limited brace buckling and plastic deformation was noted on the 2nd and 3rd floor levels and some concrete cracking was observed, but the structure appeared to be in good condition. Observation of the force-deflection hysteretic curves indicated that the structure remained essentially linear elastic in the 4th, 5th, and 6th stories, although buckling was initiated in the north brace of the fifth story. Limited energy dissipation was noted during the later cycles of response for the 2nd and 3rd levels, because of yielding and buckling of the braces. However, the first level dissipated a large amount of energy (see Fig. 4.9) without apparent brace buckling or yielding. The hysteresis loops showed significant deterioration in the stiffness and load capacity of this level during the last few cycles of vibration response. Further, Table 4.1 shows that there was significant reduction in stiffness and increase in natural period after this test.

Because of this anomaly in the energy dissipation, a more careful inspection of the structure was made, and it was discovered that the beam panel zone between the first level K-braces failed during this test. A very unusual connection detail, by U.S. standards (see Fig. 2.2b and Fig. 2.5e), was used in this zone because of the unusual erection method described earlier. First the beam splice was placed in this region of potentially large bending moment. A bolted gusset plate was used to join the beam webs and the flanges and webs were later welded with complete penetration welds. Finally, the geometry of the connection resulted in

an effective eccentricity which caused the panel to act as a short eccentric shear link. The result was a very unusual 3-piece tear pattern as shown in Fig. 4.13. The complete cause of this failure has not been precisely determined. However, it is probable that the large shear load on the panel combined with the twisting action of the beam combined to produce yielding and tearing of the connection. The tear was induced by the axial loads and end rotation of the ends of the brace and the eccentricity in the connection. These caused serious compatibility problems between the panel and gusset plate. This caused a prying action between the bolts and the welds, and led to a tear which probably initiated at the large copes provided for flange welding. This failure did not occur on any other level although significant prying and panel distortion was observed at this splice on other levels.

This damage was repaired by cutting out the panel and grinding the web down to the flanges and existing panel stiffeners. A 12mm (0.5 in) plate was then welded into place with full penetration welds. This plate was approximately 50% thicker than the original beam web. Stiffness measurements and vibration tests were then performed on the repaired structure to determine its elastic properties. Table 4.1 shows that dynamic characteristics of the structure after the repair are comparable to the initial condition of the building. The Final test for Phase I was then performed.

4.5 Final Test

Figure 4.14 shows the measured floor displacements as function of time for the Final test. The story shear force vs. displacement

relationships for all six levels are shown in Figs. 4.15-4.17 and a graphical summary of the damage is given in Fig. 4.18. Maximum deflections were approximately 3 times as large as those observed in the Moderate Test. Further, Fig. 4.14 shows that deflections were considerably larger to the north direction. Severe brace buckling was noted on the 2nd and 3rd levels during the first few seconds of the acceleration record because of the high energy input of the Miyagi-ken Oki acceleration records and because of the imperfections induced by previous testing. The braces of story 2 buckled out of plane and those of story 3 buckled in the plane of bracing. The braces were square tubes. Local tears initiated at the corners (see Fig. 4.19) because of high concentration of strains induced by plastic hinging of the brace and due to the reduced ductility from the forming process. This mode of failure appears to be consistent with observations from other research [8]. The tears and large lateral deflections of the brace reduced the stiffness of the 2nd and 3rd levels. This increased the deflection and story drift for these levels and caused further concentration of damage. A severely buckled brace is shown in Fig. 4.21 and local tearing at the bottom of a brace is shown in Fig. 4.22. The north brace of the 3rd level completely ruptured (Fig. 4.20) at 11.37 sec into the seismic record. The test was stopped at this point, even though some strength

Table 4.1 clearly illustrates that the stiffness of the structure was dramatically reduced by the brace failure.

Additional structural damage was noted during this Final Test of Phase I. In-plane brace buckling occurred on the north brace of the 4th level and to a lesser extent the north brace of the 1st level. Very limited out of plane buckling was noted on the north brace of the 5th level. Slab cracking was most severe on the 2nd and 3rd floors and decreased for the upper floors. Slab cracking generally initiated at or near the K-brace connection and center column line. Cracking was much smaller and less widely distributed on the north and west sides of the structure. The crack patterns for the Z2 and Z3 floor slabs are shown in Figs. 4.23 and 4.24. The 2nd level composite floor slab also exhibited signs of separation from the steel beam because of the large cyclic reversals induced by the bracing. Measurements indicated that the concrete slab and metal deck were separated by several centimeters (i.e., in order of 1 inch) on the Z2 level at the end of this test. The beam splice connections for the 2nd and 3rd level (i.e., Z3 and Z4 girders) experienced the same twisting prying action noted for the Z2 girder in the moderate test but fracture did not occur (see Fig. 4.25).

The maximum relative story drift of 1.9% occurred in the 2nd story. The 3rd story had similar maximum drift because of the severe brace buckling noted at this level, but all other stories had a relative story drift of less than 1%. The base shear reached a maximum value of approximately 3.2 MN (720 kips) which corresponds to 0.49 W. This ratio of the lateral strength to the dead weight seems quite large, but it should be noted that the structure was not tested with live loads or dead

loads due to walls and partitions. These loads were included in the initial gravity load design, and their absence results in a substantial increase in the reserve strength of the beams and columns. Figure 4.15 shows that considerable energy was dissipated in the lower levels and some deterioration in strength and stiffness occurred. Limited yielding could be observed in the center columns and in the beam column panel zones. This could be observed by the cracking of the paint coating on the steel surfaces. The summary of damage is shown in Fig. 4.18. However, this paint appeared to be very tough and ductile, so additional yielding most likely occurred at other locations. Inspections of the strain gage data will clarify this.

A rough idea of the energy dissipation mechanism for the building can be obtained by observing the responses of the individual members of each story level. The force-deflection response of each brace for the first story are shown in Fig. 4.26 and for the second story in Fig. 4.27. The moment-rotation response for the top and bottom of columns B1, B2, A1 and A2 are shown in Figs. 4.28-4.31, respectively and the panel zone response of each of these columns is shown in Figs. 4.32-4.35. These figures indicate that for the first story, the energy was dissipated by the braces, by hinging at the bottom of the columns and through panel zone deformation. In the second story, nonlinear brace and panel zone behavior accounted for the majority of the energy that was dissipated. The deterioration of strength and stiffness for each story may be attributed primarily to the brace behavior.

4.6 Practical Observations

Analysis of the test results are not yet complete. A tremendous volume of data is available and considerable time is needed to fully analyze the test results. This detailed analysis will be performed and reported in later publications. However, preliminary results can be noted.

First, the test illustrated the importance of the redundancy offered by dual systems in seismic design. Figure 4.36 shows the ratio of the total story shear force carried by the braces in the lowest three stories to that carried by the moment frames. Note that initially the braces carried about 80% of the total shear to 20% for all three moment frames. However, later in the tests the braces in the second and third stories were severely buckled and the moment frames carried about 60% of the lateral load. This is an example of a dual system working perfectly. Without the moment frames as a backup, the building could have been in serious trouble after the fracture of the brace.

Second, the test illustrates the importance of design details for satisfactory seismic performance. The Moderate test caused a failure at a very unusual connection detail. Failure of a single connection significantly reduced the strength and stiffness of the building, and the full consequences of the connection behavior must be considered. Finally, the general result again clearly shows the importance of providing a reliable energy dissipation mechanism within the structure. The concentrically braced frame dissipated energy through panel zone deformation, flexural yielding, and buckling and yielding of the braces. These dissipation mechanisms are reasonably well understood. However the

braces in the second and third story failed early in the Final test. This created a soft story with considerably reduced strength. Thus, had the test continued, the amount of shear transferred down to the 1st and 2nd stories would have been greatly reduced and the energy dissipated by these lower stories would also have been reduced, increasing the danger of collapse. This brace failure was probably predictable [8], and it could have caused serious problems in a real structure with the given acceleration record, since the earthquake could not be stopped early as was done in the test. It is important that engineers consider where the dissipation will occur and design the elements so that the dissipation can be achieved. This failure could be particularly serious with the design practice used in the United States, since concentrically braced frames are commonly designed without the additional stiffness and redundancy of moment resisting beam-column connections.

CHAPTER 5

PHASE II - SEISMIC TESTING OF THE ECCENTRIC BRACED BUILDING

5.1 Overview of Phase II

After the Phase I tests were complete, the concentric braces were removed, the structure was repaired and eccentric K-braces were installed. As for the Phase I structure, the objectives of the test were to determine the strength, ductility, energy absorbing capacity and failure mechanism. Correlation studies were also of interest to determine the accuracy of analytical predictions of the building's behavior. To achieve these objectives, preliminary studies and two levels of seismic testing were undertaken. In addition to these, three sinusoidal tests were also conducted.

5.2 Structural Modifications for Phase II and Preliminary Studies

After completion of the Phase I test, the structure was repaired. The residual floor displacements were all quite small, less than 7mm (.3 in) at the end of this test as shown in Fig. 5.1. The maximum residual story drift was 1/501 in the 6th story. This was approximately the same misalignment as existed in the structure prior to Phase I testing. The concrete floor slab was extensively cracked in the lower floors. Most of the cracking occurred near the major frames and the largest cracks occurred over the brace connection in the center of the south bay of Frame B. All cracks larger than 0.2mm were repaired by epoxy injection. Cracks smaller than 0.2mm could not be repaired, because the pressured epoxy could not penetrate these small cracks. The

area where epoxy injection was used is shown in Fig. 5.2 and some typical cracks are shown in Fig. 5.3. The concrete was recast at several locations where it had cracked excessively or where the slab was cut for other structural modifications such as the brace to beam connections for the Phase II structure.

The eccentric bracing was installed in the north bay (2-3) of Frame B. Lateral support was provided at both ends of the eccentric link, and shear stiffeners were attached. Details of these modifications were provided with the general description of the test structure in Chapter 2 of this report and details of the braced bay are shown in Fig. 2.7. Modifications were also made to the instrumentation. A number of potentiometers and LVDT's were removed from the south bay concentric bracing system of Phase I and used to measure deflections and deformations of the eccentric link and bracing system.

Preliminary analytical studies were conducted to determine the level of damping to use in each mode and to decide which earthquake accelerogram to use. The 1952 Taft record (see Fig. 4.5) was chosen as the input excitation and the same damping values as used for Phase I were employed for earthquake simulation testing. Only two seismic tests were planned. These would use the Taft accelerogram scaled to 65 gals ($\approx$0.065g) peak acceleration for the Elastic test and to 500 gals ($\approx$0.5g) for the Inelastic test.

Vibration tests and static unit load tests were performed at critical points of the test. Table 5.1 summarizes the dynamic properties of the structure as measured at different times during the test program. This table clearly shows that the Phase II structure had a shorter period

and was somewhat stiffer than the Phase I structure. The eccentric shear links added flexibility to the structure, but the braces were larger than those used for Phase I. The net effect was a slight increase in stiffness. However, the Phase II structure had reduced lateral resistance. This occurred because the beam and column sizes were selected for the Phase I structure and were not changed for Phase II. An ideal eccentrically braced frame would require a different distribution of member size and stiffness, but this was not practical for this multi-phase test program. It was believed that the structure would provide a good test of this type of system even though the design was less than optimum.

5.3 Elastic Test

The Elastic Test was conducted with the Taft acceleration record scaled to 65 gal (about 6.5%g). It was designed to examine the elastic behavior, to evaluate the parameters used in the COLA test system, and to check the instrumentation system. Figure 5.4 shows the displacement as a function of earthquake time for each floor. These displacements are quite small. They were only one-half of those predicted in the linear-elastic dynamic analysis, and maximum deflections and story drifts were only about 1/3 of that observed in the Phase I Elastic test. At the time, it was thought that the damping had been underestimated for the analysis. However, later studies revealed that the discrepancy was the result of a small difference between the analytical and actual fundamental period [9]. The analytical model had a period of 0.595 sec compared to the measured value of 0.565 sec. Even though this was only a 5% difference, it resulted in a difference of about a factor of 2 between

the measured and computed responses as shown in Fig. 5.5. Thus, elastic response to the Taft accelerogram is very sensitive to small changes in period in this frequency range.

5.4 Inelastic Test

The Inelastic test was then performed to determine the strength, ductility and failure mechanism for the Phase II building. The Taft acceleration record was scaled to a peak acceleration of 500 gal (about 50%g) for this purpose. Figure 5.6 shows the displacement response of each floor. Figures 5.7-5.9 shows the story shear vs. story drift for all the six stories. Examination of Fig. 5.7 shows that considerable energy was dissipated in the first two levels, but relatively little inelastic behavior occurred in the upper four stories.

The Phase II Inelastic test resulted in a much larger number of inelastic cycles than the Phase I testing, but Phase I produced larger displacements and story drifts and caused considerably more damage. The maximum story drift noted in the Phase II Inelastic test was 1/200 in the first story and an average of 1/250 over the entire structure.

Most of the energy dissipation occurred in the eccentric links. The shear link response for the first two stories and for the second two stories are shown in Figs. 5.10 and 5.11, respectively, where the shear force is approximated as the vertical component of the measured brace force. Examination of the curves in Figs. 5.10 and 5.11 shows that no deterioration in the structure had occurred and the building appeared to have considerable strength and ductility remaining. This is also evident in Figs. 5.12-5.17 which show various member responses.

5.5 Sinusoidal Tests

As a result of the minimal damage and relatively small story drifts and displacements noted with the Phase II Inelastic test, the members of the JTCC recommended that three additional tests be conducted. These tests were to be performed so that the strength, ductility and final failure mechanism could be determined since none of these were revealed by the Inelastic test. Each test was to be conducted using the pseudo-dynamic testing technique with a sinusoidal ground acceleration. The initial conditions at each level were to be selected to approximate a steady-state response in the "first mode," and up to two complete cycles of response were to be obtained, time permitting, for each test. The target interstory drifts of the first story were about 1/200, 1/100 and 1/50 for the first, second and third tests, respectively. However, a maximum interstory drift of 1/40 was not to be exceeded at any level. Also, the tests were to be stopped if the damage became so great that it would cause great delays in conducting future phases of the joint program. A further constraint was that the tests should be complete in only four days of testing. This time constraint limited the testing to one complete cycle at each response level.

The story displacements vs. time for the three Sinusoidal tests are shown in Fig. 5.18. These curves are not smooth sine waves because, for the second cycle, the pseudodynamic method was used only for the loading portions of the test. Unloading was accomplished by manually releasing the pressure on the actuators in 5 or 6 steps to speed up the test. The story shear vs. interstory displacement for the six stories for the Sinusoidal tests are shown in Figs. 5.19-5.21. The structure developed

story drifts which were larger than those developed in the Phase I test. The maximum base shear was approximately 3.3 MN (750 kips) which corresponds to 0.51W. This is greater strength than would be expected in most real building structures because portions of the dead load and all of the live load were not supported during the test. Fig. 5.22 shows the amount of deformation that was typical for the shear links at the first and second levels during the first cycle of the Sinusoidal test and at the maximum displacements for the Inelastic test. During the second cycle, tears and severe yielding in the brace gusset plates initiated in one corner and at the end of the brace is shown in Fig. 5.23.

Figure 5.19 reveals that unexpected strength degradation occurred in the response of the first two stories. Figures 5.24 and 5.25 show plots of the ratio of the first story shear carried in the braces to the total story shear for the first three stories for the Inelastic and Sinusoidal tests, respectively. These curves indicate that there was deterioration in the ability of the braces to carry their portion of the lateral loads for the lowest two stories. For the Inelastic test the braces carried about 80% of the total shear initially. This percentage dropped to about 55% for the first story at about 14 to 15 seconds when the link was undergoing large inelastic deformations and then increased to about 60% near the end of the test. This was not unexpected. For the Sinusoidal tests, however, the braces in the first story carried about 60% of the total shear during the initial cycle, but this dropped to less than 40% of the total shear as the story displacement increased. This ratio went from 80% to 50% for the second story.

The source of the problem was the brace-to-girder connection at the Z2 level. The gusset plate yielded and then buckled near the end of the second cycle of the Sinusoidal test. When this occurred, the end of the brace moved out-of-plane and caused a large torque to develop in the girder adjacent to the shear link. The girder suffered large inelastic torsional deformation, but the transverse braces held the shear link nearly in plane. This inelastic action created a soft spot at the end of the brace. Thus, even with large story drifts, the brace was unable to develop and maintain large axial force. Although the link was in excellent condition, the brace was no longer able to transfer force into it and, therefore, its strength and energy absorbing capacity were not fully utilized. The damage to the brace-to-girder connection for the braces in the first story are shown in Fig. 5.26. This behavior occurred to some extent for both the north and south braces in the first two stories.

The effects of the buckled gusset plates can be seen in Fig. 5.27 which shows the shear vs. story displacement relationships for the braces and for the frames of the first story. The solid line for the braces represents the measured values and the dashed line represents the expected behavior without buckling of the gusset plates. The strength and energy absorbing capacity of the first story was significantly reduced because of the detail failure. Similar behavior was observed for the second story but to a smaller degree. The deterioration in performance of the structure would have been greater if lateral bracing had not been provided at each end of the link.

Considerable yielding also occurred throughout the members of the first three stories. As should be expected, a large percentage of the energy dissipation occurred within the shear links. The shear force vs. shear deformation for the shear links at the six floors are shown in Figs. 5.28-5.30. The deterioration in the response of the links implied by Fig. 5.28 was the result of the gusset plate failure rather than a deterioration of the link. The yielding zones for the first story columns extended upward over one meter from the base as shown in Fig. 5.31. The B2 column in the first story may have been near collapse, but further investigation is needed to verify this. All of the panel zones in the A, B, and C Frames in the first three stories experienced considerable inelastic deformations. Selected member responses are shown in Figs. 5.32-5.43.

5.6 Practical Observations

The maximum story displacements and the maximum story drifts for the Elastic, Inelastic and Sinusoidal tests are shown in Figs. 5.44 and 5.45, respectively. These figures indicate that, even with the gusset plate failures, the structure demonstrated excellent ductility. The figures also reveal that the structure was not an optimum design. Most of the energy dissipation occurred in the first three stories. For an optimum eccentric braced frame, the maximum story drifts would be nearly equal at all levels and all stories would participate equally in the energy dissipation.

The failure of the gusset plates had considerable impact upon the structural behavior. It reduced the shear force which could be carried

by the braces as noted earlier. Further, the post-test natural period increased by 19% over that measured prior to testing. This increase in natural period would suggest that gusset plate failures on the braces of the lower two floors resulted in about a 30% reduction in the overall stiffness of the building. This indicates the importance of connection design. If the members are to dissipate energy through inelastic action, it is imperative that connection failures be avoided. The strength required of most connections of members that are expected to dissipate energy must be substantially greater than the nominal strengths of the members.

Although much energy dissipation occurred in the shear links as expected, the member responses shown above indicate that other areas of the structure also provided significant energy dissipation. This is particularly true of the column panel zones. These elements performed exceedingly well even though they were underdesigned by U.S. standards.

CHAPTER 6

PHASE III AND PHASE IV - MOMENT FRAME TEST AND NONSTRUCTURAL COMPONENT TEST

6.1 Phase III - Moment Frame Test

Upon completion of Phase II, the braces were removed from the north bay of the Frame B and an additional test was conducted on the moment frames. Table 5.1 indicates that the natural period of the Phase III moment frame was 1.28 sec. This suggests that the elastic stiffness of the moment frame was 20 to 25% of that measured in the concentrically and eccentrically braces frames of Phase I and II. This is consistent with the elastic level responses of the Phase I and Phase II structures where the frames carried about 20% of the total shear. Further, Chapter 3 of this report has indicated that the predicted lateral resistance of the moment frame was 30 to 40% of that predicted for the Phase I and II structures.

The building was subjected to the 1940 El Centro Earthquake with 350 gal peak acceleration. The time dependent floor displacements are shown in Fig. 6.1. The story shear vs. story displacement for the first two stories are shown in Fig. 6.2. These plots show that the structure was more flexible and somewhat weaker as expected, but the inelastic behavior was stable. It is quite remarkable that after being subjected to several major earthquakes, the frames were still performing well. The maximum base shear was approximately 1.23 MN (278 kips) which was approximately 19% of the total weight of the structure. This percentage

is again moderately large because the test structure did not include the full dead load or any live load.

6.2 Phase IV - Nonstructural Component Tests

After completion of the Phase II test, nonstructural elements were attached to the building and additional cyclic testing was conducted. The nonstructural elements included precast concrete and glass fiber reinforced concrete panels, lightweight concrete walls, concrete block partitions, suspended ceilings, plastered and gypsum board partitions, and walls with steel doors attached and openings for large glass panels. Original plans called for inclusion of glass panels in the test, but they were eliminated due to cost. The design of these elements is frequently regarded as a responsibility of the architect, but details for the attachment of these elements to the structure are usually designed by the structural engineer. These elements contribute a great deal of mass and stiffness to the vibrating structure, and so engineers must be concerned with their seismic performance.

There are wide variations in practice on the design, construction and installation of these elements both within the U.S. and between the U.S. and Japan. This variation severely complicated the Phase IV research. It was possible to test only a small number of details and variations in design, and so the JTCC formed a subcommittee of researchers and practicing engineers to select typical elements from both the U.S. and Japanese practice. The full variation of the elements tested in this phase is described in other publications [10,11], but Table 6.1 contains a brief summary of some of these elements and their

locations in the test structure. Panels located in Frames A, B or C were essentially subjected to in-plane deformation. Panels in Frames 1, 2 and 3 were subjected to out-of-plane deformation. Some corner element details were tested to check the interface of these elements. The nonstructural elements were manufactured and installed in the structure at locations noted in Table 6.1.

In seismic design, it is recognized that large lateral deflections will occur during major earthquakes, and attachment details must have adequate strength and ductility to prevent failure and subsequent loss of life. Two general attachment concepts for wall panels were used during this test and they are illustrated in Fig. 6.3. The sway type connection is frequently used in the U.S. It employs a rigid bolted attachment at the floor with slotted holes at the top. This presumably allows story drift through bolt slip at the slotted holes. A rocking mechanism is often used in Japan. This mechanism permits 3-dimensional movement at all attachment points. There were also several methods for permitting structural movement required by these two concepts and some of these can be seen in some of the attachment details shown in Fig. 6.4. Some of the details assumed movements were accommodated with short bolts or anchors and oversize or slotted holes. Others permitted movement with long, flexible rods which yielded to permit large inelastic deformations.

The Phase IV testing did not use seismic acceleration simulation as employed in the first 3 phases. Instead, each floor was subjected to a cyclic story drift as shown in Fig. 6.5. The story drift levels can then be correlated with drift levels noted in the Phase I, II and III results. For example, story drifts of 1/400, 1/150 and 1/50 are typical

of the maximum story drifts that were observed in the Elastic, Moderate, and Final Tests of Phase I. It must be noted that there are severe limitations with this test method. It does not consider the mass and velocity and acceleration of the nonstructural panel, since a true dynamic test is required to include these dynamic components of the response. However, the test does provide a reasonable indication of the behavior of the elements under large story drifts, and the effects of the elements on the strength and stiffness of the structure. Extensive instrumentation was attached to the nonstructural elements and their connections. Electronic strain gages and LVDT's were used, and mechanical and manual measurements were combined with frequent observations of the structure and the test elements.

Because of the wide range of instrumentation, a full evaluation of the test results will not be available until a later date, and it will be published in another paper. However, some tentative observations may be made. Joint slip was first observed at story drifts in the order of 1/700. Initiation of cracking in joint sealants was first noted at story drifts in the order of 1/500. Damage to the nonstructural elements increase dramatically with increasing story drift, and it was sensitive to the type of installation detail and errors in installation. The construction personnel appeared to be very conscientious by U.S. standards, but a number of errors in the installation of nonstructural elements were noted. Several premature failures could be attributed to these errors in installation. The long ductile rod attachment detail generally performed much better than the short bolt-slotted hole concept. It permitted larger movements and transferred smaller forces

than the slot hole element. As a result, nonstructural elements generally suffered less damage with these attachments. The corner elements appeared to be a source of major problem, and more study is needed in this area.

Ceiling tile elements suffered no damage until the story drifts reached 1/150, and the damage was significant only after the story drift exceeded 1/125. Several attachment details were regarded as being in a dangerous condition after the story drift exceeded 1/60. Two types of door and door jamb assemblies were tested. Both were built by Japanese manufacturers, but one was designed for seismic applications in that it was designed to accommodate larger movements. The ordinary doors became impossible to operate at story drifts greater than approximately 1/500, and the seismic designed doors were impossible to open at displacements greater than 1/125.

Finally, it should be noted that the nonstructural elements had considerable impact on the structural properties. Table 5.1 illustrates that nonstructural elements reduced the natural period by 30%, and this would suggest that the overall structural stiffness was increased by more than 100%. The stiffness decreased with damage to these elements. After 8 cycles (maximum story drift 1/350) however, most of this additional stiffness had been lost.

CHAPTER 7

PRACTICAL IMPLICATIONS

This report is the initial report on the results of a major research program into the seismic behavior of steel structures. An enormous body of data is available from these tests and considerable time will be needed to fully evaluate the test results. However, some important practical observations for building designers were made in Chapters 4, 5 and 6. These are summarized below.

1. The Phase I test illustrated the importance of the redundancy offered by dual systems. After severe buckling and fracture of several braces, the moment frames carried the majority of the total shear and, thus, demonstrated a dual system working to perfection. Without the moment frames as a backup the building could have been in serious trouble after the fracture of the brace.

2. The Phase I and Phase II tests showed the importance of providing reliable energy dissipating mechanisms within the structure. The concentrically braced frame dissipated energy through buckling and yielding of the braces and the eccentrically braced frame dissipated energy through shear link deformation. In addition, both frames dissipated considerable energy through panel zone deformation and flexural yielding. These dissipation mechanisms are reasonably well understood. However, the braces in the second and third stories of the Phase I structure failed early in the Final test. This created a soft story with considerably reduced strength. Thus, had the test continued, the amount of shear transferred down to the first and

second stories would have been greatly reduced, increasing the danger of collapse. This type of premature fracture of braces must be avoided. It is important that engineers consider where the dissipation will occur and design the elements so that dissipation can be achieved. This failure could be particularly serious with the design practice used in the United States, since concentrically braced frames are commonly designed without the additional stiffness and redundancy of moment resisting beam-column connections.

3. Both the Moderate test of Phase I and the Sinusoidal Tests of Phase II clearly illustrated the importance of connection design on the seismic performance of the structure. Both tests resulted in a connection failure which significantly reduced the strength, stiffness and ductility of the structure. Structural engineers must recognize that seismic design for extreme earthquakes requires inelastic energy dissipation in the members, and connections must be designed to remain functional at loads and deformations well above service conditions.

4. Many nonstructural elements failed or were severely damaged at deformations well below those expected during a severe earthquake. This damage represents an economic loss and in some cases a serious safety issue. Much of this damage was related to the attachment details used in the structure and accuracy with which they were erected. Attachment details must be capable of permitting large movements with minimal resistance, and if movements are restricted the attachment and the nonstructural element must be capable of developing the strength and ductility required to prevent failure.

5. It is not possible to directly compare the concentrically braced frame of Phase I with the eccentrically braced frame of Phase II, because they had different strength levels and they were tested under different seismic excitations. However, it is apparent that the eccentrically braced frame behaved quite well. It had good strength and stiffness and a stable energy dissipation mechanism as predicted in small scale tests. The brittle nature of the braces in the Phase I structure indicates that caution must be exercised in the design of braced frames without the backup of a moment resisting frame.
6. The moment frame also had very stable energy dissipation characteristics but it was a relatively flexible structure.
7. Finally, the test frame showed a remarkable level of strength, stiffness and ductility even though it was tested under several major earthquake simulations. It illustrates that a properly designed and detailed steel building would have considerable ductility and should perform well during a major earthquake.

REFERENCES

1. Uniform Building Code, International Conference of Building Officials, Pasadena, CA 1979.

2. Watabe, M. and Ishiyama, K., "Earthquake Resistant Regulations for Building Structures in Japan," Earthquake Resistant Regulations A World List, 1980.

3. Askan, 6, Lee, S. J., and Lu, Le-Wu. "Design Studies of the Six Story Steel Test Building," Fritz Engineering Laboratory, Lehigh University, Report No. 467.3, June 1983.

4. Roeder, C. W., and Popov, E. P., "Eccentrically Braced Steel Frames for Earthquakes," ASCE, Journal of Structural Division, ST 3, Vol. 104, March 1978.

620.6

5. Okamoto, S., Kaminosono, T., Nakoshima, M., and Kato, H., "Techniques for Large Scale Testing at BRI Large Scale Structure Test Laboratory," BRI Research Paper 101, Ministry of Construction, Japan 1983. (ISSN 0453-4972).

6. Mahin, S. A., and Shing, P. B., "Pseudodynamic Method for Seismic Performance Testing," ASCE, Journal of Structural Division, Vol. III, No. ST 7, July 1985.

620.6

7. Midorikawa, M., personal communication.

8. Gugerli, H., and Goel, S. C., "Inelastic Cyclic Behavior of Steel Bracing Members," Report UMEE 82R1, University of Michigan, Ann Arbor, MI 1982.

9. Boutros, M. K. and Goel, S. C. "Analytical Modeling of Braced Steel Structures," Report UMCE 85-7, University of Michigan, Ann Arbor, MI, 1985.

10. Ito, H. "Progress Report - Nonstructural Element Test Phase," Sixth Joint Technical Coordinating Committee Meeting, Royal Lahaina, Maui, Hawaii, June 1985.

11. Wang, M. L. "Preliminary Results - Nonstructural Element Test Phase," Sixth Joint Technical Corrdinating Committee Meeting, Royal Lahaina, Maui, Hawaii, June 1985.

12. Wang, M. L. "Nonstructural Element Test Phase," U.S. Side Final Report, NSF Grant CEE 82-08012, Center for Environmental Design, University of California, Berkeley, CA, October 17, 1986.

Table 2.1 Column Schedule

	C1	C2	C3	C4	C5
6 - 5	W10x49	W10x33	W10x33	W10x33	W12x40
4 - 3	W12x65	W12x53	W10x39	W10x60	W12x72
2	W12x79	W12x65	W12x50	W12x79	W12x103
1	W12x87	W12x87	W12x65	W12x106	W12x136

Table 2.2 Girder Schedule

	G1	G2	G3	G4
R - 6F	W16x31 w/ 2-19mm[1] @ 200 mm	W16x31 w/ 1-19mm @ 150 mm	W18x35 w/ 1-19mm @ 300 mm	W21x50 w/ 1-19mm @ 300 mm
5F	W16x31 w/ 2-19mm @ 200 mm	W18x35 w/ 1-19mm @ 150 mm	W18x35 w/ 1-19mm @ 300 mm	W21x50 w/ 1-19mm @ 300 mm
4F	W18x35 w/ 2-19mm @ 200 mm	W18x35 w/ 1-19mm @ 150 mm	W18x35 w/ 1-19mm @ 300 mm	W21x50 w/ 1-19mm @ 300 mm
3F	W18x35 w/ 2-22mm @ 200 mm	W18x40 w/ 1-19mm @ 150 mm	W18x35 w/ 1-19mm @ 300 mm	W21x50 w/ 1-19mm @ 300 mm

[1] Indicates size and spacing of shear studs in composite floor system (typical)

Table 2.3 Miscellaneous Member Schedule

	Floor Beam b1	Phase I Brace	Phase II Brace
6 - 5	W16x31 w/ 19mm @ 300mm[1]	ST 4x4x3/16	ST 8x6x5/16
4	W16x31 w/ 19mm @ 300mm	ST 5x5x1/4	ST 8x6x3/8
3 - 2	W16x31 w/ 19mm @ 300mm	ST 6x6x1/4	ST 8x6x3/8
1	W16x31 w/ 19mm @ 300mm	ST 6x6x1/4	ST 8x6x3/8

[1] Indicates size and spacing of shear studs in composite floor system (typical)

Table 2.4 Slab Thicknesses in mm Measured from Bottom of Deck to Top of Slab

Floor level	B 3 Column	B 1-2 0.4 m west	B 1-2 0.4 m east
2F	185	185 110	185 105
3F	170	170 100	170 95
4F	175	170 100	170 100
5F	185	165 95	165 95
6F	180	165 95	170 95
RF		165 90	165 90

Table 2.5 Mechanical Properties of W Shapes.

(Average values from three flange specimens)

Member Size	σ_u ton/cm^2 (ksi)	σ_y ton/cm^2 (ksi)	σ_{uy} ton/cm^2 (ksi)	Est ton/cm^2 (ksi)	ε_u %	ε_{st} %	ε_{max} %
W 10×33	4.60 (65.3)	3.07 (43.6)	3.21 (45.6)	47 667	19.25	2.50	31.2
W 10×39	4.54 (64.5)	2.94 41.7	3.08 43.7	52 738	21.16	2.27	32.0
W 10×49	4.75 (67.5)	3.24 (46.01)	3.42 (48.6)	37 525	18.84	2.15	32.01
W 10×60	4.69 (66.6)	3.00 (42.6)	3.19 (45.3)	51 (724)	19.20	1.73	32.3
W 12×40	4.59 (65.2)	2.87 (40.75)	3.01 (42.74)	54 (767)	19.82	2.00	32.2
W 12×50	4.51 (64.04)	2.70 (38.34)	2.79 (39.62)	51 (724)	19.77	1.83	33.7
W 12×53	4.38 (62.2)	2.59 (36.78)	2.86 (40.61)	41 (582)	19.48	1.53	32.0
W 12×65	4.56 (64.75)	2.85 (40.47)	3.02 (42.88)	45 (639)	19.33	2.03	32.8
W 12×72	4.59 (65.18)	2.94 (41.75)	3.00 (42.60)	43 (611)	18.85	1.86	32.3

Table 2.5 Cont.

Member Size	σ_u ton/cm^2 (ksi)	σ_y ton/cm^2 (ksi)	σ_{uy} ton/cm^2 (ksi)	E_{st} ton/cm^2 (ksi)	ε_u %	ε_{st} %	ε_{max} %
W 12×79	4.59 (65.18)	2.87 (40.75)	3.04 (43.17)	44 (625)	19.05	1.89	32.4
W 12×87	4.70 (66.74)	2.91 (41.32)	3.10 (44.02)	58 (824)	17.98	2.00	32.8
W 12×106	4.54 (64.47)	2.59 (36.78)	2.75 (39.05)	57 (809)	20.23	1.38	32.6
W 12×136	4.56 (64.75)	2.61 (37.06)	2.65 (37.63)	62 (880)	21.05	1.52	33.5
W 16×31	4.43 (62.91)	2.84 (40.33)	2.92 (41.46)	50 (710)	19,83	1.81	32.0
W 18×35	4.63 (65.75)	3.07 (43.59)	3.19 (45.30)	46 (653)	20.5	2.57	32.0
W 18×40	4.79 (68.02)	3.03 (43.03)	3.20 (45.44)	43 (610)	18.87	1.87	30.6
W 21×50	4.49 (63.76)	2.77 (39.33)	2.93 (41.61)	52 (738)	19.98	1.77	31.0

Table 2.6 Mechanical Properties of Square Tubes.

(Average values from three coupons)

Tube Size (in)	σ_u ton/cm^2 (ksi)	σ_y ton/cm^2 (ksi)	σ_{uy} ton/cm^2 (ksi)	E_{st} ton/cm^2 (ksi)	ε_u %	ε_{st} %	ε_{max} %
6×6×0.25	4.73 (67.17)	3.95 (56.09)	4.00 (56.80)	34 (483)	10.71	1.11	32.9
5×5×0.25	4.71 (66.88)	4.10 (58.22)	4.10 (58.22)	30 (426)	8.93	1.15	33.2
5×5×0.18	4.68 (66.46)	3.88 (55.10)	3.87 (54.95)	34 (483)	11.85	1.65	35.2
6×6×0.50	4.88 (69.29)	4.38 (62.20)			7.35		34.9
4×4×0.18	5.06 (71.85)	4.33 (61.49)	4.37 (62.10)	26 (369)			29.4
6×6×0.25	4.63 (65.75)	3.89 (55.24)	3.89 (55.24)	34 (483)	10.71	0.97	33.9
6×6×0.25	4.72 (67.02)	4.34 (61.63)			6.36		35.8
6×6×0.25	4.79 (68.02)	3.96 (56.23)	3.96 (56.23)	38 (540)	11.25	1.23	34.3

Table 2.7 Mechanical Properties of Concrete.
(Average of 2 cylinders)

Floor Level	Day of Test	σ_u ton/cm^2 (ksi)	E_c ton/cm^2 (ksi)
2F	29	0.280 (3.98)	144 (2045)
3F	26	0.290 (4.12)	169 (2400)
4F	29	0.278 (3.95)	143 (2031)
5F	26	0.306 (4.35)	160 (2272)
6F	29	0.300 (4.26)	148 (2102)
RF	26	0.305 (4.33)	151 (2144)

Table 3.1 Dimensions for Load Cell in mm as shown in Fig. 3.7.

Story Level								ℝ-12 (SM50A)			ℝ-16 (SM50A)			ℝ-25 (SM50B)		
	A	A´	H	t_1	t_2	t_3	t_4	B	B´	R	C	C´	R	D	D´	R
1	$165.^{1}$	$165.^{1}$	$202.^{4}$	$25.^{4}$	$25.^{4}$	$25.^{4}$	$25.^{5}$	$114.^{3}$	$114.^{3}$	$6.^{35}$	127	127	$12.^{7}$	$182.^{4}$	$182.^{4}$	$40.^{4}$
	$165.^{1}$	$165.^{1}$	$202.^{3}$	$25.^{4}$	$25.^{5}$	$25.^{4}$	$25.^{4}$				□$152.^{4}$×$152.^{4}$×$12.^{7}$					
	$165.^{1}$	$165.^{1}$	$202.^{3}$	$25.^{6}$	$25.^{6}$	$25.^{4}$	$25.^{5}$									
2-3	159	159	$202.^{4}$	$12.^{9}$	$12.^{8}$	$12.^{7}$	$12.^{8}$	$133.^{35}$	$133.^{35}$	5	$139.^{7}$	$139.^{7}$	$6.^{35}$	$182.^{4}$	$182.^{4}$	$27.^{7}$
	$158.^{9}$	$158.^{9}$	$202.^{2}$	$12.^{6}$	$12.^{8}$	$12.^{7}$	$12.^{9}$									
	$158.^{8}$	$158.^{8}$	$202.^{4}$	$12.^{9}$	$12.^{9}$	$12.^{9}$	$12.^{9}$				□$152.^{4}$×$152.^{4}$×$6.^{35}$					
	$158.^{8}$	$158.^{9}$	$202.^{3}$	$12.^{9}$	$12.^{9}$	$12.^{7}$	$12.^{8}$									
	$158.^{9}$	159	$202.^{4}$	$12.^{9}$	$12.^{7}$	$12.^{7}$	$13.^{0}$									
4	$133.^{4}$(3)	$133.^{3}$(4)	177	$12.^{7}$	$12.^{7}$(8)	$12.^{8}$	$12.^{8}$	$107.^{95}$	$107.^{95}$	5	$114.^{3}$	$114.^{3}$	$6,^{35}$	157	157	$27,^{7}$
	$133.^{4}$	$133.^{3}$	177	$13.^{0}$	$12.^{9}$	$12.^{9}$	$12.^{9}$				□ 127×127×$6,^{35}$					
5	$131.^{7}$	$131.^{7}$	177	$9.^{2}$	$9.^{2}$	$9.^{2}$	$9.^{2}$	$113.^{29}$	$113.^{29}$	5	$117.^{86}$	$117.^{86}$	$4.^{57}$	157	157	$24.^{14}$
	$131.^{7}$	$131.^{7}$	177	$9.^{2}$	$9.^{1}$	$9.^{1}$	$9.^{2}$				□127×127×$4.^{57}$					
	$131.^{7}$	$131.^{6}$	177	$9.^{2}$	$9.^{2}$	$9.^{2}$	$9.^{2}$									
6	$106.^{1}$	$106.^{1}$	$151.^{3}$	$9.^{2}$	$9.^{3}$	$9.^{2}$	$9.^{2}$	$87.^{89}$	$87.^{89}$	5	$92.^{46}$	$92.^{46}$	$4.^{57}$	$131.^{6}$	$131.^{6}$	$24.^{14}$
	$106.^{1}$	$106.^{1}$	$151.^{3}$	$9.^{3}$	$9.^{2}$	$9.^{2}$	$9.^{2}$				□$101.^{6}$×$101.^{6}$×$4.^{57}$					
	$106.^{2}$	$106.^{2}$	$151.^{6}$	$9.^{2}$	$9.^{2}$	$9.^{3}$	$9.^{3}$									

Table 4.1 Dynamic Properties of Phase 1 Structure

	Natural Period (Secs)		
	1st Mode	2nd Mode	3rd Mode
Initial Condition	.61	.227	.133
After Moderate Test	.707	--	--
After Repair	.620	.225	.133
After Final Test	.840	.253	.160

Table 5.1 Dynamic Properties of the Test Structure

	Natural Period (Secs)		
	1st Mode	2nd Mode	3rd Mode
Phase I Initial Cond.	.61	.227	.133
Phase II Initial Cond.	.57	.201	--
Phase II Final Cond.	.68	.230	--
Phase III Initial Cond.	.68	.441	.255
Phase IV Initial Cond.	.87	.270	.130
Phase IV After 8 Cycles	1.13	.389	.207

Table 6.1 Nonstructural Test Specimens

Specimen Type	Design	Location on Structure	Remarks
Precast Concrete Panels	US Design	South Bay of Frames A & B on 2F & 4F & Frame 1 @ 2F & 4F	Normal Weight Concrete Sway Type
Precast Panels	Japan Design	North Bay of Frames C on 2F, 3F, & 4F	Light Weight Concrete Rocking Type
GRC Panels	US Design	Frame 1 on 2F	Sway Type Fiberglass Reinforcement
GRC Panels	Japan Design	North Bay of Frame A on 2F, 3F & 4F	Rocking Type Fiberglass Reinforcement
Lath & Plaster Walls	Japan Design	South Bay of Frames A & C on 5F & 6F	Light Gage Steel Frame
Suspended Ceiling	Japan Design	2F, 3F, 4F & 5F	Supported by Light Gage Steel Frame - 3 Types
Steel Door in Partition	Japan Design	Frame B on 3F & 6F	Ordinary Type and Seismic Type - Installed in Concrete Block Partitions

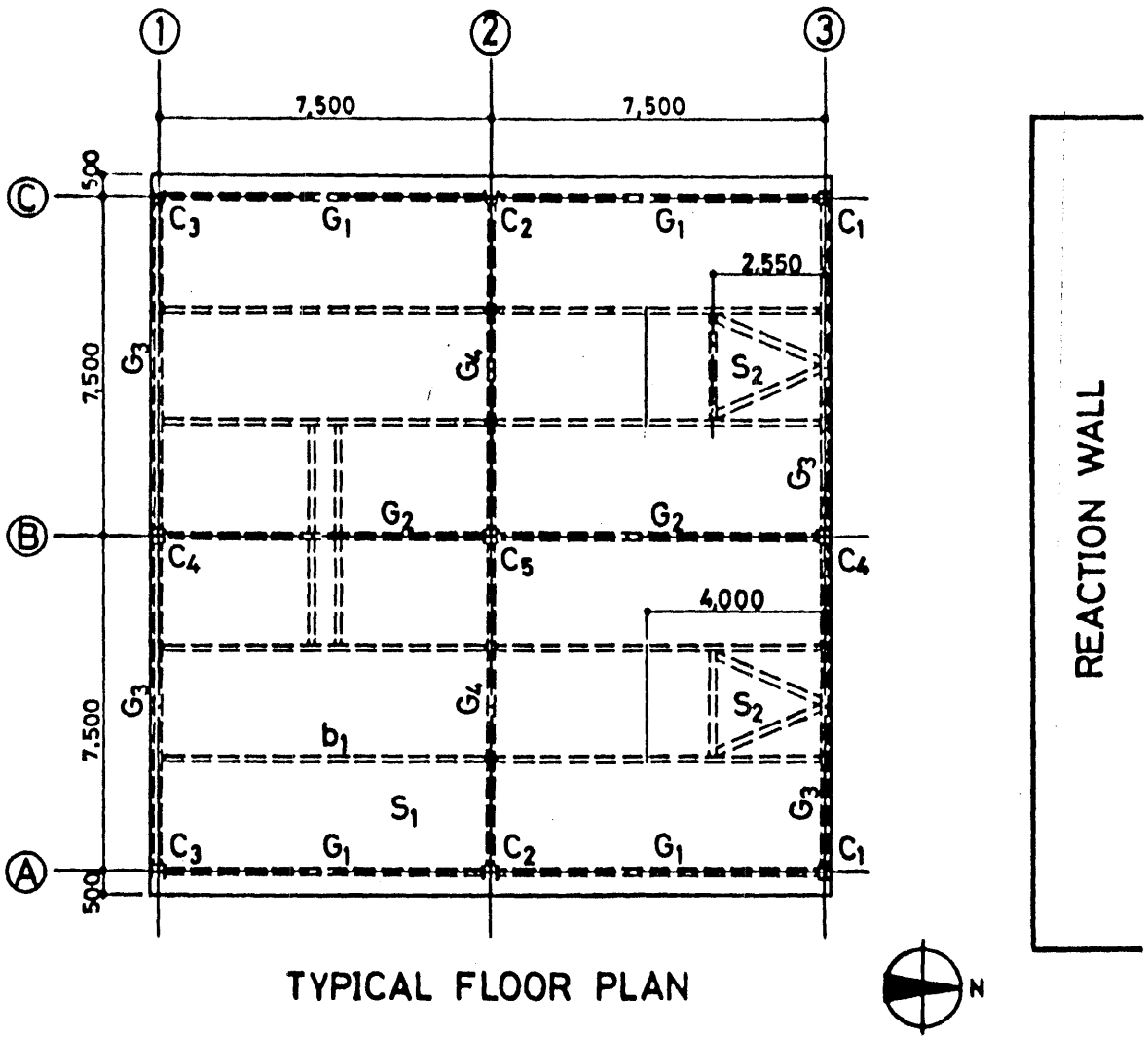

Fig. 2.1 General floor plan of the full-scale test structure

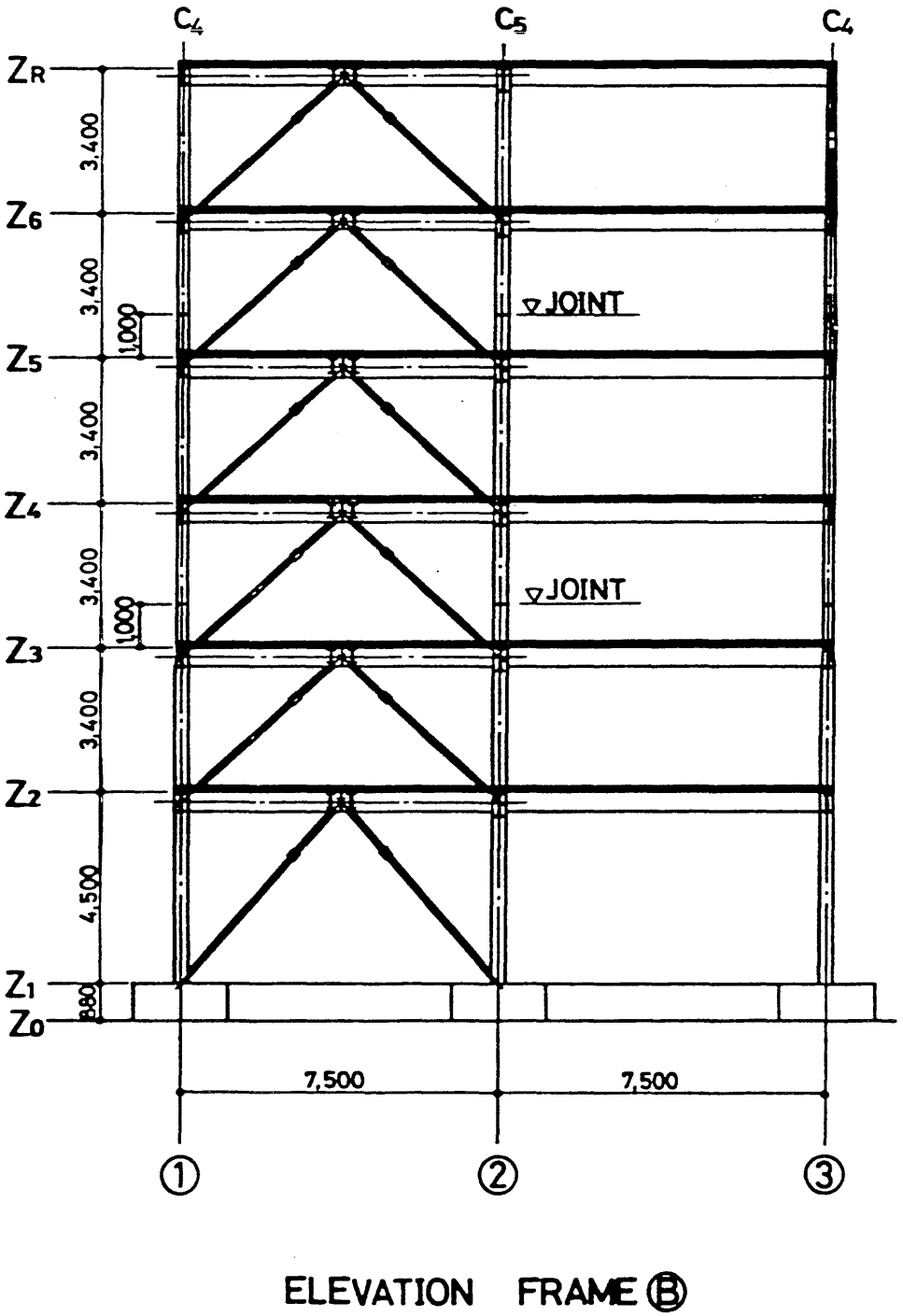

Fig. 2.2a Elevation view of Frame B for the concentric braced test structure of Phase I - full frame

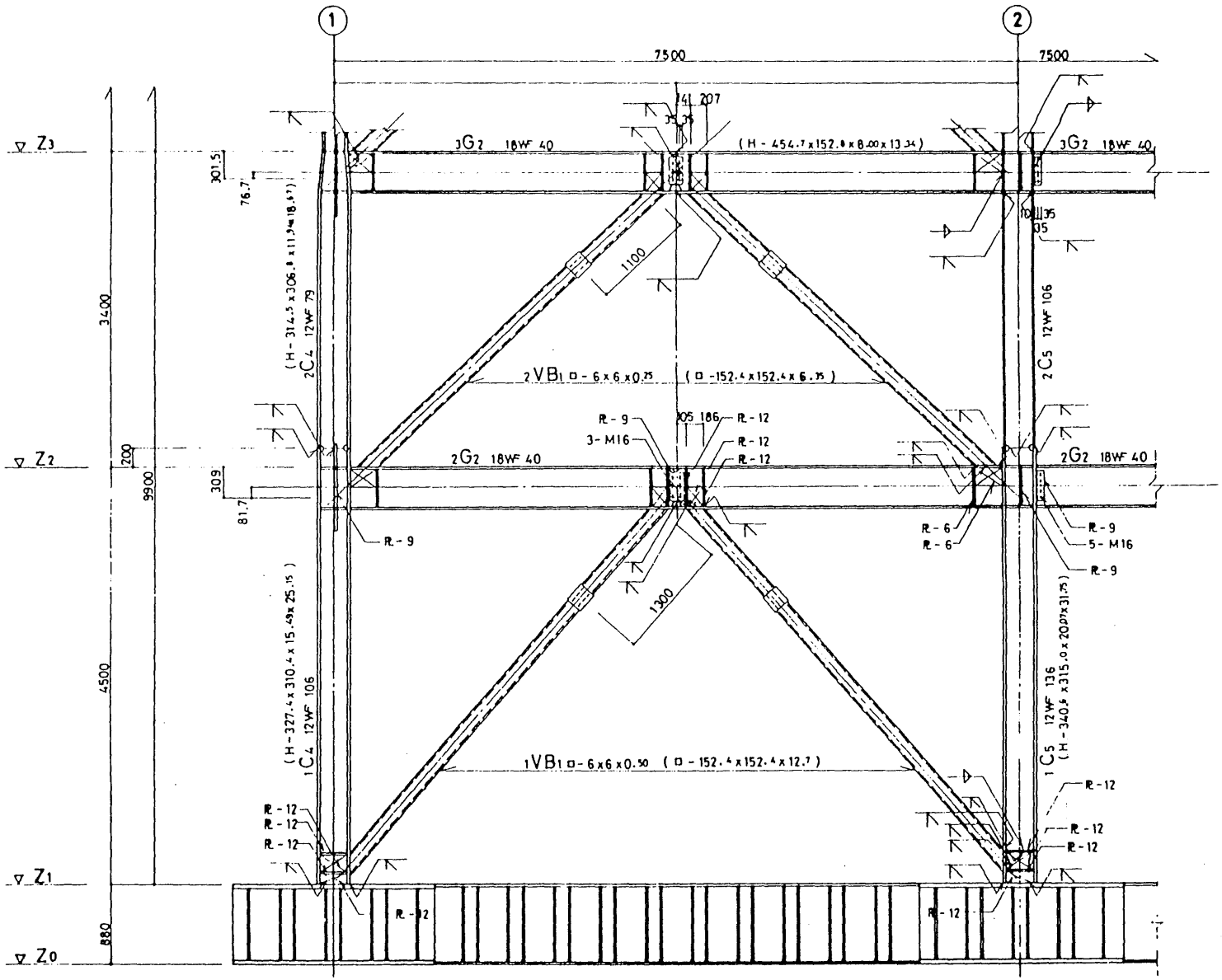

Fig. 2.2b Elevation view of Frame B for the concentric braced test structure of Phase I - story 1 and story 2 of 1-2 bay

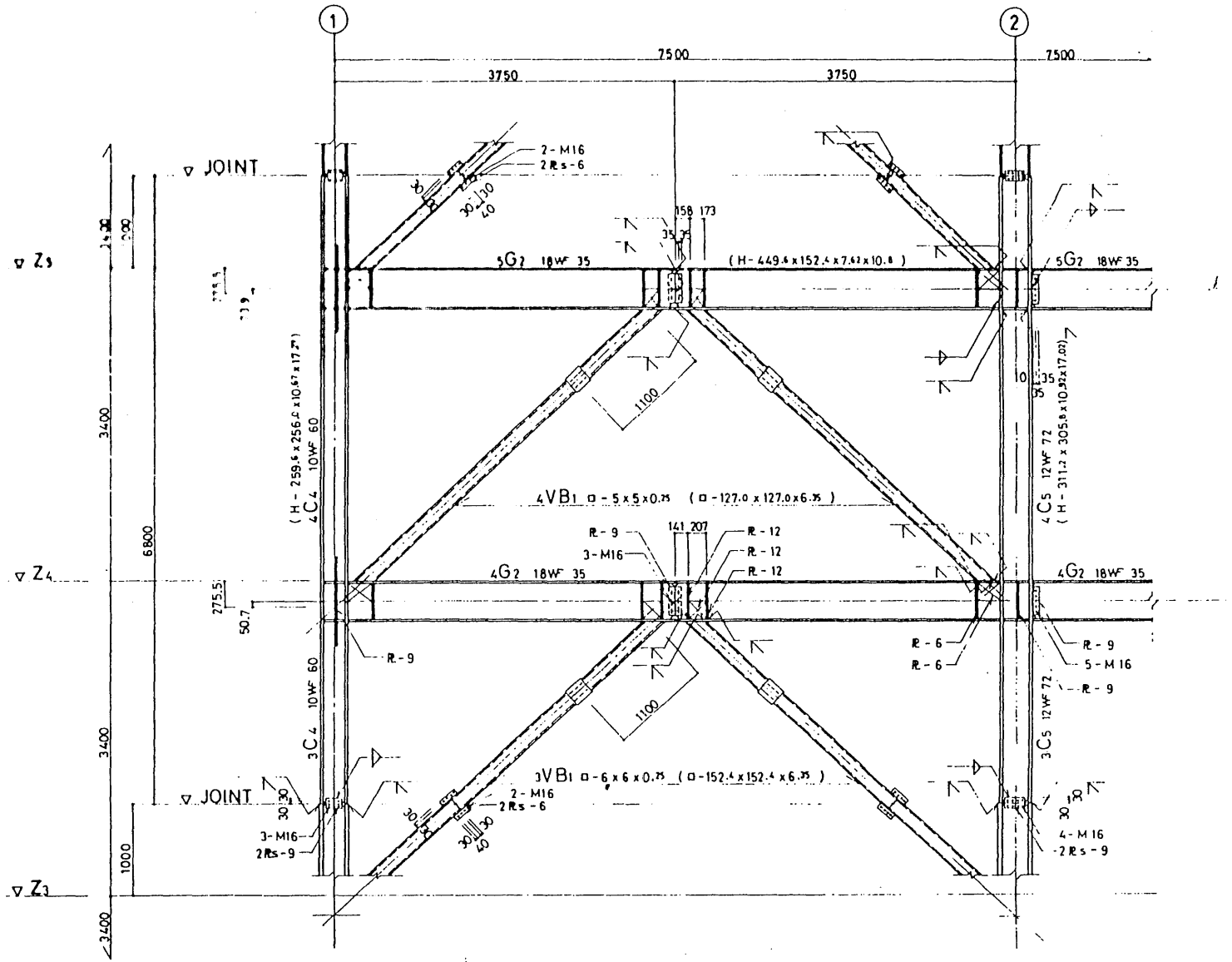

Fig. 2.2c Elevation view of Frame B for the concentric braced test structure of Phase I - story 3 and story 4 of 1-2 bay

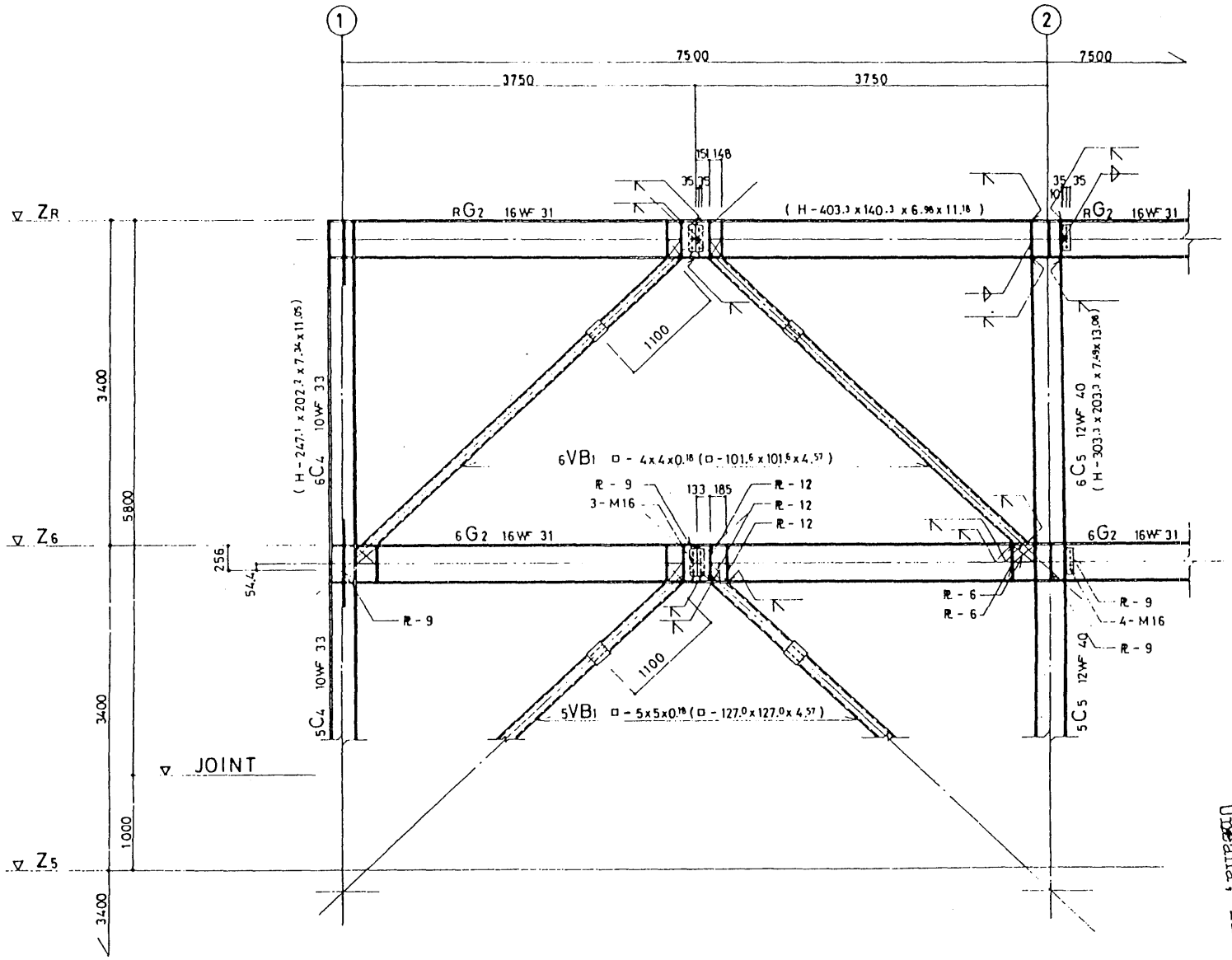

Fig. 2.2d Elevation view of Frame B for the concentric braced test structure of Phase I - story 5 and story 6 of 1-2 bay

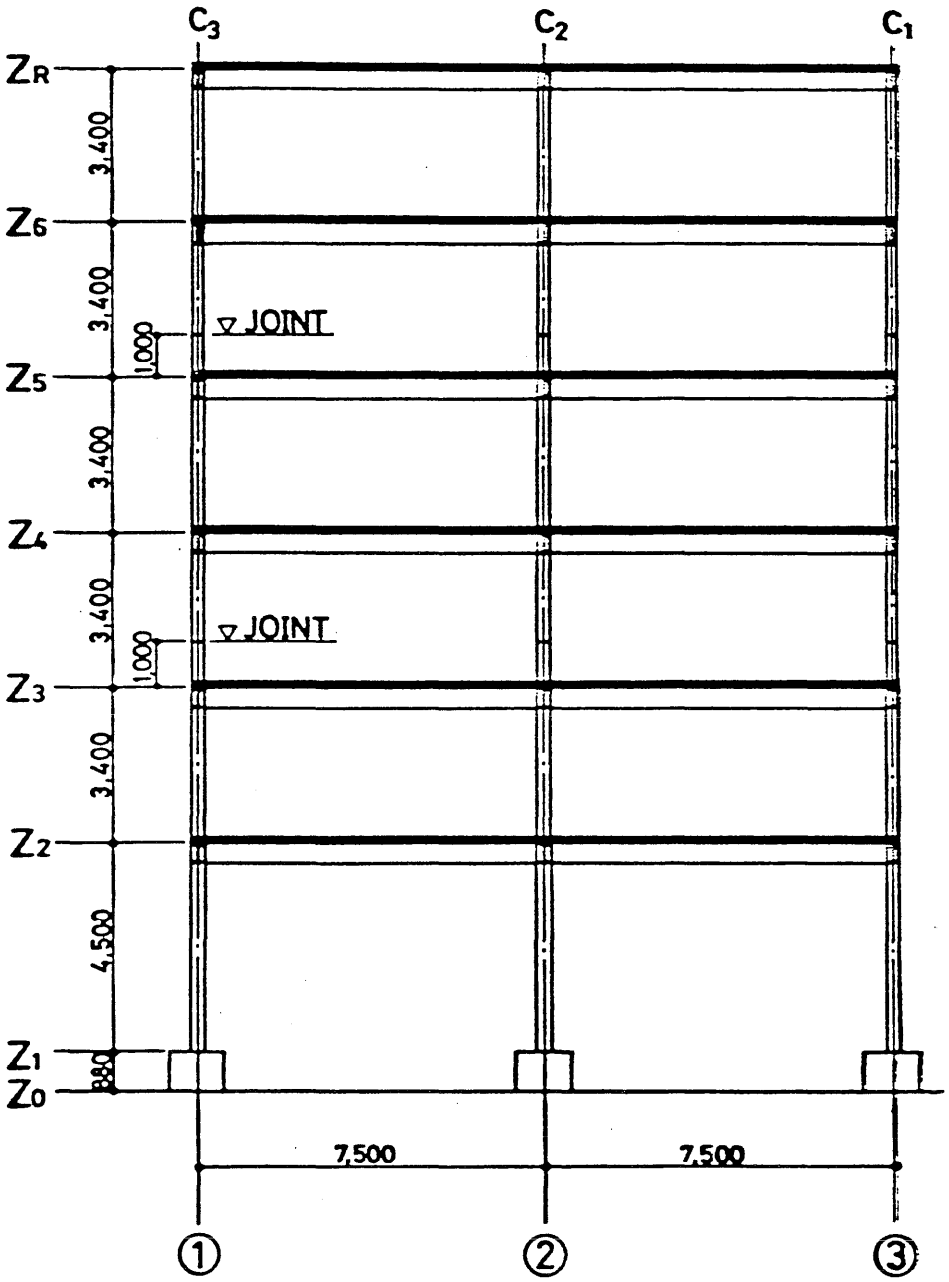

ELEVATION FRAME Ⓐ.Ⓒ

Fig. 2.3 Elevation view of Frame A and Frame C for the concentric braced test structure of Phase I

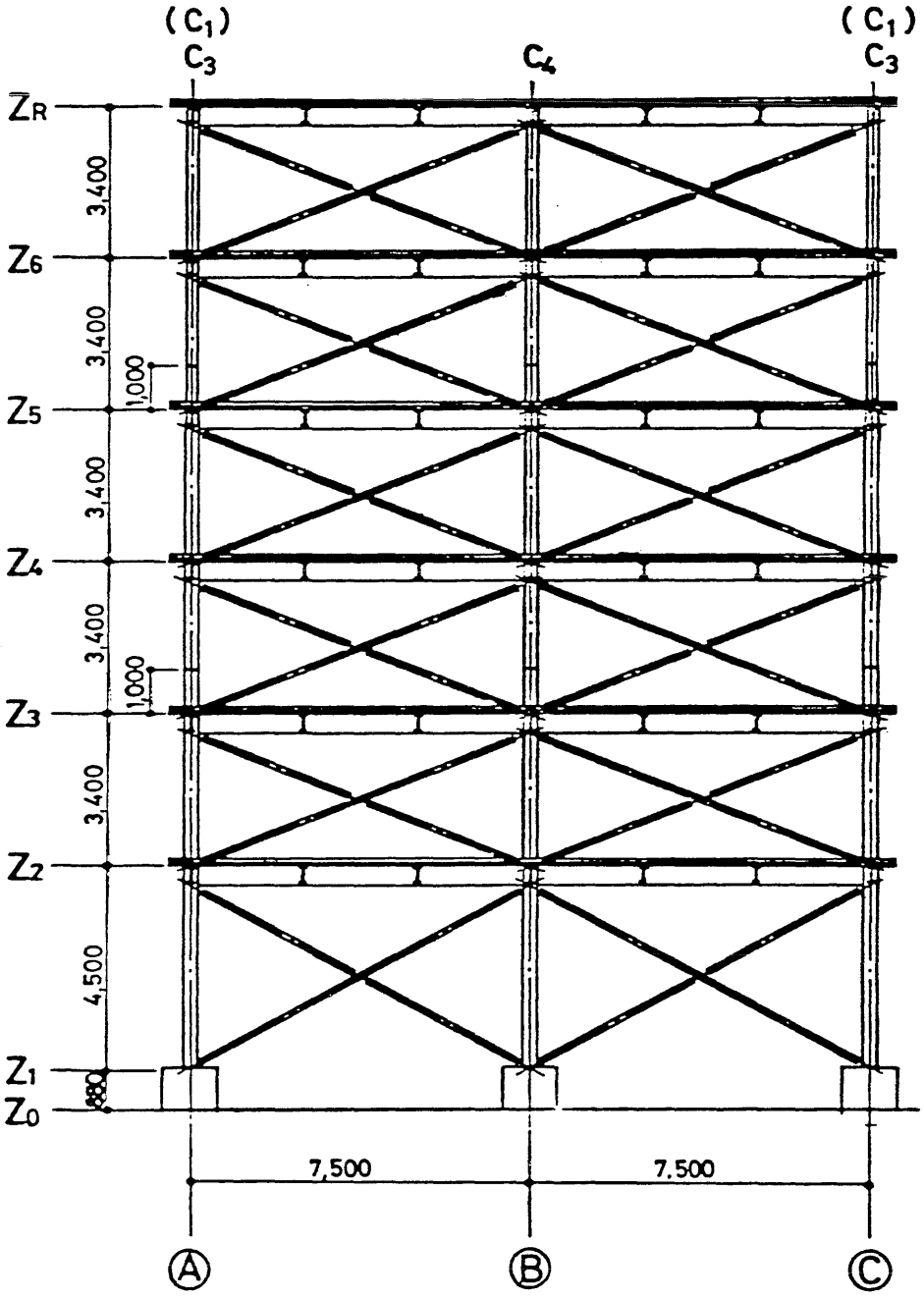

ELEVATION FRAME①③

Fig. 2.4 Elevation view of Frame 1 and Frame 3 for the concentric braced test structure of Phase I

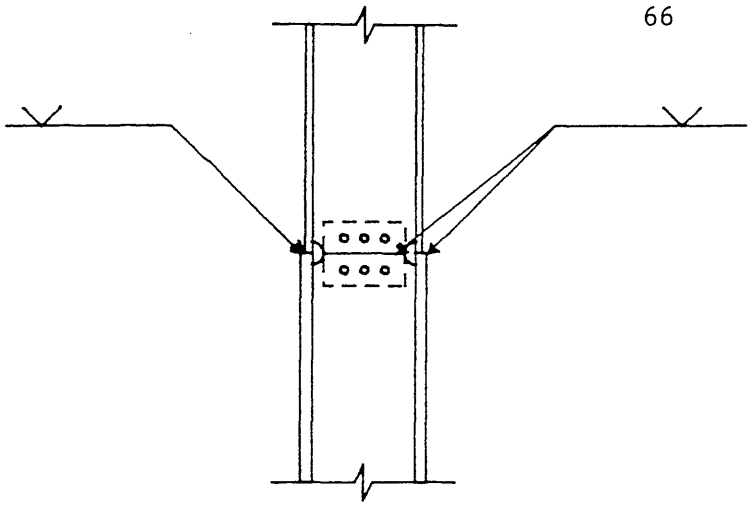

a) TYPICAL COLUMN SPLICE

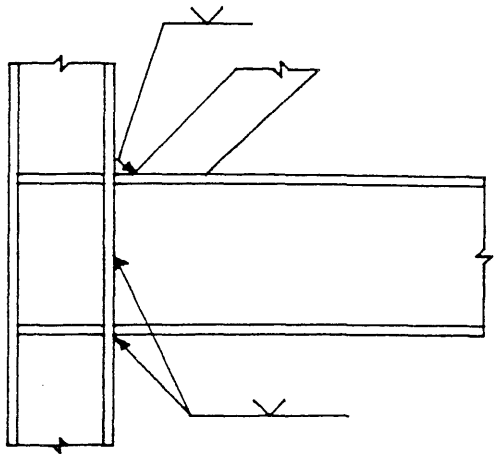

b) TYPICAL BEAM-COLUMN-BRACE CONNECTION FRAME B

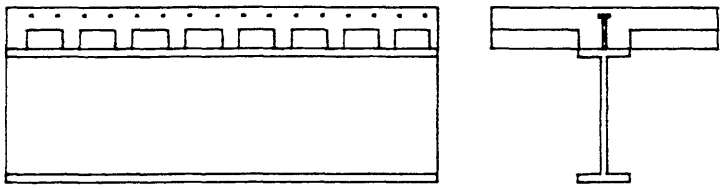

c) TYPICAL SHEAR CONNECTOR DETAIL FOR COMPOSITE BEAMS

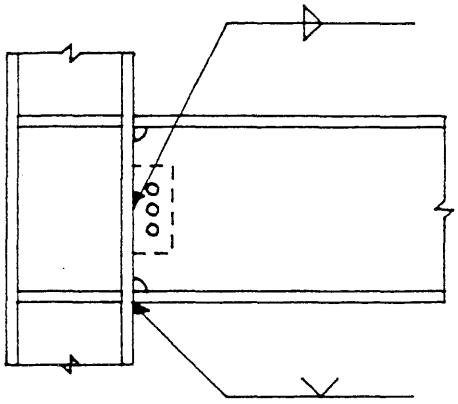

d) BEAM-COLUMN CONNECTION

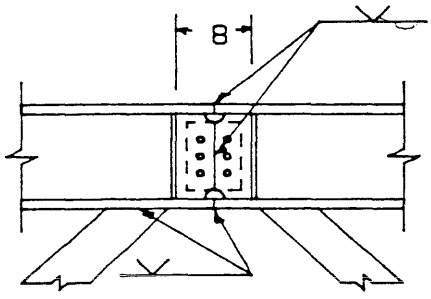

e) TYPICAL BRACE-BEAM CONNECTION PHASE 1

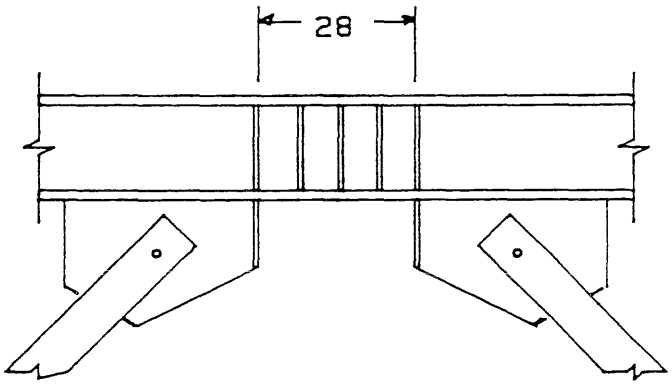

f) TYPICAL BRACE-BEAM CONNECTION PHASE 2

Fig. 2.5 Typical connection details

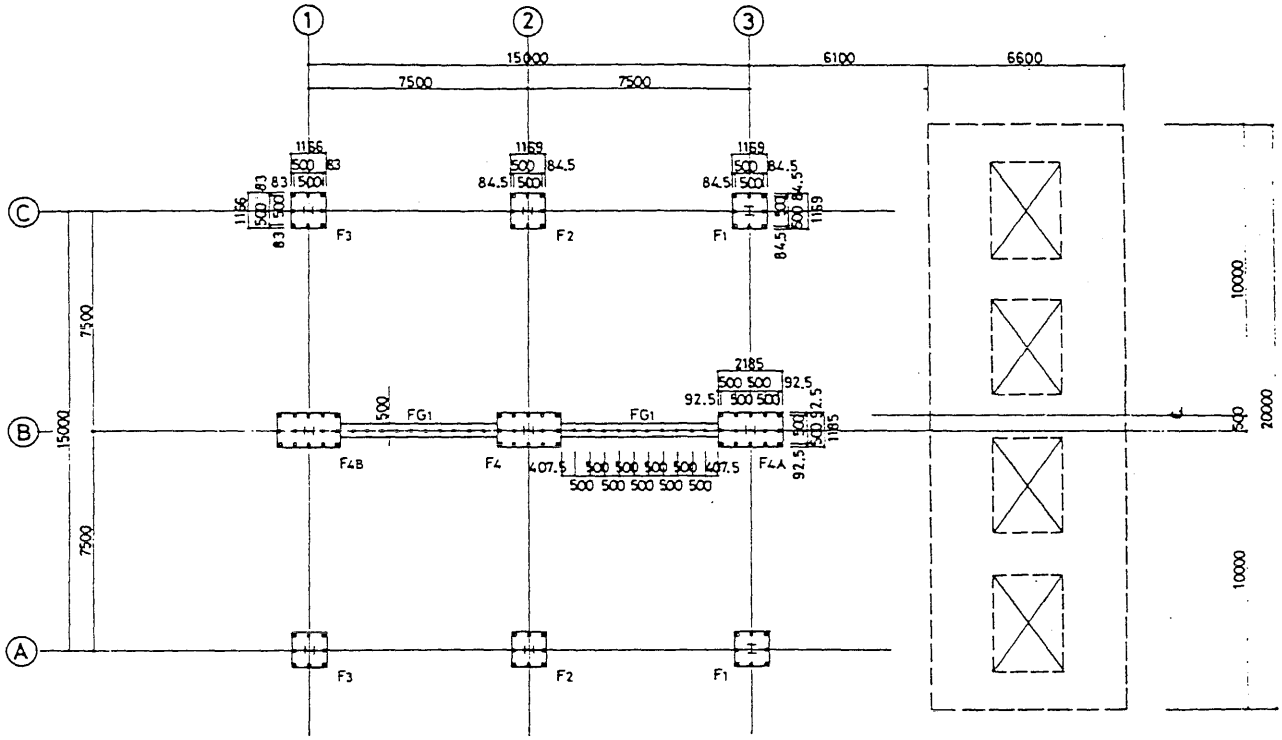

Fig. 2.6 Plan view of the foundation

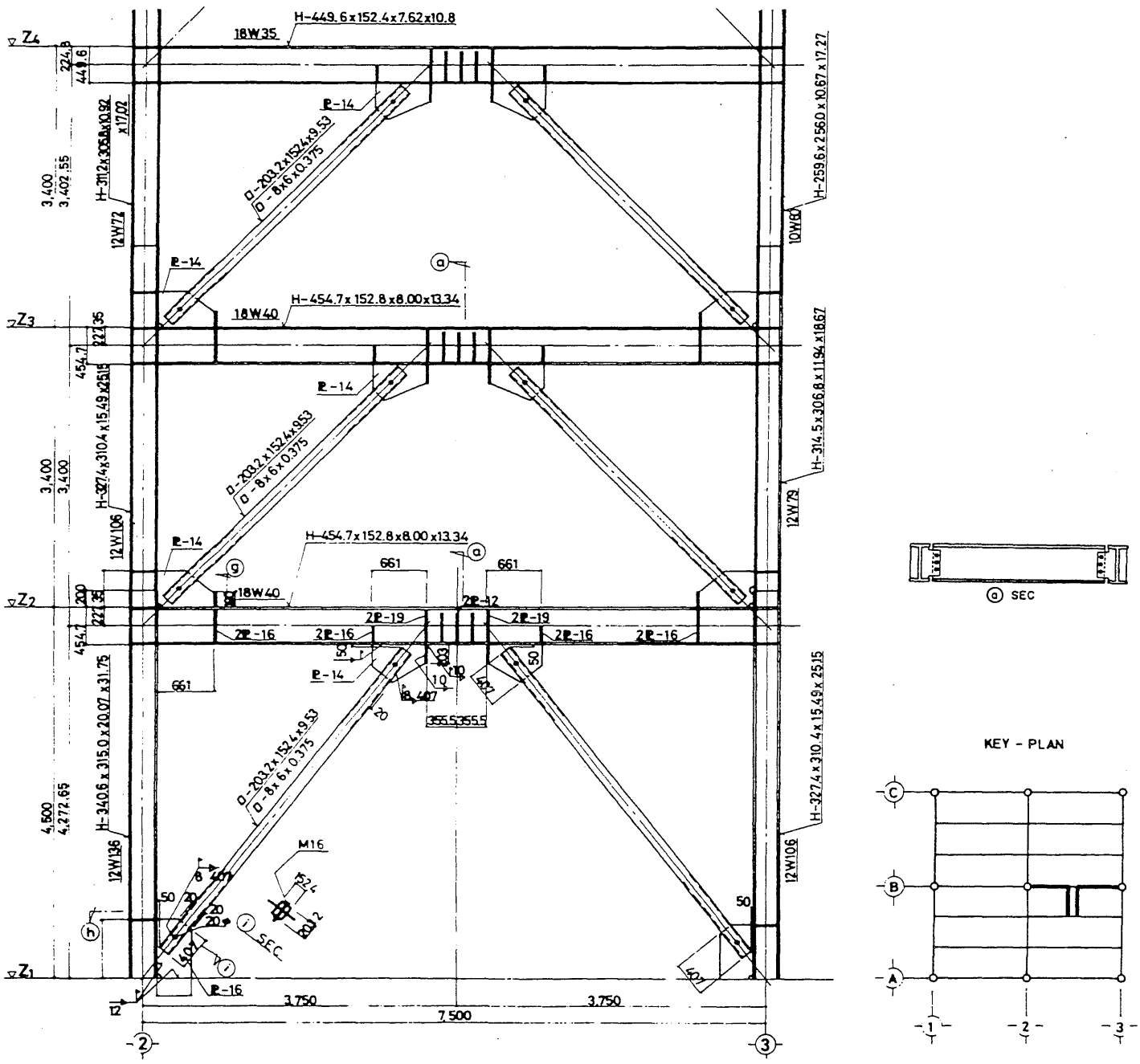

Fig. 2.7 Elevation view of Frame B for the eccentric braced test structure of Phase II

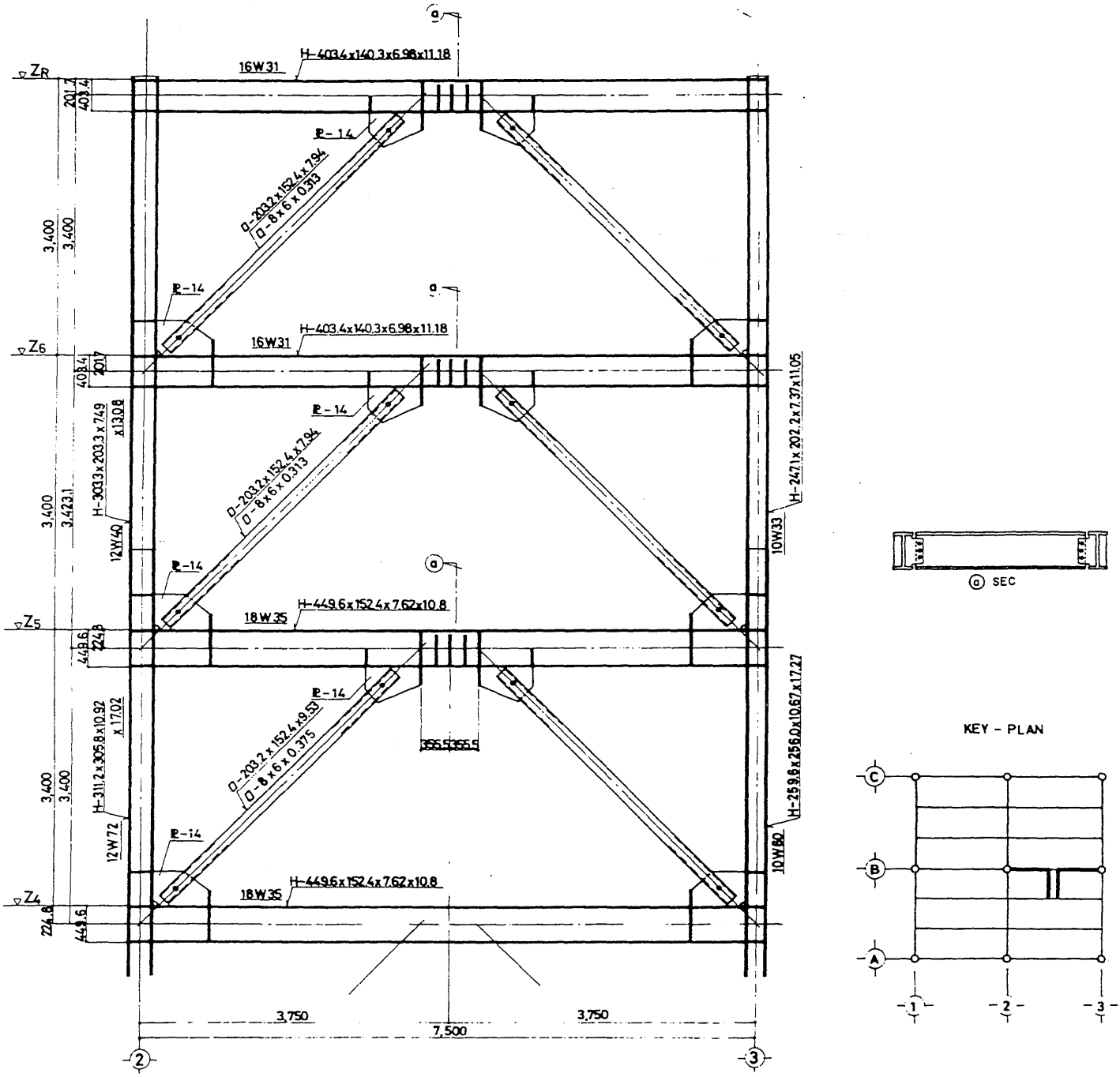

Fig. 2.7 (continued)

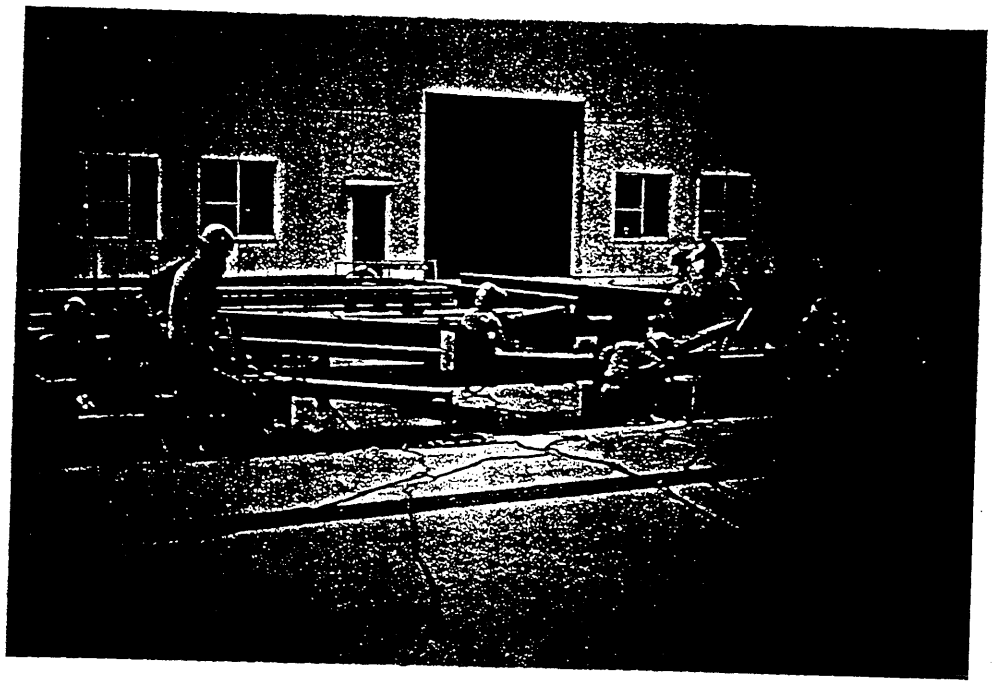

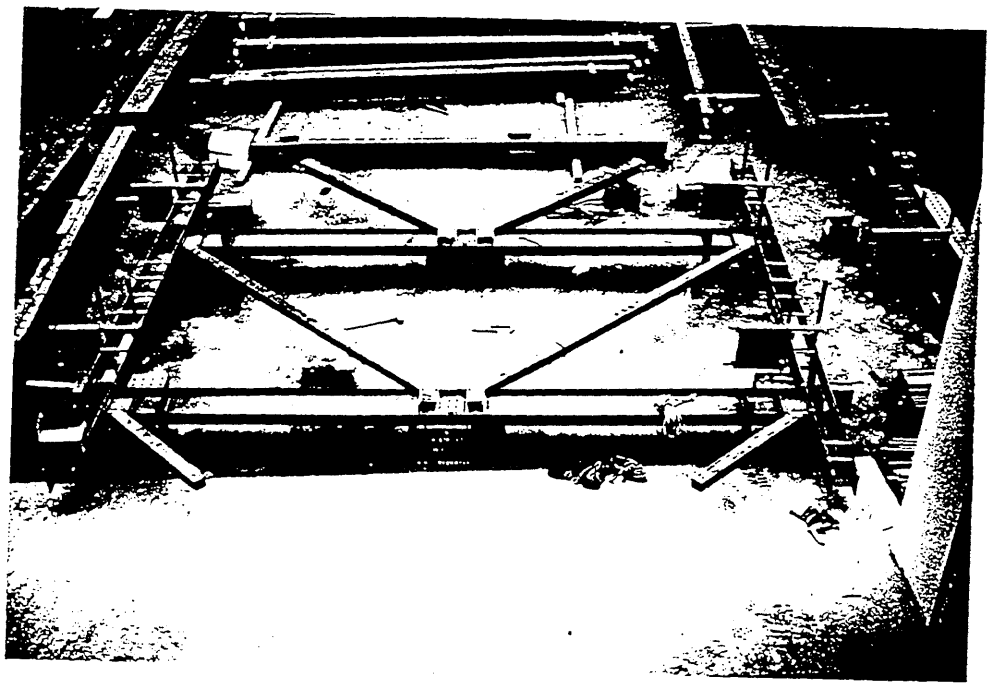

Fig. 2.8 Layout and splicing of one two-story unit of the braced 1-2 bay of Frame B

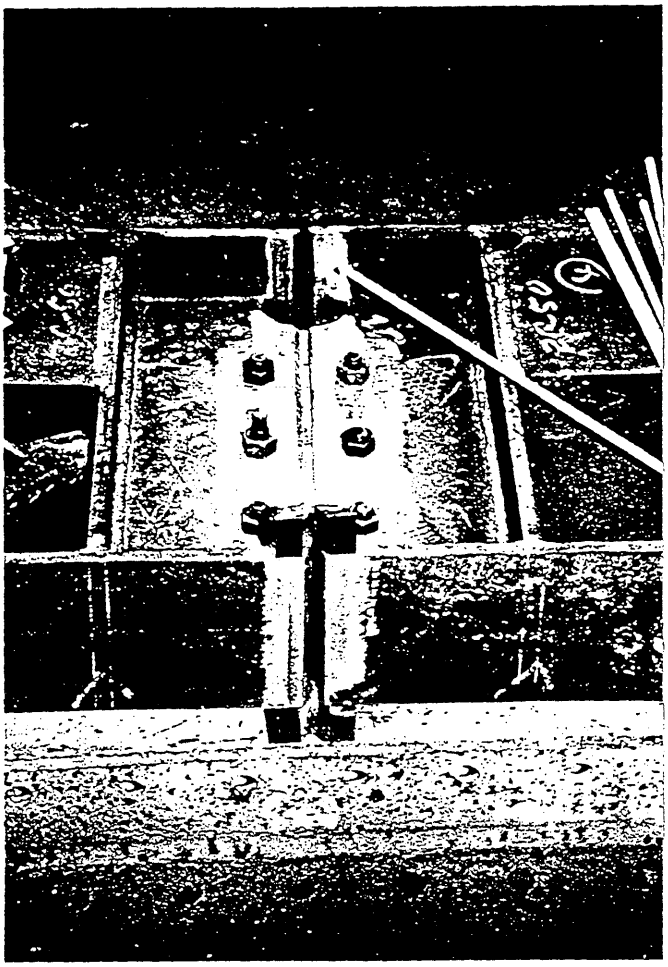

(a)

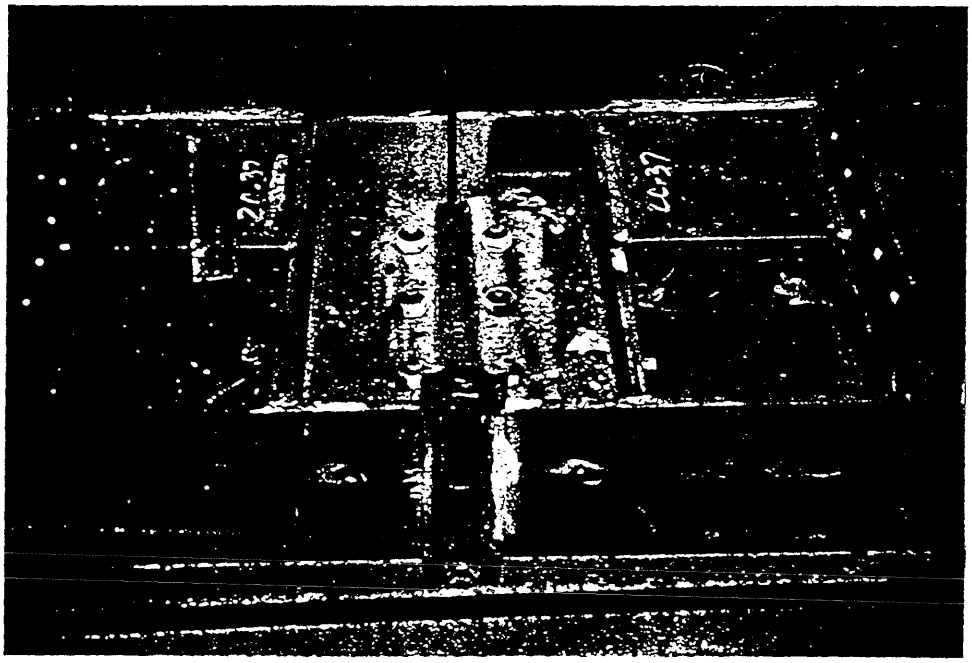

(b)

Fig. 2.9 Beam splice detail for the braced 1-2 bay of Frame B (a) before welding; (b) after welding

(a)

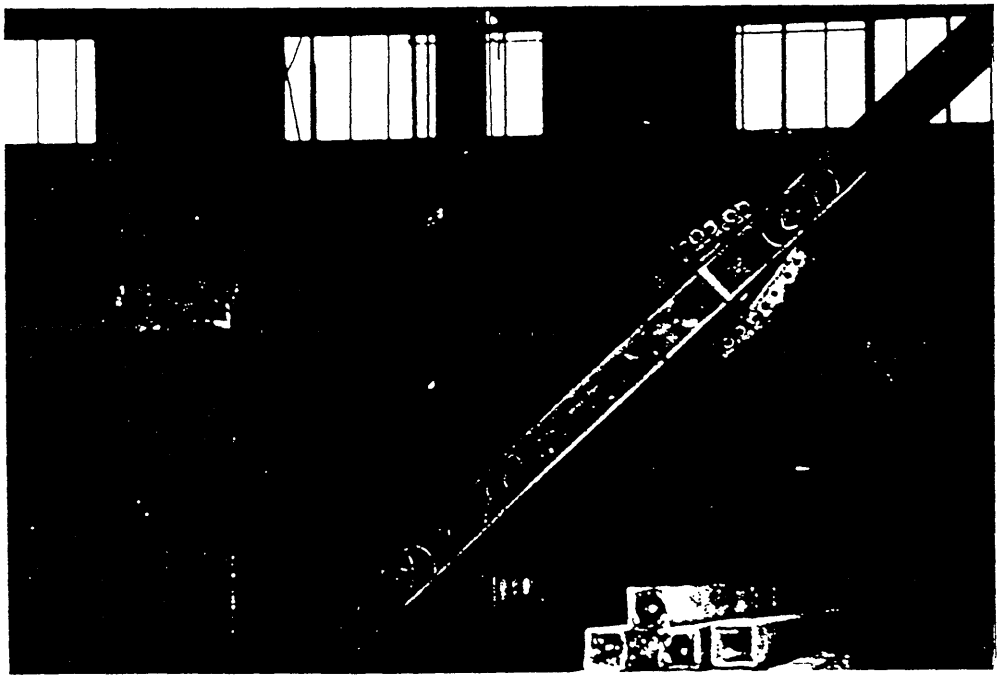

(b)

Fig. 2.10 Erection of a two story section of the braced 1-2 bay of Frame B: (a) aligning the brace ends for temporary connection; (b) temporary connection detail

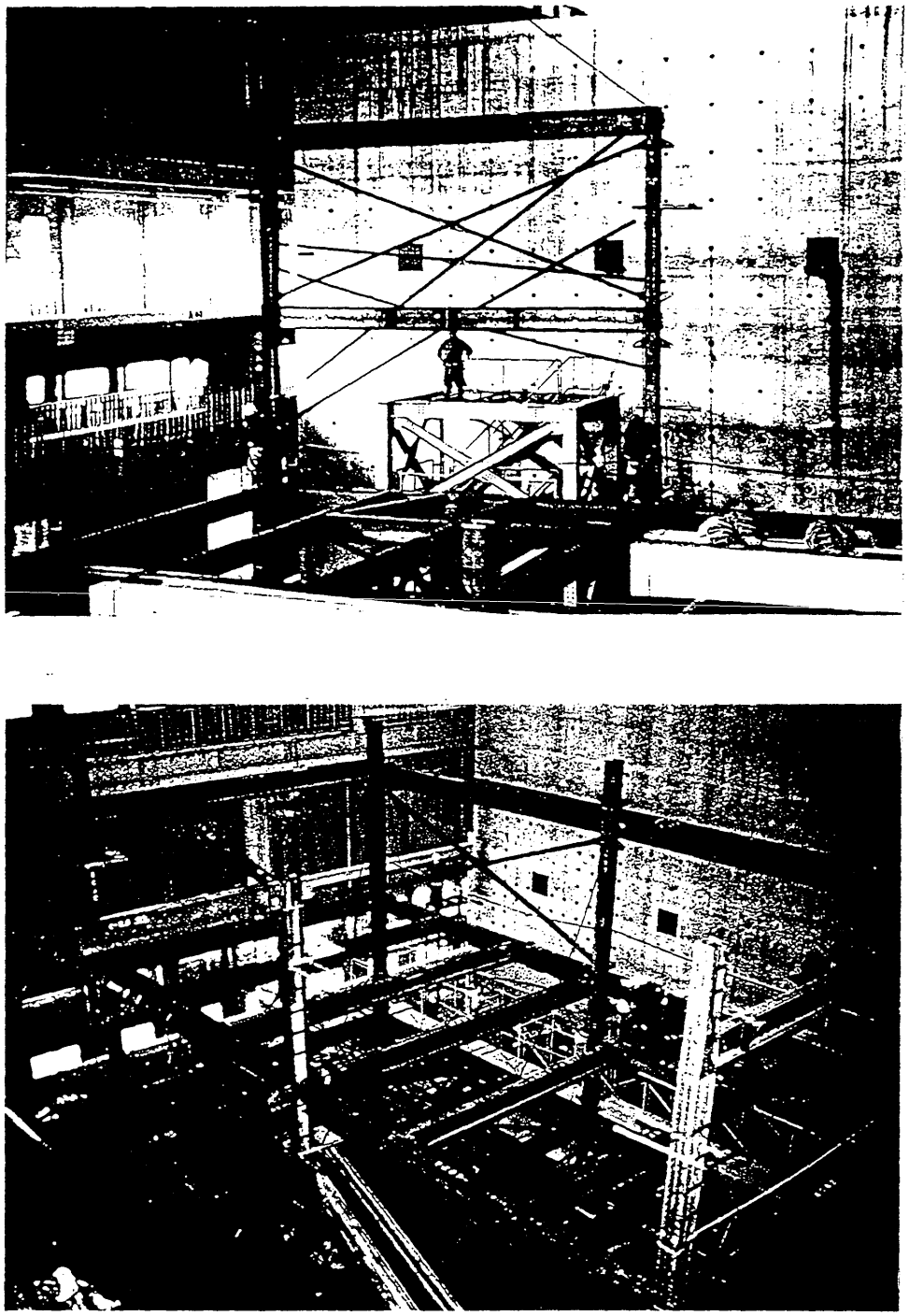

Fig. 2.11 Erection of the test building

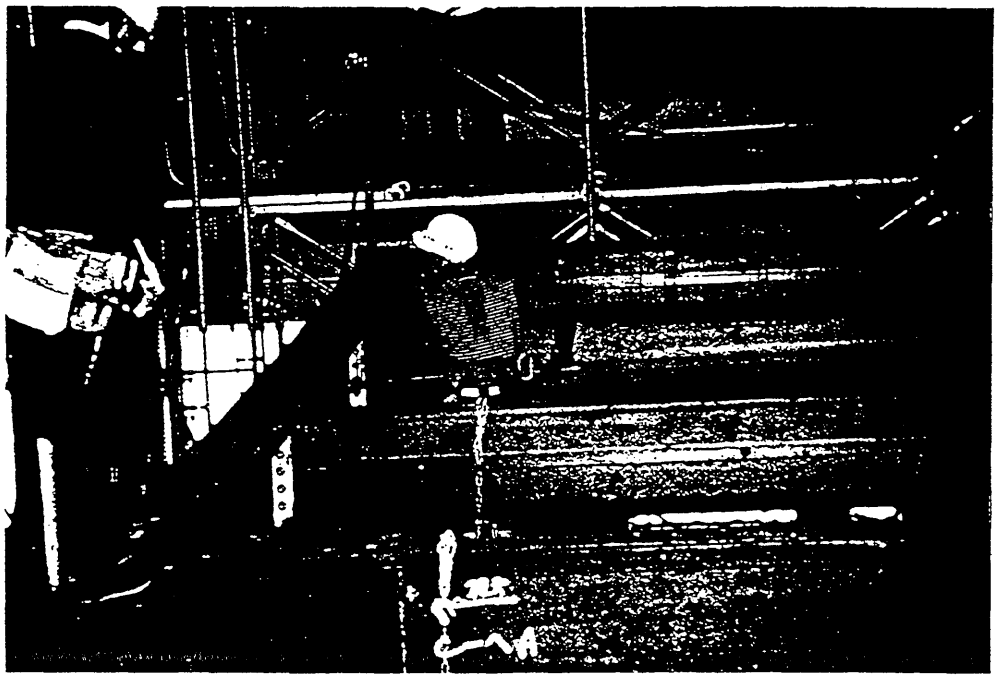

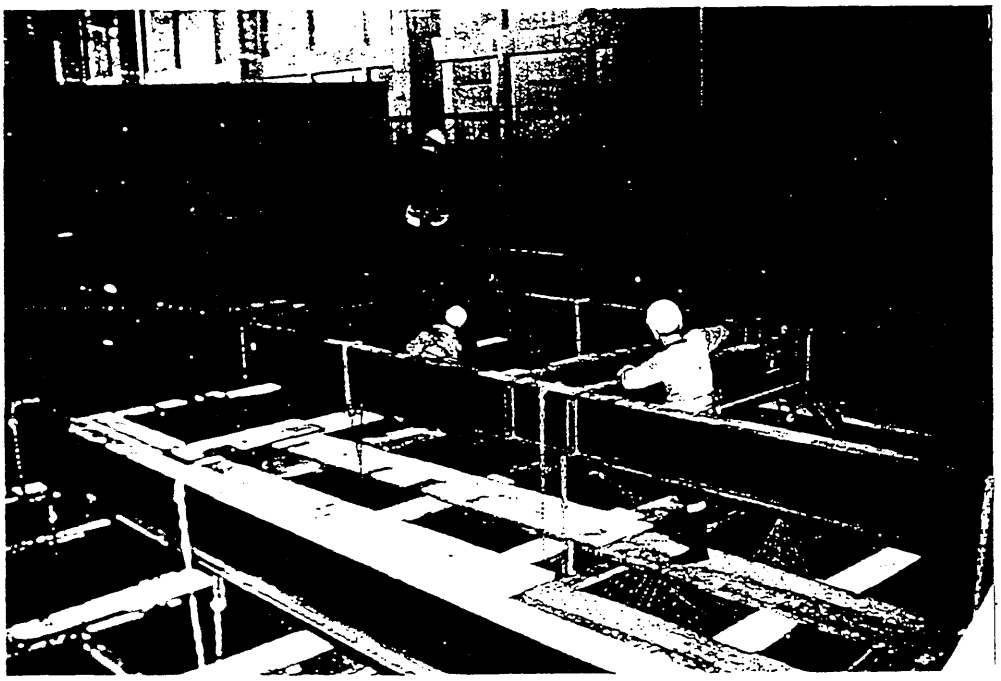

Fig. 2.12 Final tightening of the high strength bolts

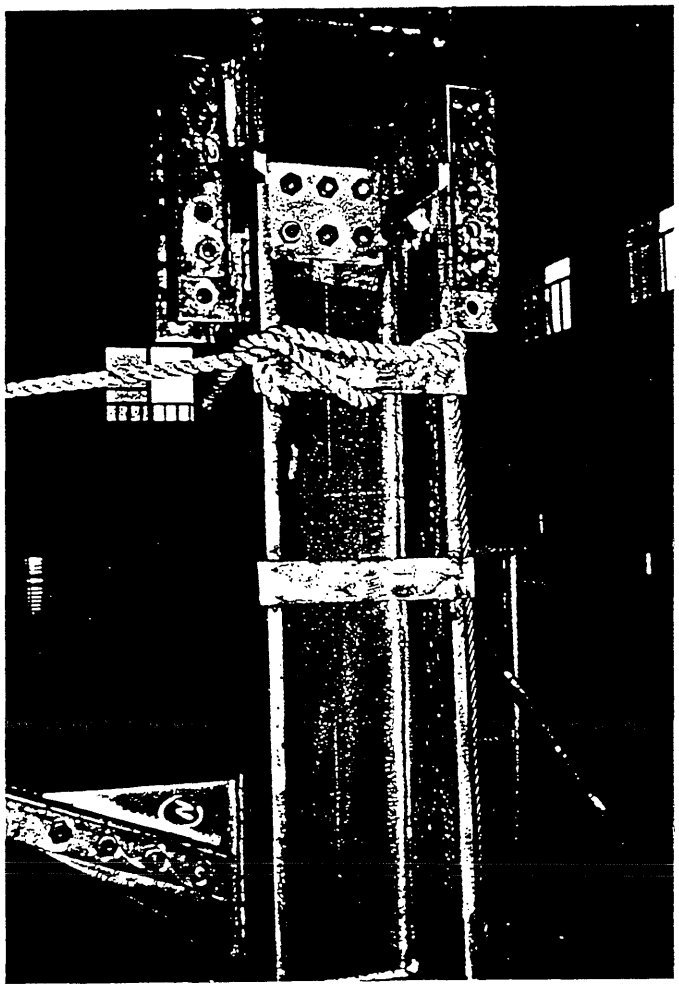

(a)

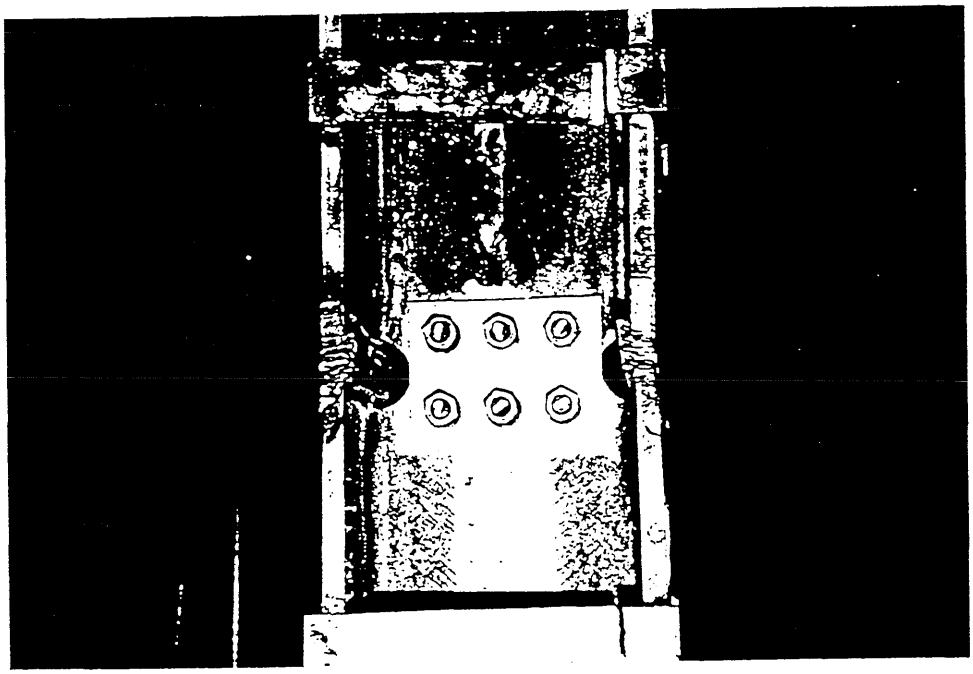

(b)

Fig. 2.13 (a) temporary column splice
(b) final column splice with full penetration groove welds

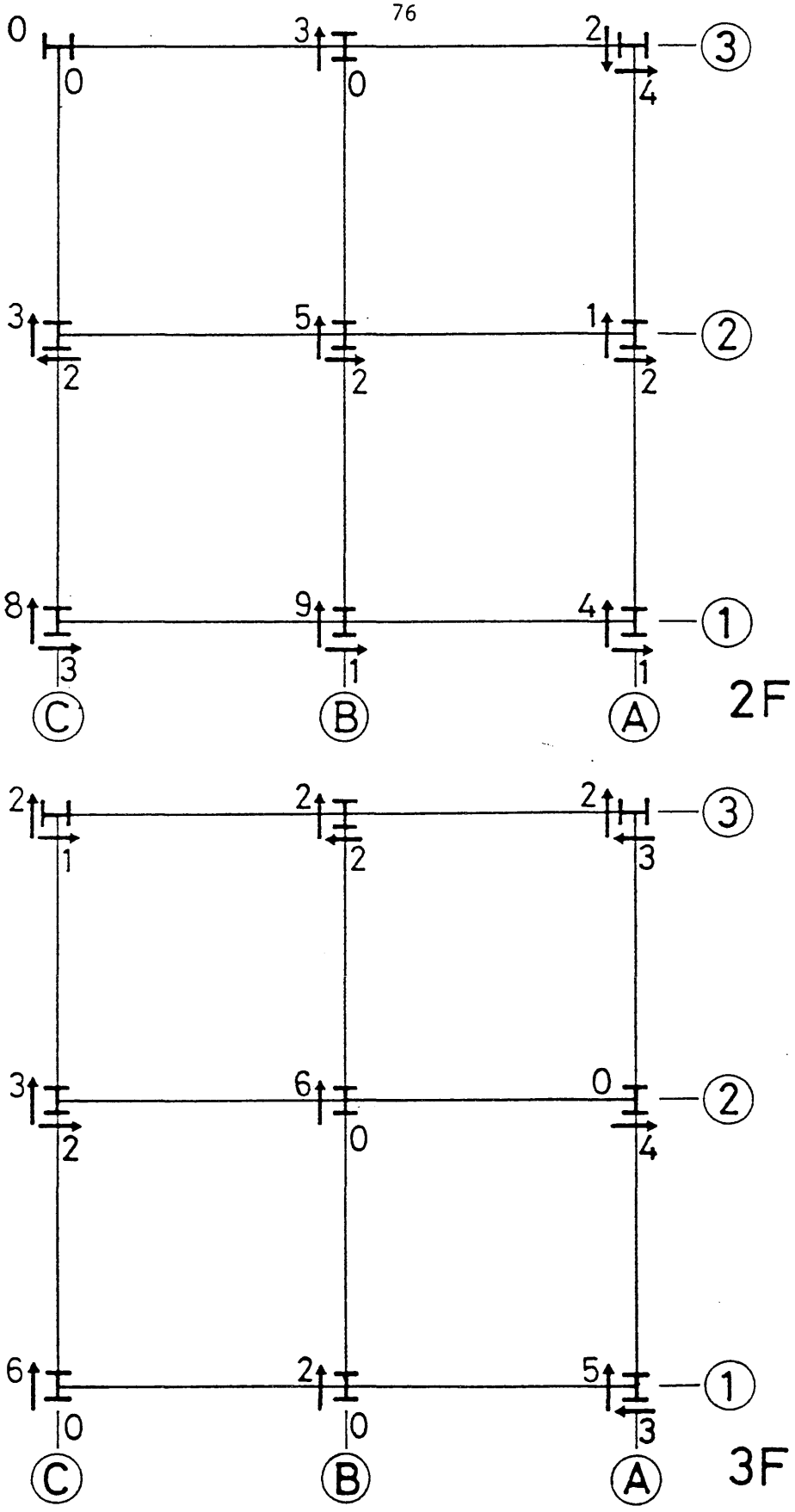

Fig. 2.14 Departures from vertical for the columns at the Z2 and Z3 levels

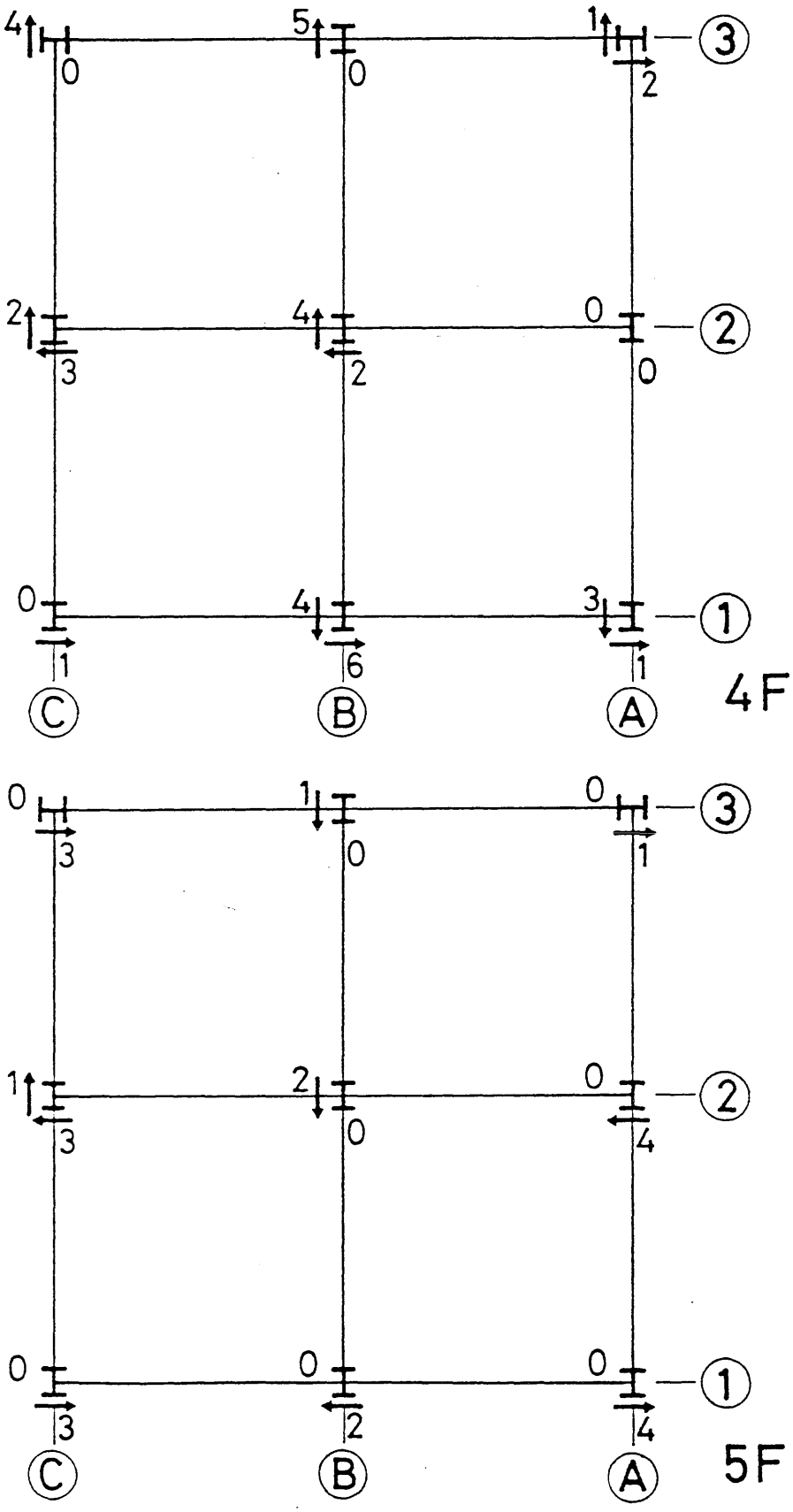

Fig. 2.15 Departures from vertical for the columns at the Z4 and Z5 levels

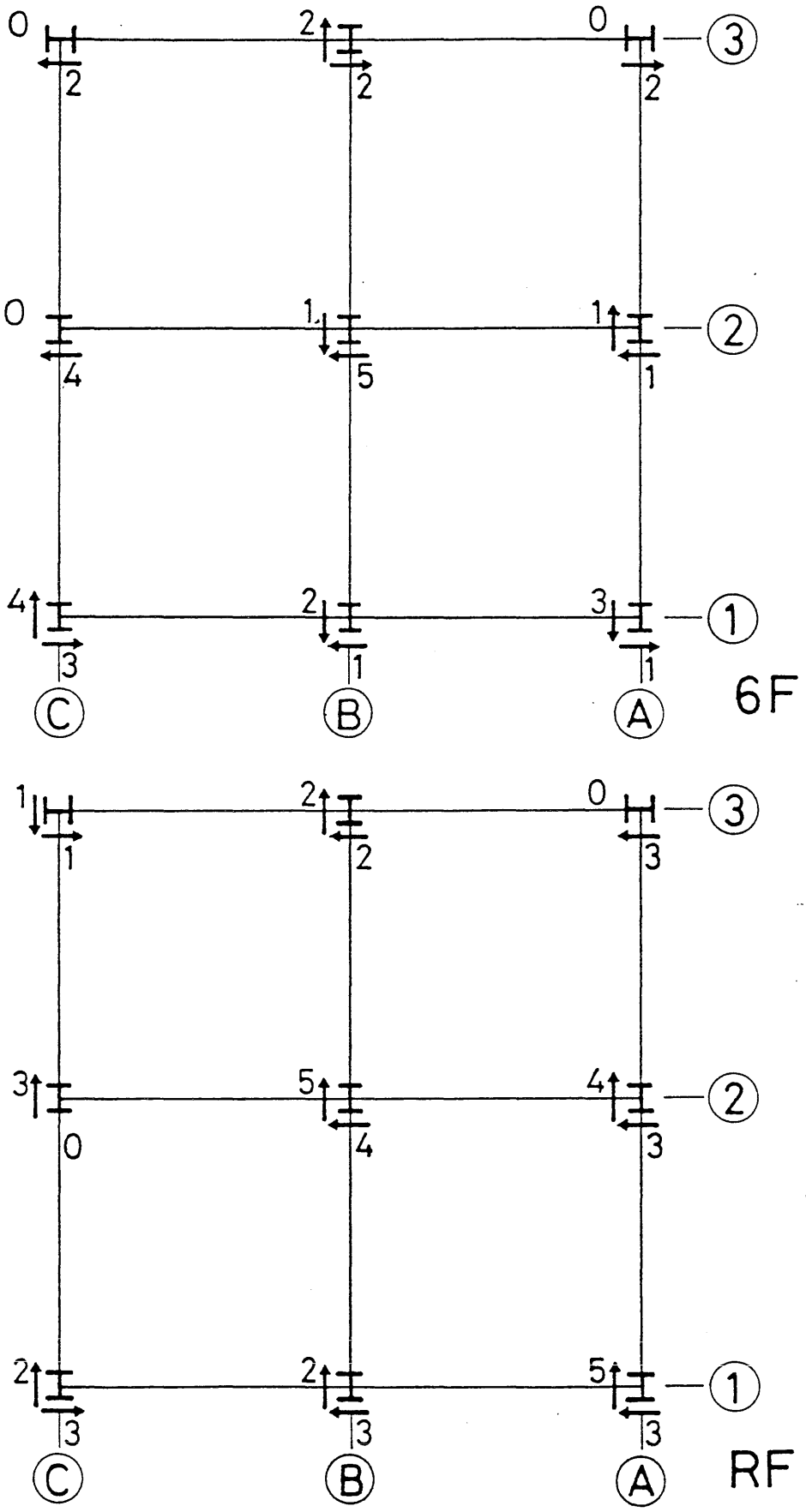

Fig. 2.16 Departures from vertical for the columns at the Z6 and ZF levels

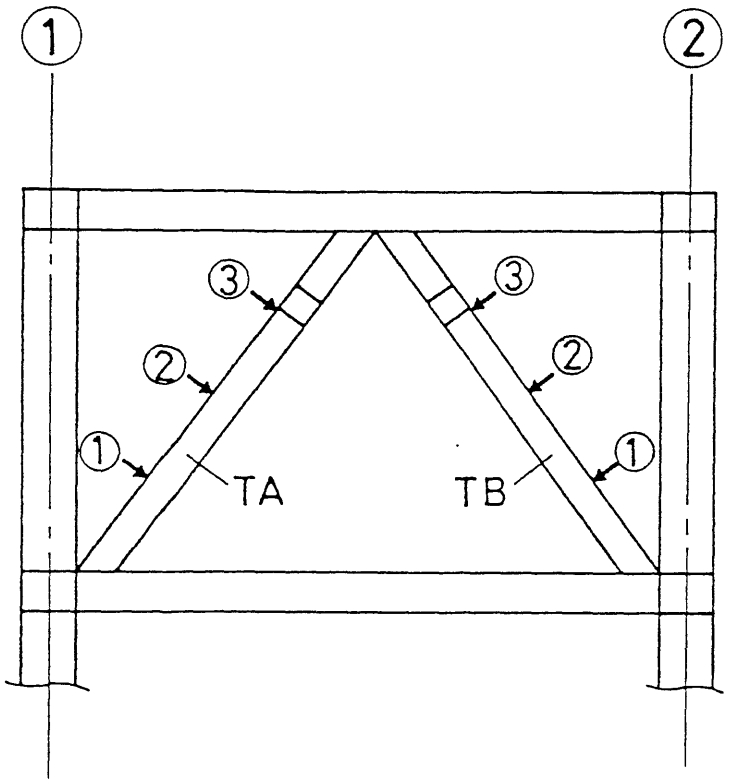

X direction, out of plane of B frame, positive towards A frame.

Y direction, in plane of B frame, positive upward

		X direction			Y direction		
		①	②	③	①	②	③
ZR ~ Z6	TA	+4	+4	+3	0	0	-1
	TB	0	0	0	-1	-3	-2
Z6 ~ Z5	TA	+2	+3	+2	0	0	-1
	TB	-6	-6	-5	-2	0	0
Z5 ~ Z4	TA	-1	-1	-3	+1	+3	+4
	TB	1	0	+2	0	0	0
Z4 ~ Z3	TA	+2	+2	+2	+2	+2	0
	TB	0	0	+1	-8	-3	+1
Z3 ~ Z2	TA	-1	-4	-6	+1	+2	+3
	TB	0	+1	+2	-1	0	-1
Z2 ~ Z1	TA	0	-1	-2	+2	+2	+2
	TB	-1	-2	-2	+7	+9	+7

Fig. 2.17 Departures from a straight line for the concentric braces of Frame B

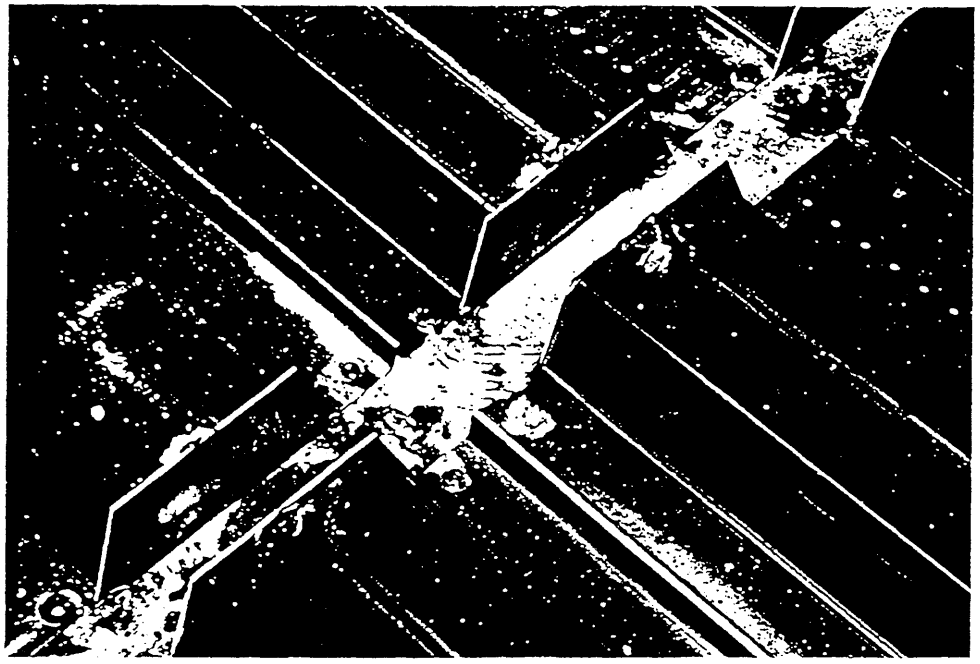

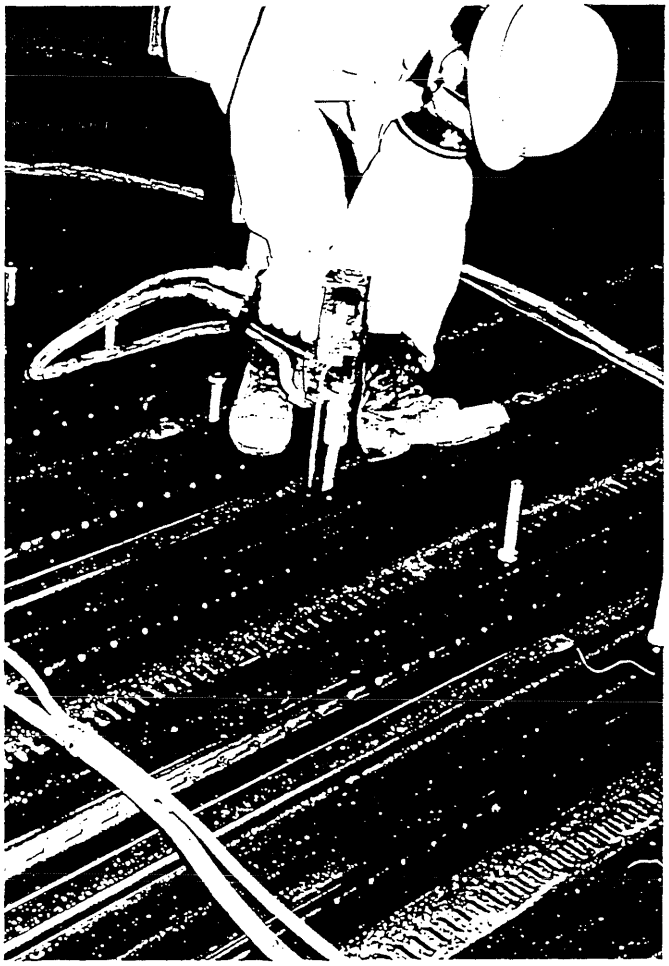

Fig. 2.18 Installation of metal deck and steel shear studs

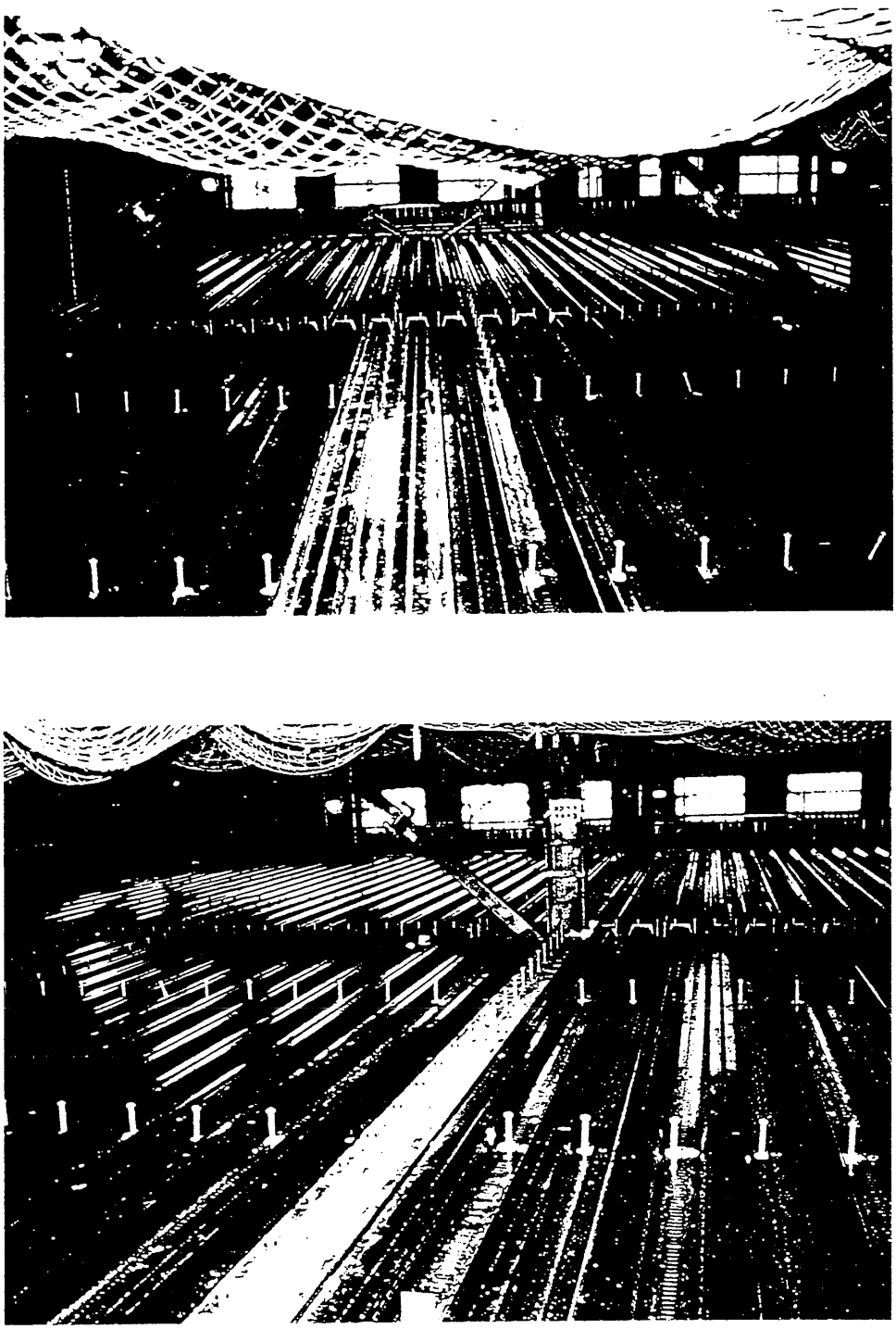

Fig. 2.19 Metal floor deck and studs after installation was completed

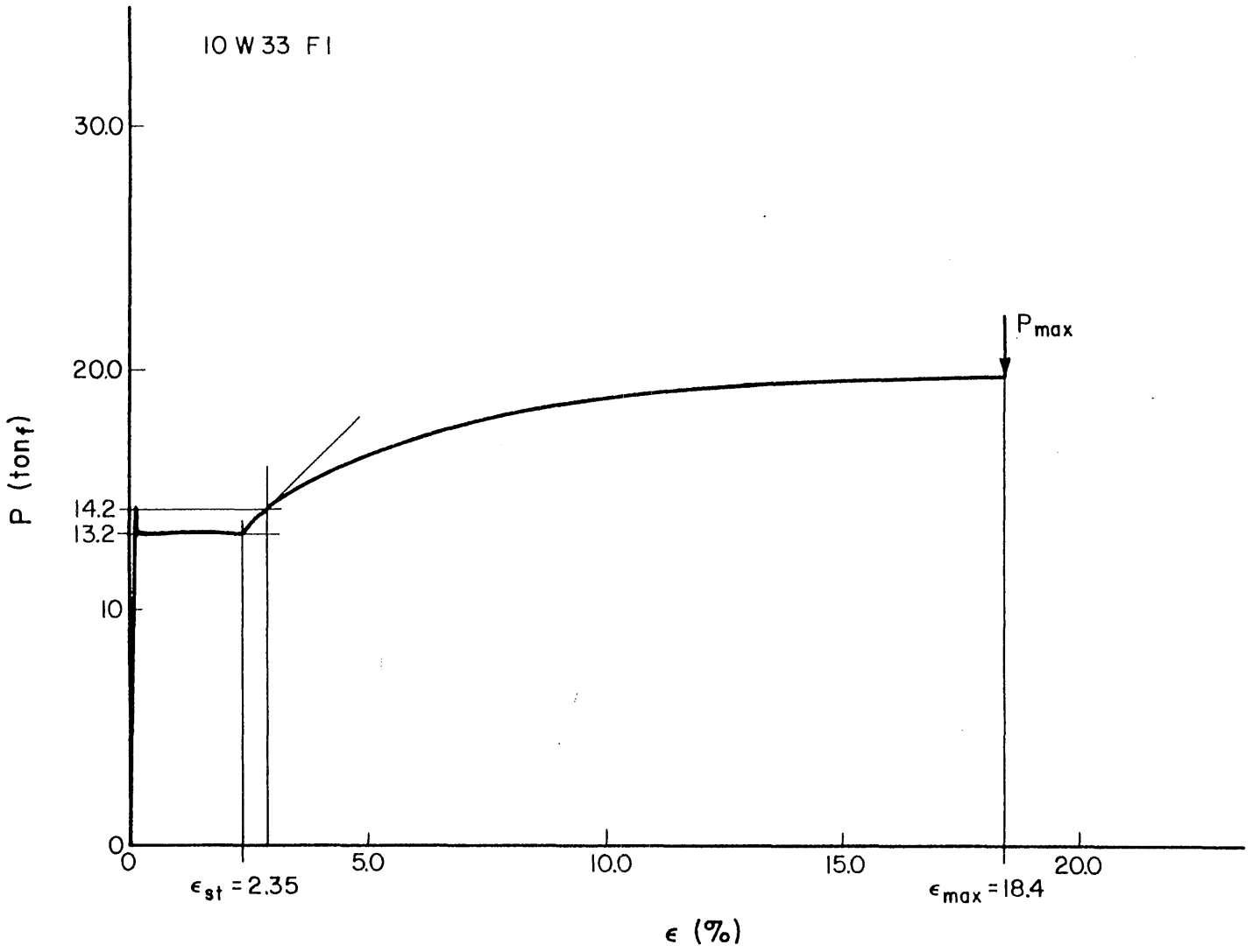

Fig. 2.20 Typical stress vs. strain curves for material from W shapes used in the test structure

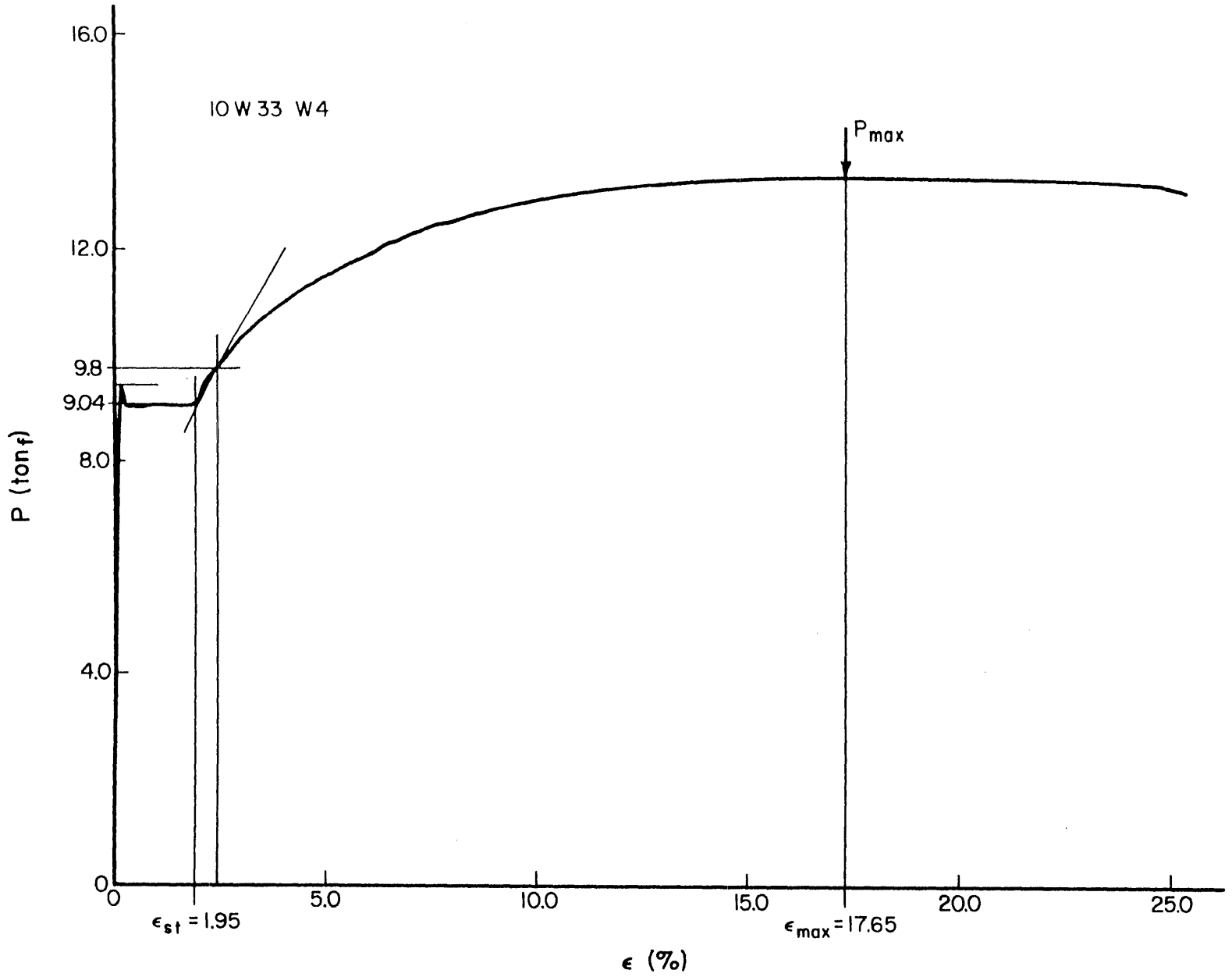

Fig. 2.21 Typical stress vs. strain curves for material from W shapes used in the test structure

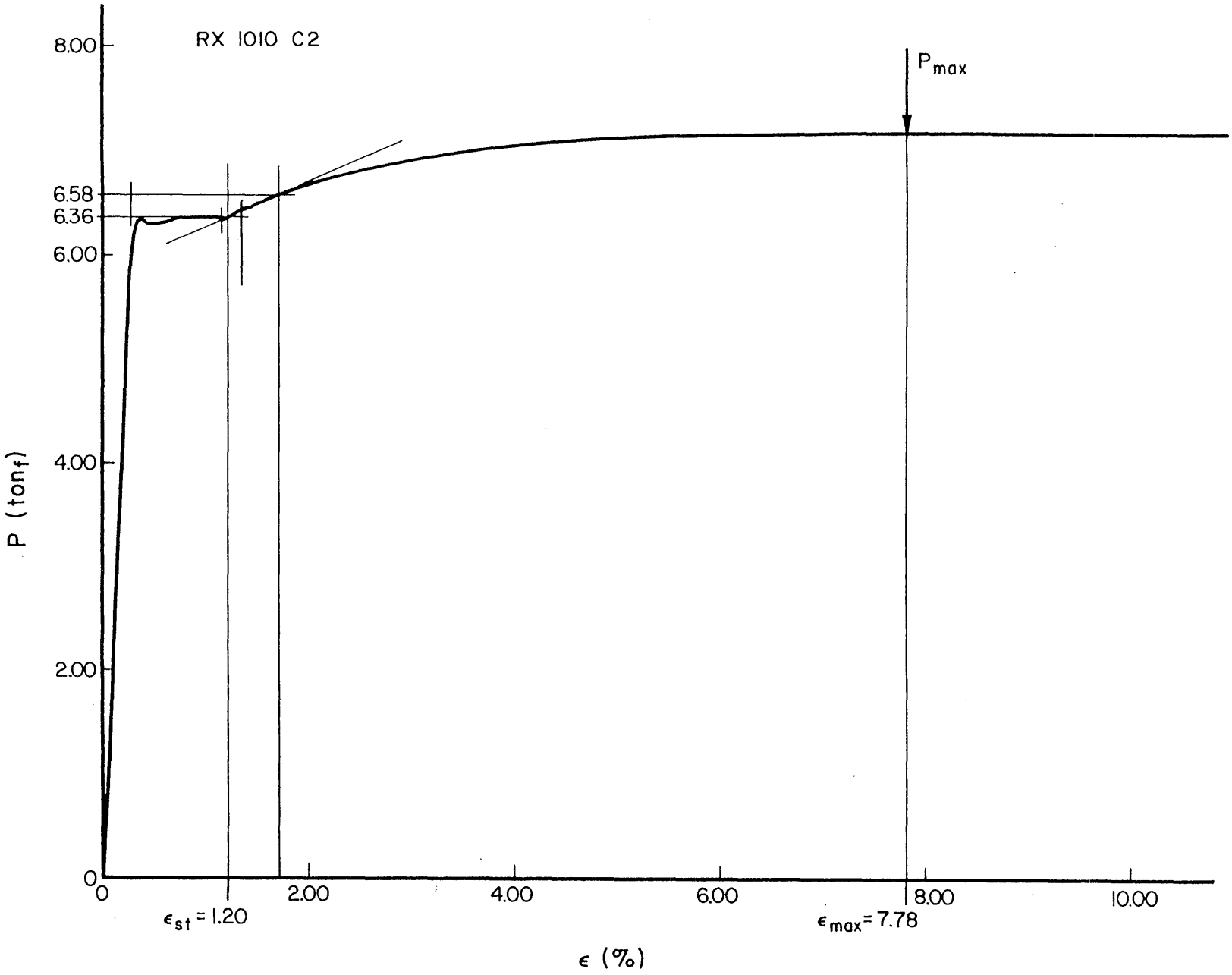

Fig. 2.22 Typical stress vs. strain for material from the concentric braces used in Frame B of the test structure

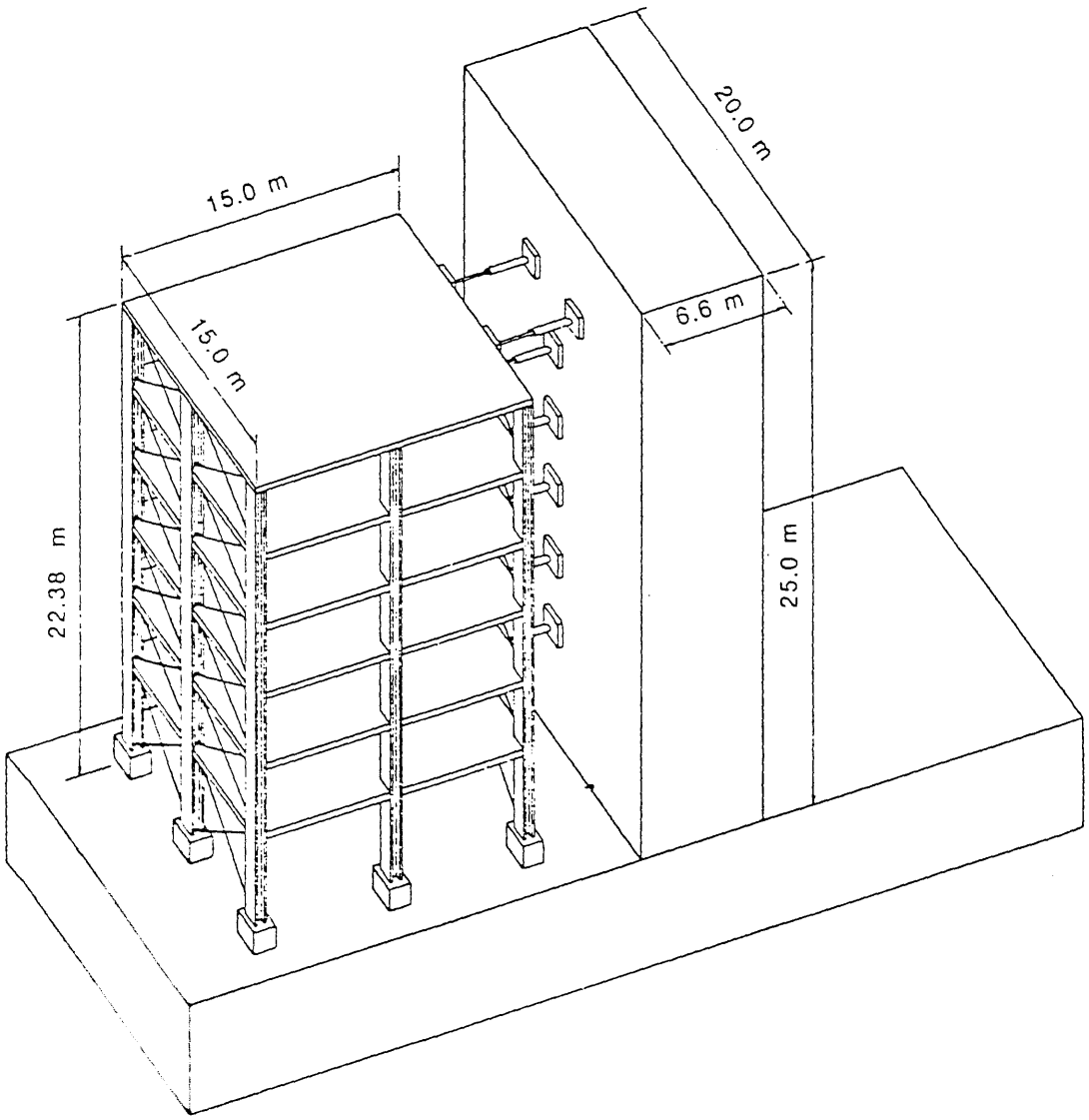

Fig. 3.1 Schematic of test specimen standing next to reaction wall (from Ref. 12)

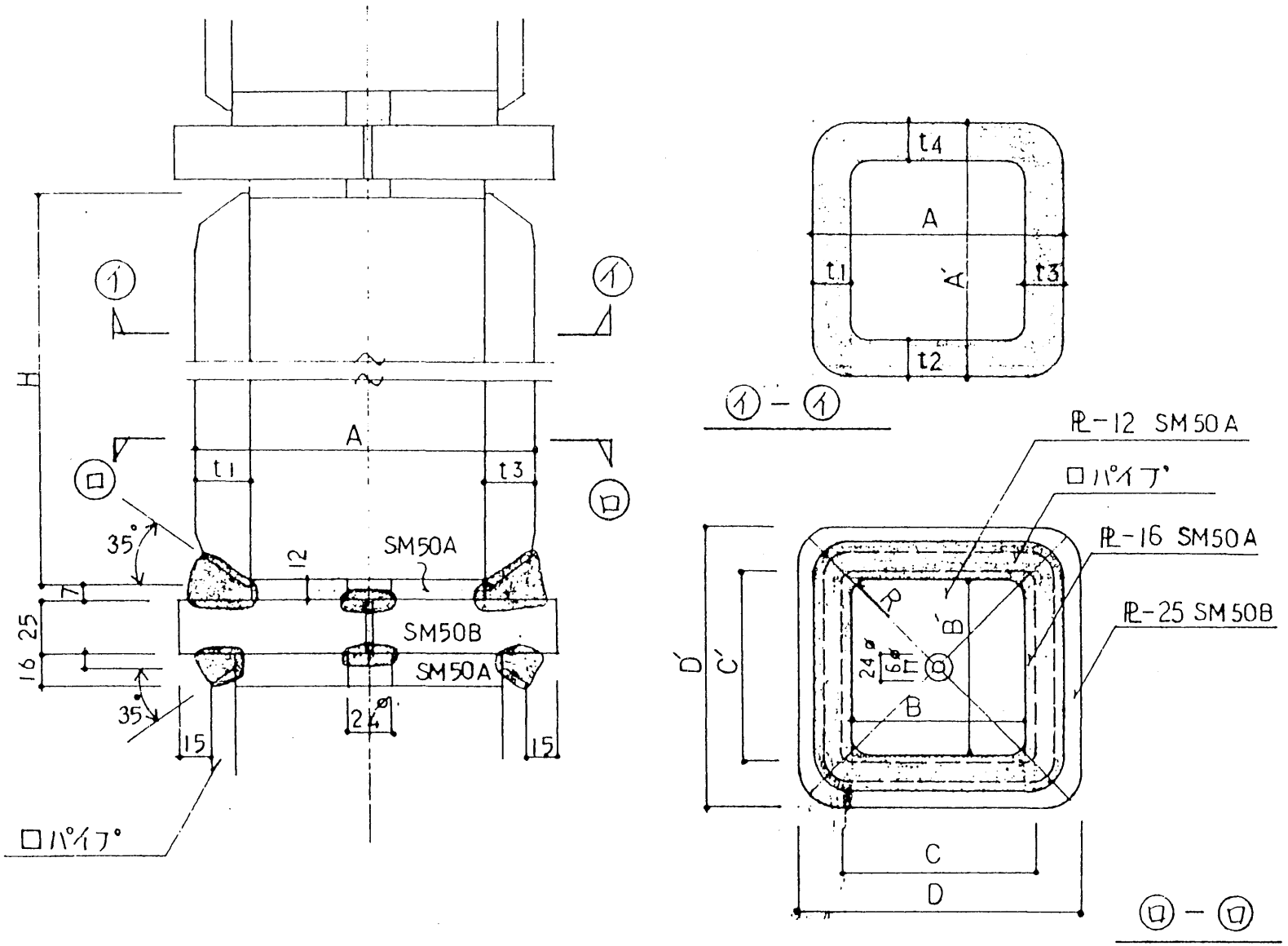

Fig. 3.2 Detail of load cell mounted within each brace in the Phase I structure--dimensions given in Table 3.1

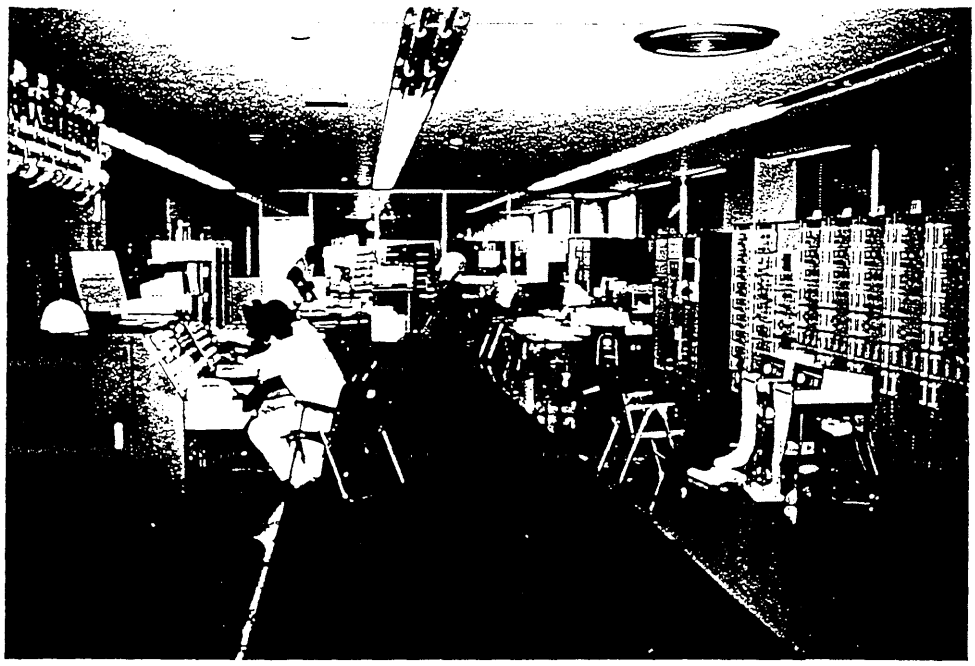

Fig. 3.3 Control room of Large Size Structure Laboratory of BRI

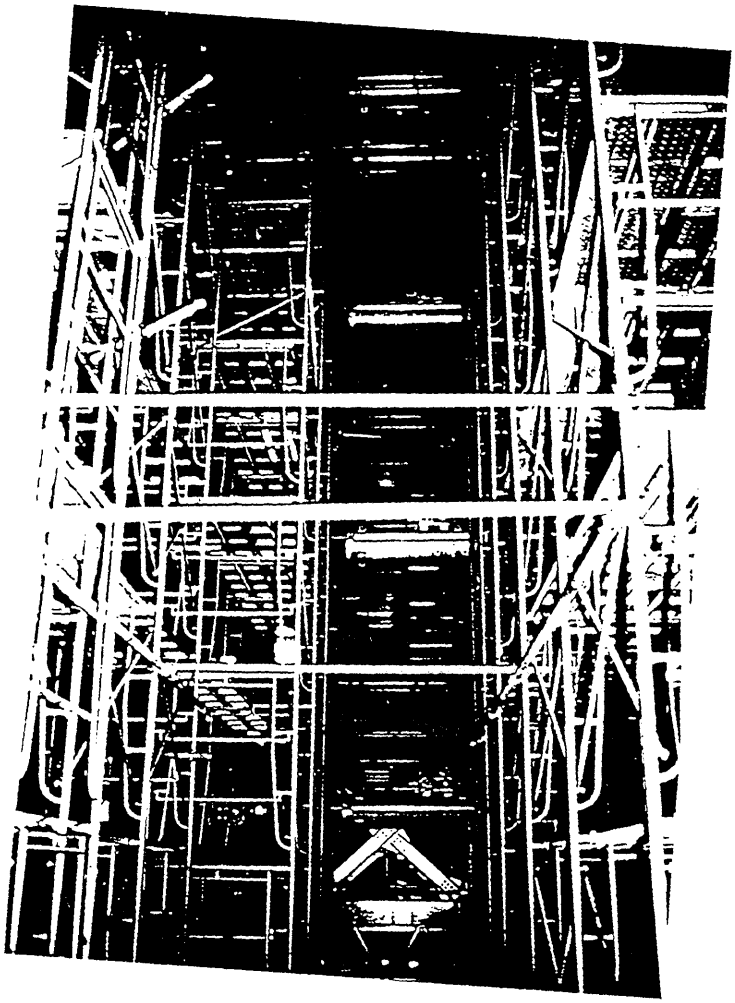

FIG. 3.- Actuators in place with temporary scaffolding on the right and left

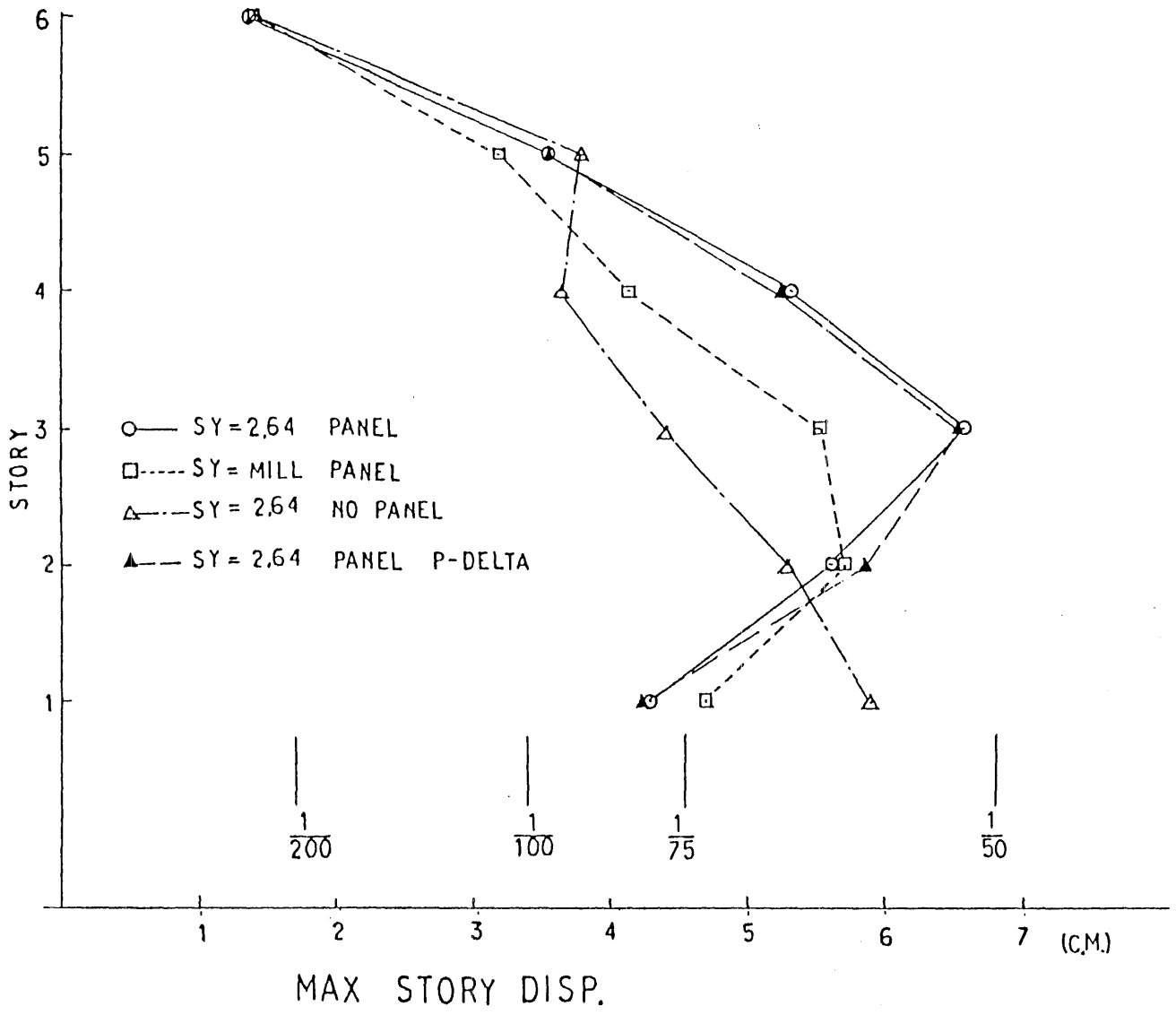

Fig. 4.1 Analytical results from preliminary studies (from Ref. 7)

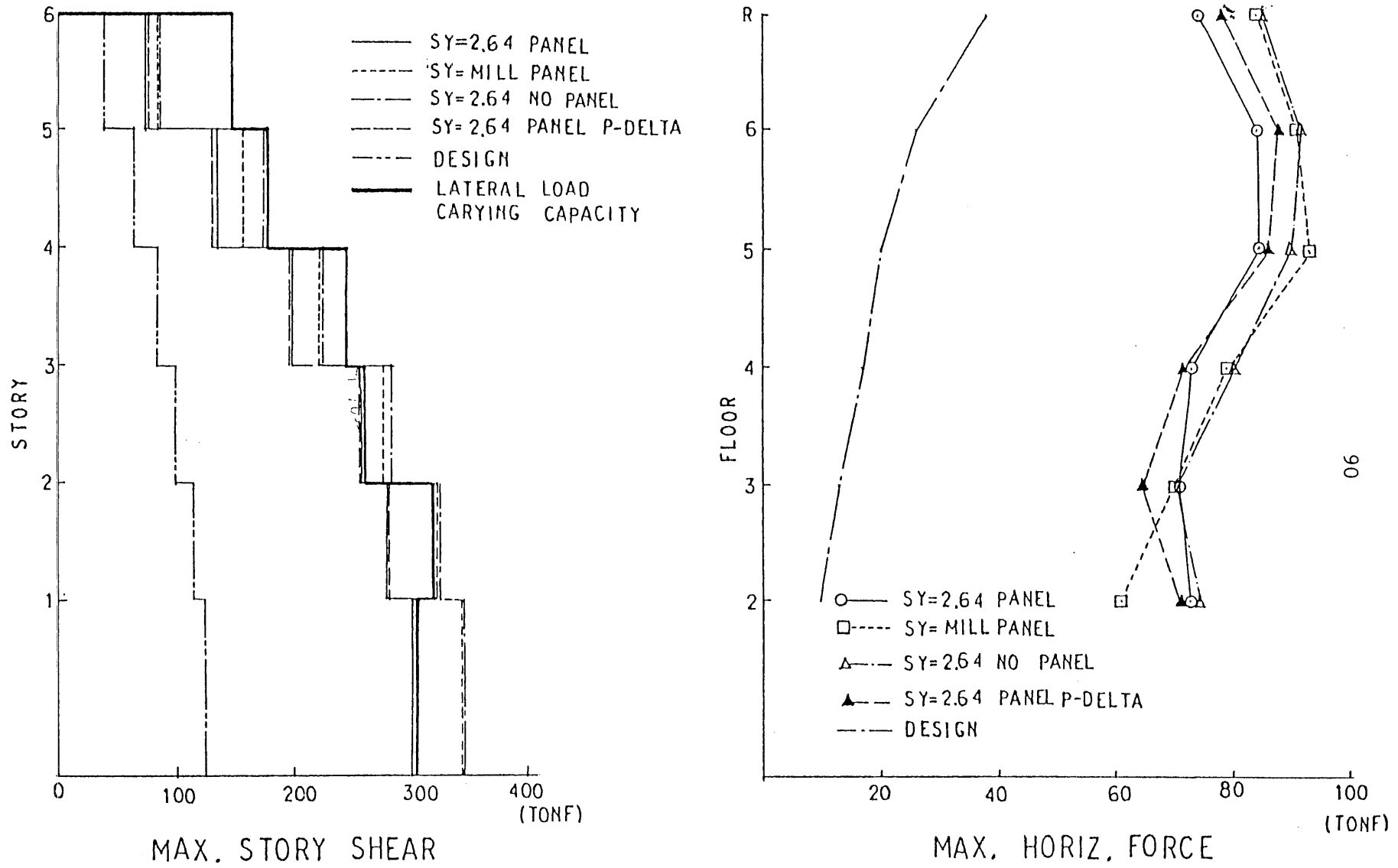

Fig. 4.2 Analytical results from preliminary studies (from Ref. 7)

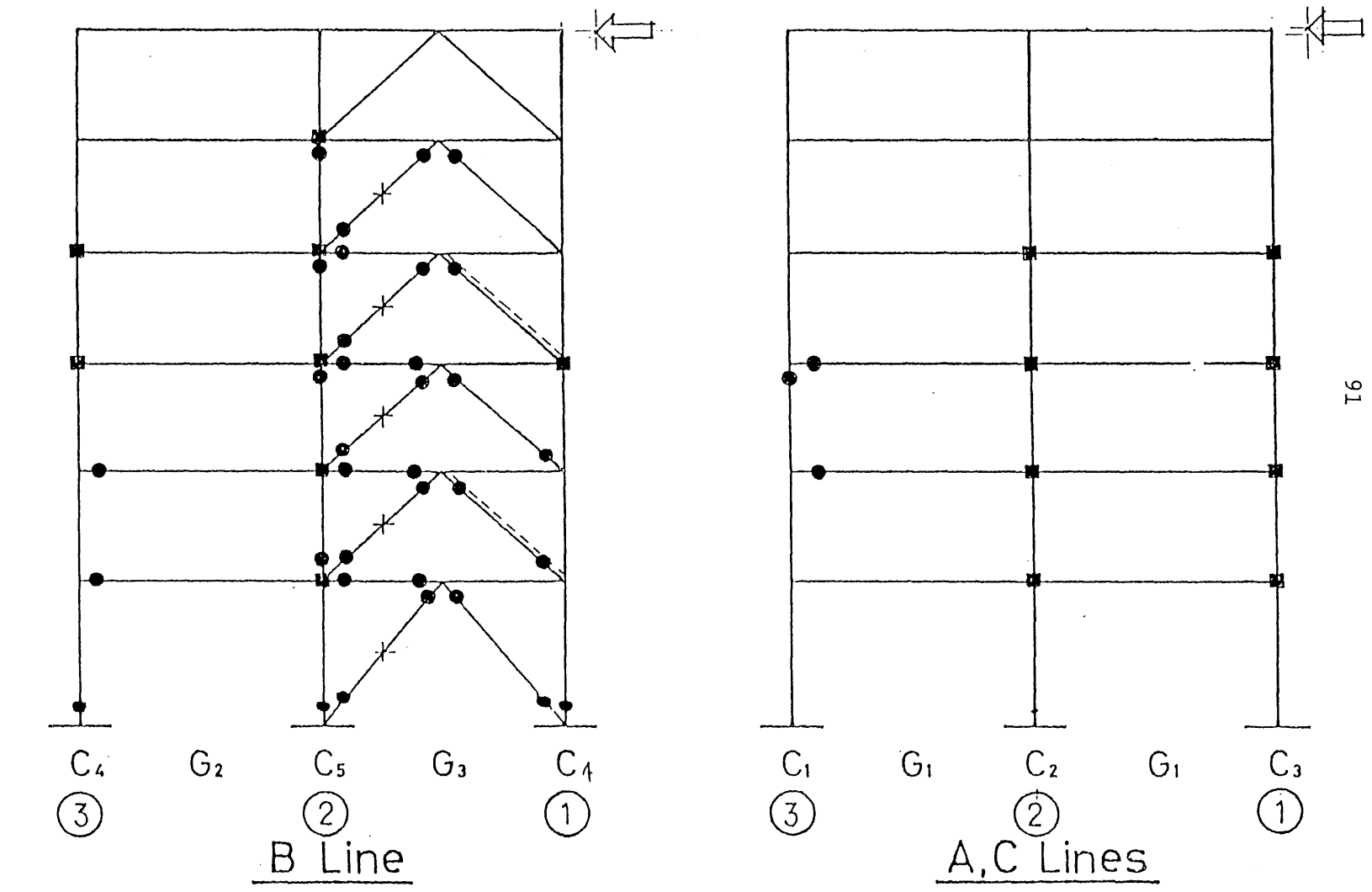

Fig. 4.3 Analytical results from preliminary studies (from Ref. 7)

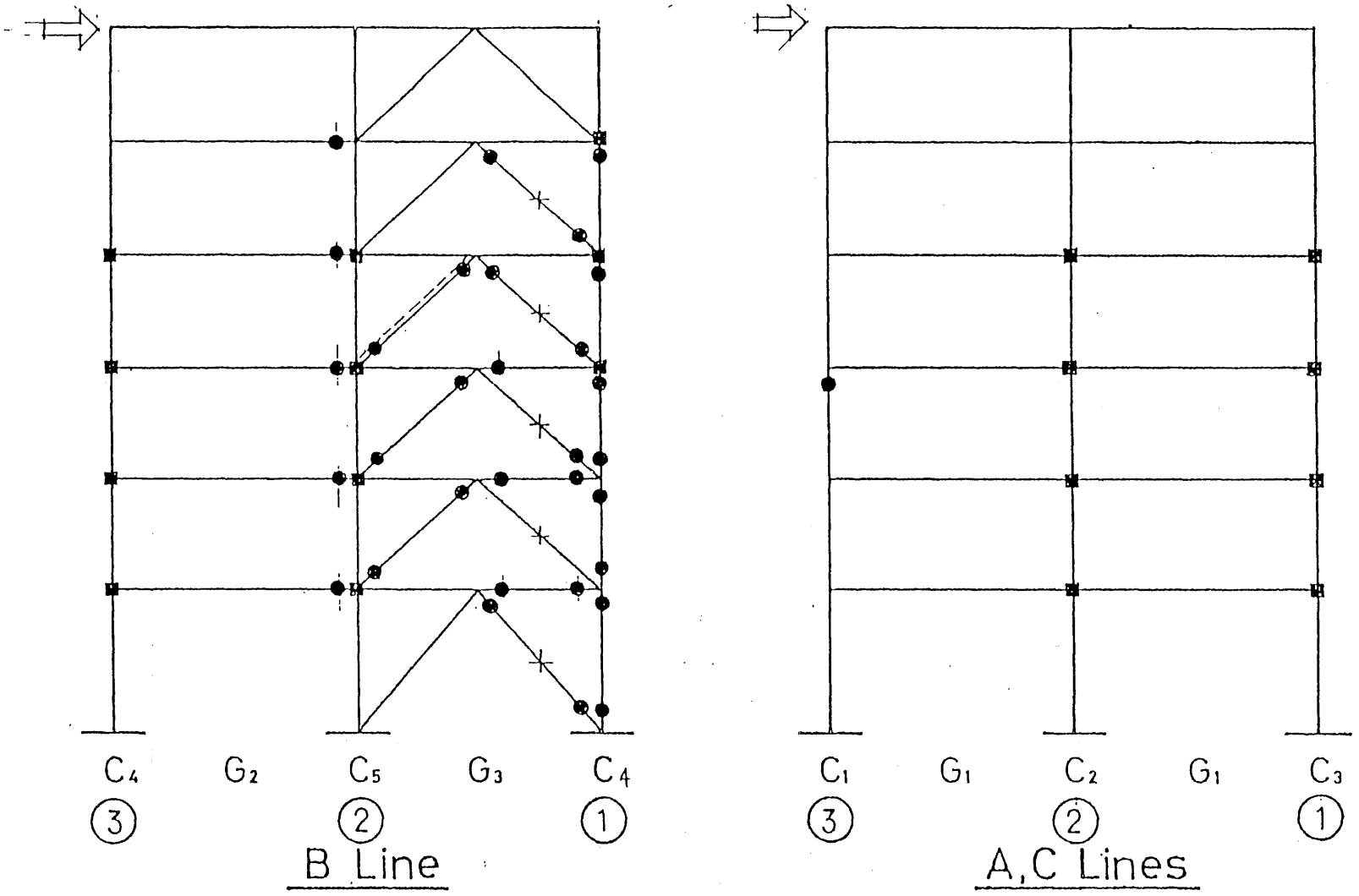

Fig. 4.4 Analytical results from preliminary studies (from Ref. 7)

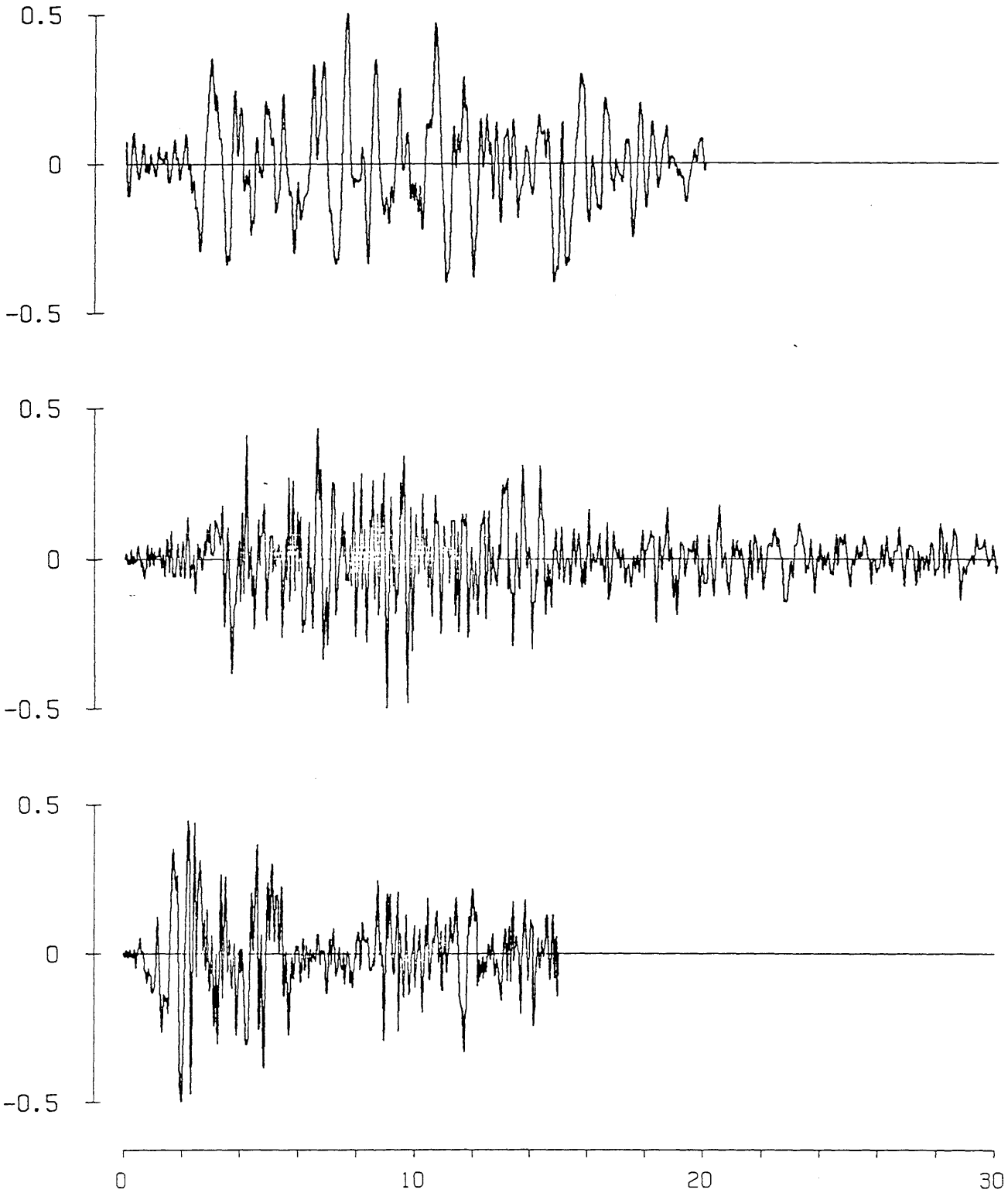

Fig. 4.5 (a) Miyagi-ken Oki accelerogram used in Phase I
(b) Taft accelerogram used in Phase II
(c) El Centro accelerogram used in Phase III

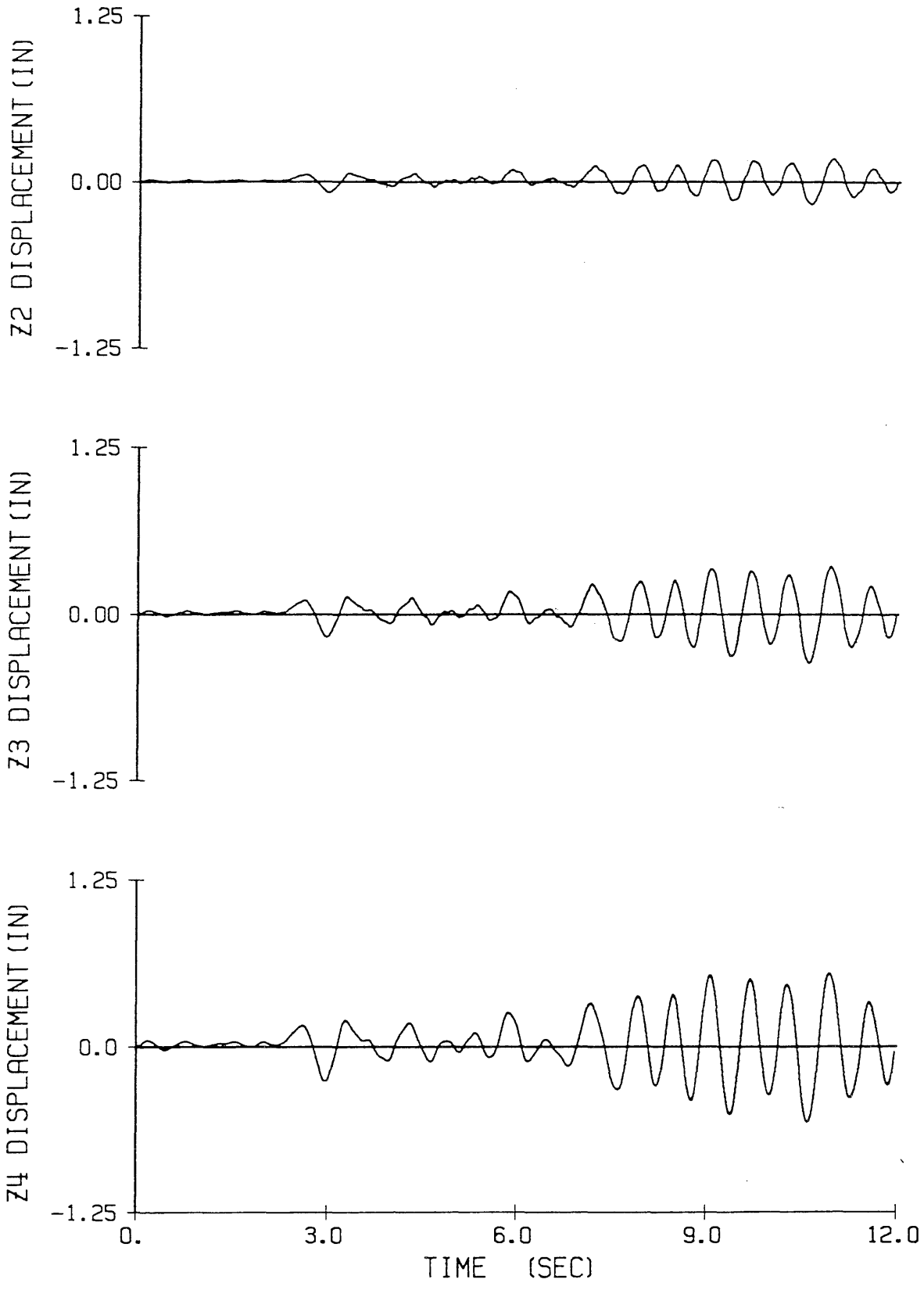

Fig. 4.6 Floor displacements vs. time for the Phase I Elastic test

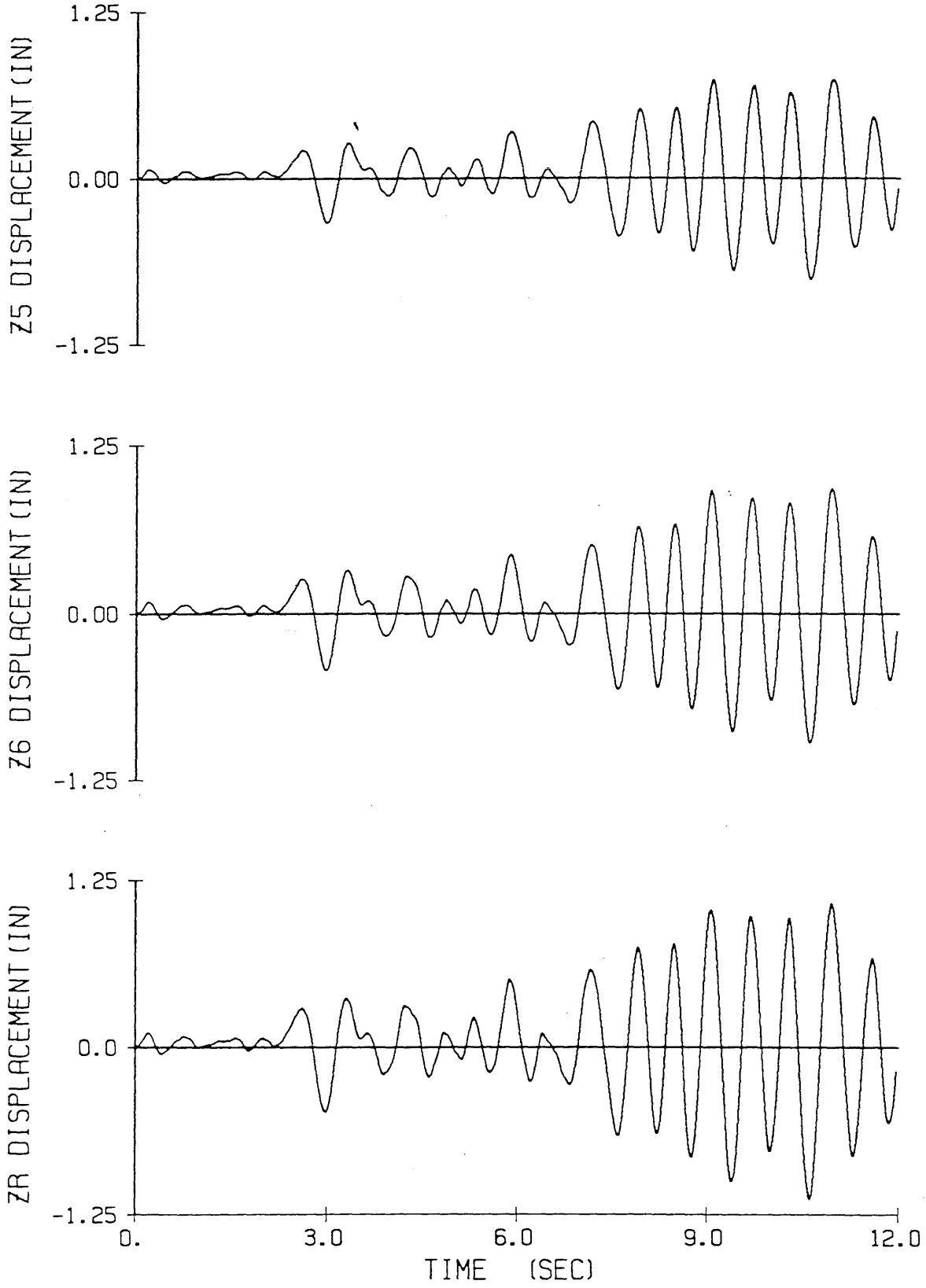

Fig. 4.6 (continued)

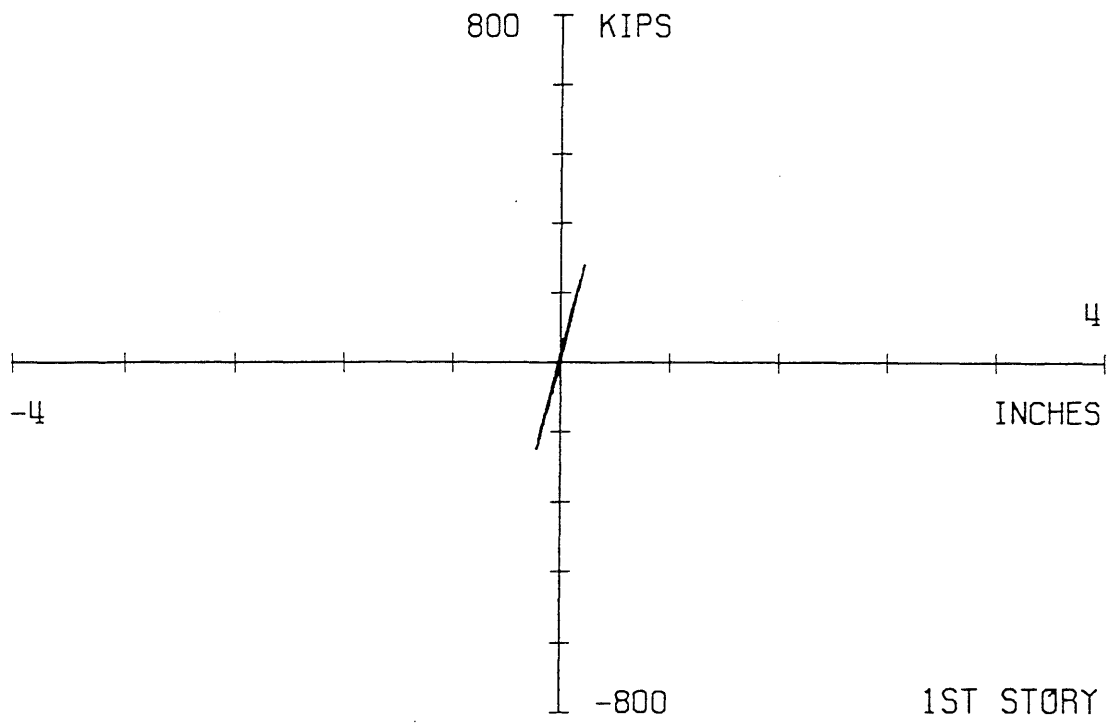

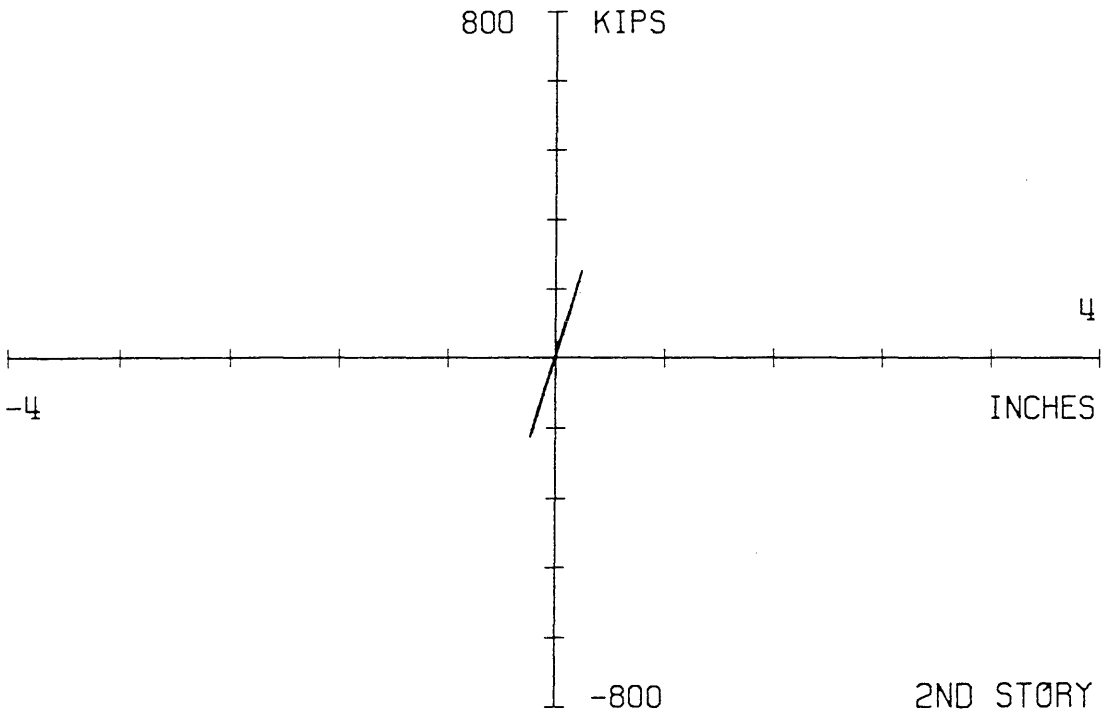

Fig. 4.7 Story shear vs. story displacement for the first and second stories for the Phase I Elastic test

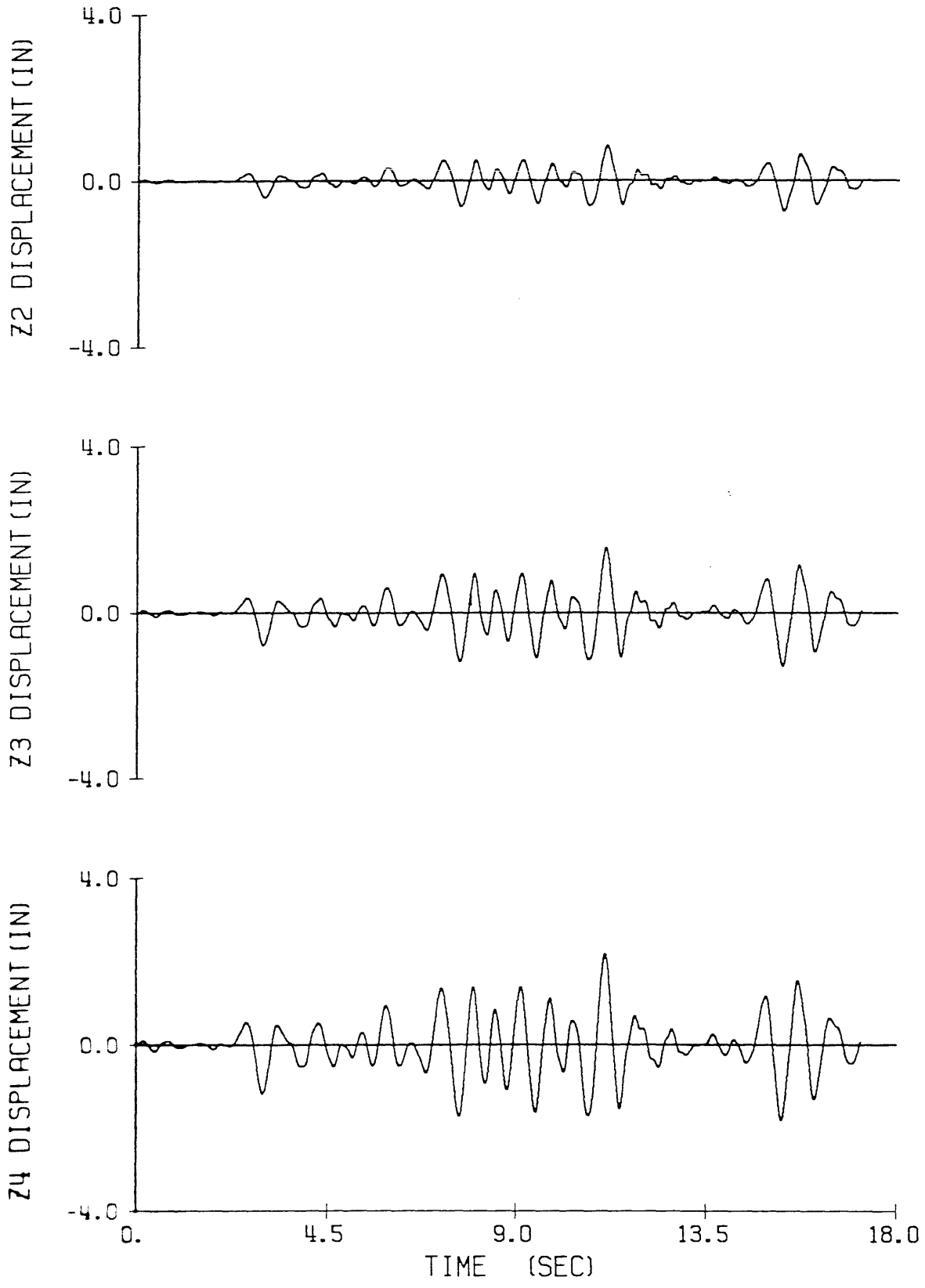

Fig. 4.8 Floor displacements vs. time for the Phase I Moderate test

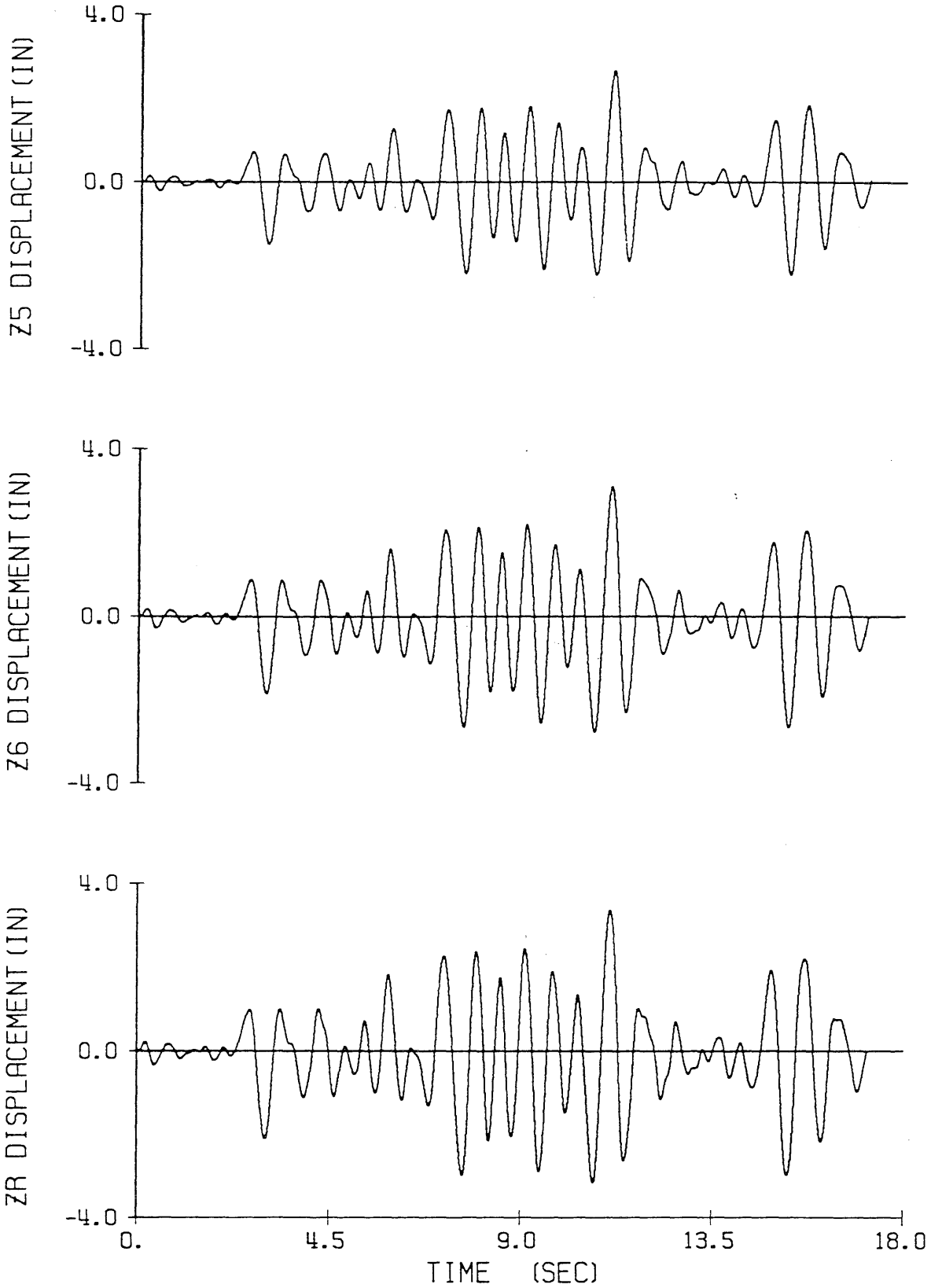

Fig. 4.8 (continued)

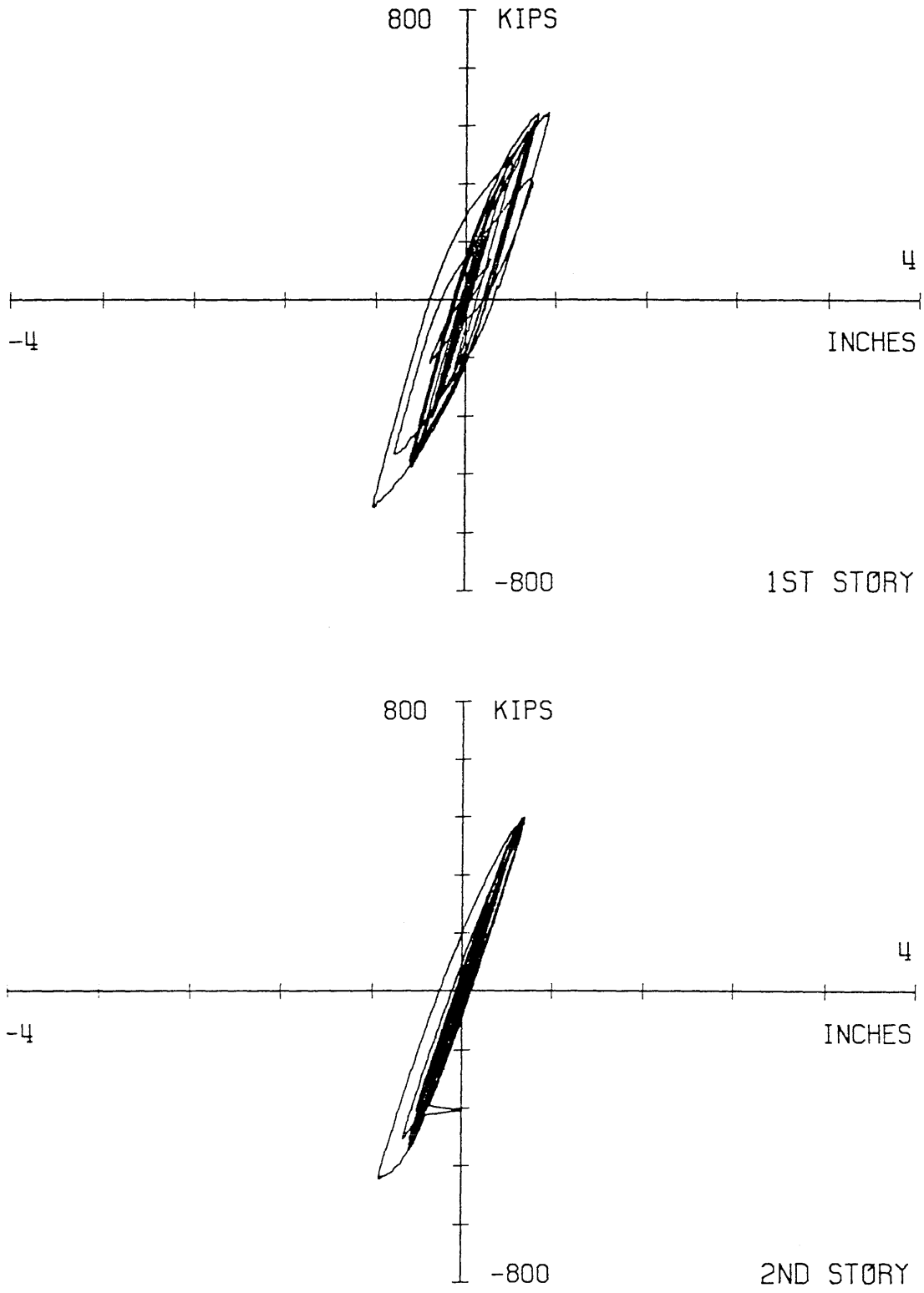

Fig. 4.9 Story shear vs. story displacement for the first and second stories for the Phase I Moderate test

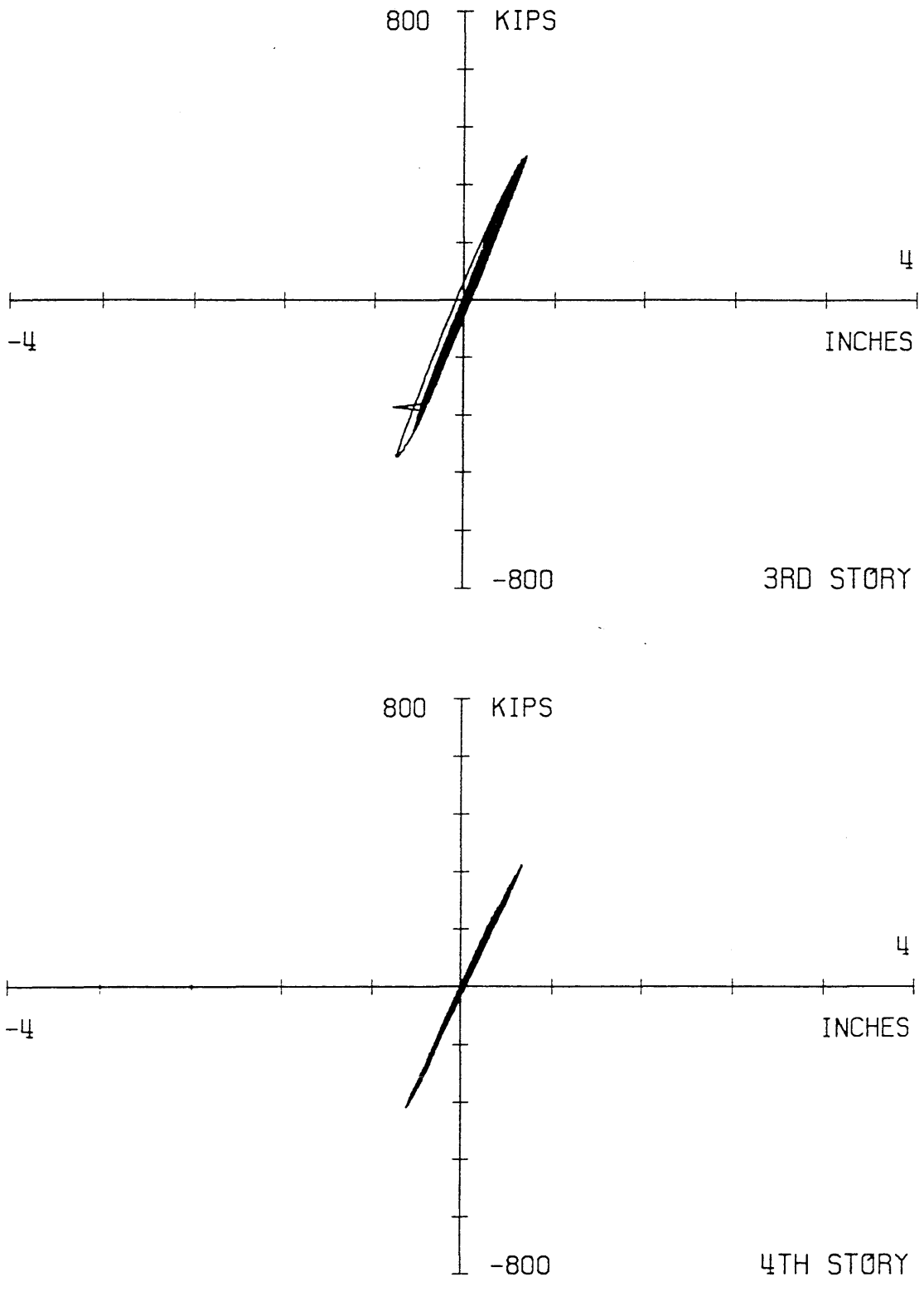

Fig. 4.10 Story shear vs. story displacement for the third and fourth stories for the Phase I Moderate test

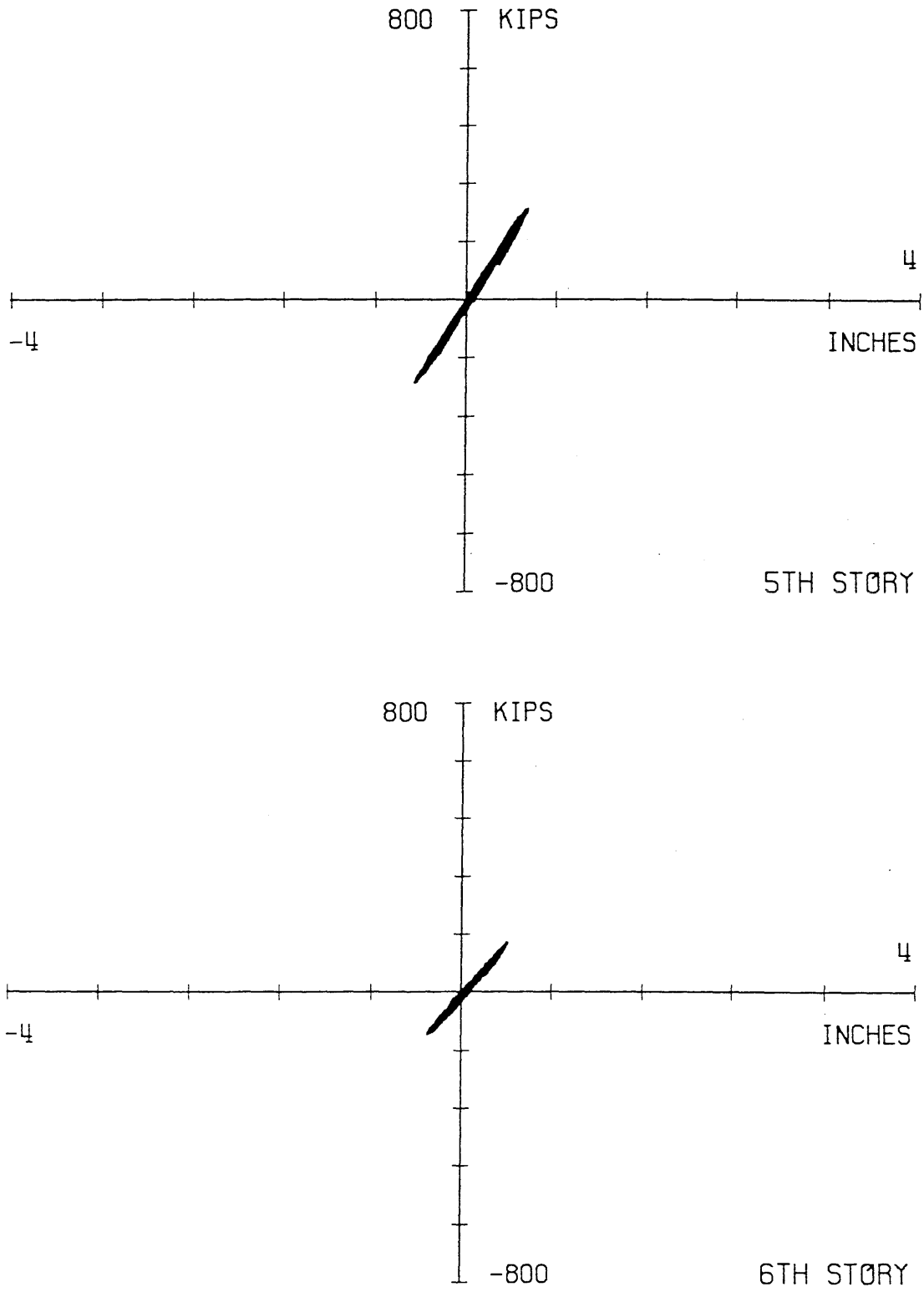

Fig. 4.11 Story shear vs. story displacement for the fifth and sixth stories for the Phase I Moderate test

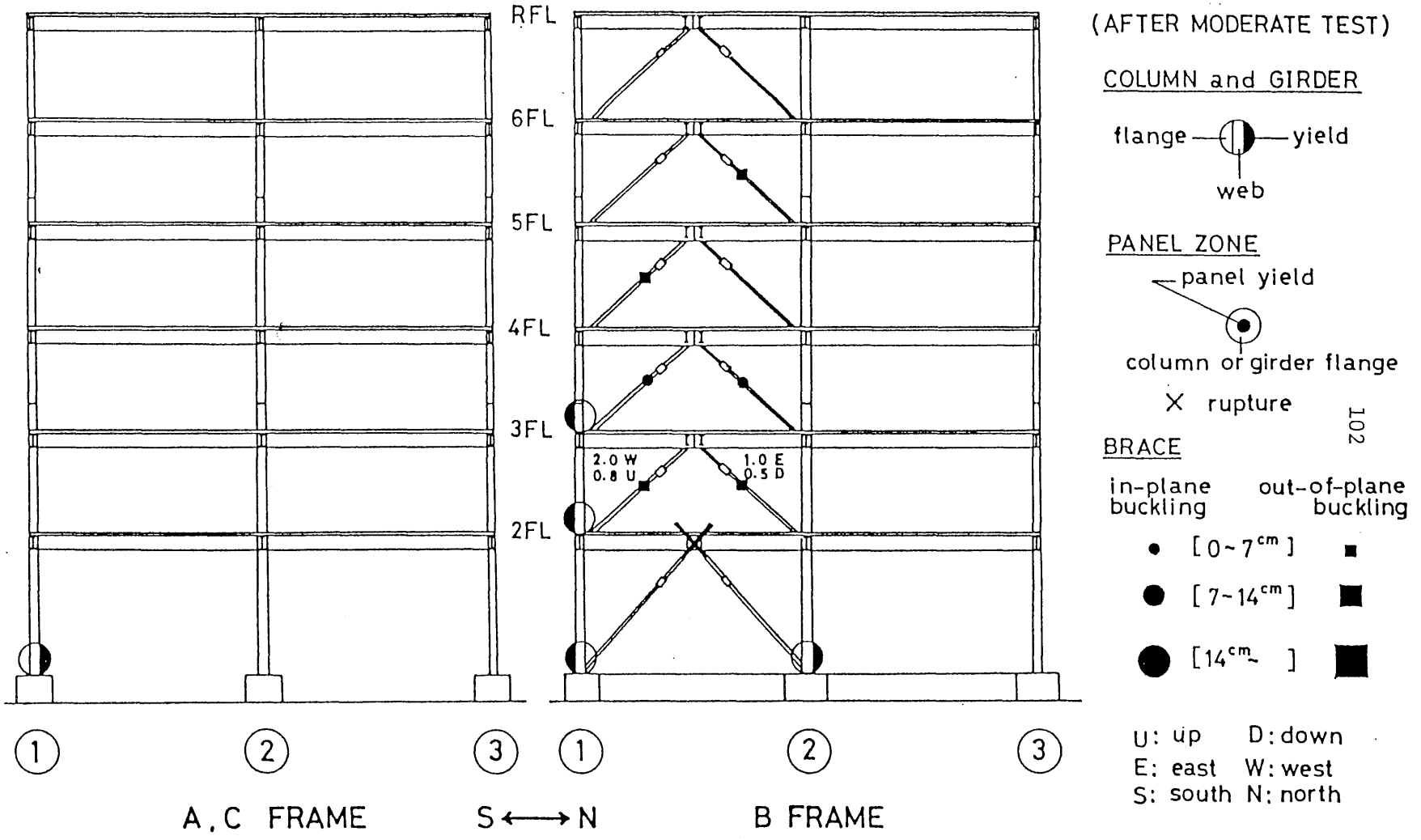

Fig. 4.12 Summary of damage observed after the Phase I Moderate test

Fig. 4.13 Tearing of the connection splice link at the center of the concentric braced bay during the Phase I Moderate test

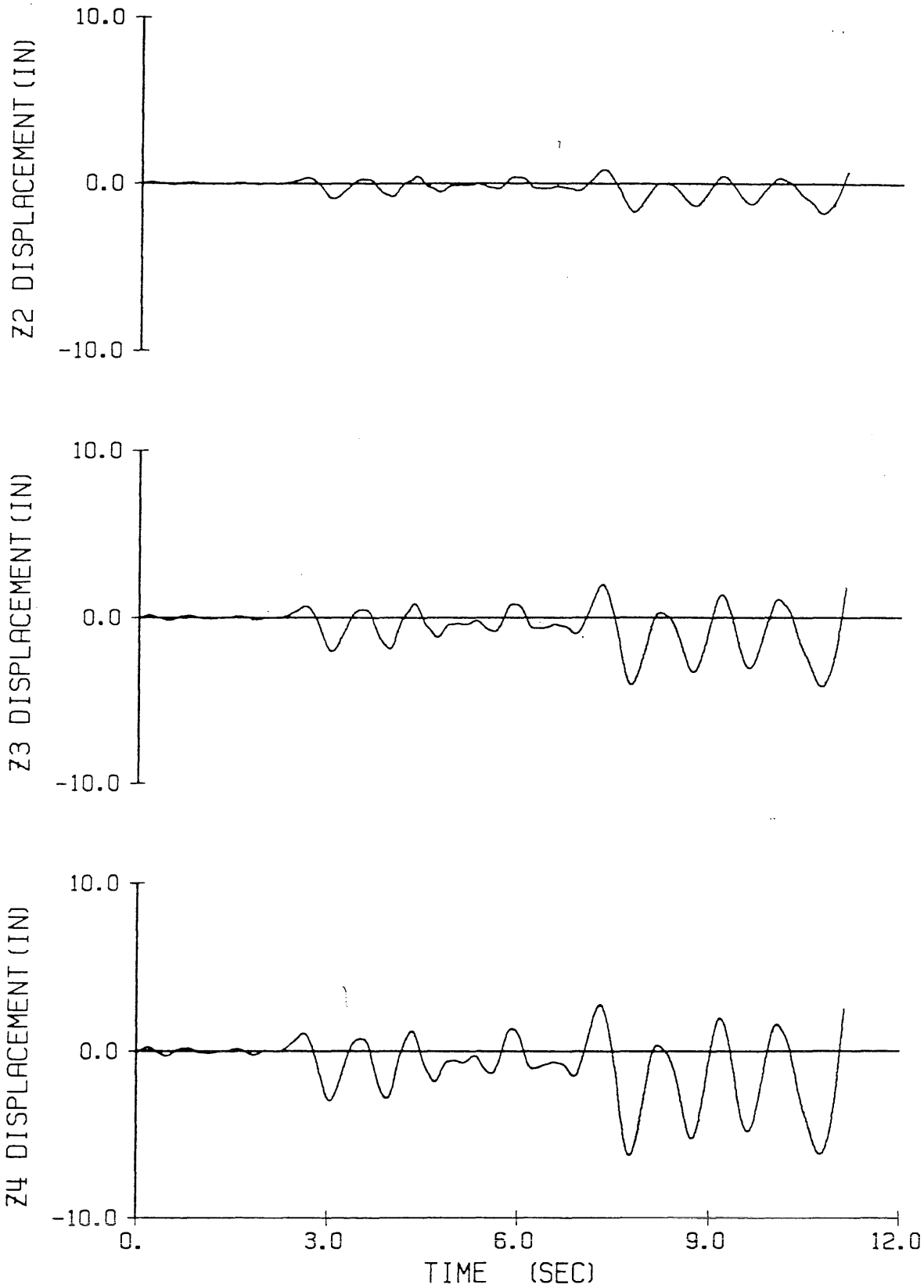

Fig. 4.14 Floor displacements vs. time for the Phase I Final test

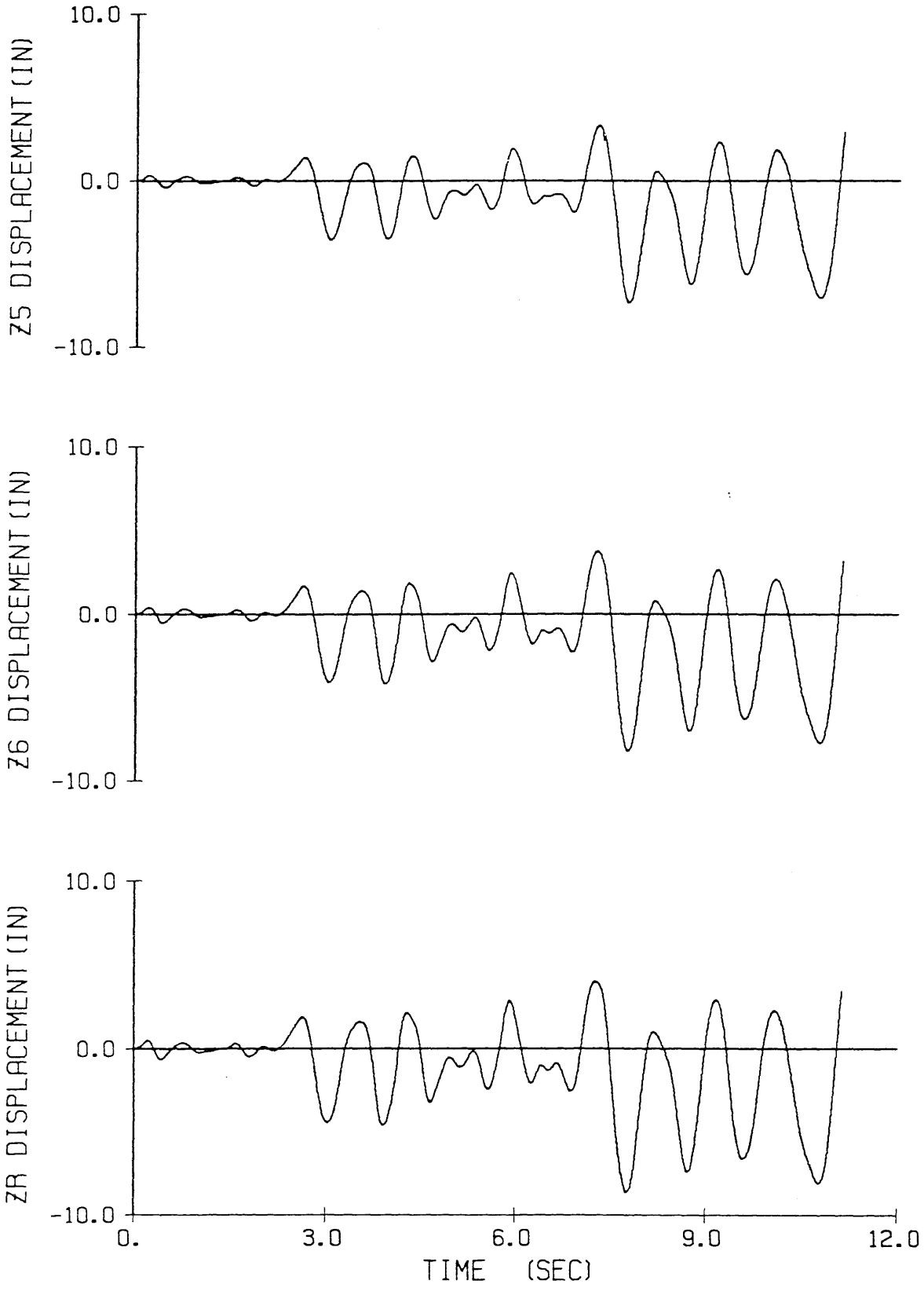

Fig. 4.14 (continued)

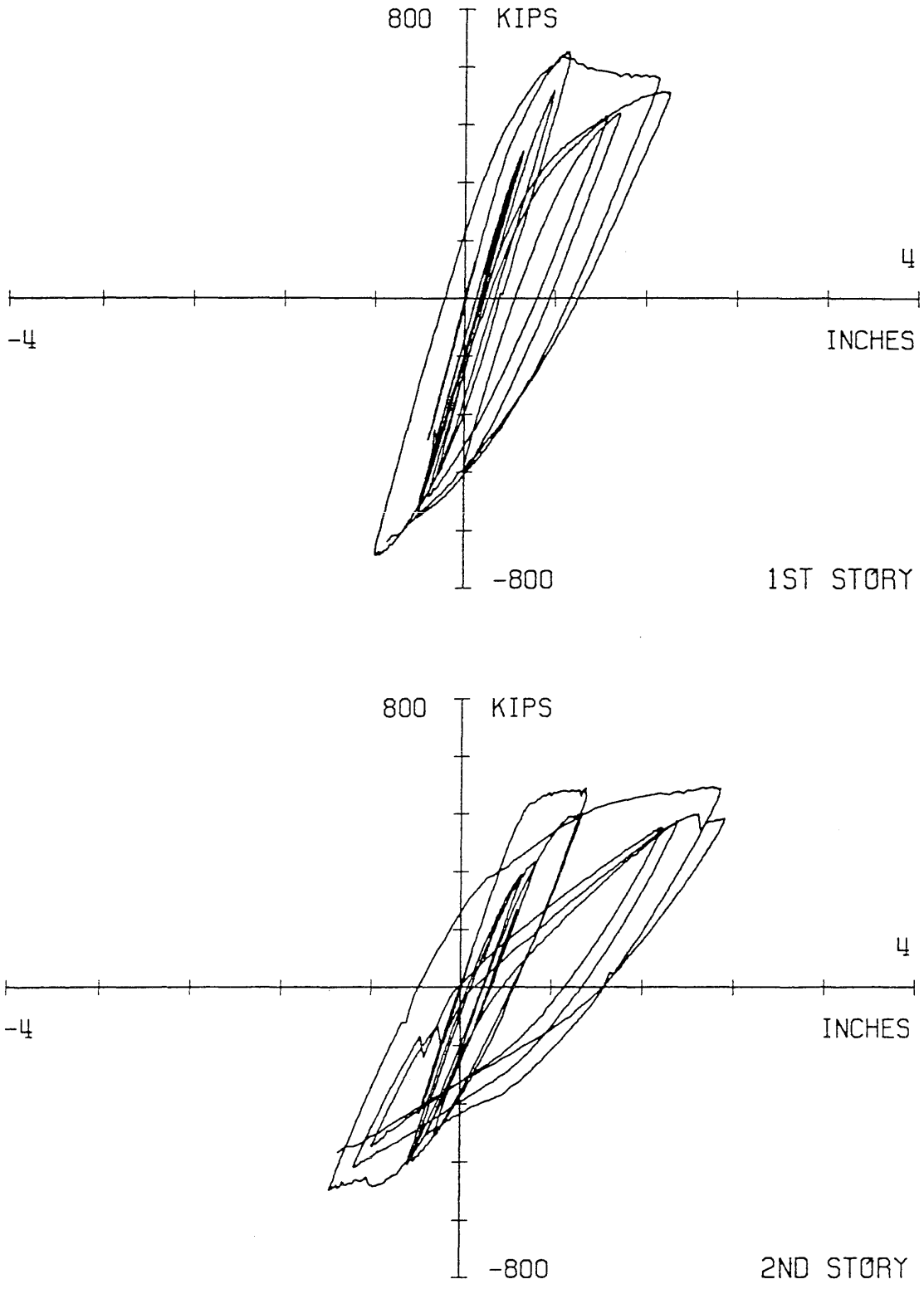

Fig. 4.15 Story shear vs. story displacement for the first and second stories for the Phase I Final test

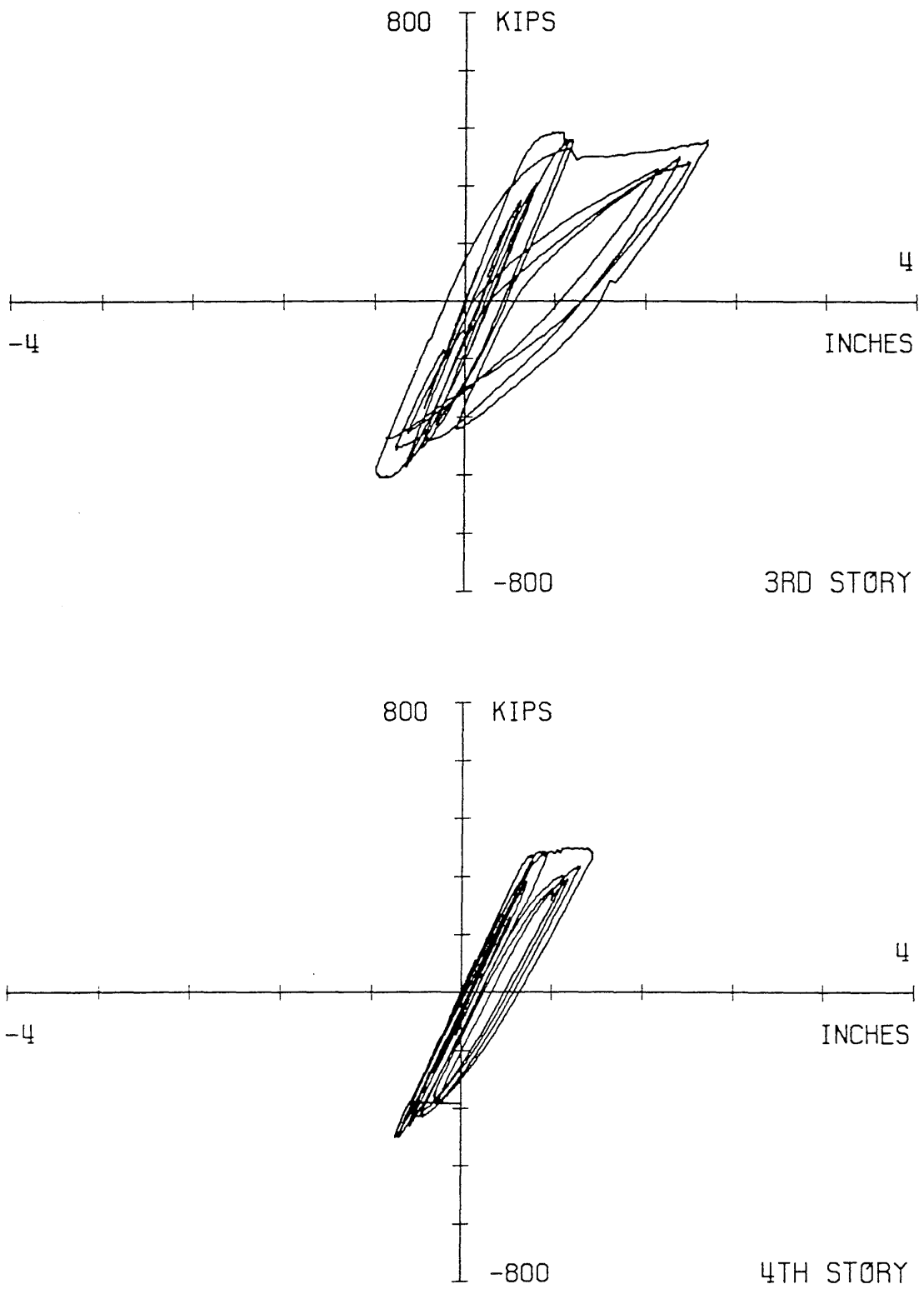

Fig. 4.16 Story shear vs. story displacement for the third and fourth stories for the Phase I Final test

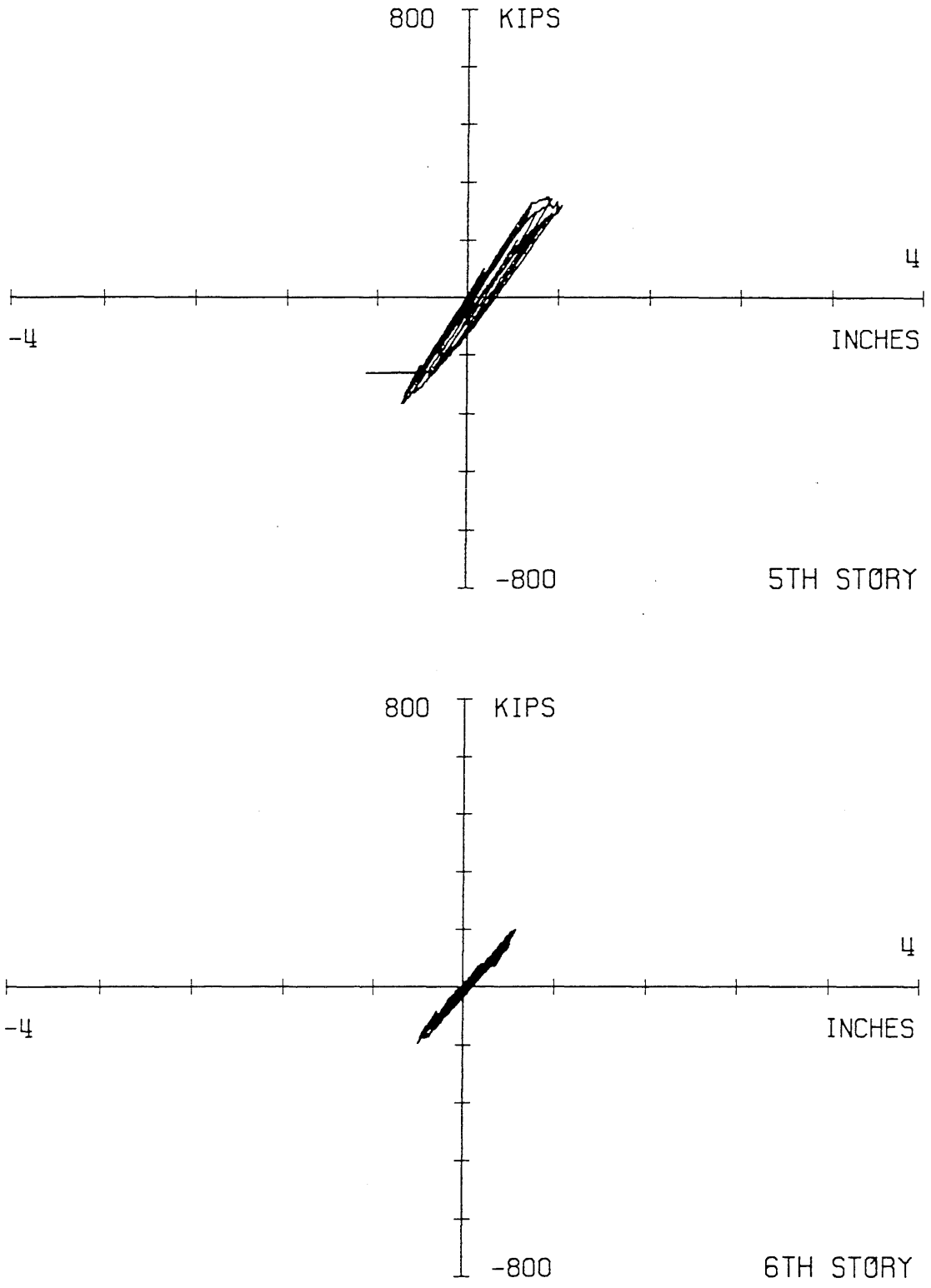

Fig. 4.17 Story shear vs. story displacement for the fifth and sixth stories for the Phase I Final test

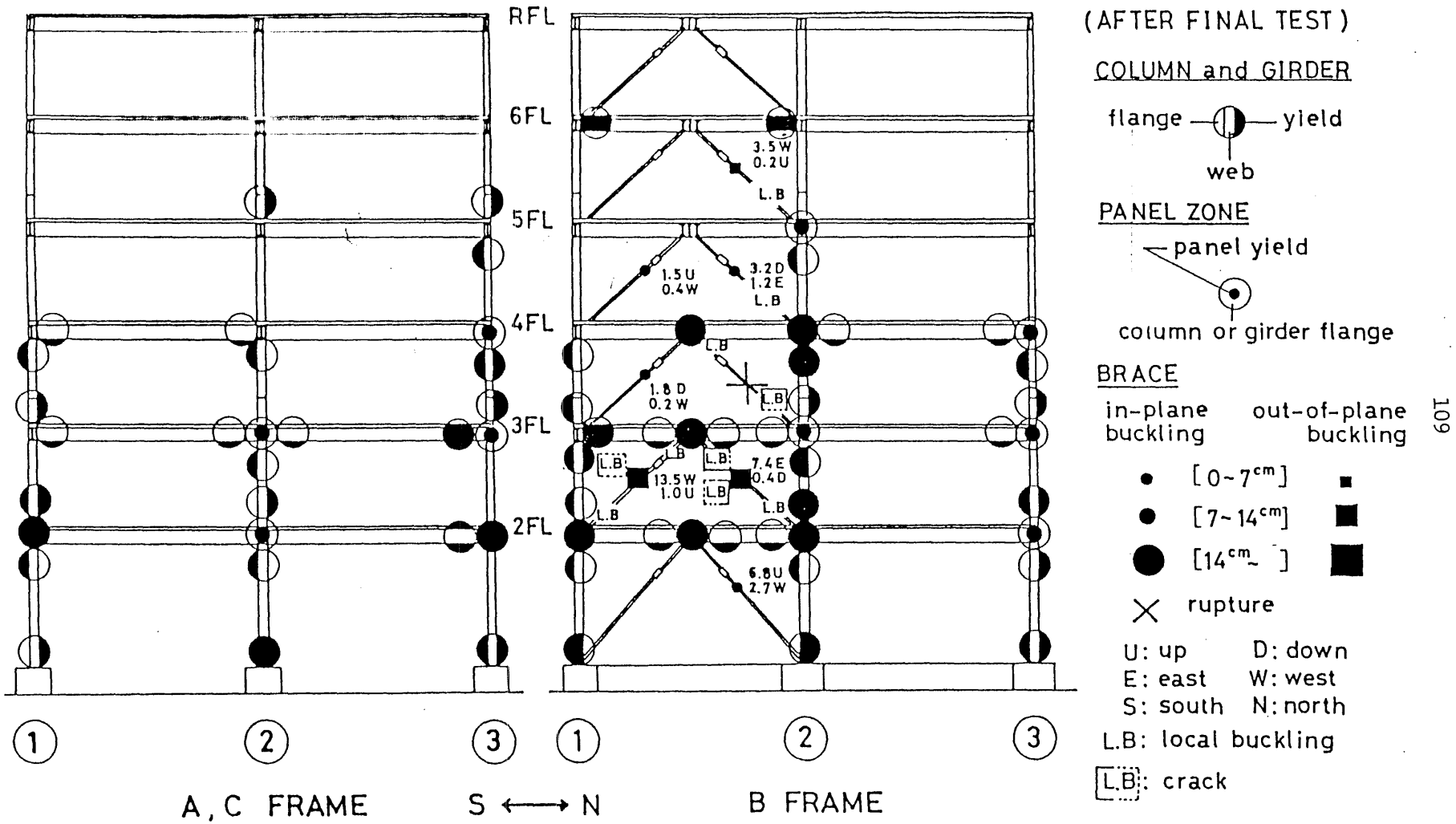

Fig. 4.18 Schematic of damage observed after the Phase I Final test (from Ref. 7)

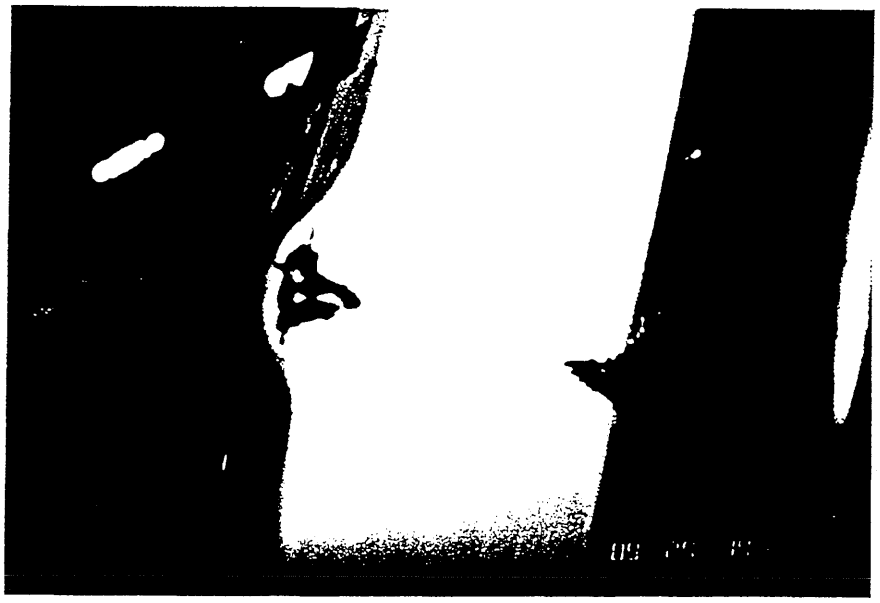

Fig. 4.19 Typical local tears in the braces of the B Frame that occurred during the Phase I Final test

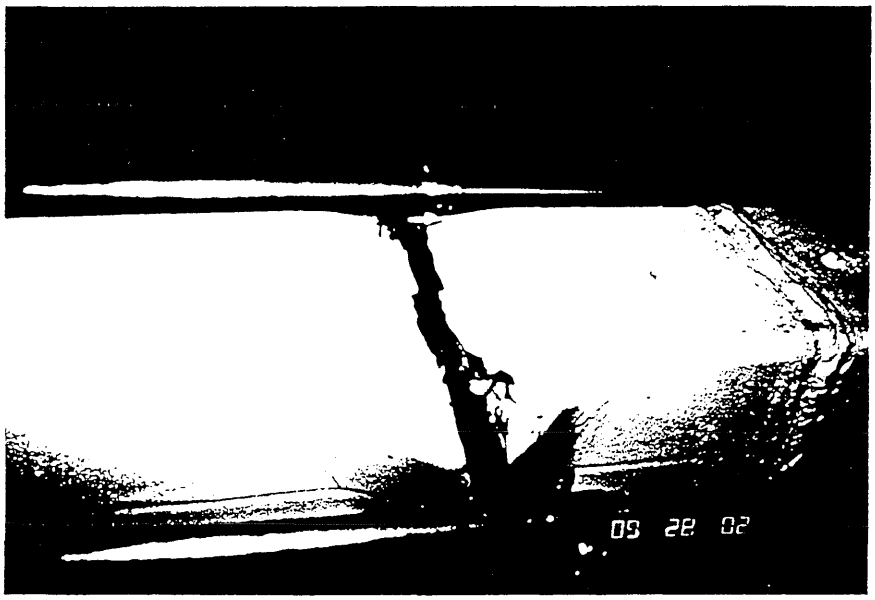

Fig. 4.20 Fracture of the north brace of the third story during the Phase I Final test

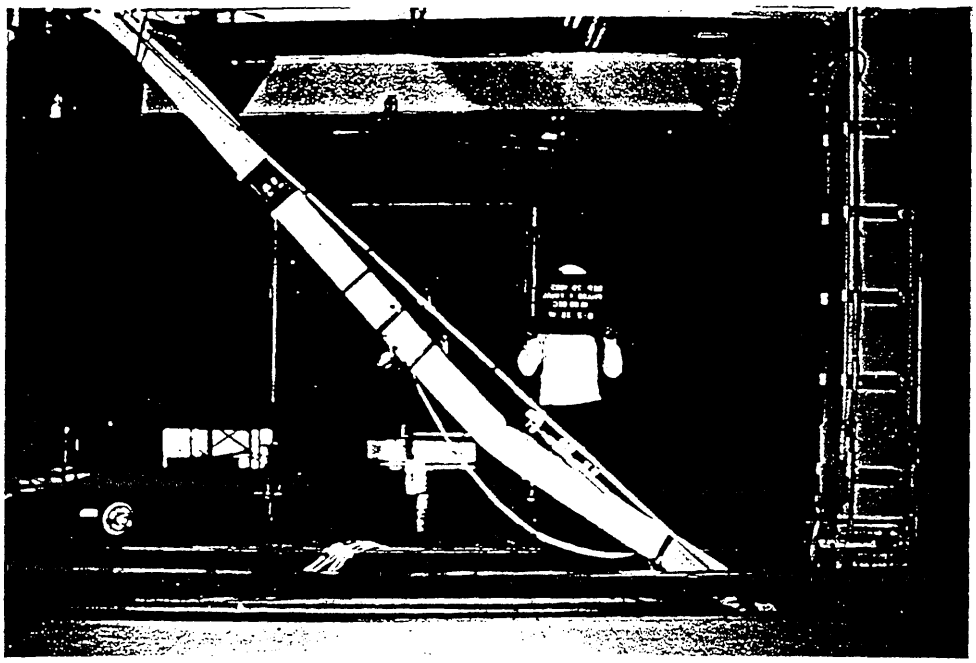

Fig. 4.21 In-plane buckling of brace during the Phase I Final test

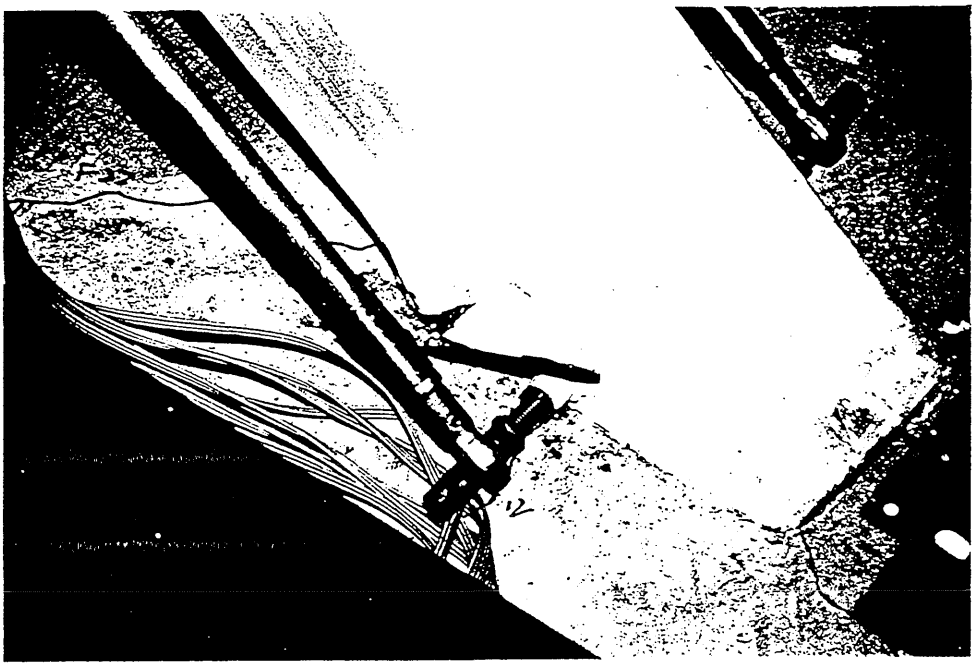

Tears initiating in the corners at the bottom of a brace during the Phase I Final test

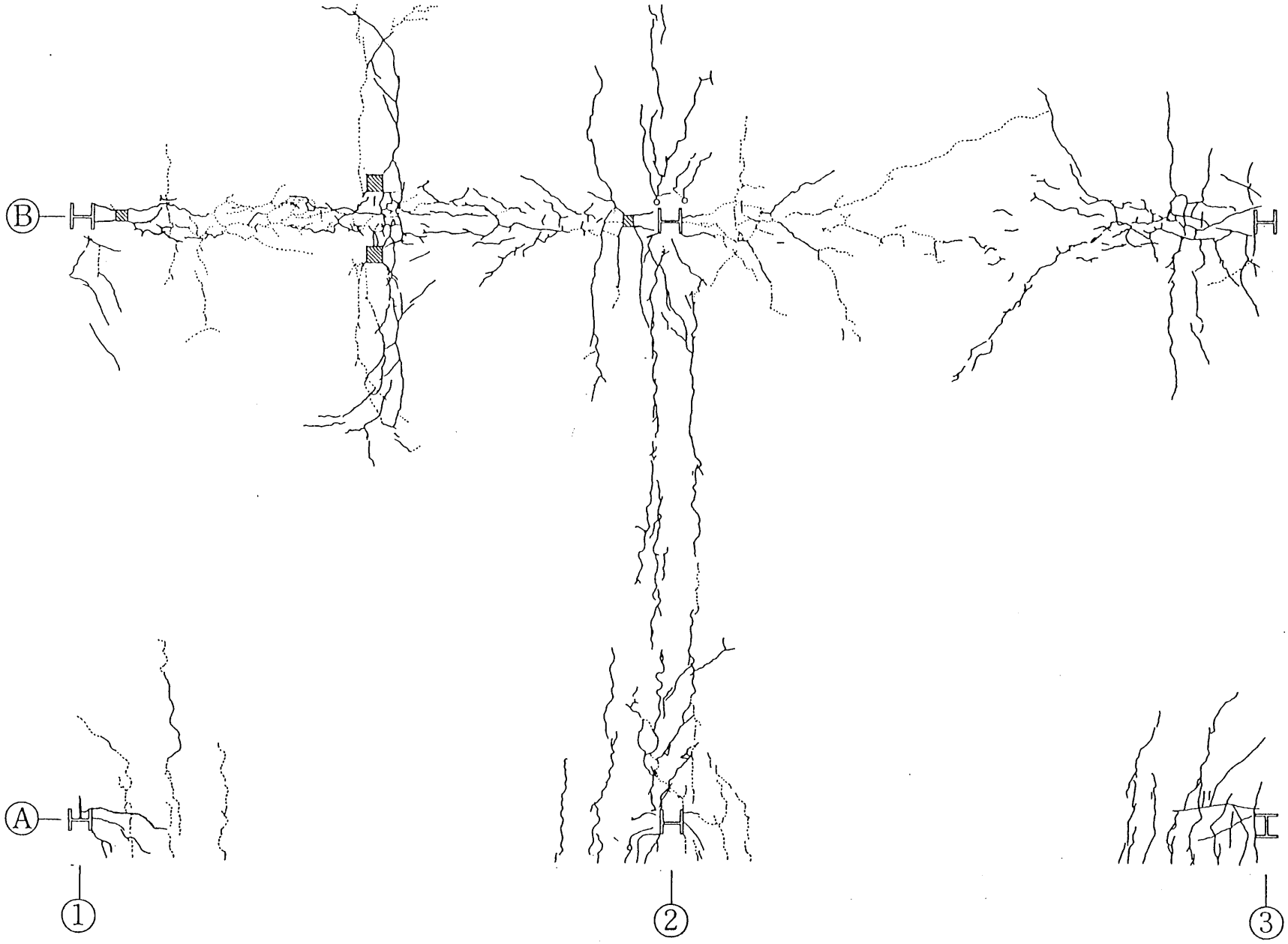

Fig. 4.23 Pattern of cracks following the Phase I Final test for the floor at the Z2 level

Fig. 4.24 Pattern of cracks following the Phase I Final test for the floor at the Z3 level

Fig. 4.25 Warping of the splice plate at the center beam splice in the 1Z bay of Frame B at the Z3 level as a result of twisting prying action during the Phase I Final test

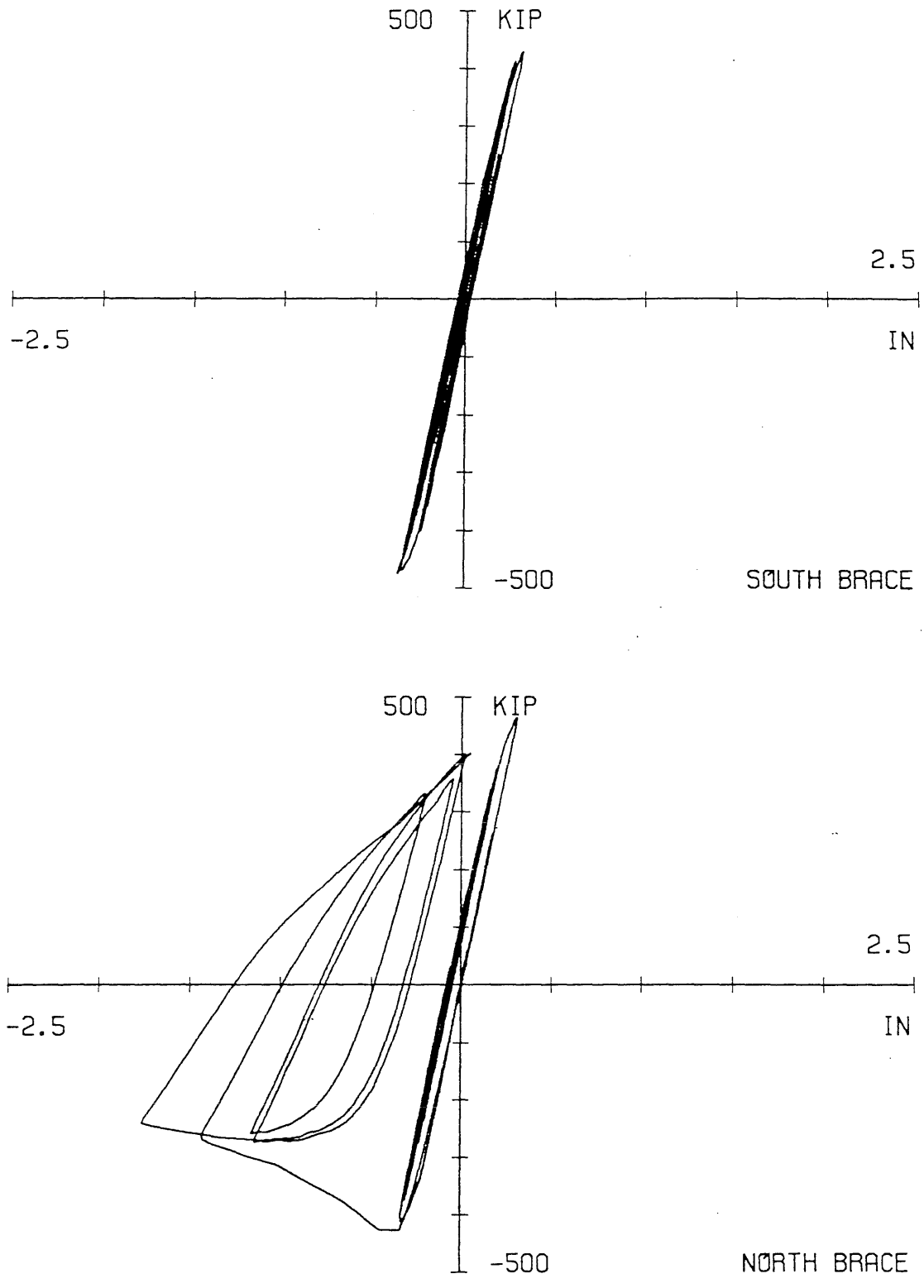

Fig. 4.26 Force-deflection relationship for the braces of the first story for the Phase I Final test

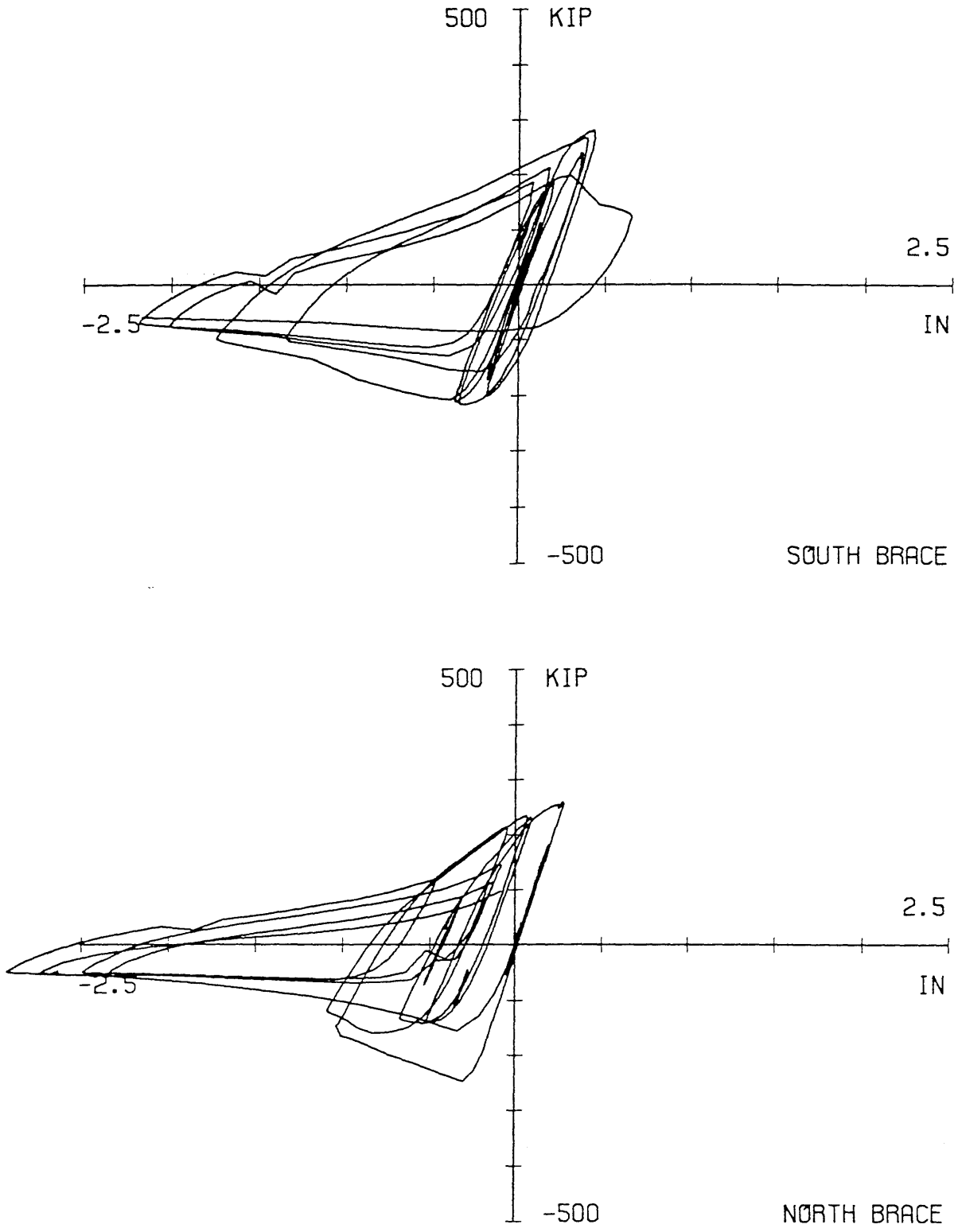

Fig. 4.27 Force-deflection relationship for the braces of the second story for the Phase I Final test

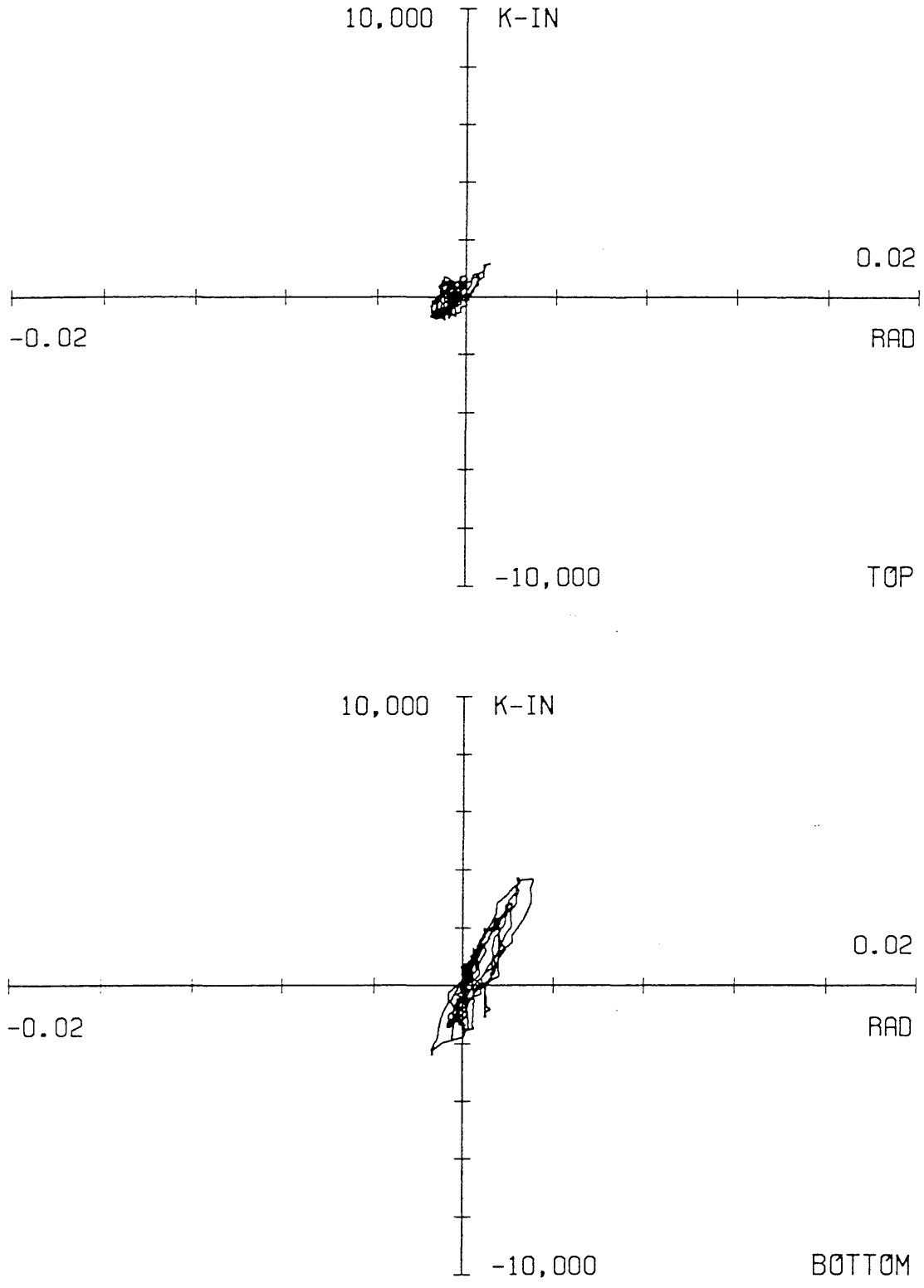

Fig. 4.28 Moment-rotation relationship for the top and bottom of the B1 column of the first story during the Phase I Final test

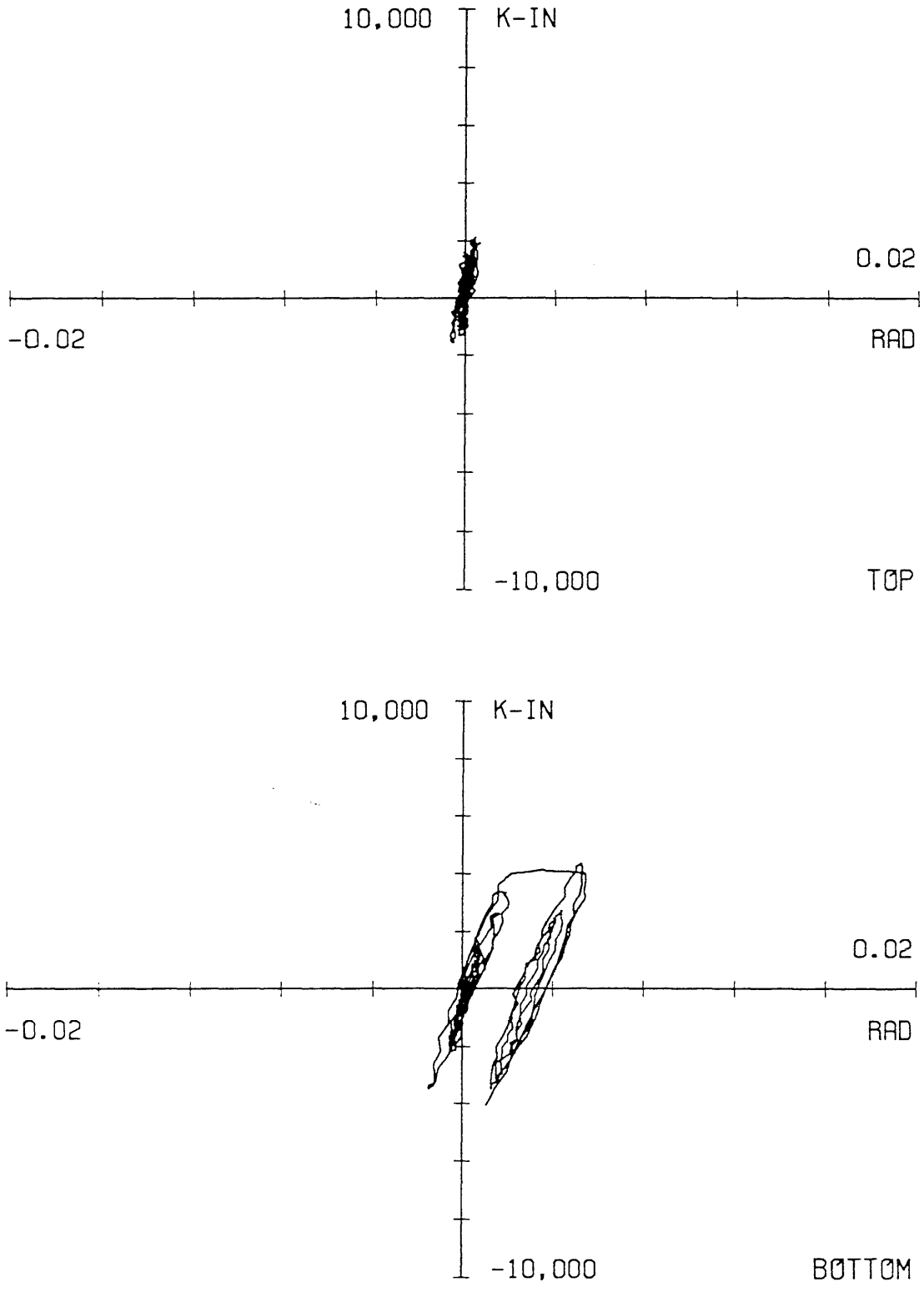

Fig. 4.29 Moment-rotation relationship for the top and bottom of the B2 column of the first story during the Phase I Final test

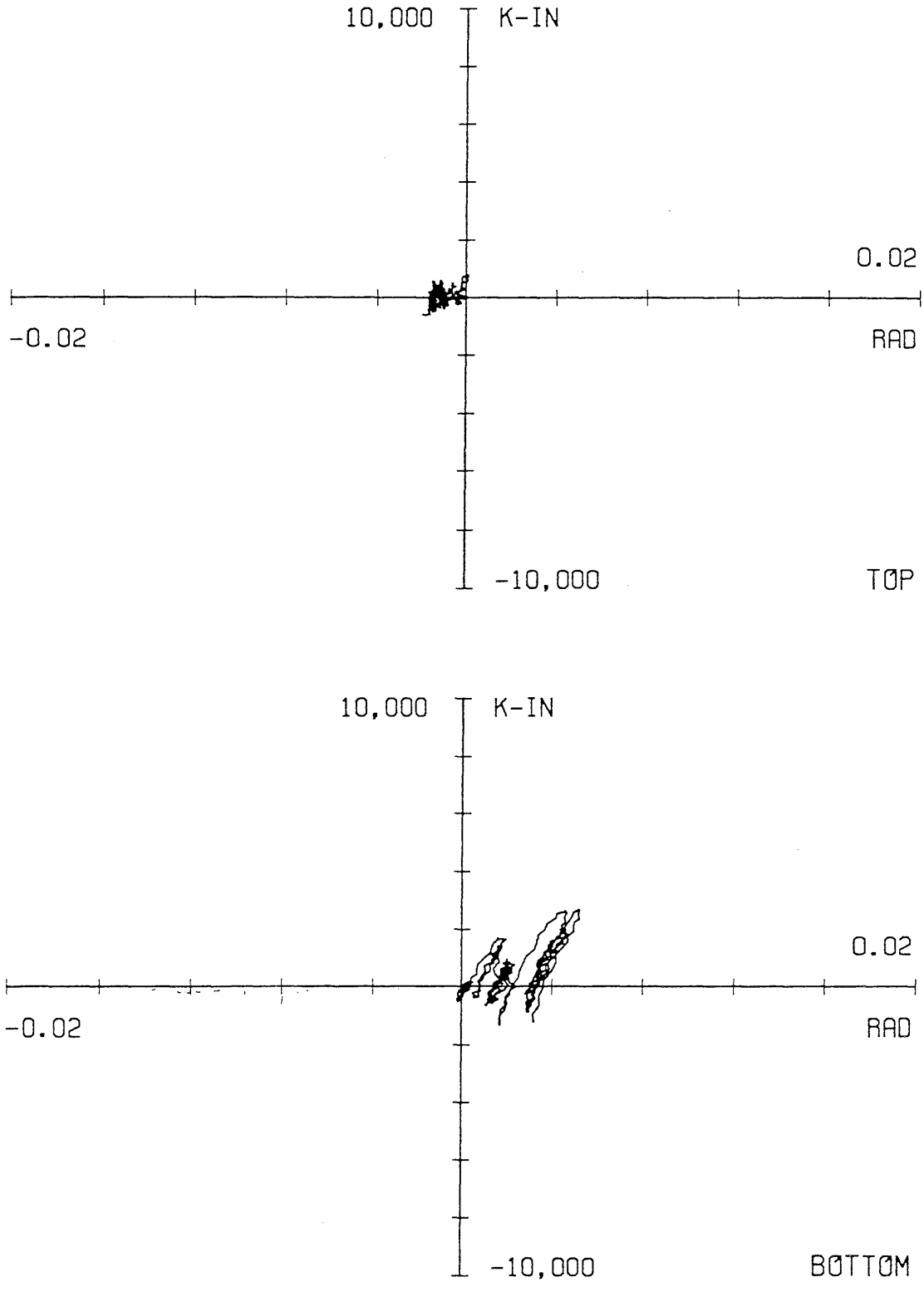

Fig. 4.30 Moment-rotation relationship for the top and bottom of the A1 column of the first story during the Phase I Final test

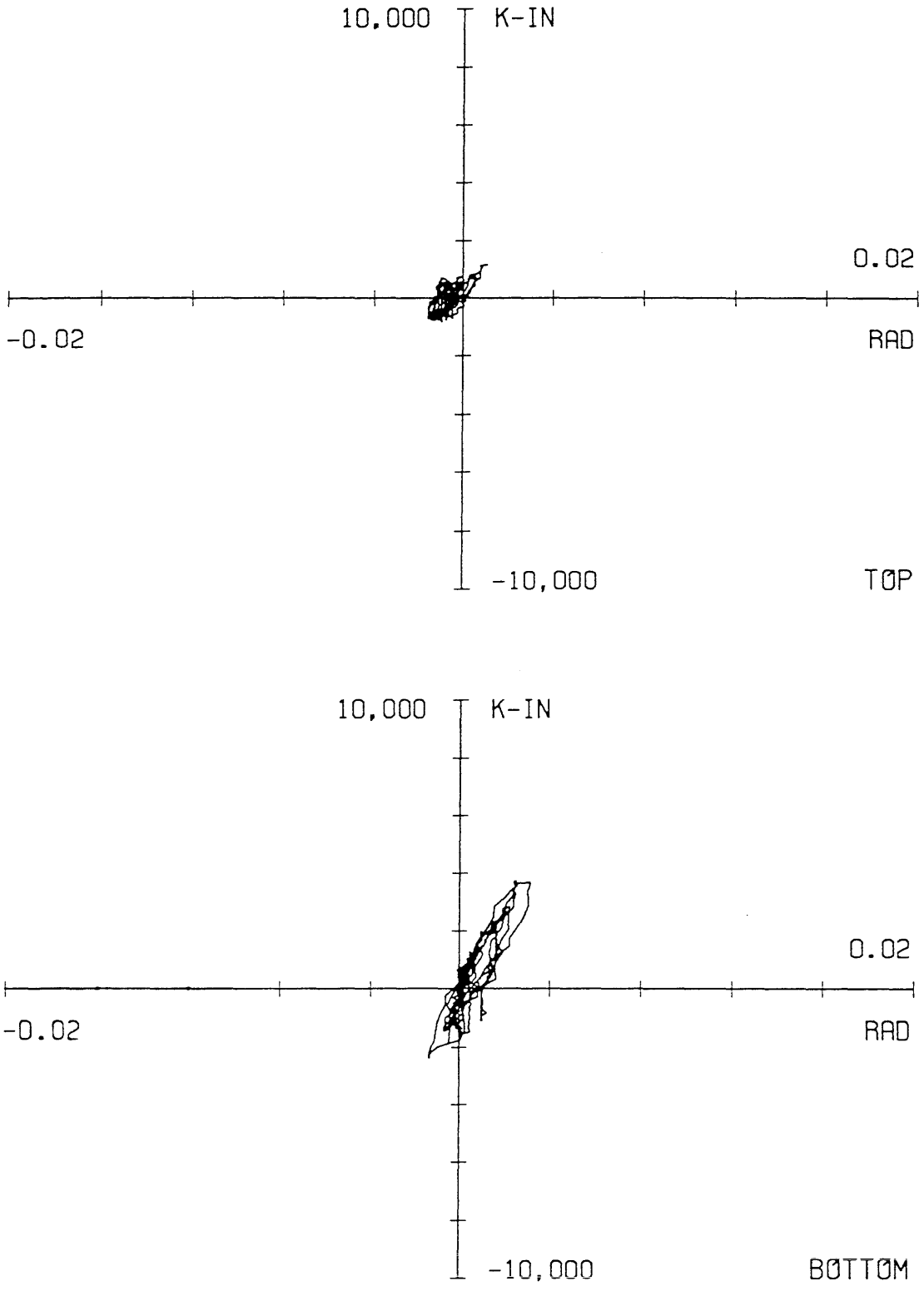

Fig. 4.31 Moment-rotation relationship for the top and bottom of the A2 column of the first story during the Phase I Final test

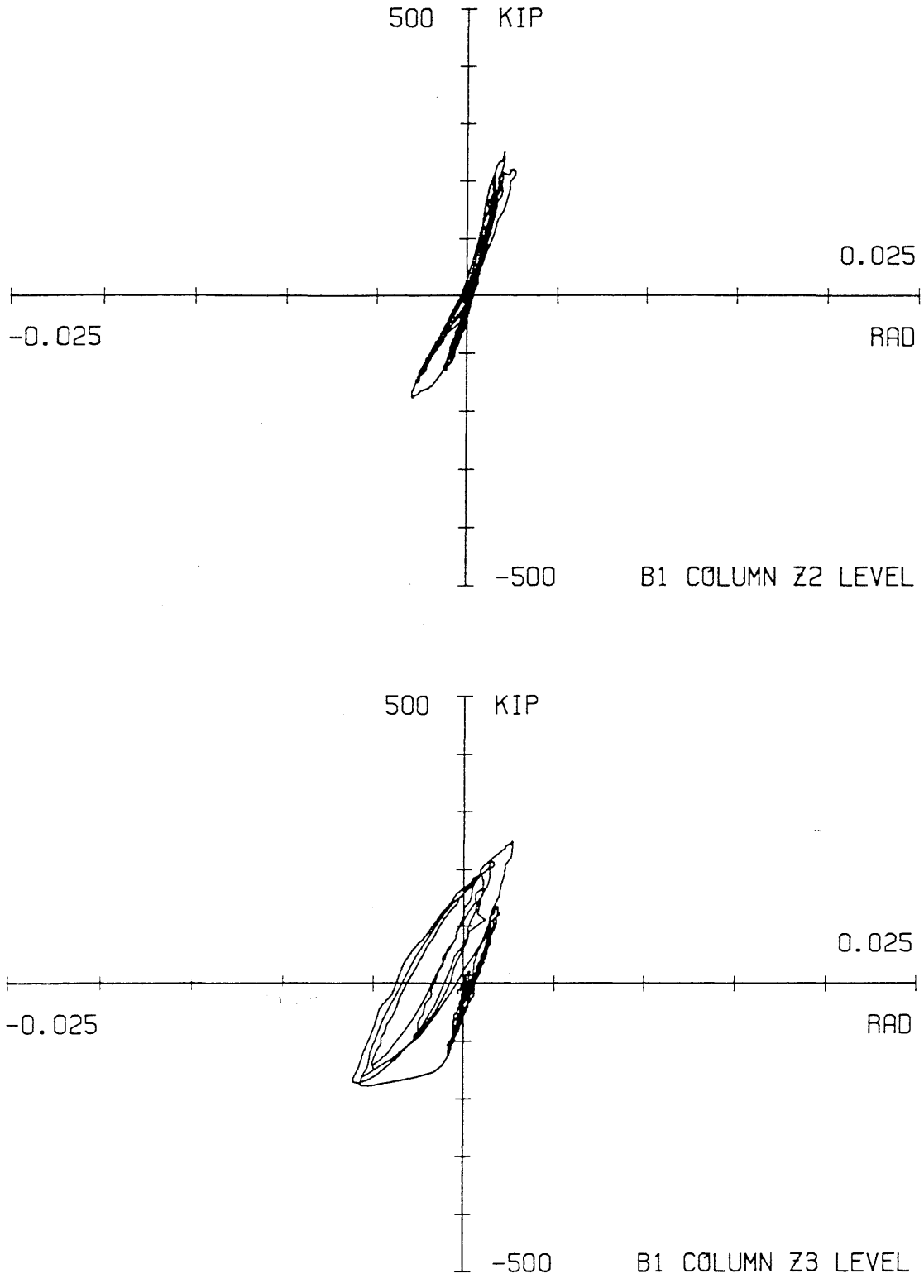

Fig. 4.32 Panel zone response for the B1 column at the Z2 and Z3 levels during the Phase I Final test

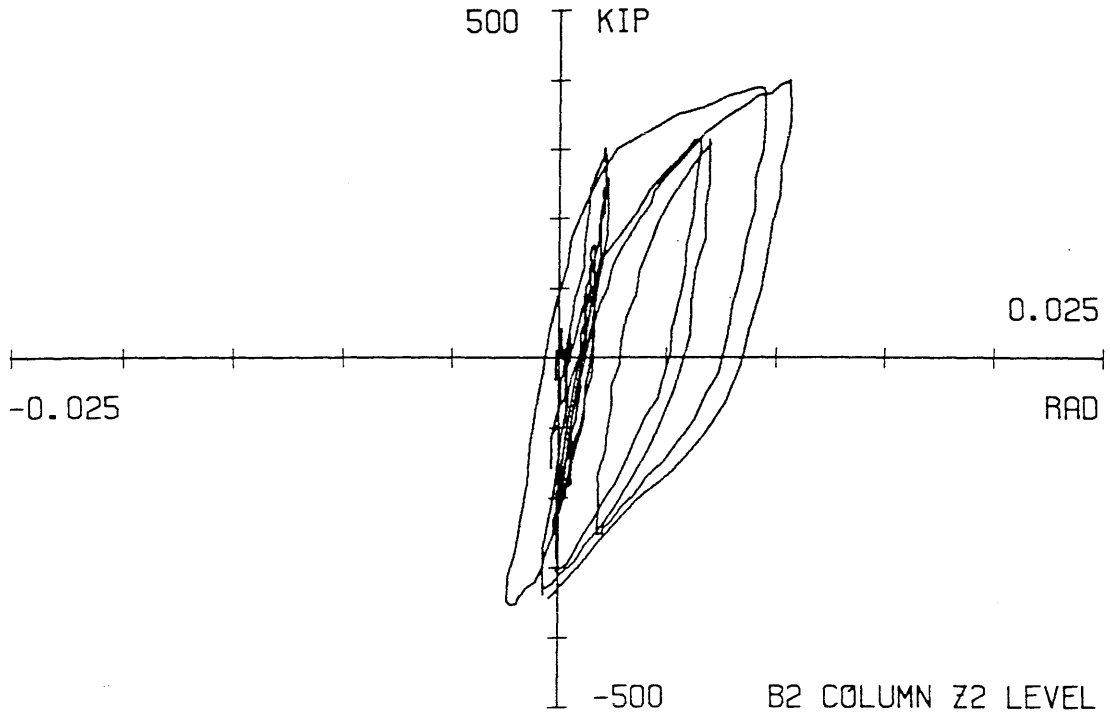

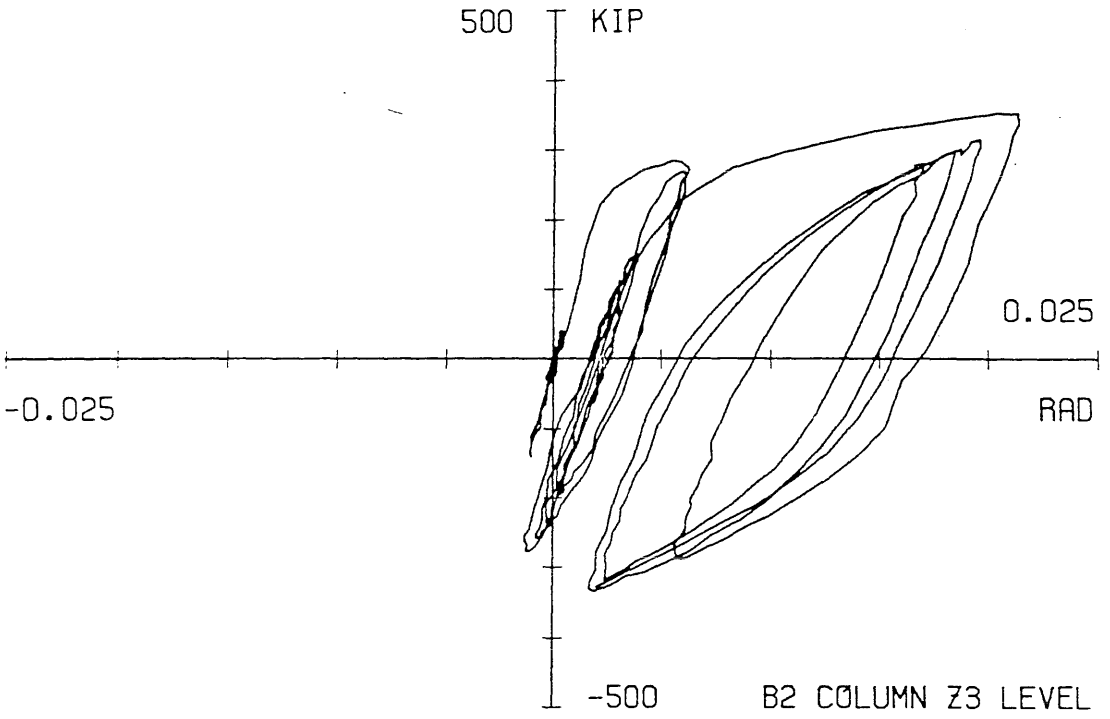

Fig. 4.33 Panel zone response for the B2 column at the Z2 and Z3 levels during the Phase I Final test

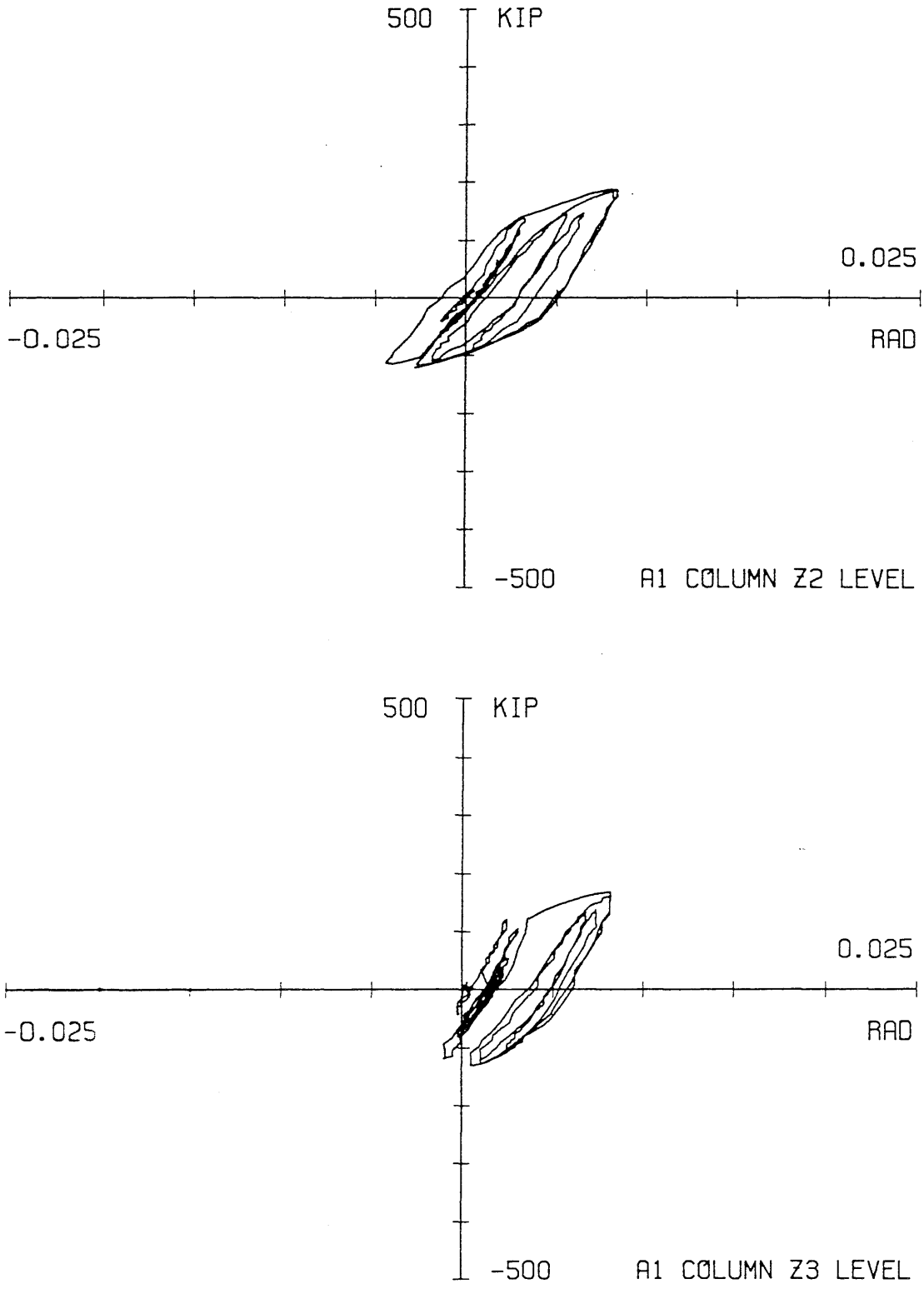

Fig. 4.34 Panel zone response for the A1 column at the Z2 and Z3 levels during the Phase I Final test

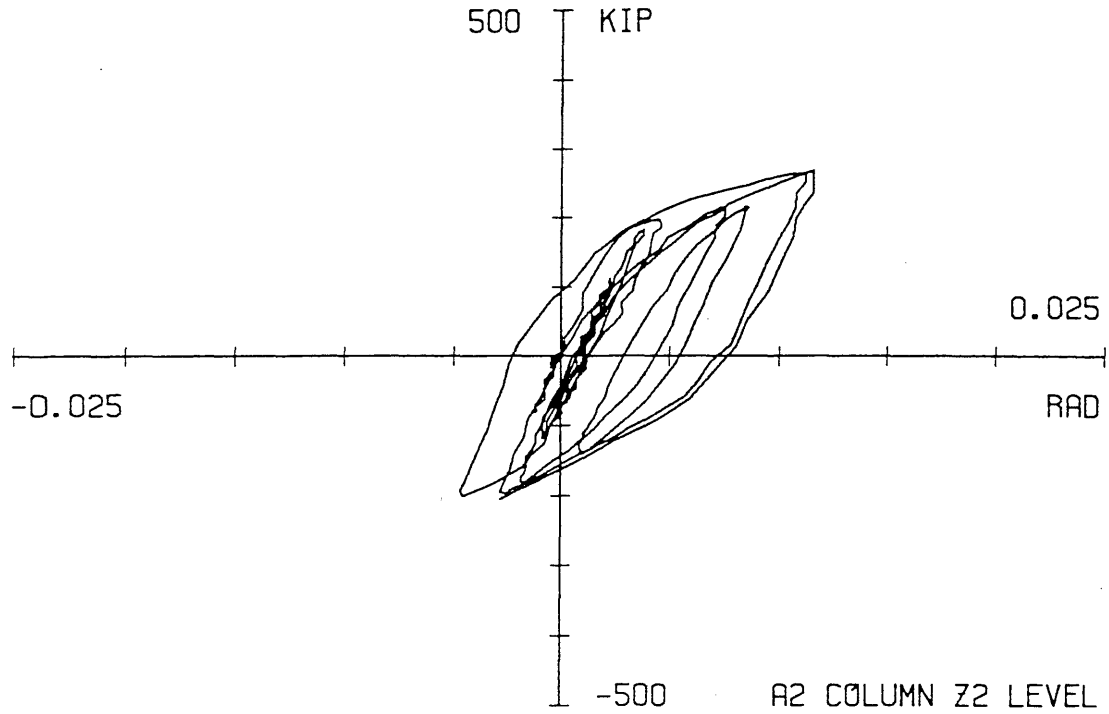

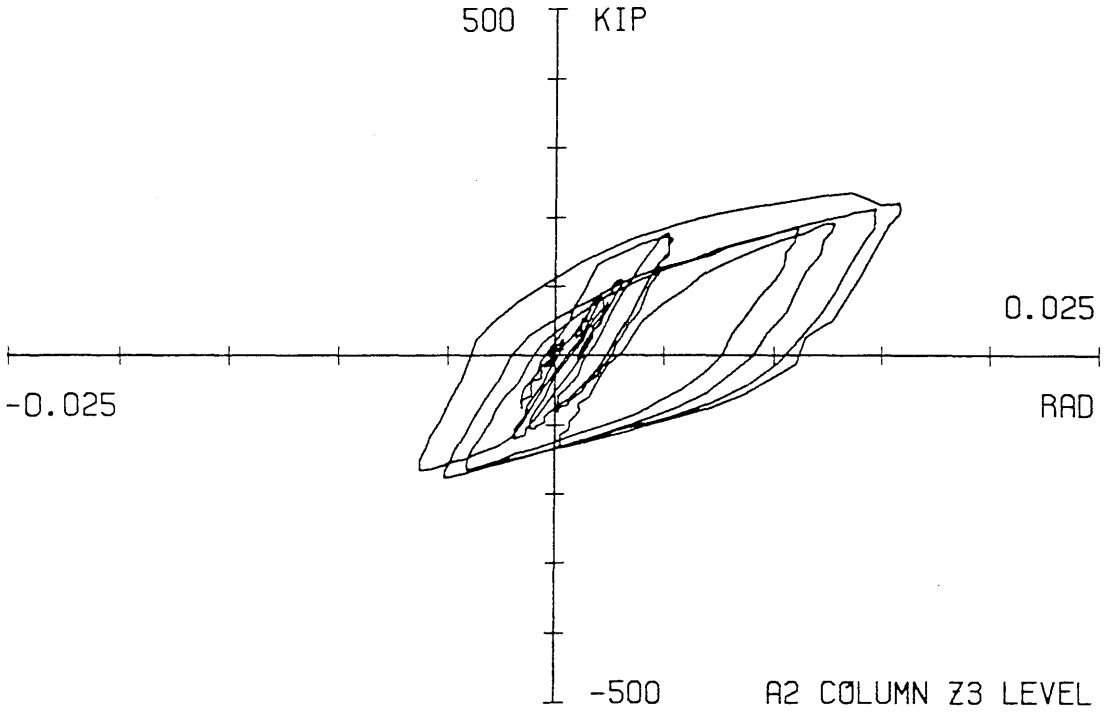

Fig. 4.35 Panel zone response for the A2 column at the Z2 and Z3 levels during the Phase I Final test

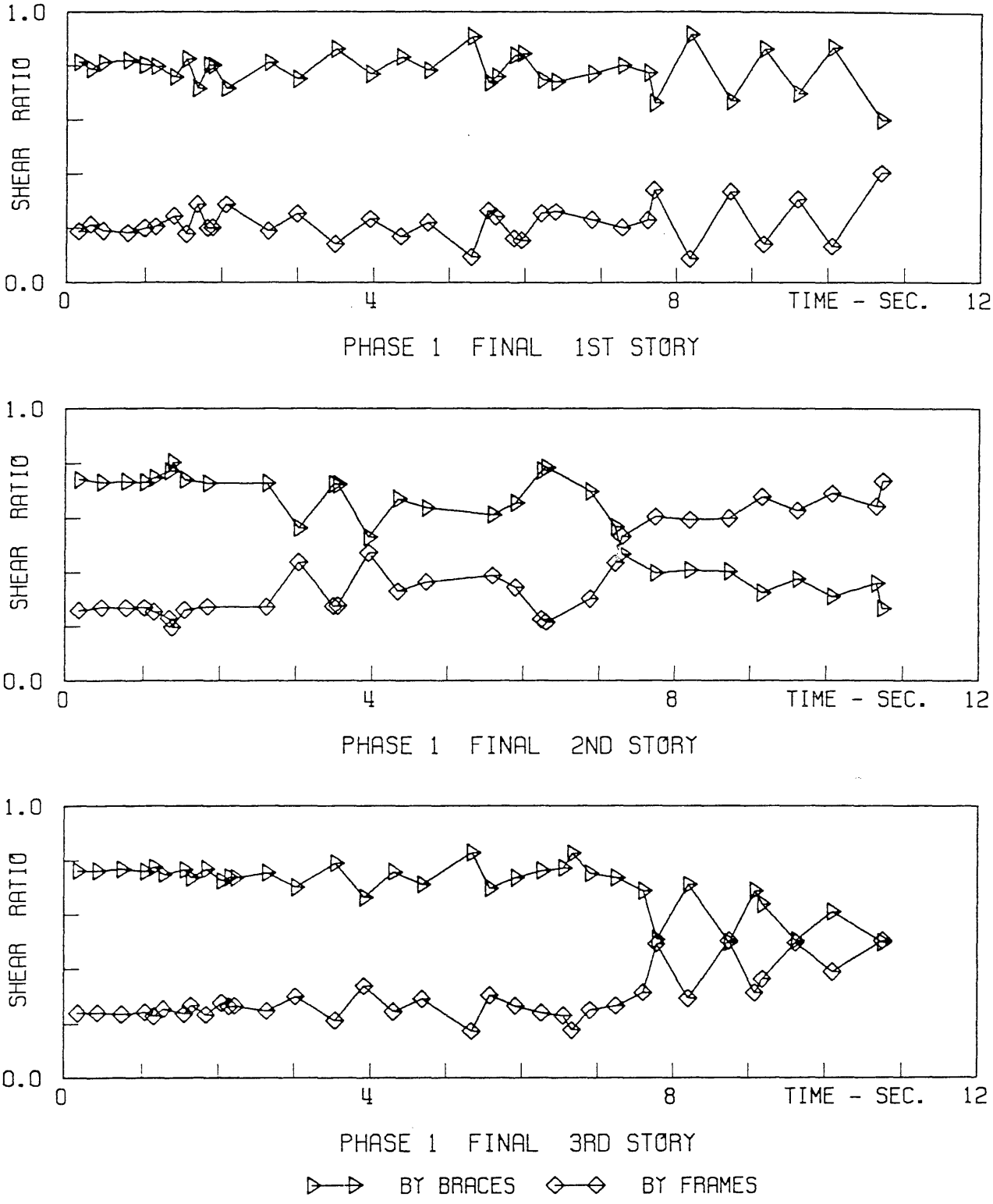

Fig. 4.36 Ratio of shear carried by the braces to the total shear for the third story during the Phase I Final test

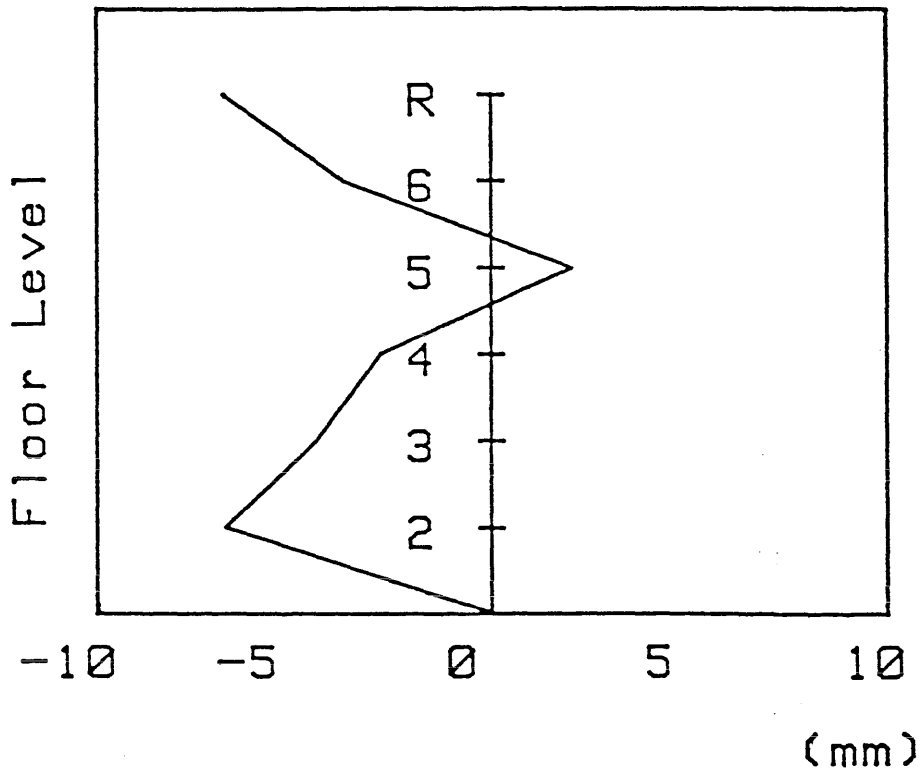

Fig. 5.1 Residual floor displacements after the Phase I Final test

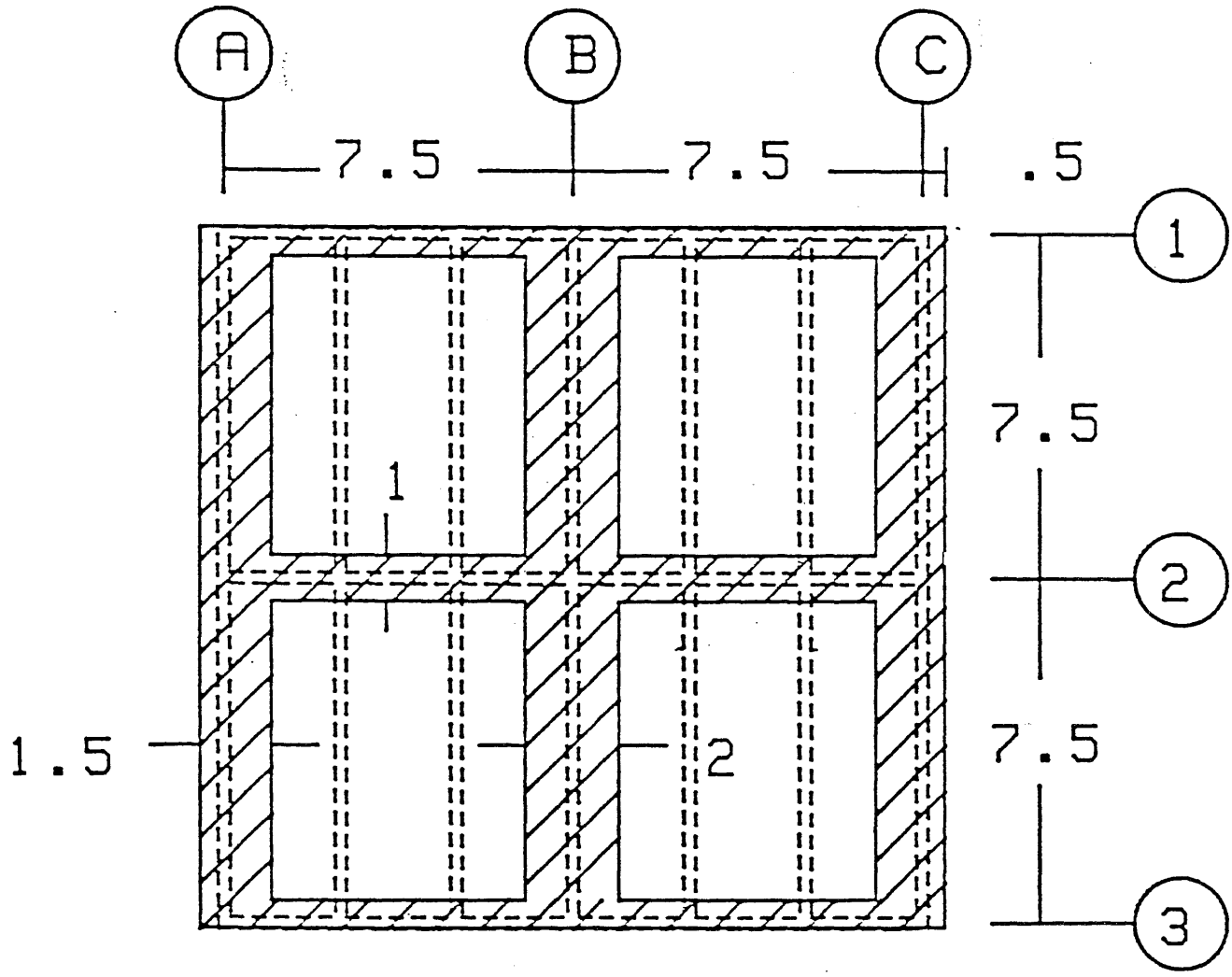

Fig. 5.2 Locations on each floor where epoxy injection was used to repair cracks resulting from the Phase I tests

Fig. 5.3 Typical cracks prior to repair

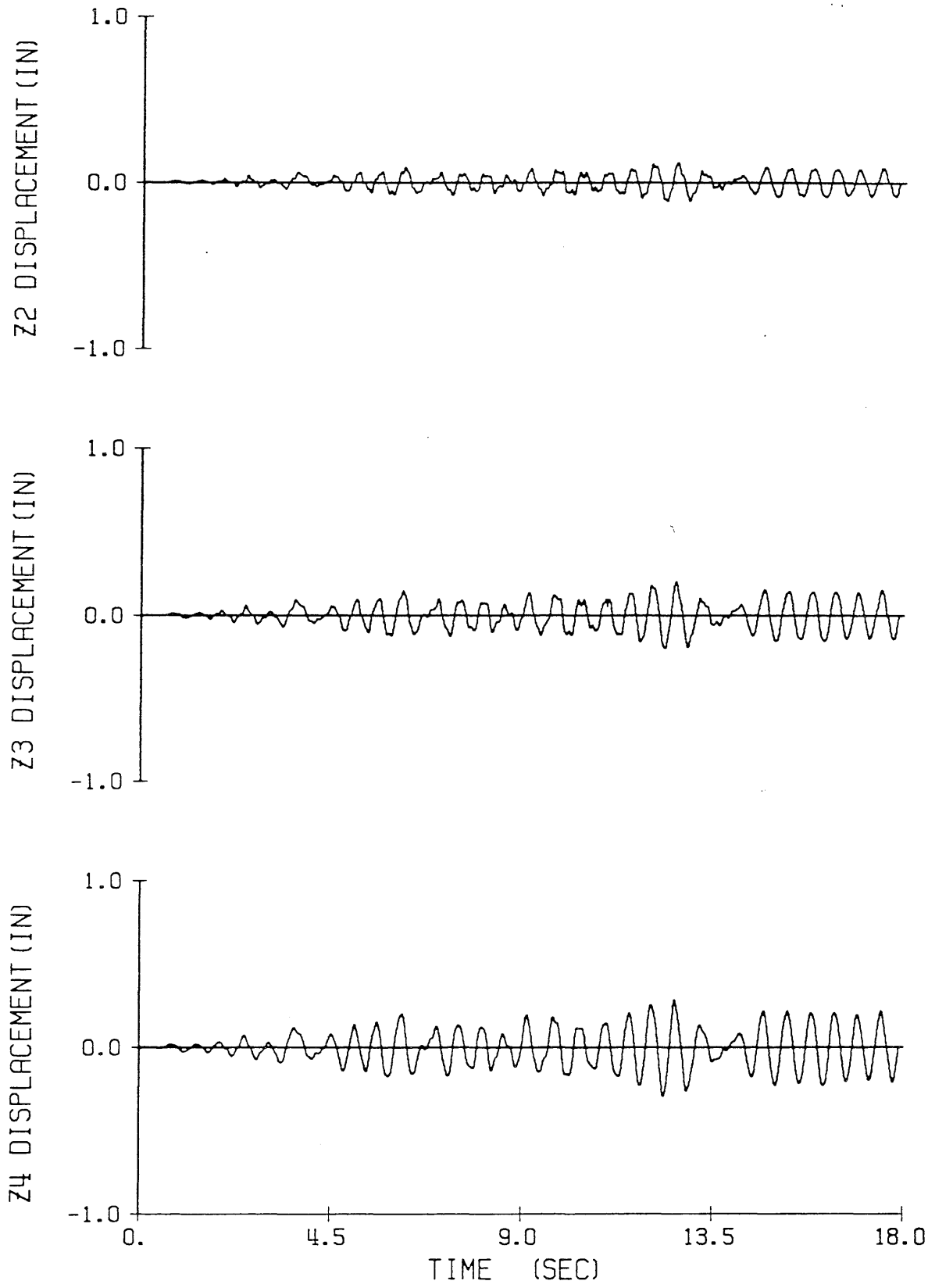

Fig. 5.4 Floor displacement vs. time for the Phase II Elastic test

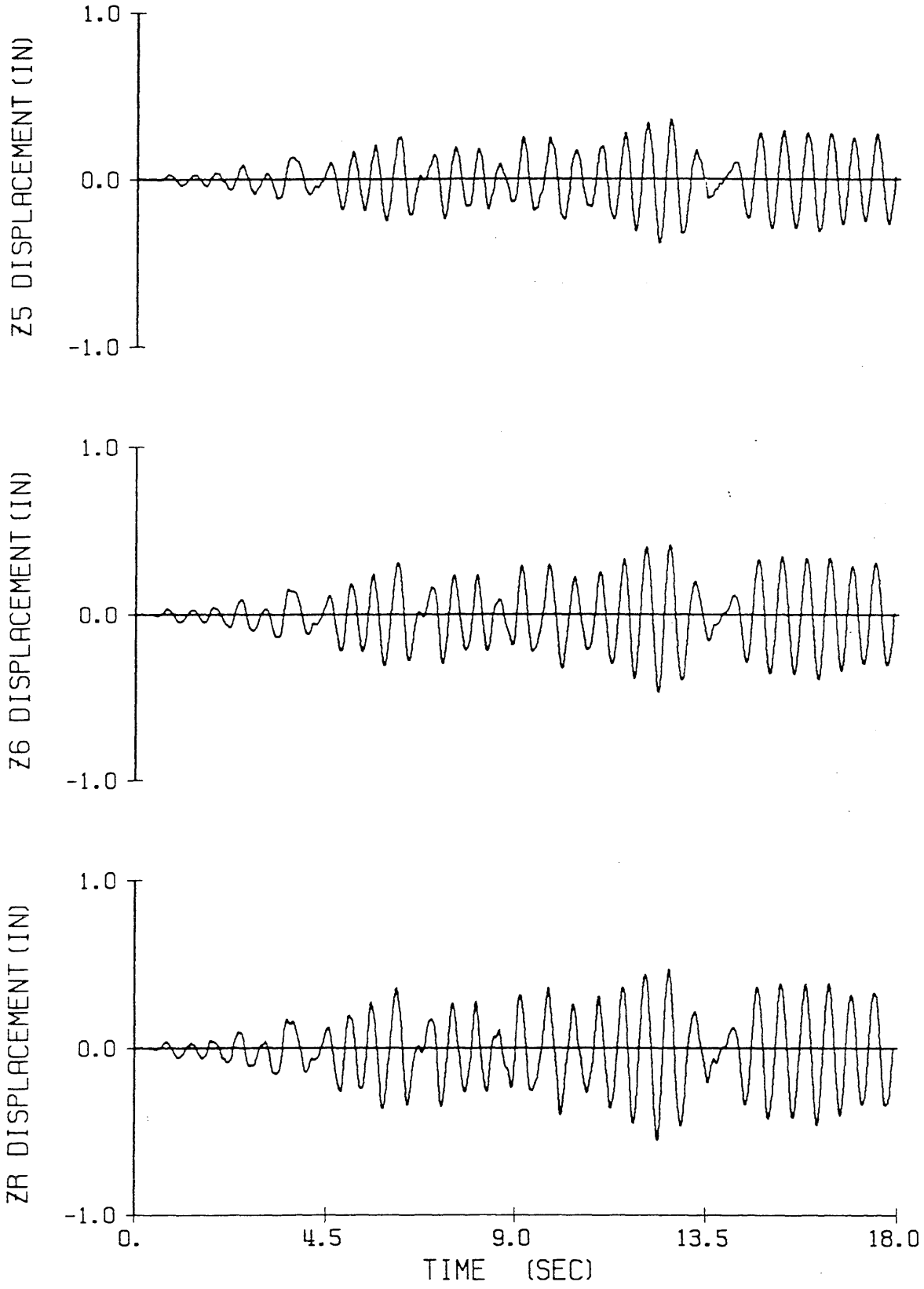

Fig. 5.4 (continued)

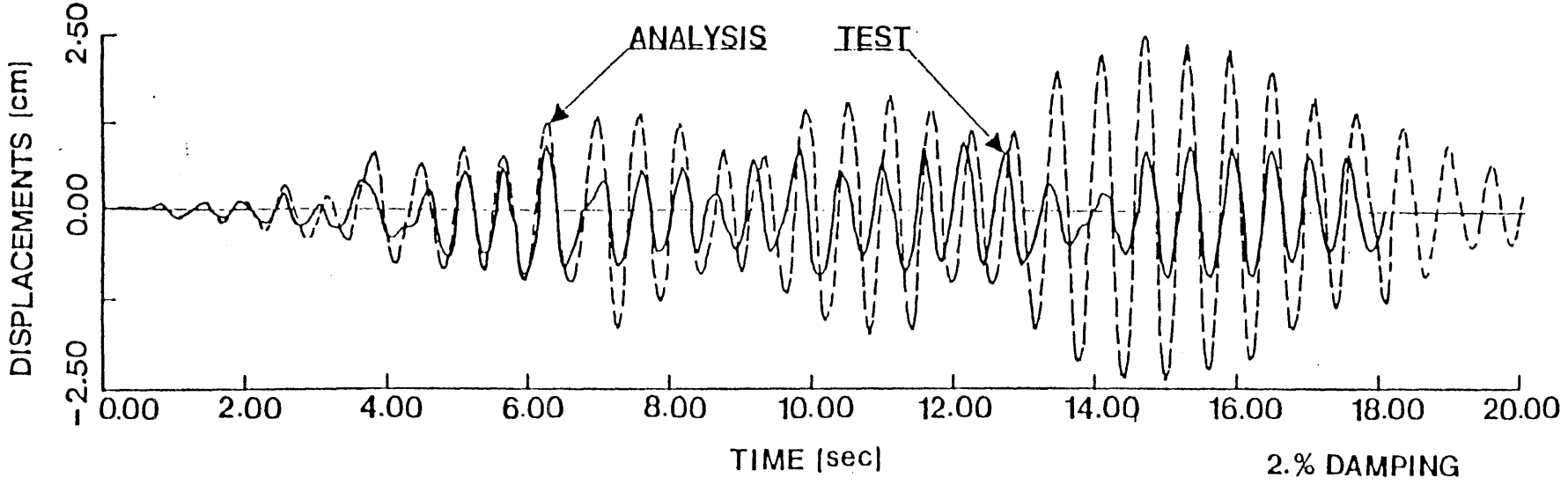

Fig. 5.5 Measured and computed displacements for the ZR level during the Phase II Elastic test (from Ref. 9)

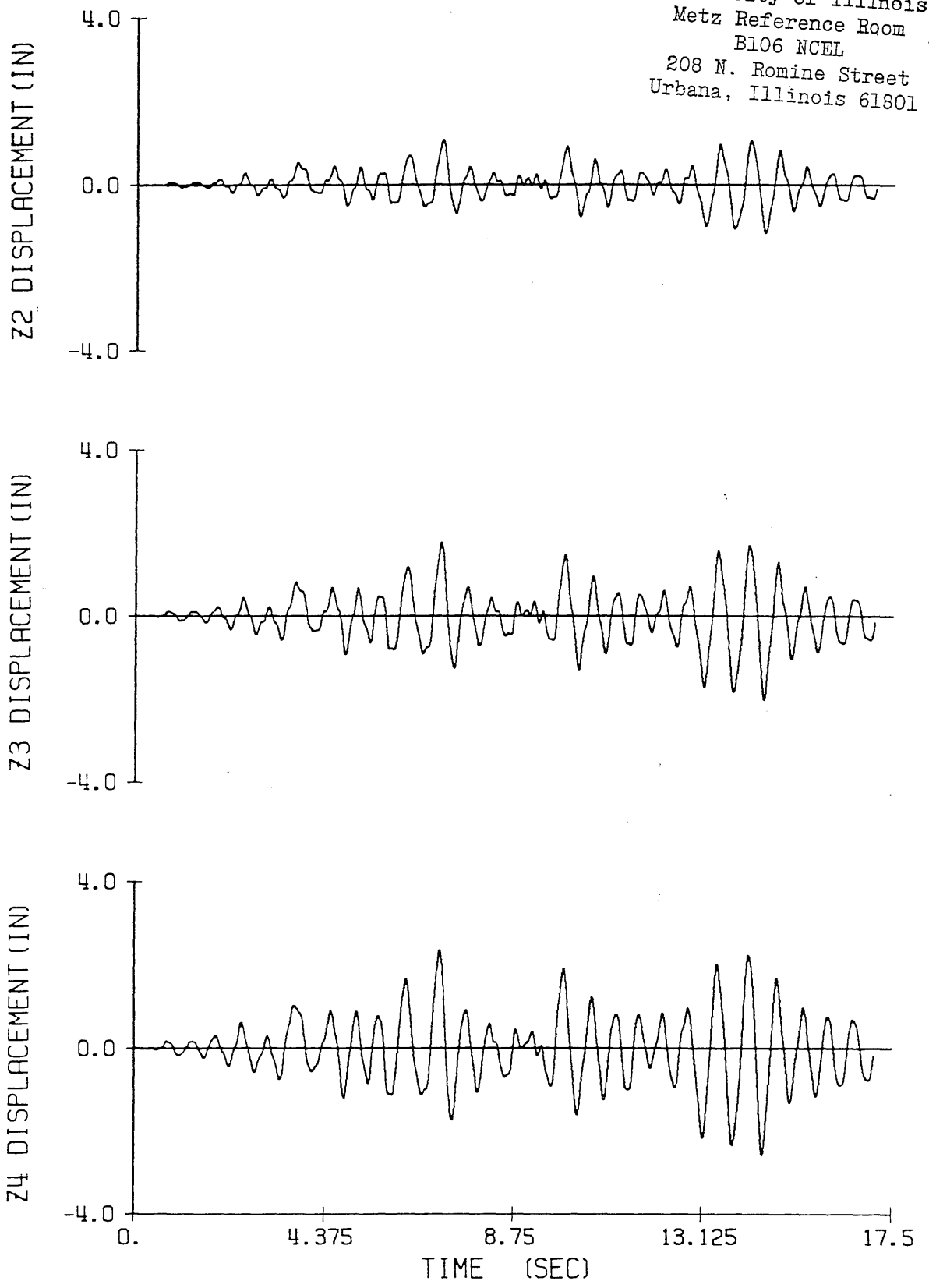

Fig. 5.6 Floor displacements vs. time for the Phase II Inelastic test

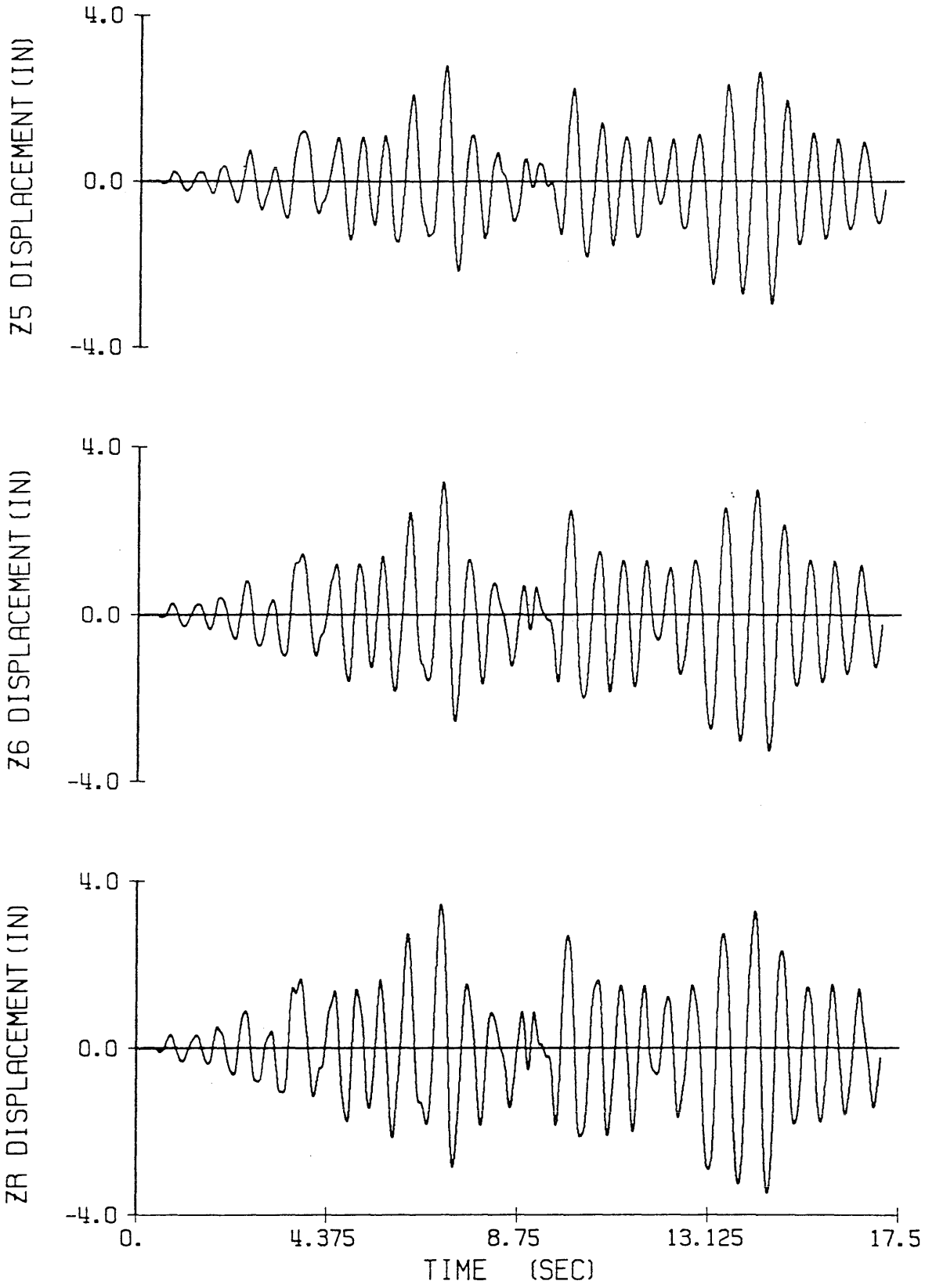

Fig. 5.6 (continued)

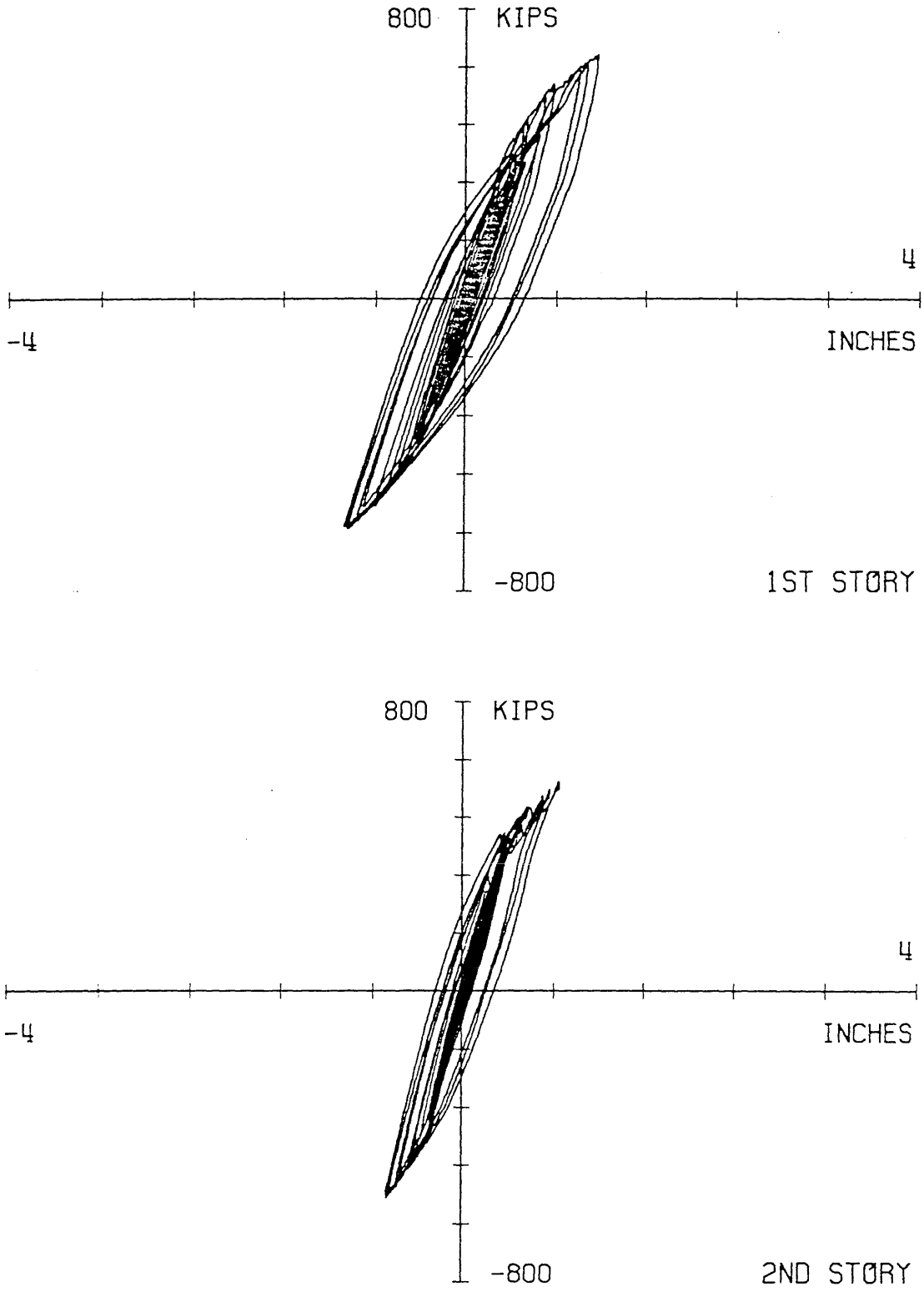

Fig. 5.7 Story shear vs. story displacement for the first and second stories for the Phase II Inelastic test

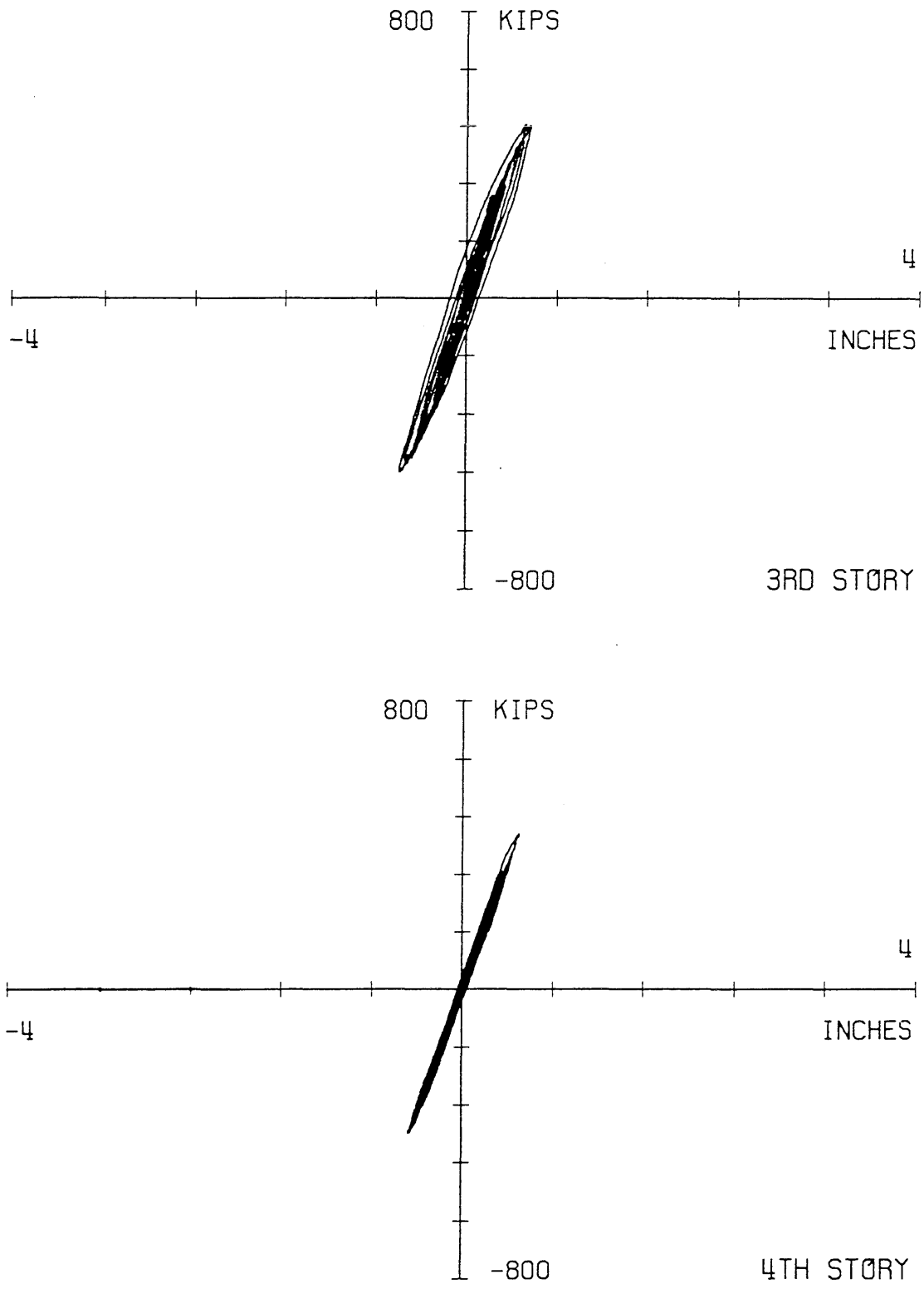

Fig. 5.8 Story shear vs. story displacement for the third and fourth stories for the Phase II Inelastic test

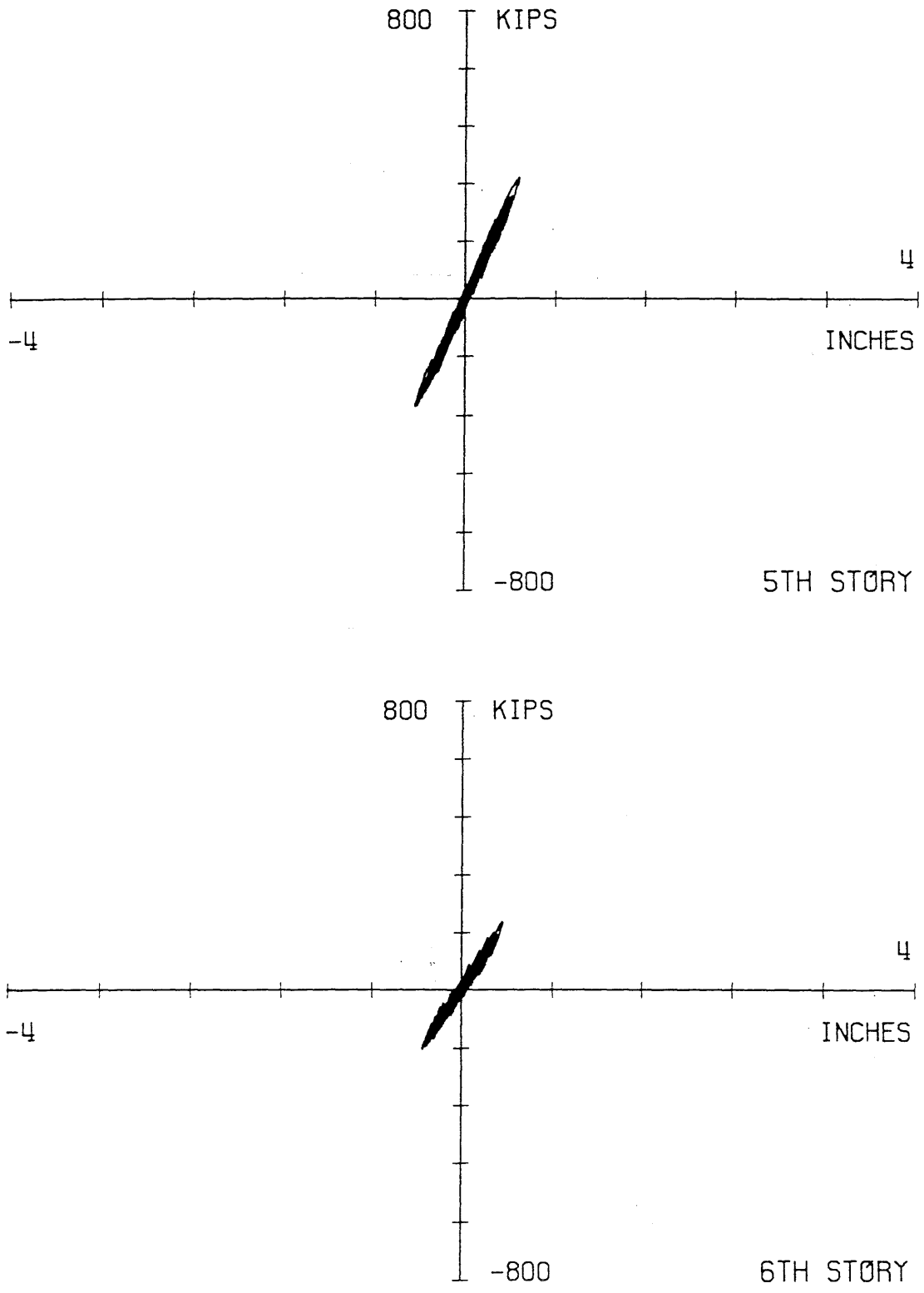

Fig. 5.9 Story shear vs. story displacement for the fifth and sixth stories for the Phase II Inelastic test

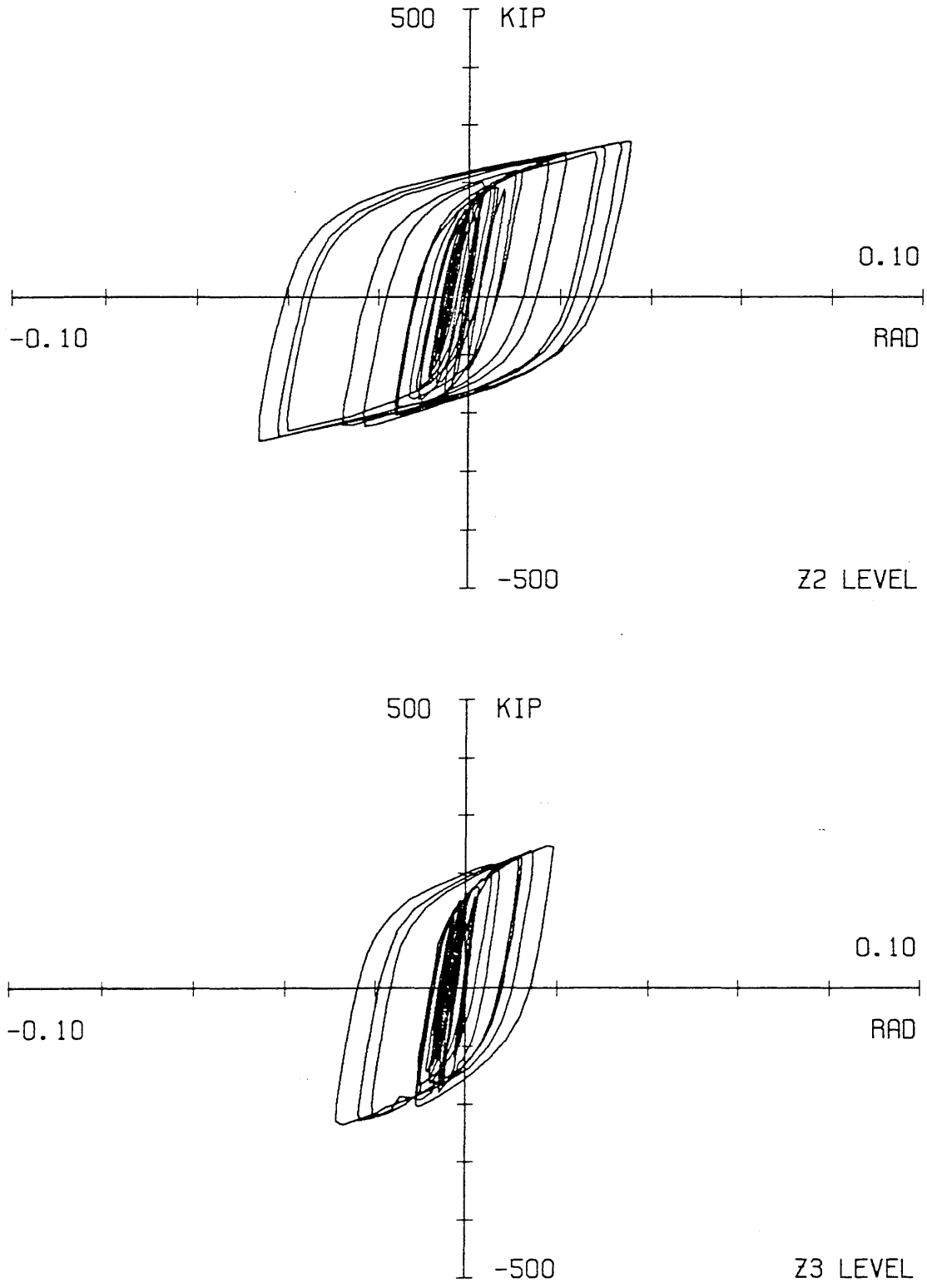

Fig. 5.10 Shear link response at the Z2 and Z3 levels during the Phase II Inelastic test

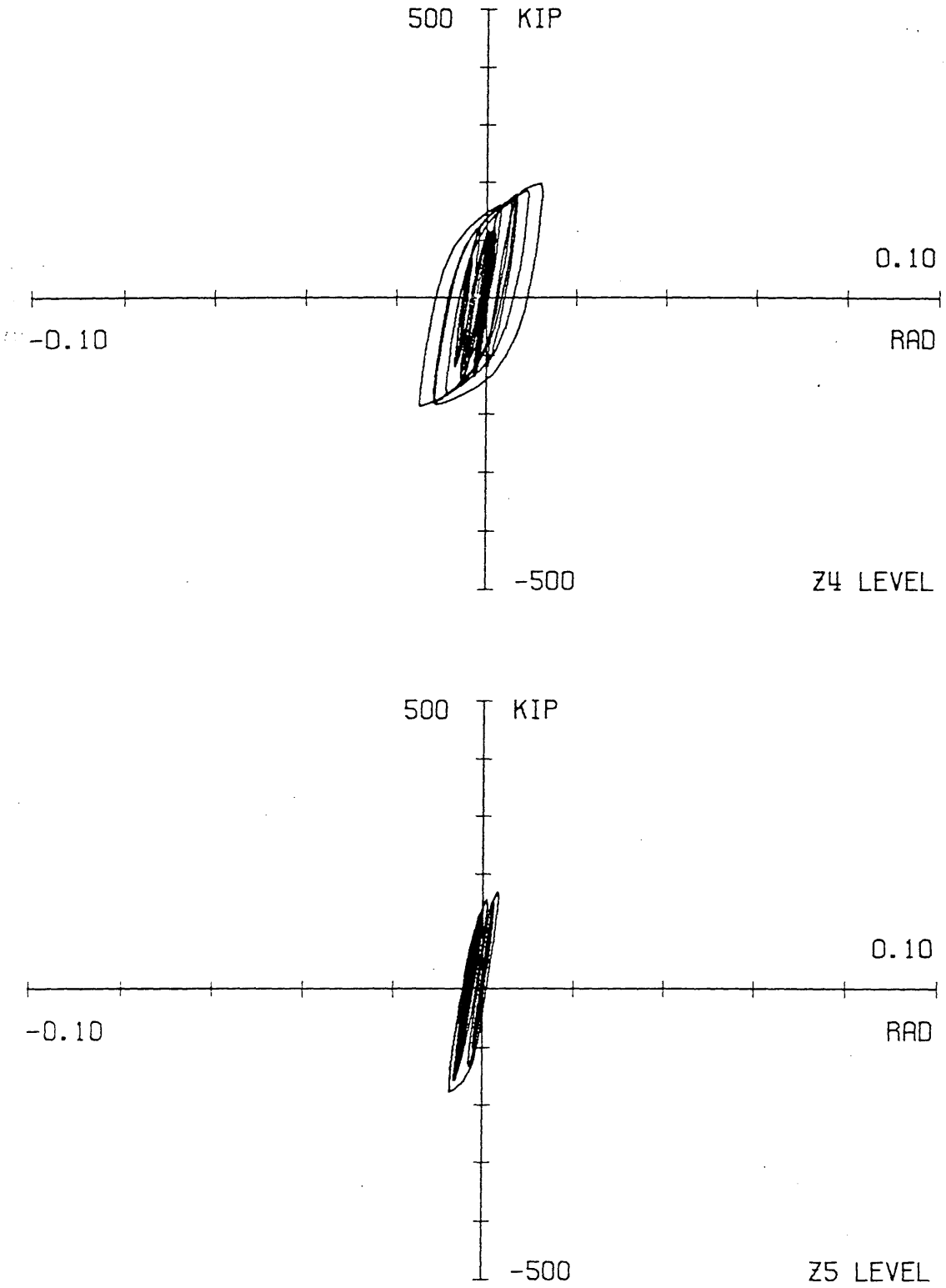

Fig. 5.11 Shear link response at the Z4 and Z5 levels during the Phase II Inelastic test

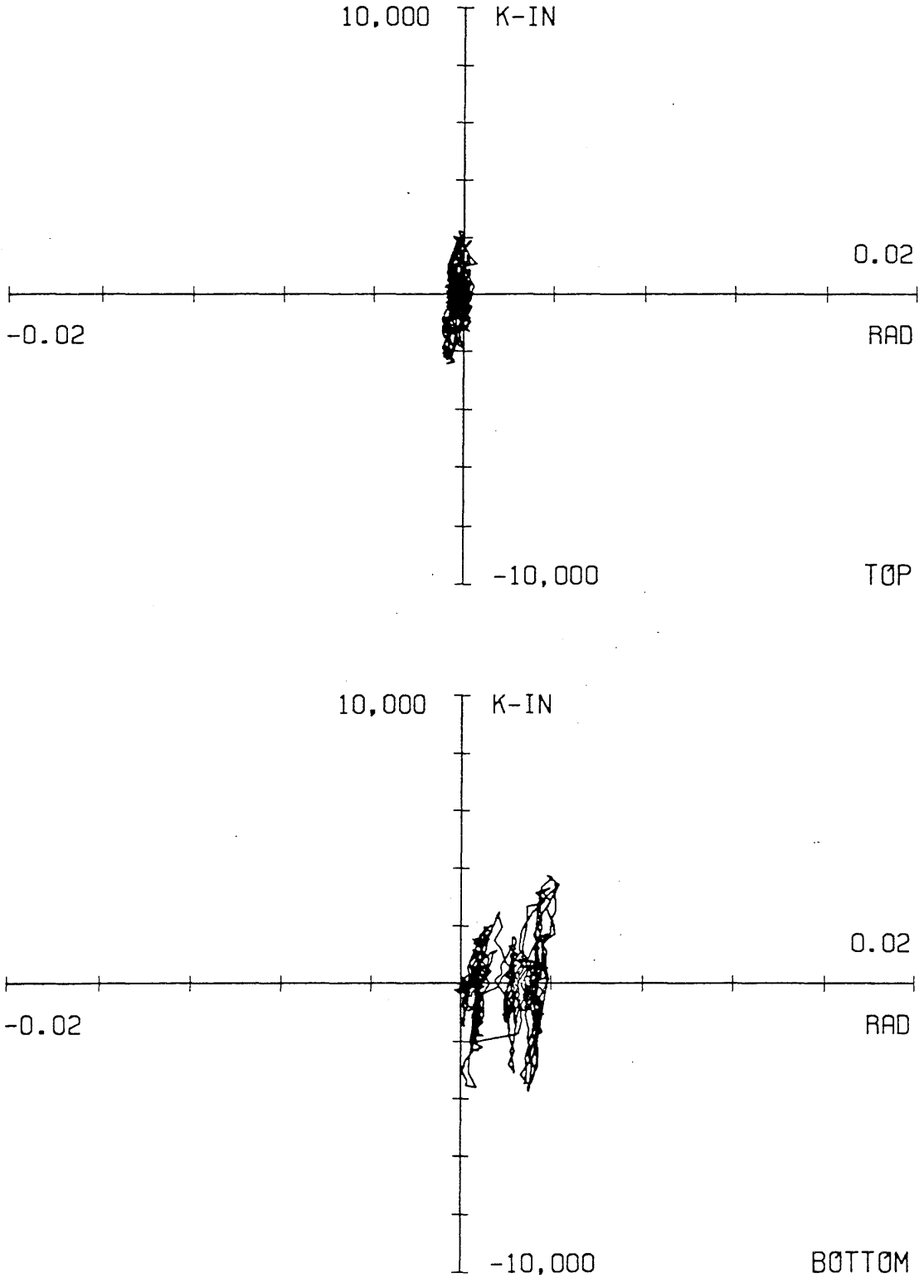

Fig. 5.12 Moment-rotation relationships for the top and bottom of the B1 column of the first story during the Phase II Inelastic test

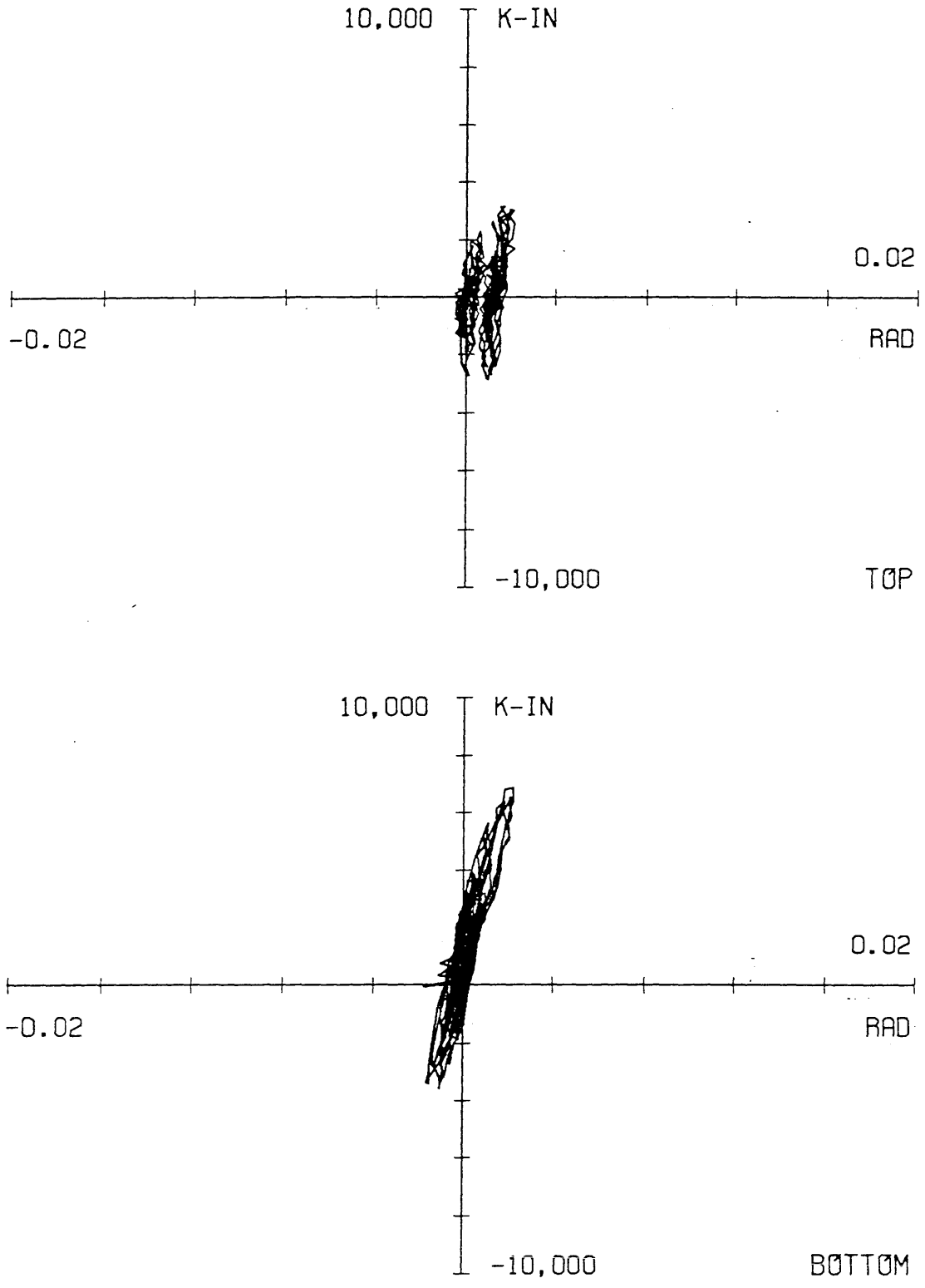

Fig. 5.13 Moment-rotation relationships for the top and bottom of the B2 column of the first story during the Phase II Inelastic test

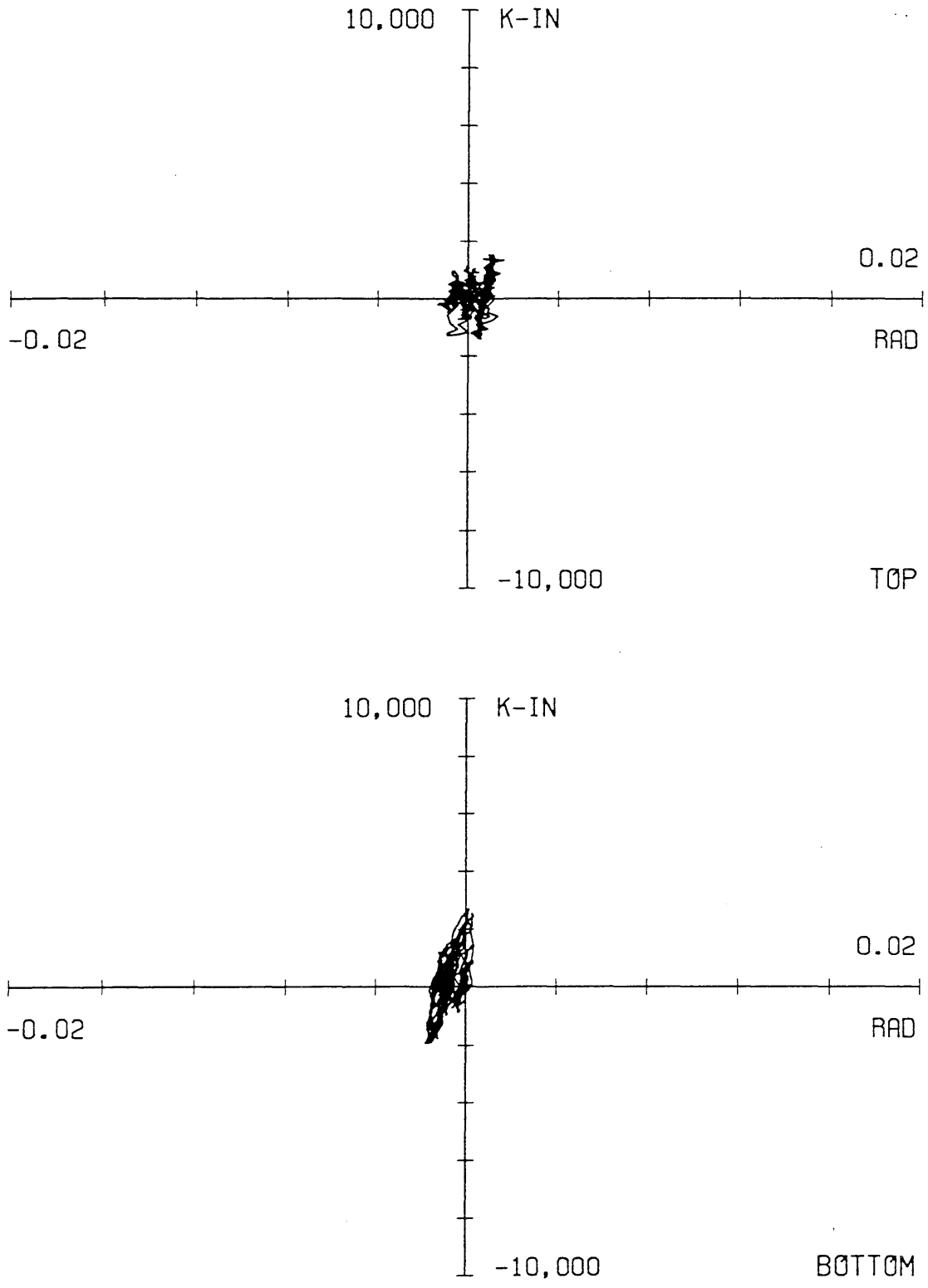

Fig. 5.14 Moment-rotation relationships for the top and bottom of the A1 column of the first story during the Phase II Inelastic test

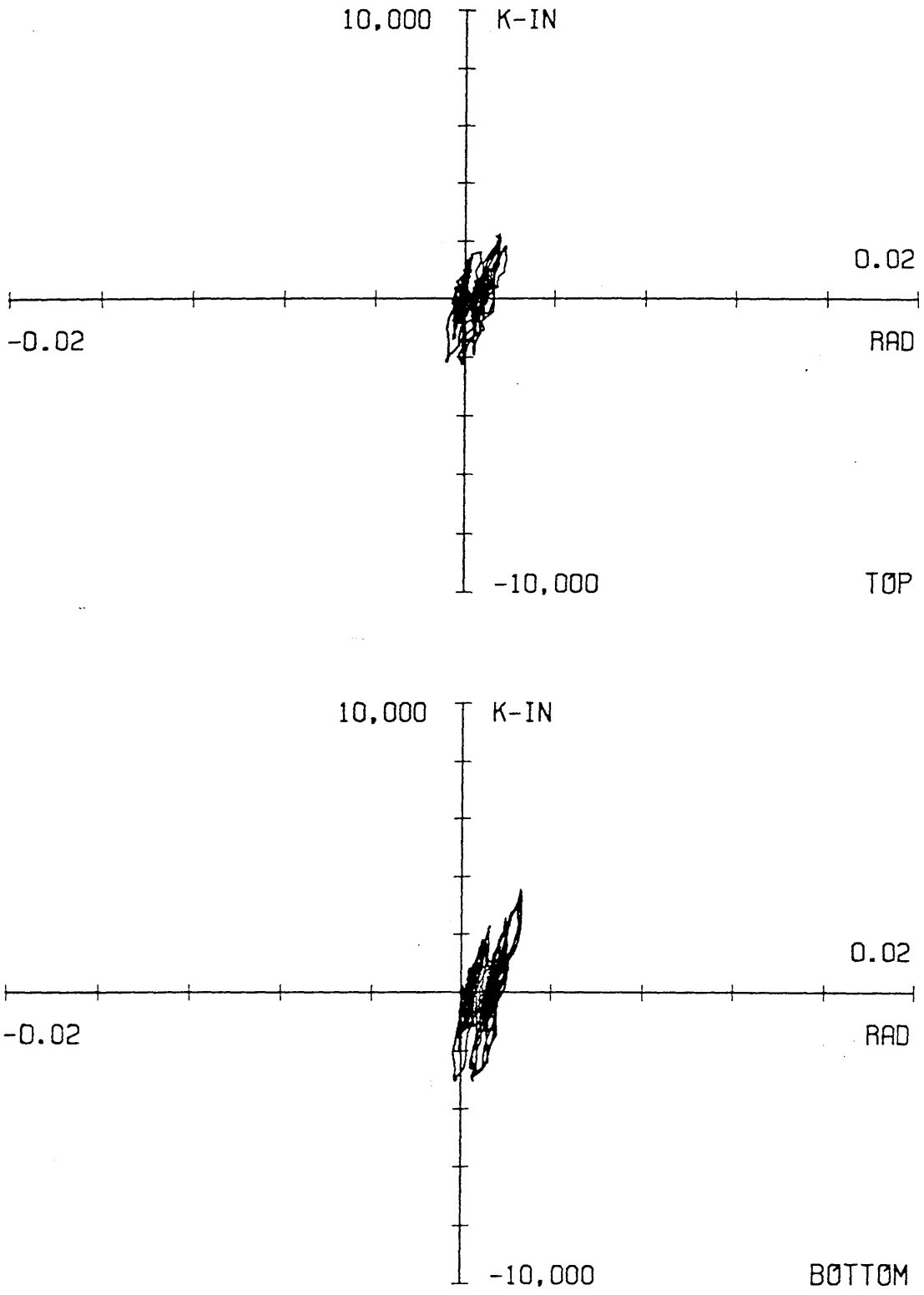

Fig. 5.15 Moment-rotation relationships for the top and bottom of the A2 column of the first story during the Phase II Inelastic test

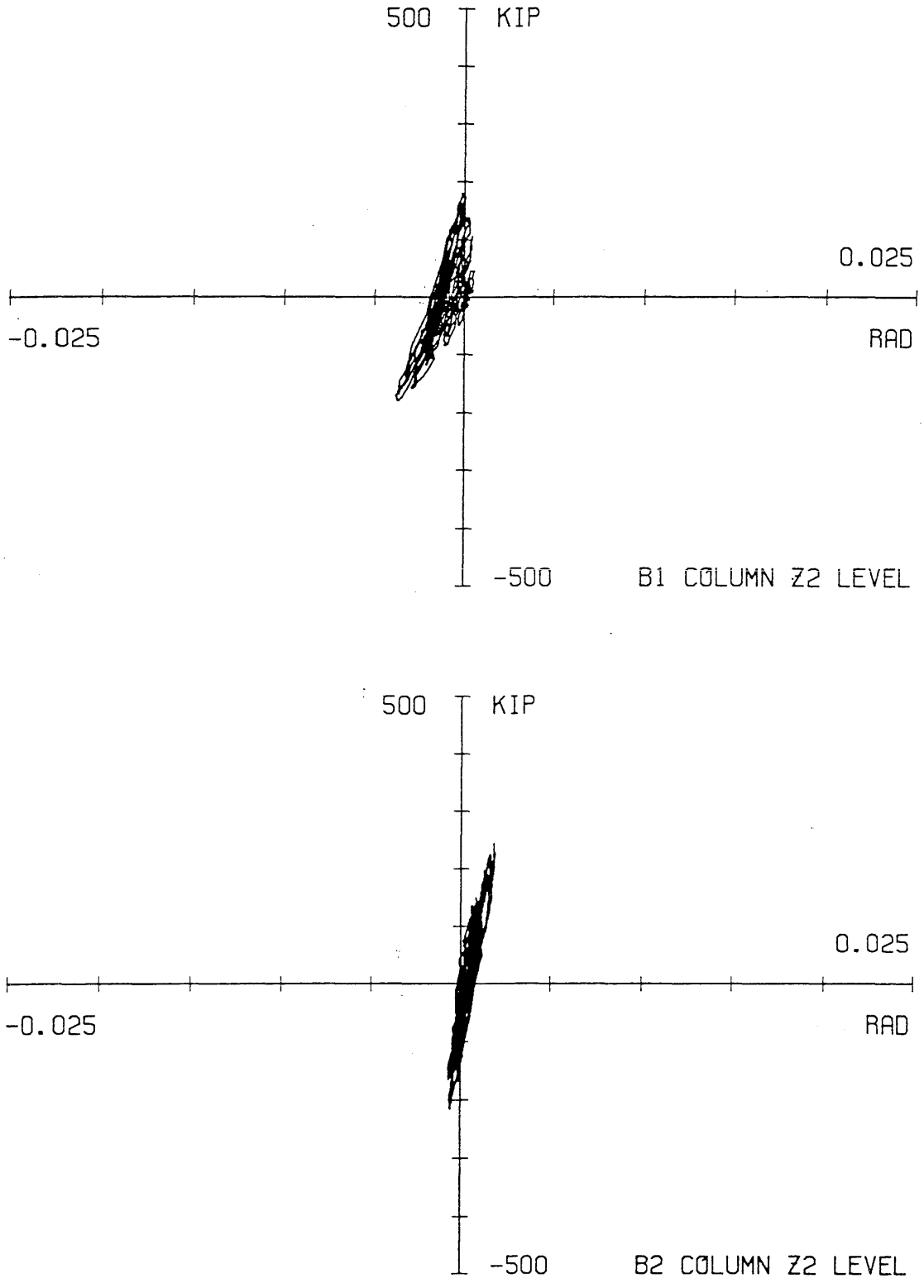

Fig. 5.16 Panel zone response for the B1 and B2 columns at the Z2 level for the Phase II Inelastic test

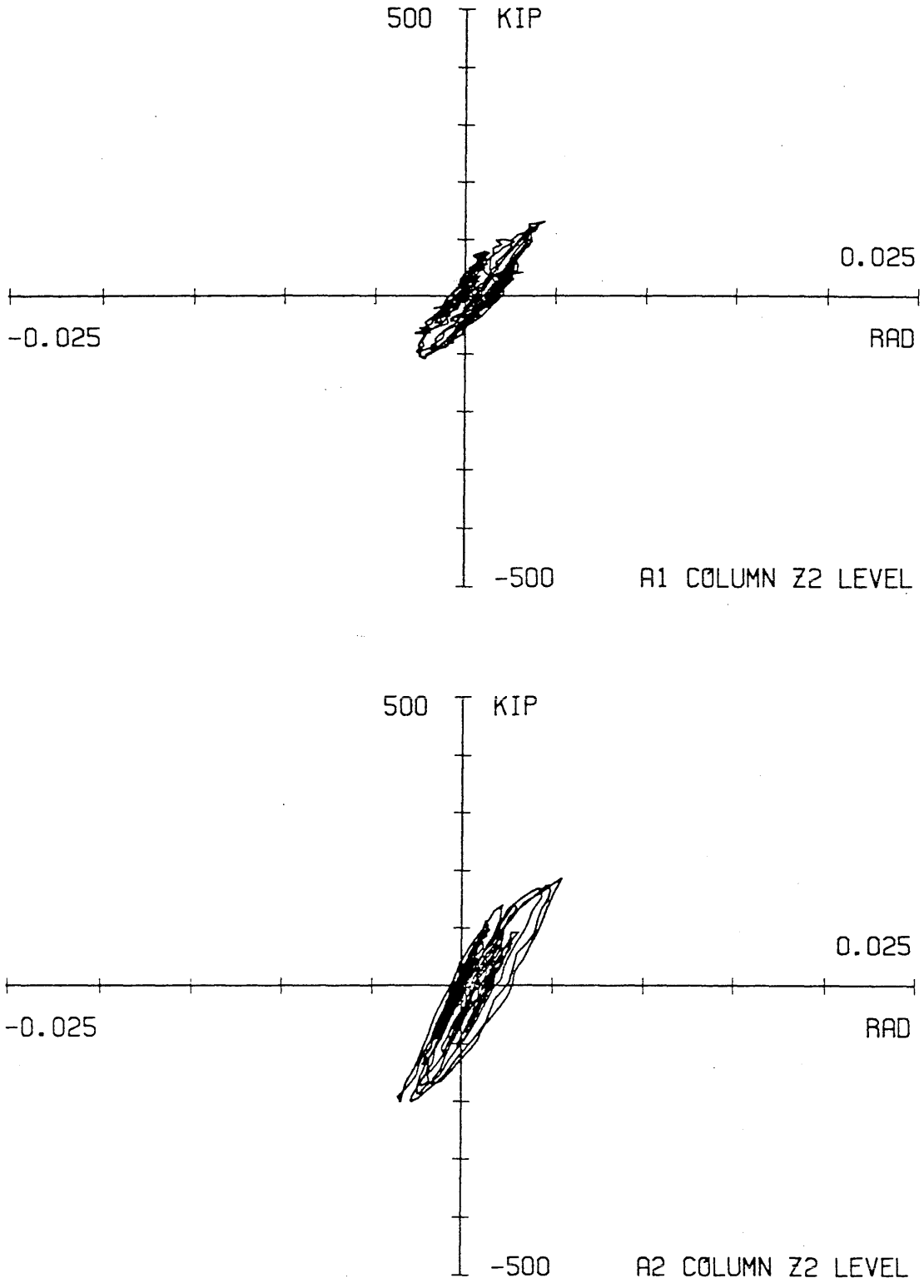

Fig. 5.17 Panel zone response for the A1 and A2 columns at the Z2 level for the Phase II Inelastic test

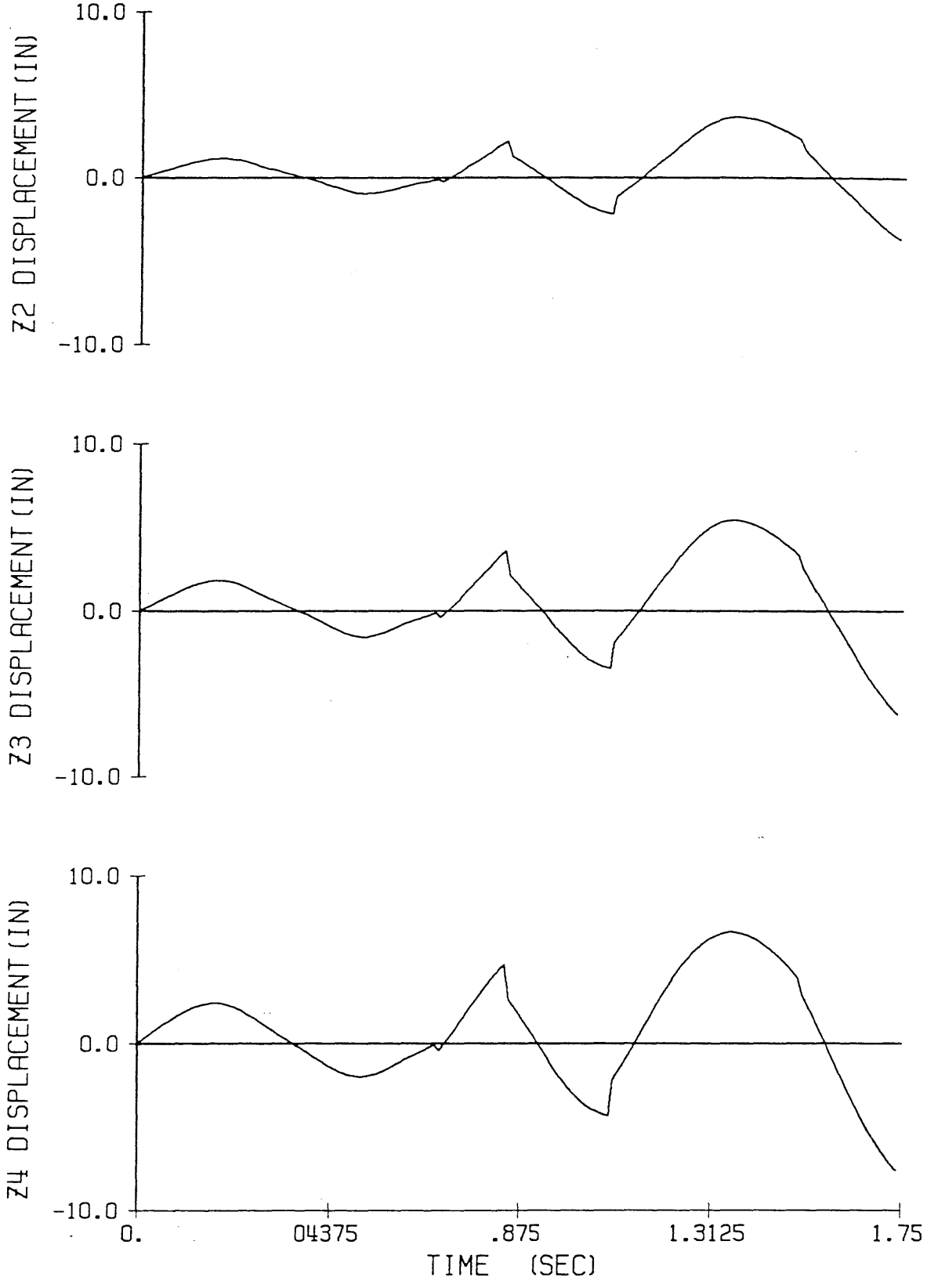

Fig. 5.18 Floor displacements vs. time for the Phase II Sinusoidal tests

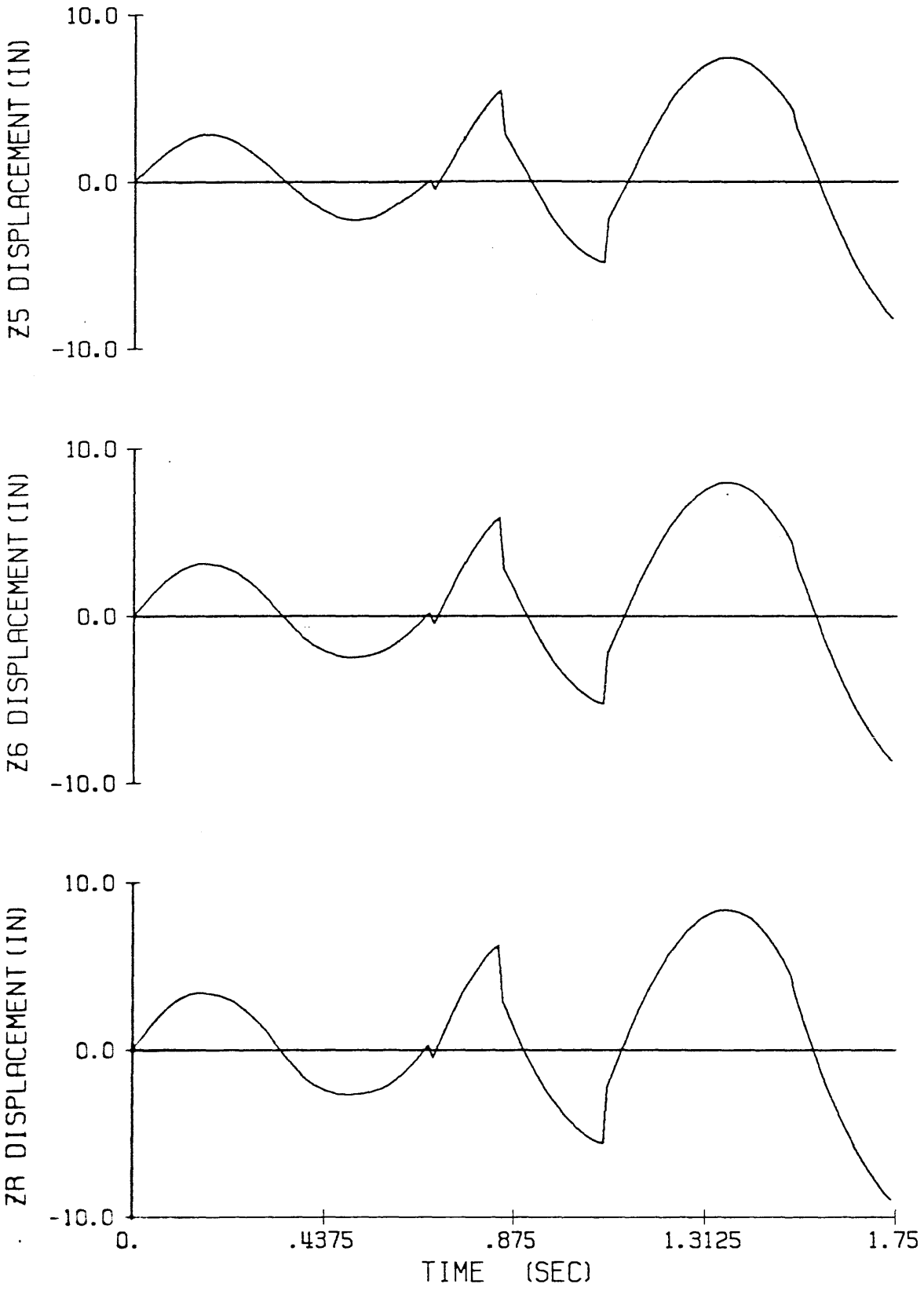

Fig. 5.18 (continued)

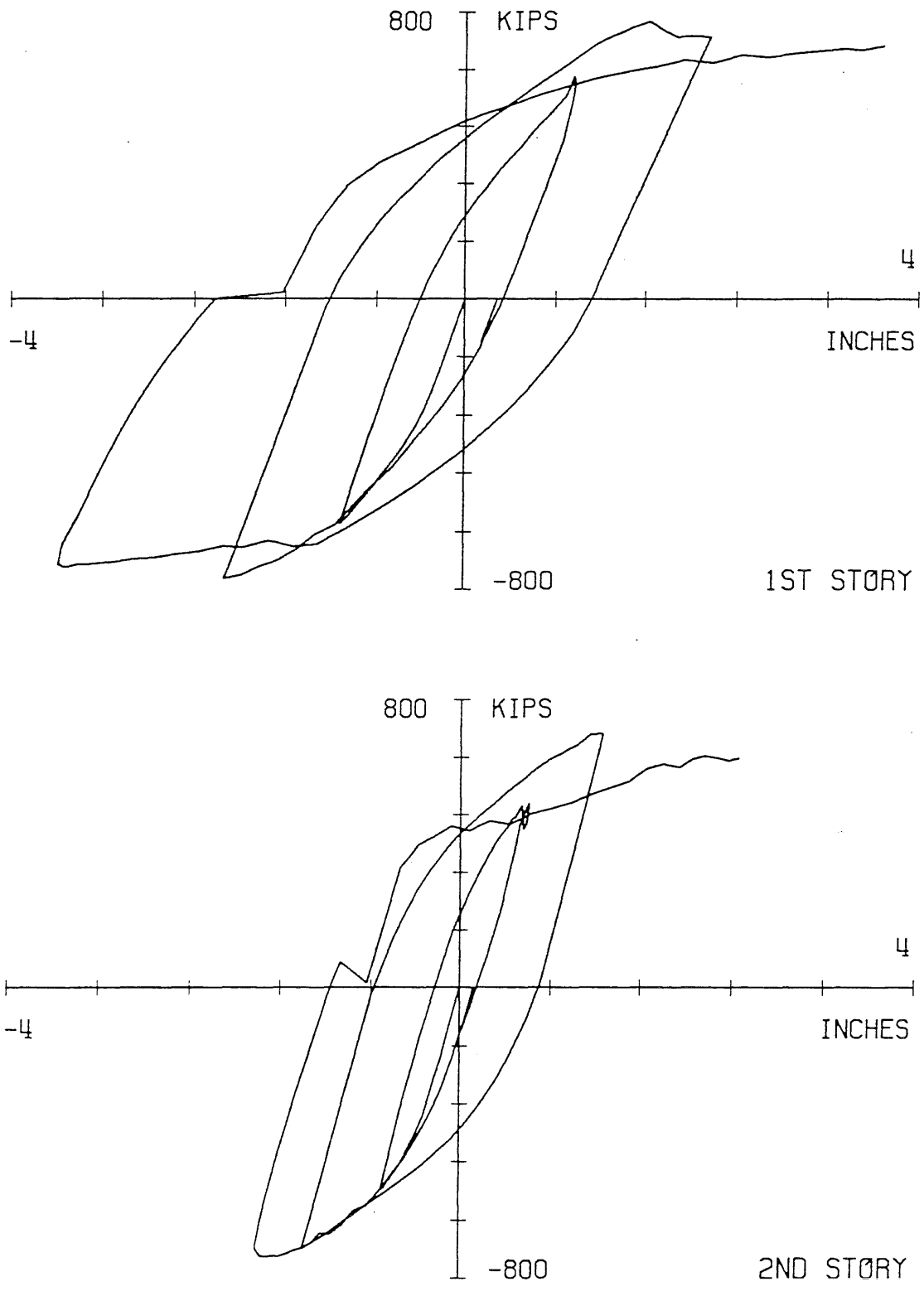

Fig. 5.19 Story shear vs. story displacement for the first and second stories for the Phase II Sinusoidal tests

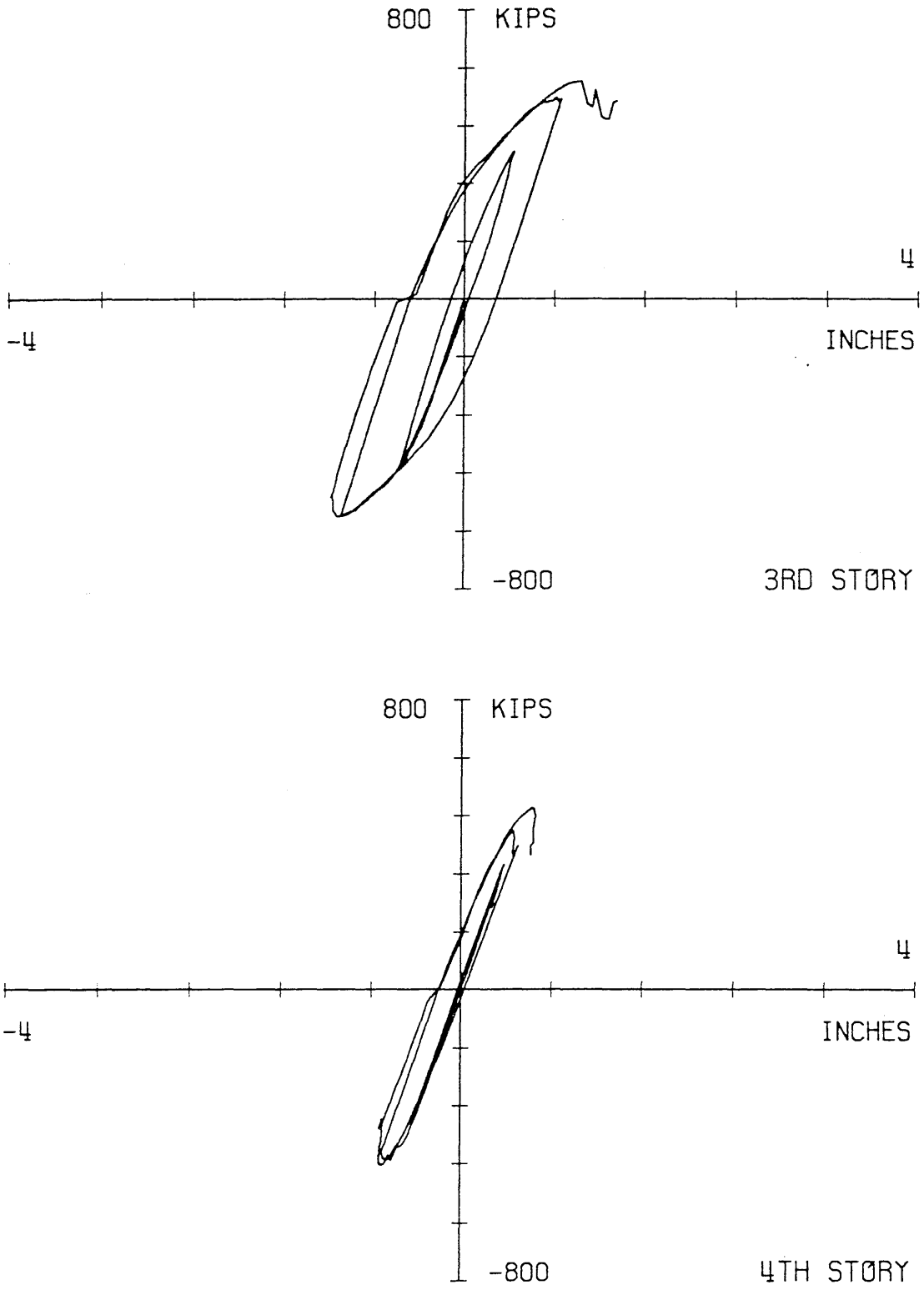

Fig. 5.20 Story shear vs. story displacement for the third and fourth stories for the Phase II Sinusoidal tests

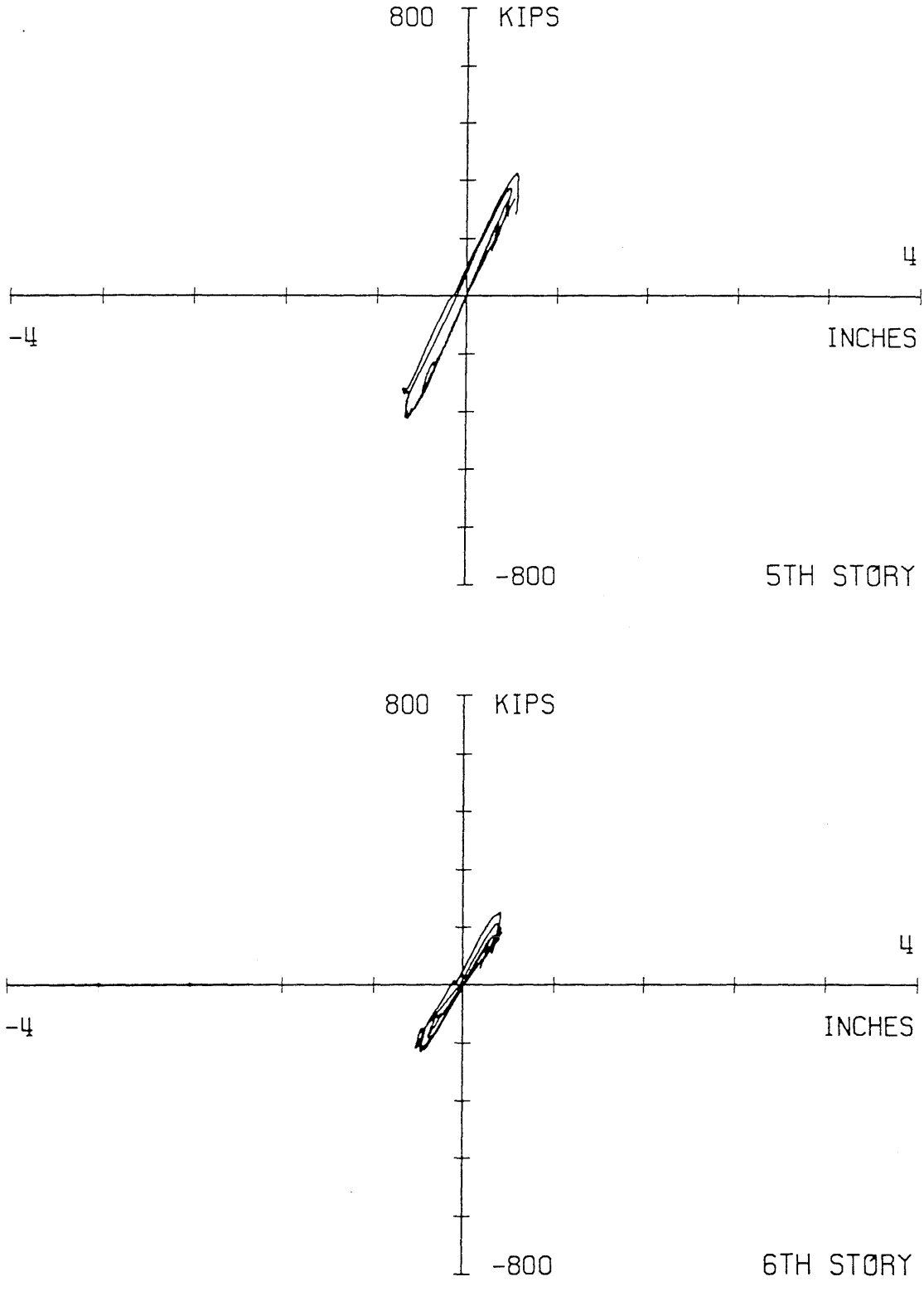

Fig. 5.21 Story shear vs. story displacement for the fifth and sixth stories for the Phase II Sinusoidal tests

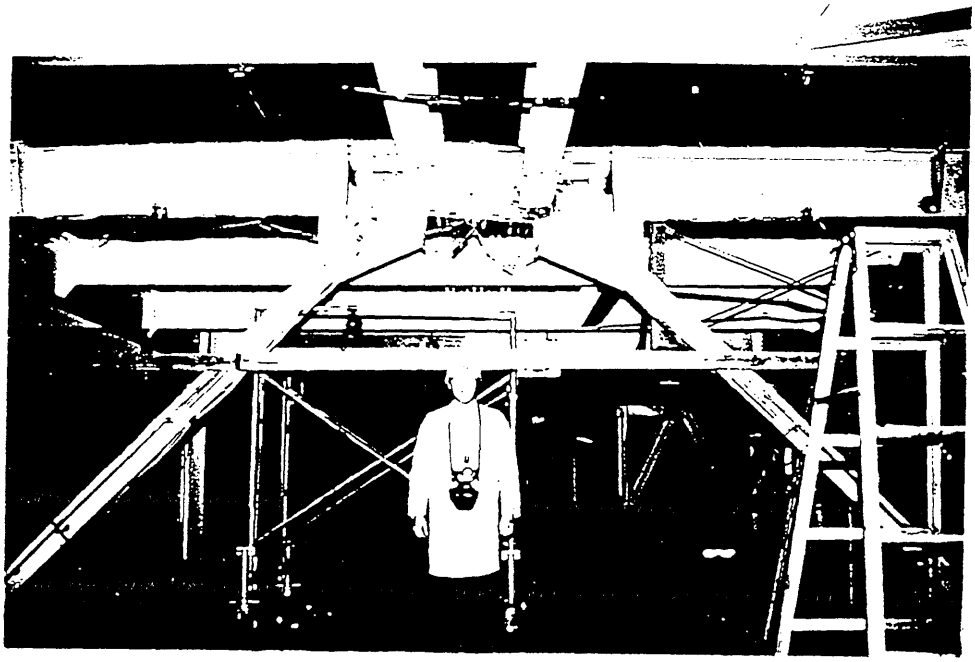

Fig. 5.22 Maximum deformation in the shear link at the 23 level during the Phase II Inelastic test and during the first cycle of the Sinusoidal test

Fig. 5.23 Yielding and tearing of the gusset plate at the Z2 level during the second cycle of the Sinusoidal test

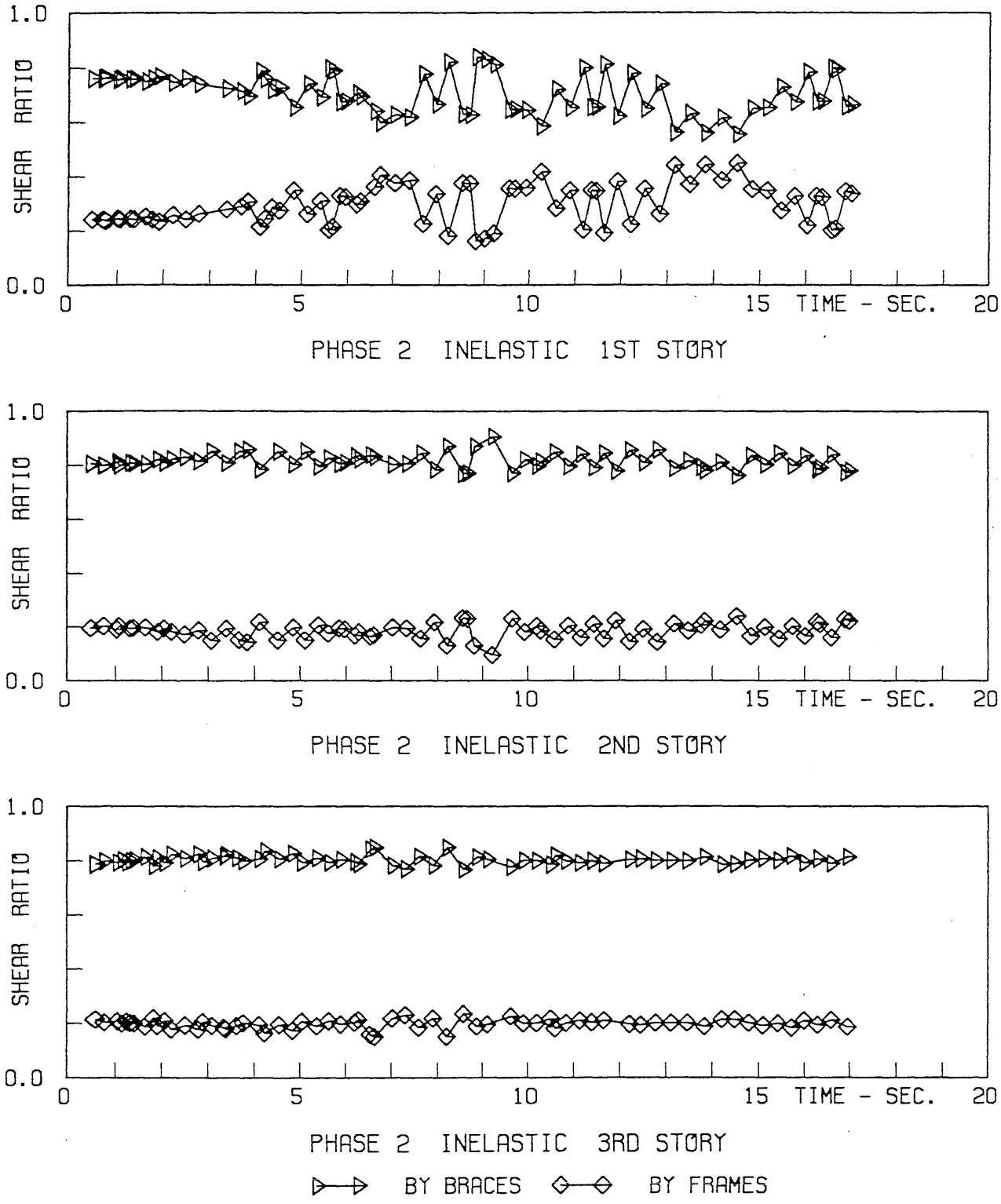

Fig. 5.24 Ratio of story shear carried by the braces to the total story shear for the first, second and third stories during the Phase II Inelastic tests

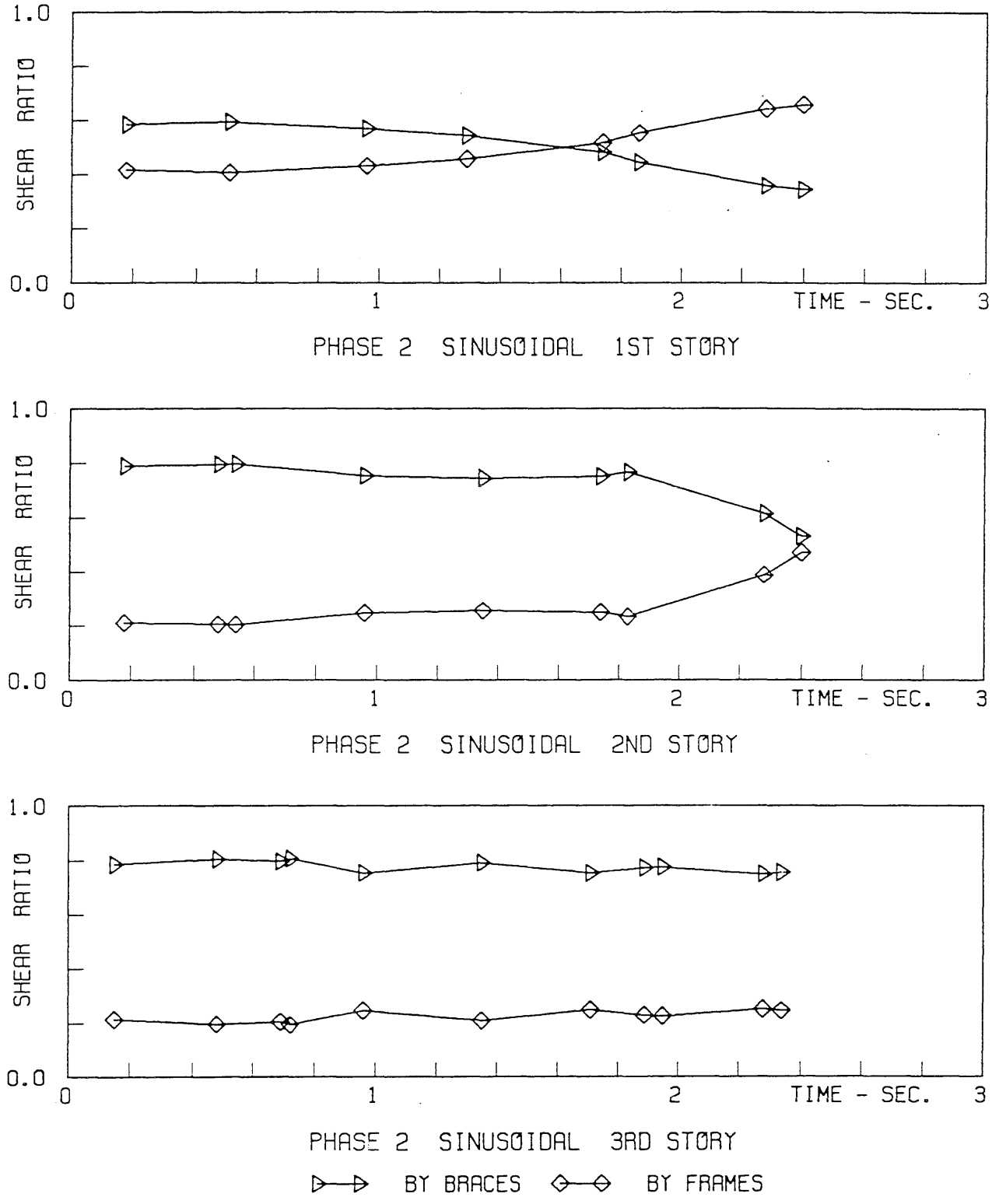

Fig. 5.25 Ratio of story shear carried by the braces to the total story shear for the first, second and third stories during the Phase II Sinusoidal tests

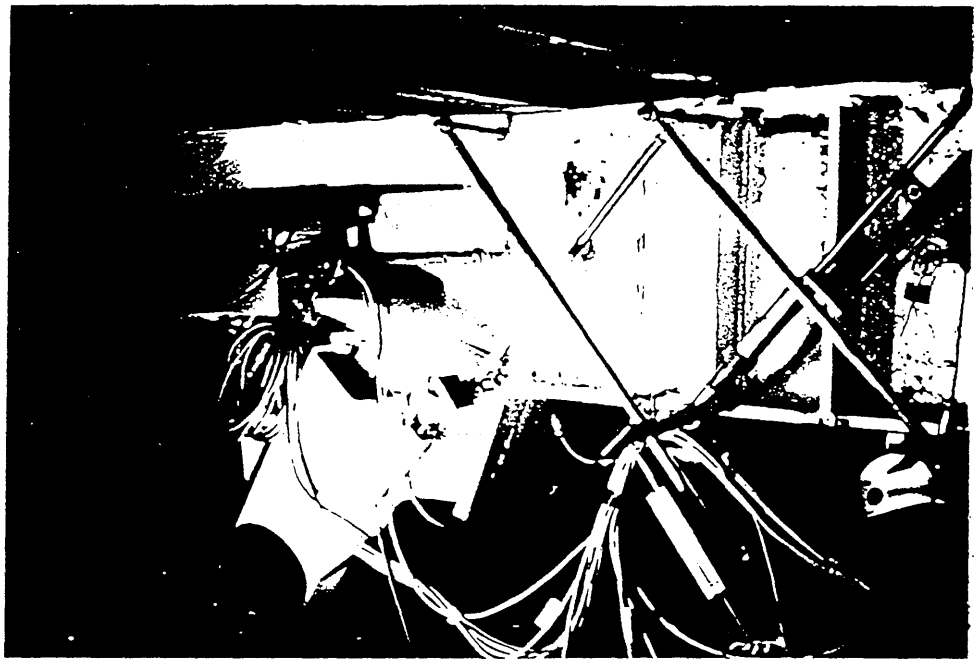

West side of shear link of 2F girder at maximum negative floor displacement

West side of north-brace gusset plate at 2F girder

Fig. 5.26 Damage to the brace-to-girder connection for the braces in the first story during the Phase II Sinusoidal tests

Looking up at 2F girder shear link at maximum negative displacement

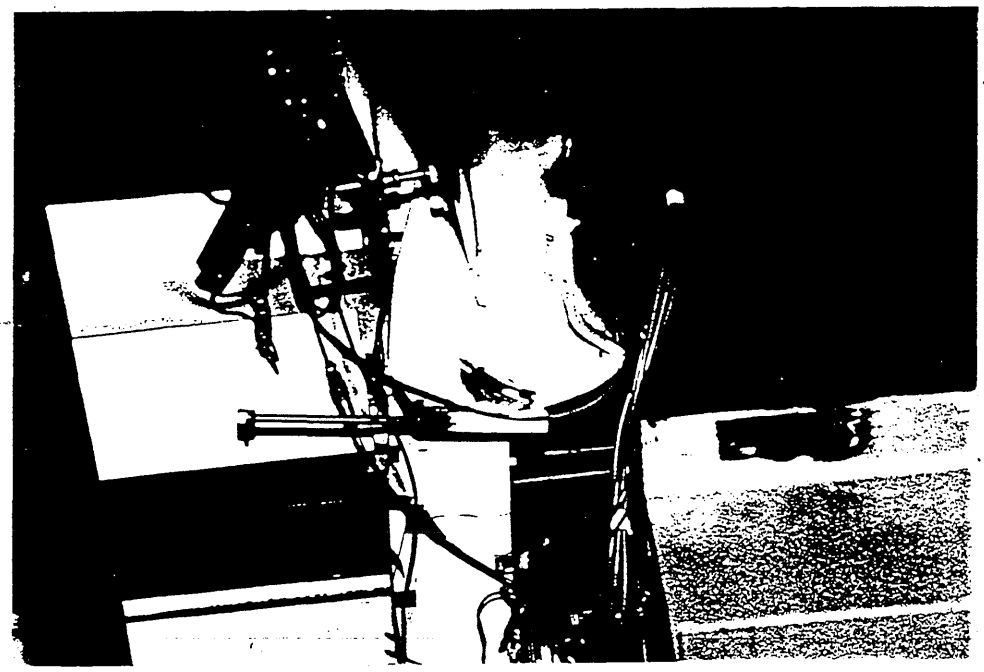

Looking up at 2F girder shear link at maximum negative displacement for

Fig. 5.26 (continued)

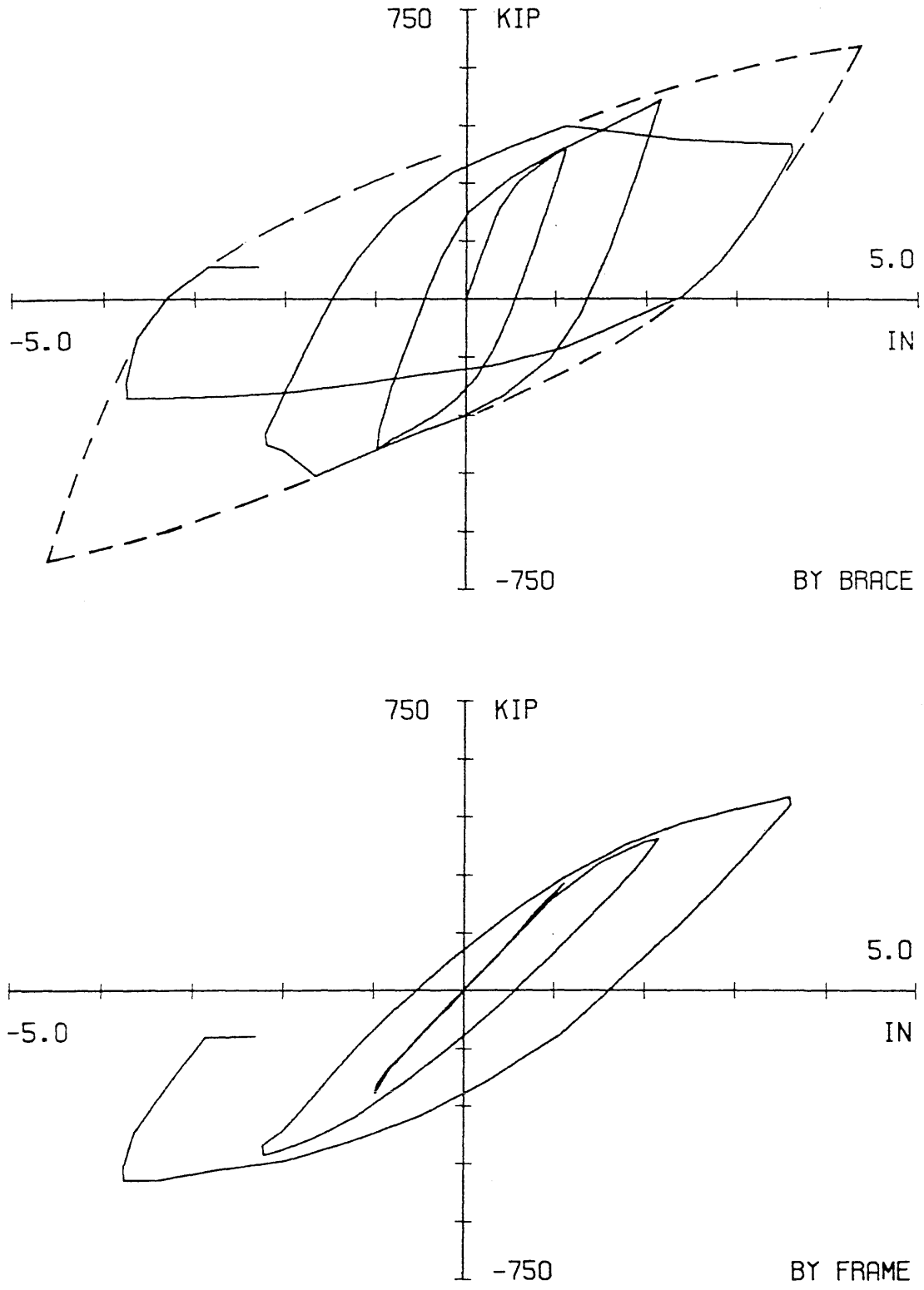

Fig. 5.27 Story shear vs. story displacements as carried (a) by the braces and (b) by the moment frames of the first story during the Phase II Sinusoidal tests

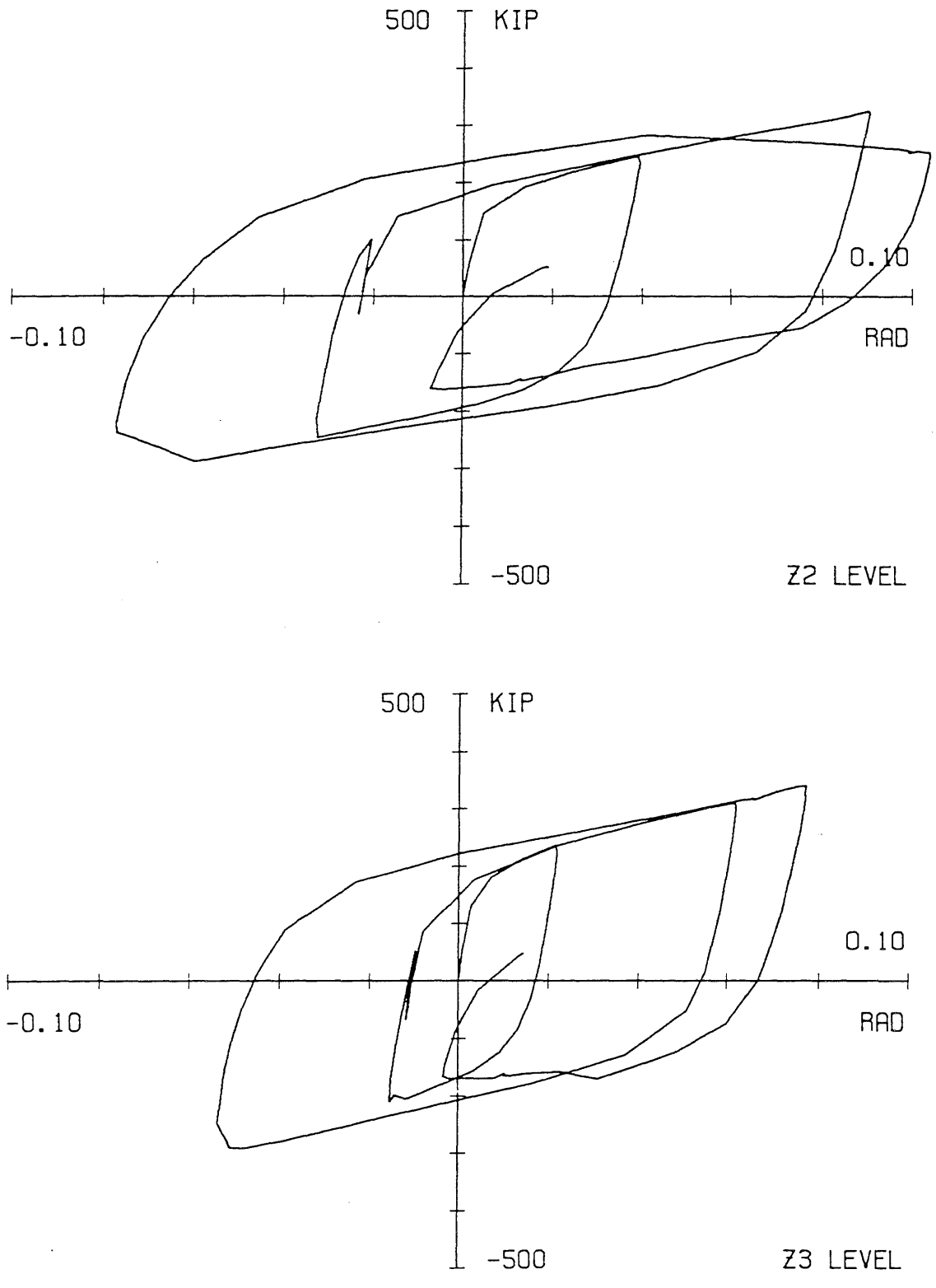

Fig. 5.28 Shear link response at the Z2 and Z3 levels during the Phase II Sinusoidal tests

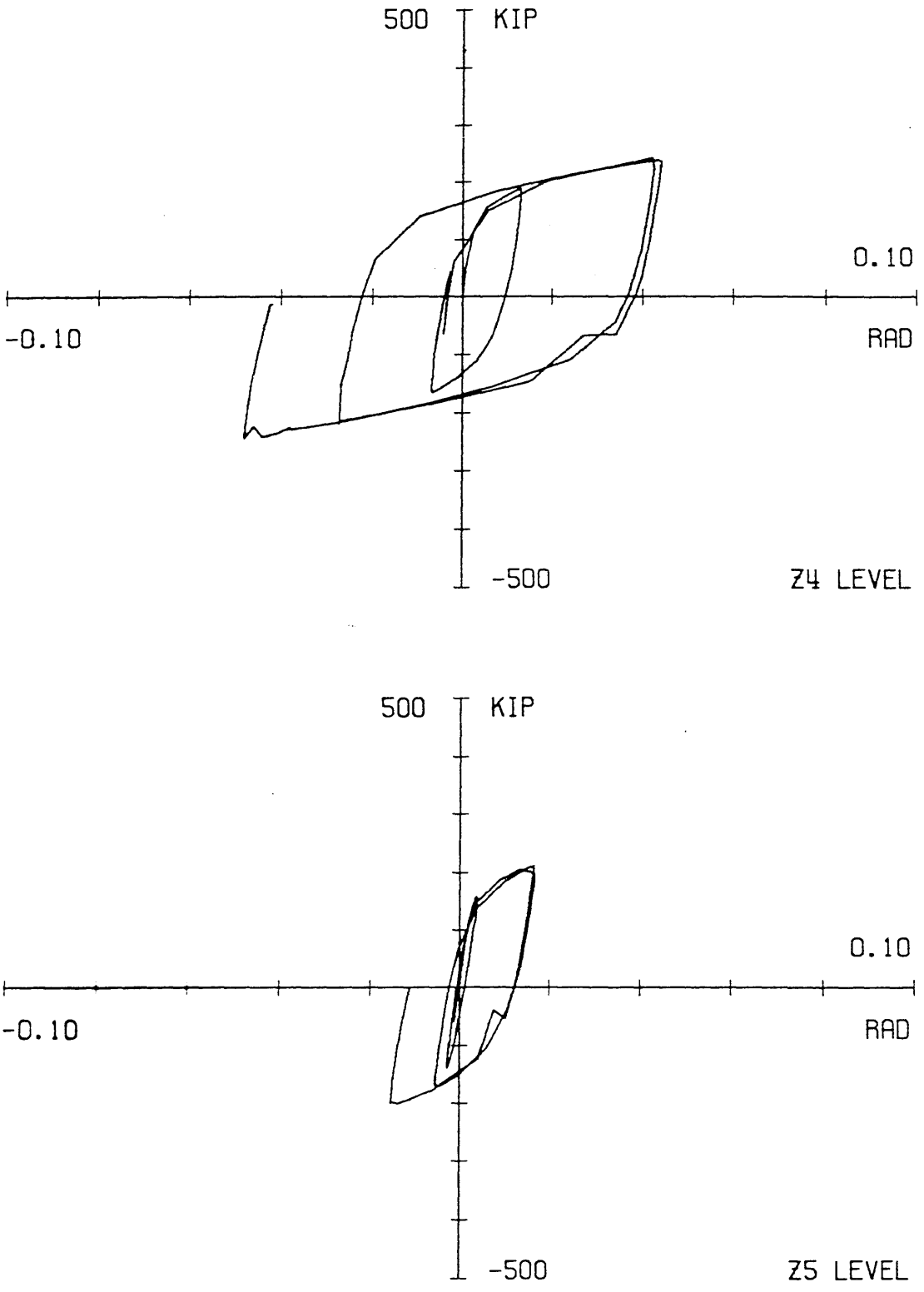

Fig. 5.29 Shear link response at the Z4 and Z5 levels during the Phase II Sinusoidal tests

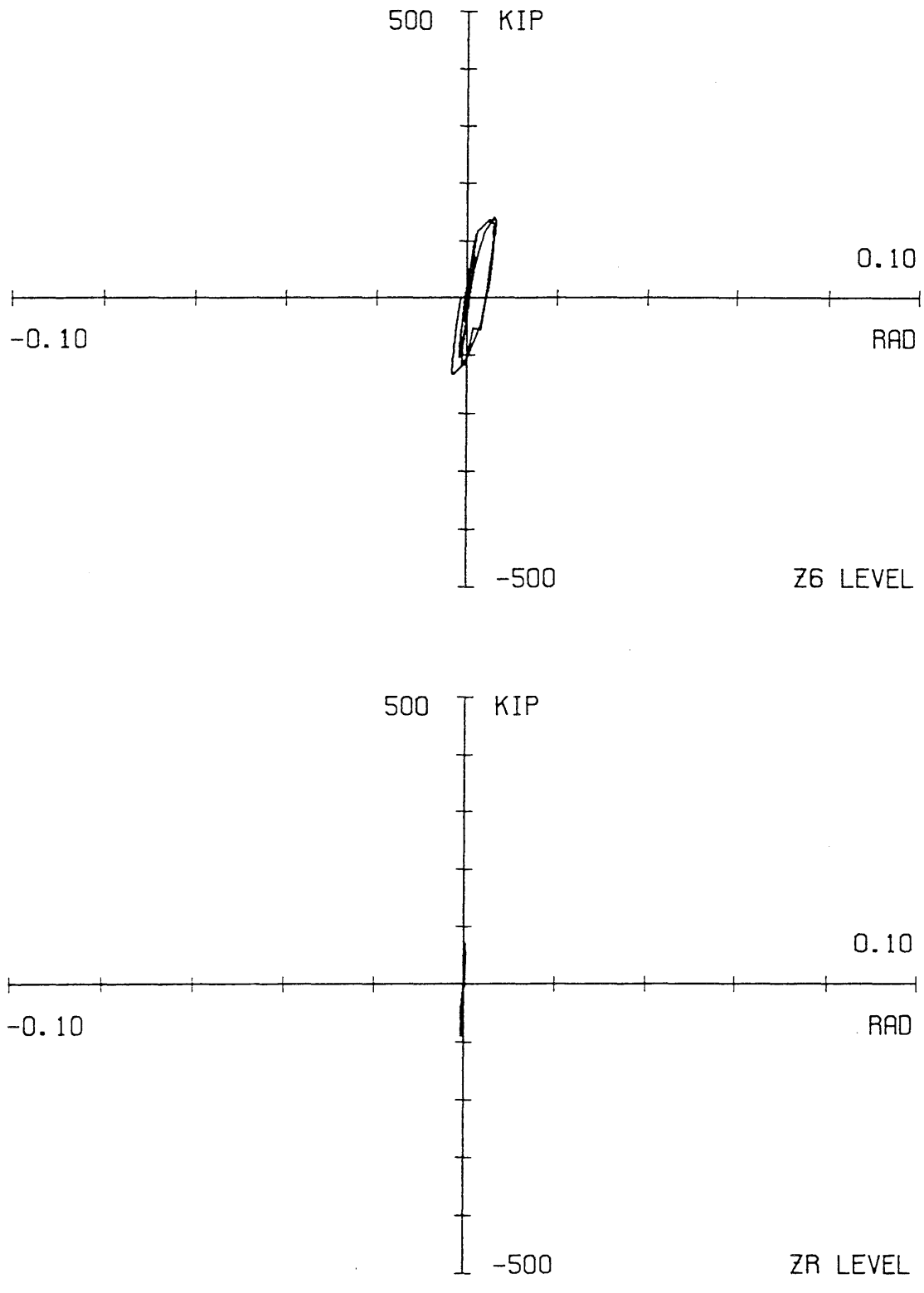

Fig. 5.30 Shear link response at the Z6 and ZR levels during the Phase II Sinusoidal tests

Fig. 5.31 Yielding at the bottom of the B2 column during the Sinusoidal tests

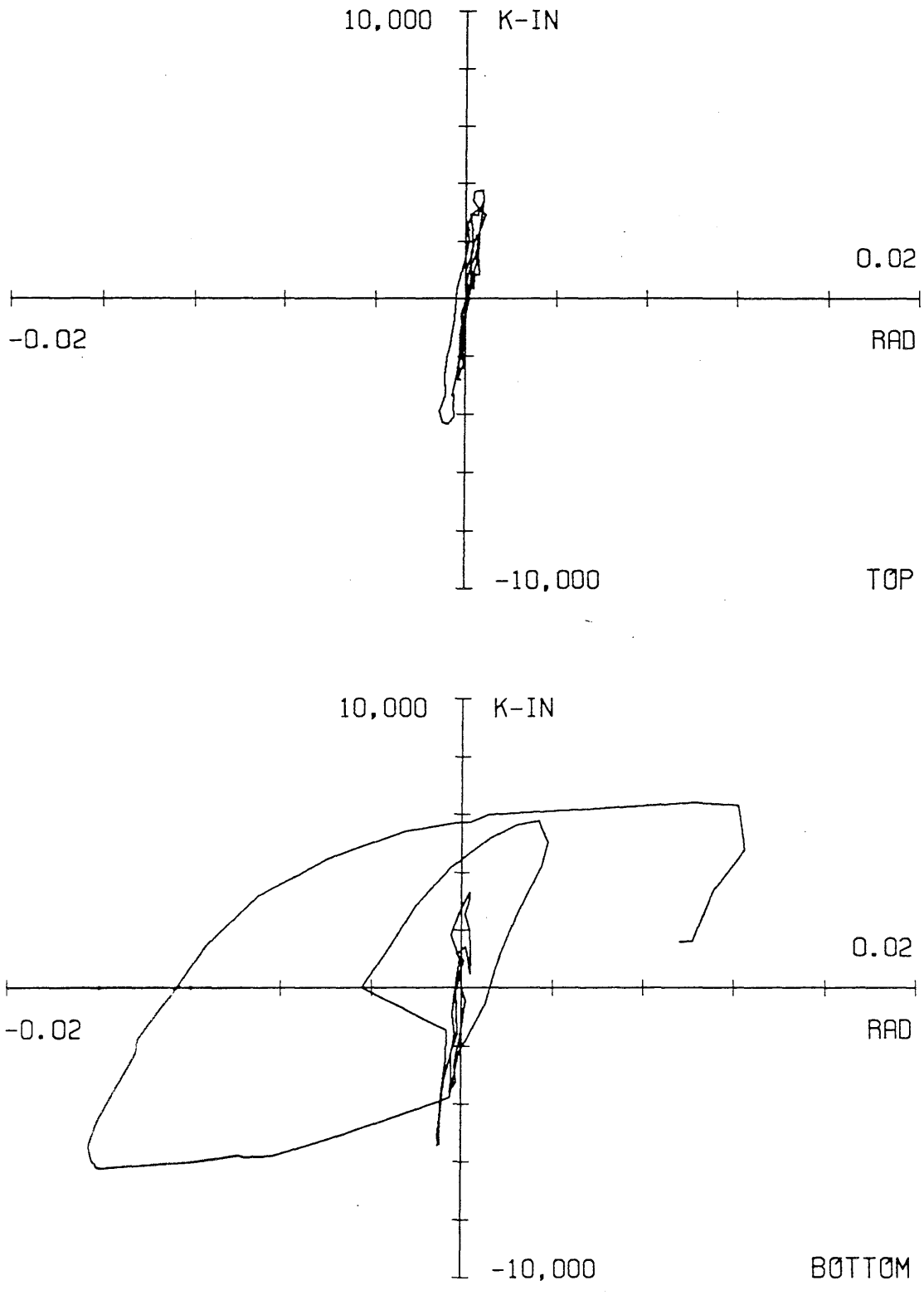

Fig. 5.32 Moment-rotation relationships for the top and bottom of the B1 column of the first story during the Phase II Sinusoidal tests

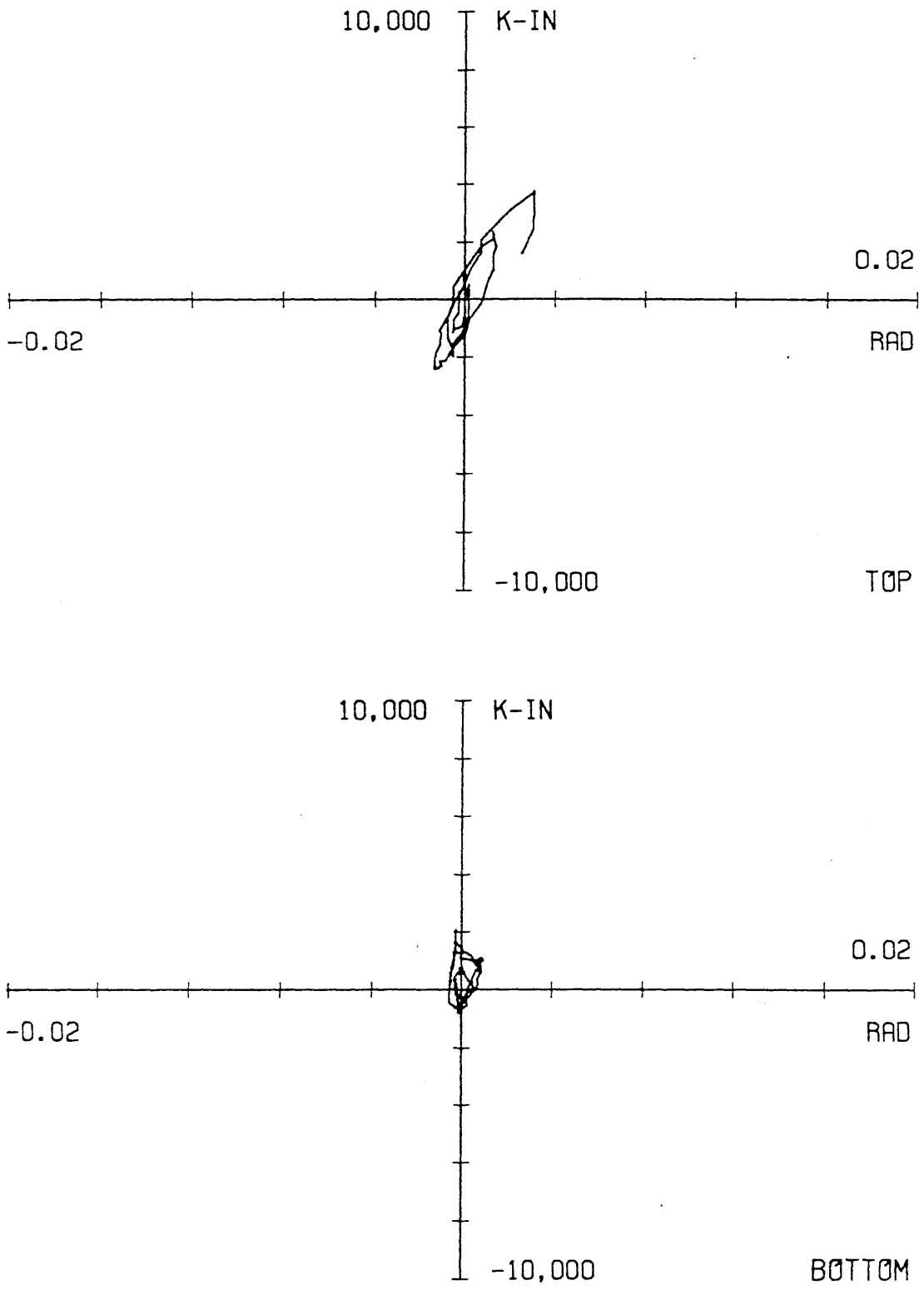

Fig. 5.33 Moment-rotation relationships for the top and bottom of the B1 column of the second story during the Phase II Sinusoidal tests

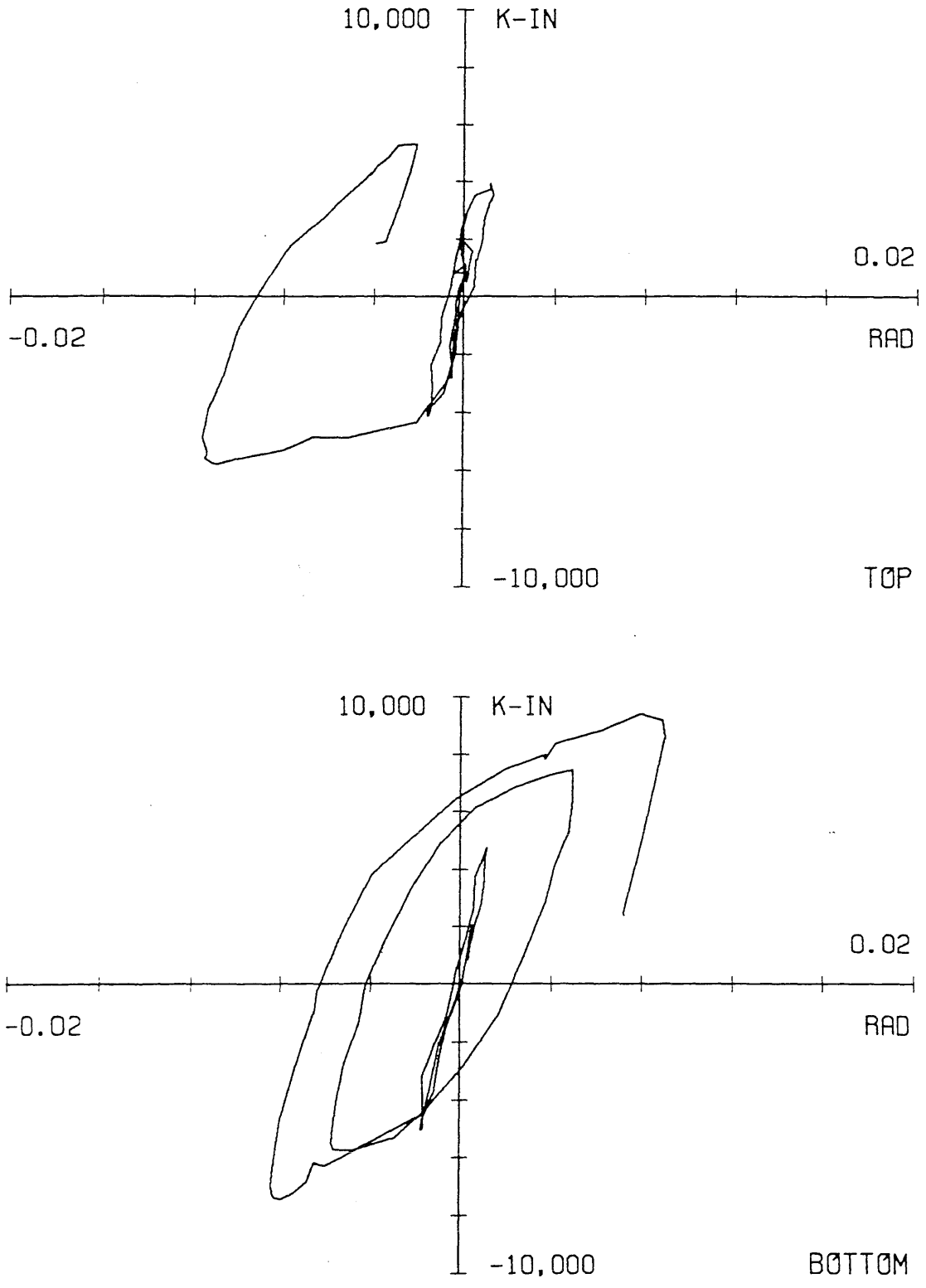

Fig. 5.34 Moment-rotation relationships for the top and bottom of the B2 column of the first story during the Phase II Sinusoidal tests

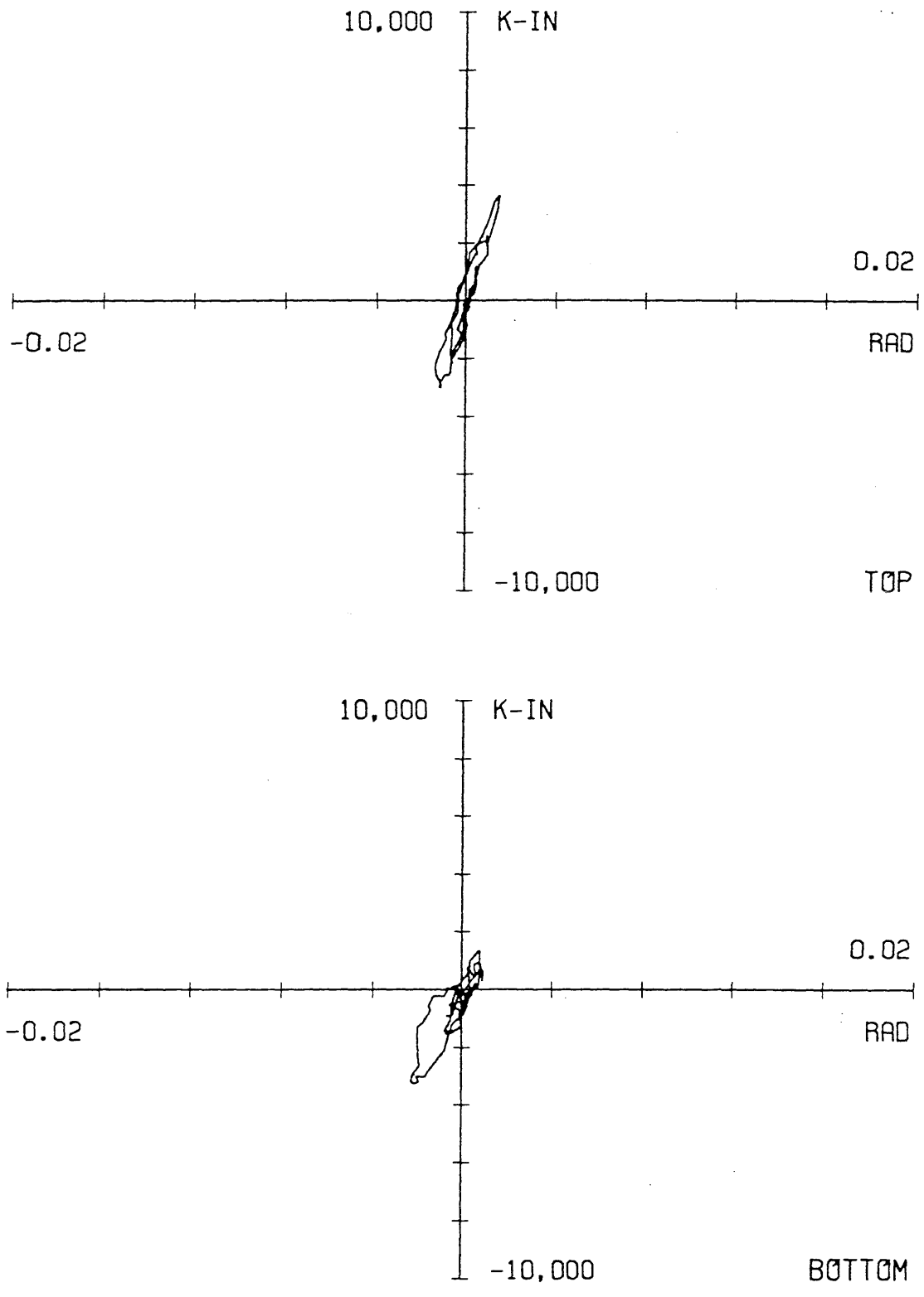

Fig. 5.35 Moment-rotation relationships for the top and bottom of the B2 column of the second story during the Phase II Sinusoidal tests

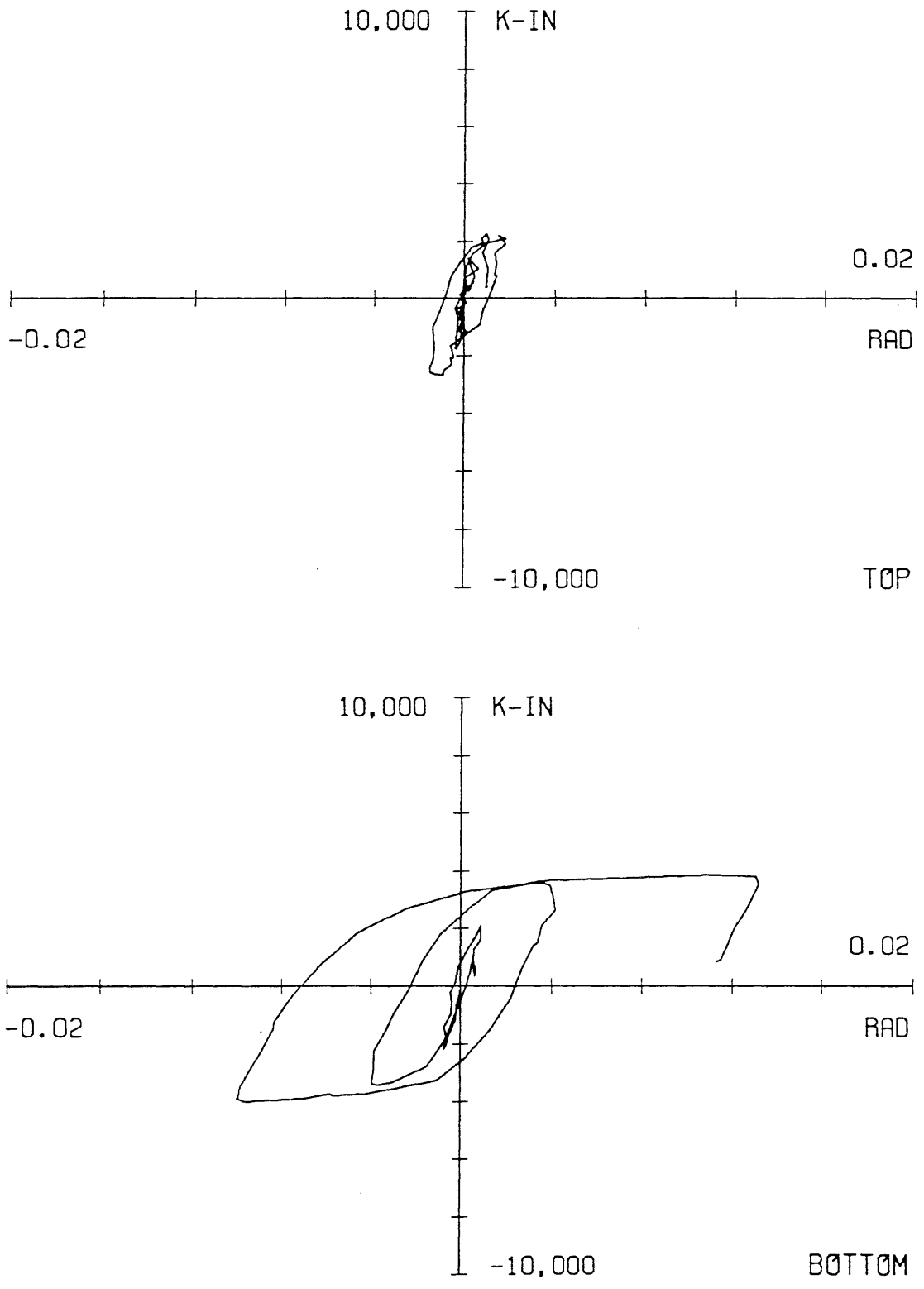

Fig. 5.36 Moment-rotation relationships for the top and bottom of the A1 column of the first story during the Phase II Sinusoidal tests

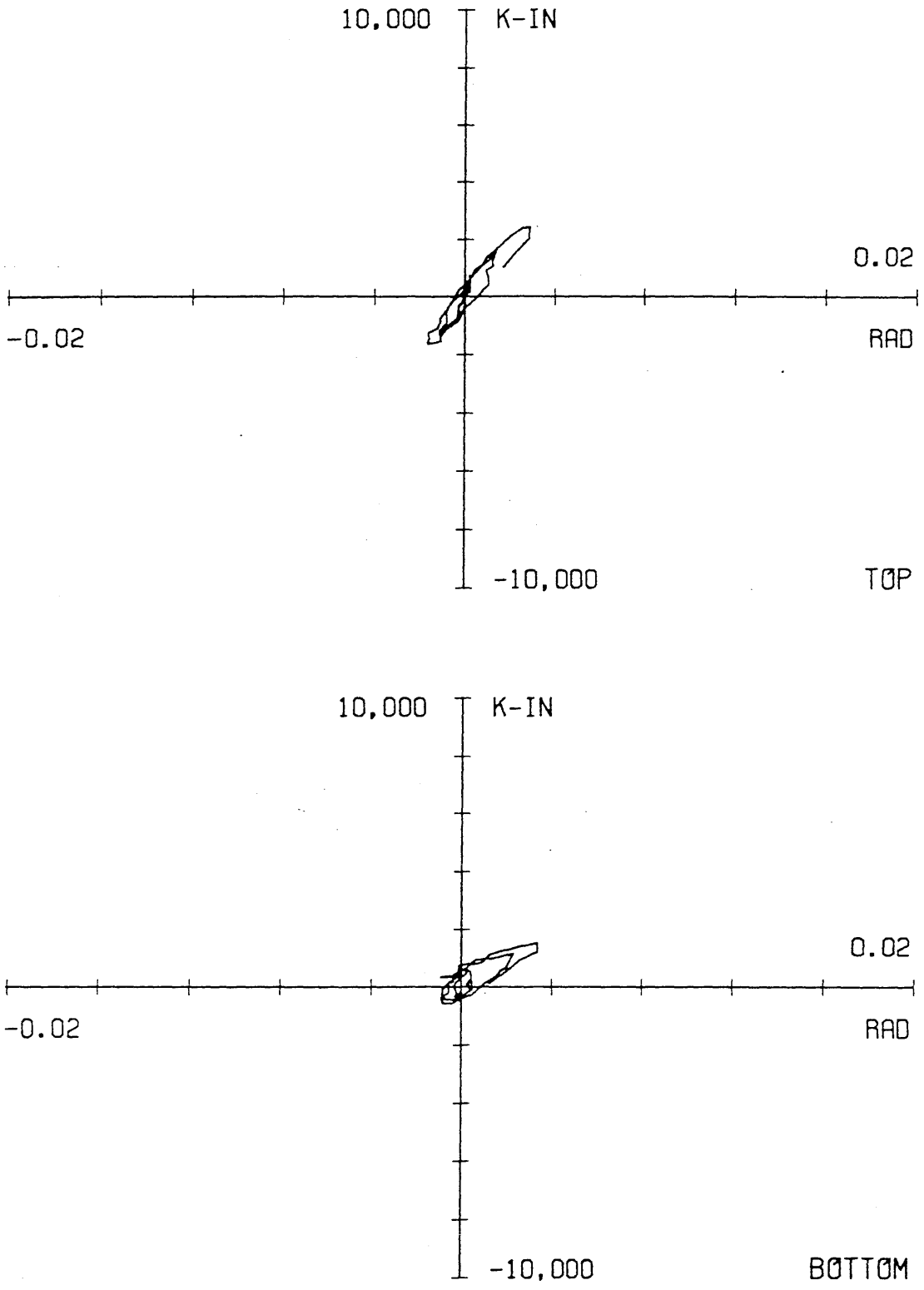

Fig. 5.37 Moment-rotation relationships for the top and bottom of the A1 column of the second story during the Phase II Sinusoidal tests

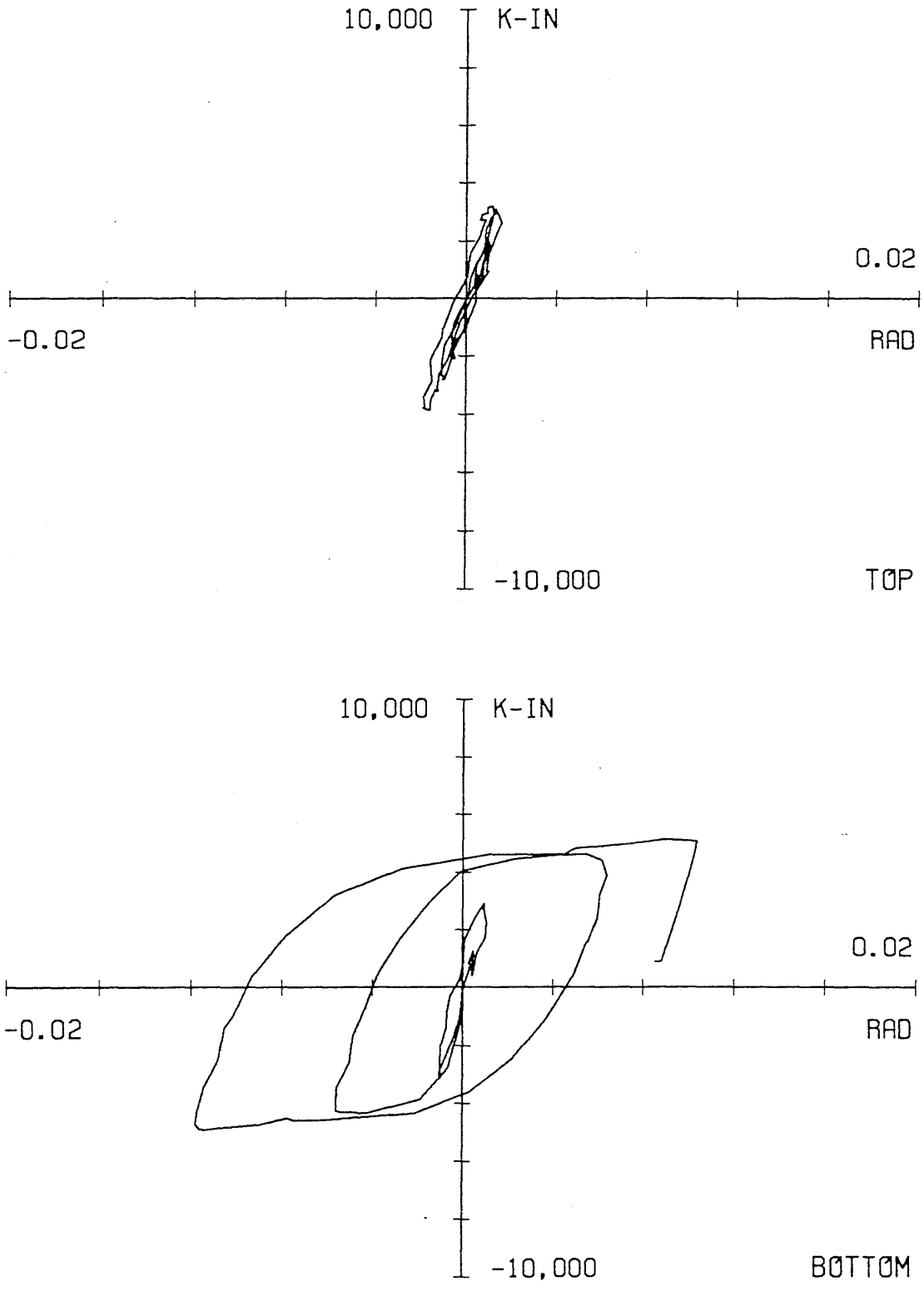

Fig. 5.38 Moment-rotation relationships for the top and bottom of the A2 column of the first story during the Phase II Sinusoidal tests

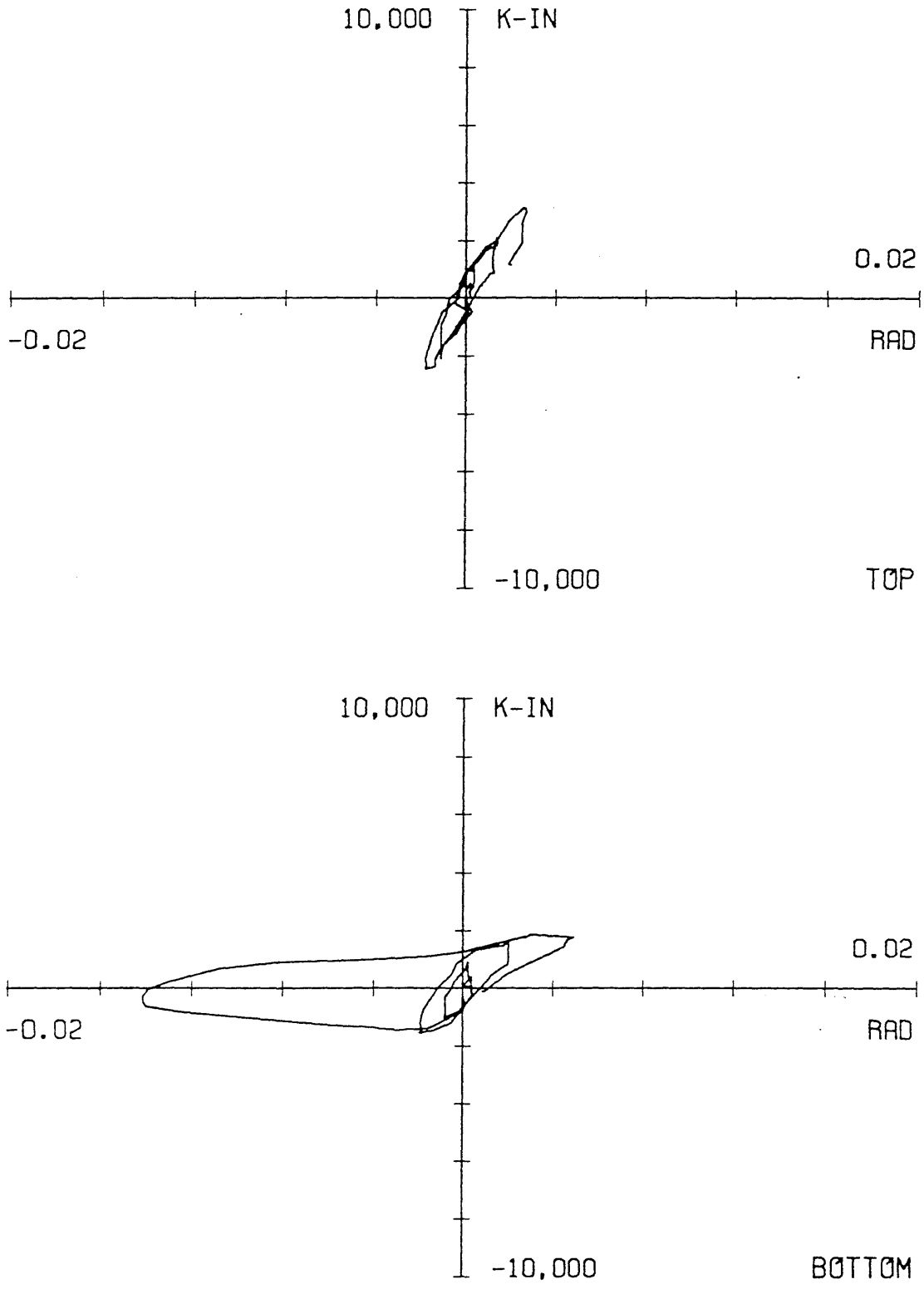

Fig. 5.39 Moment-rotation relationships for the top and bottom of the A2 column of the second story during the Phase II Sinusoidal tests

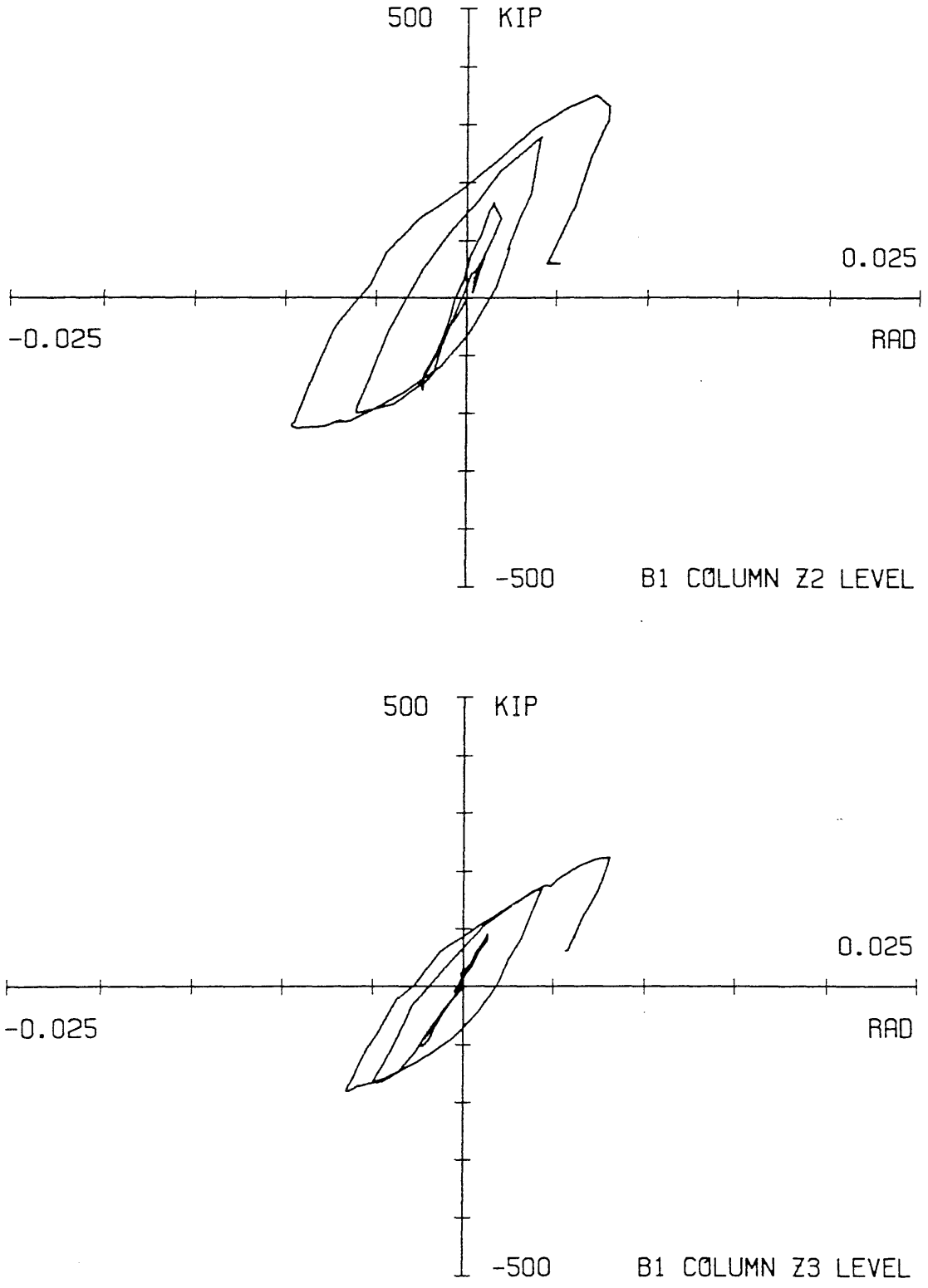

Fig. 5.40 Panel zone response for the B1 column at the Z2 and Z3 levels during the Phase II Sinusoidal tests

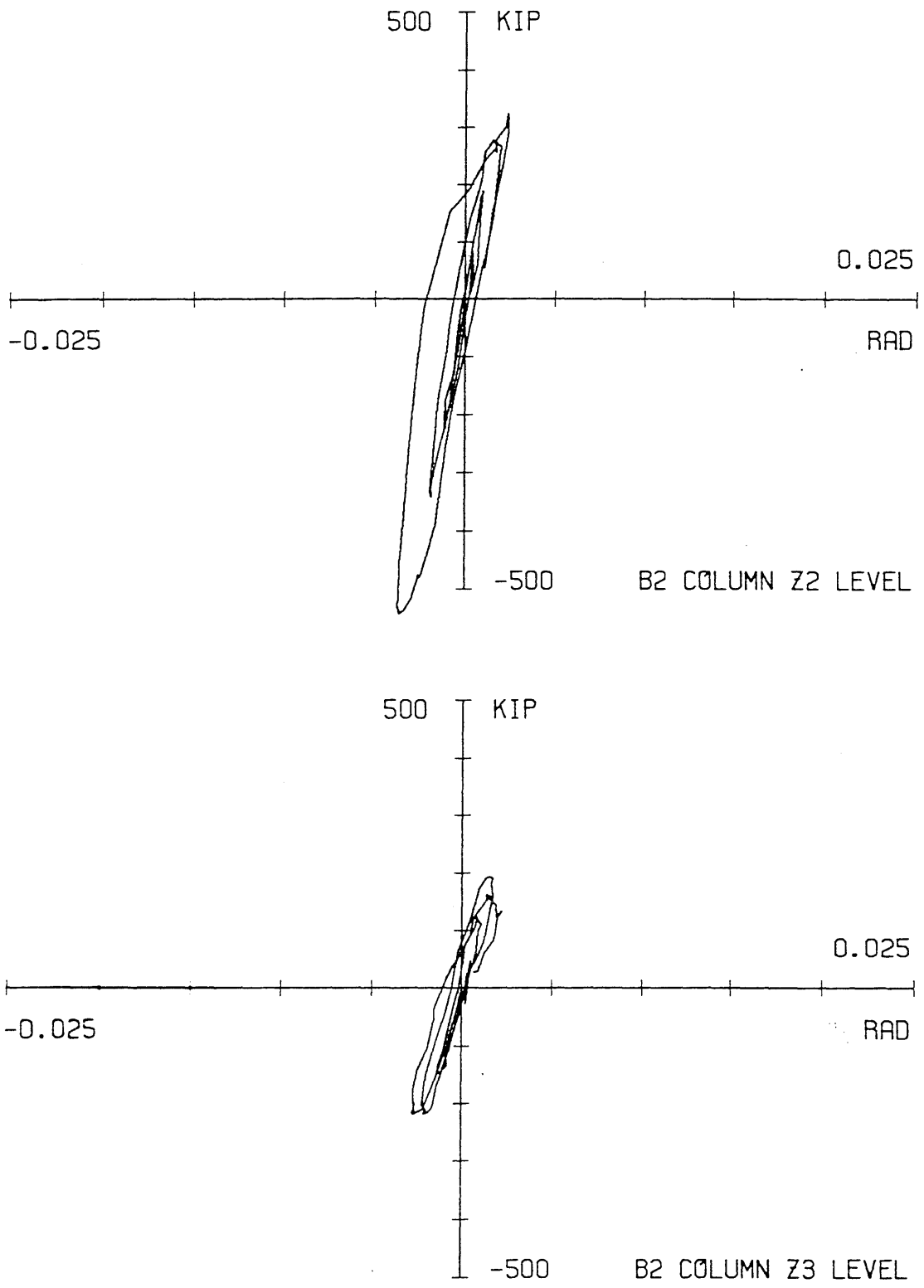

Fig. 5.41 Panel zone response for the B2 column at the Z2 and Z3 levels during the Phase II Sinusoidal tests

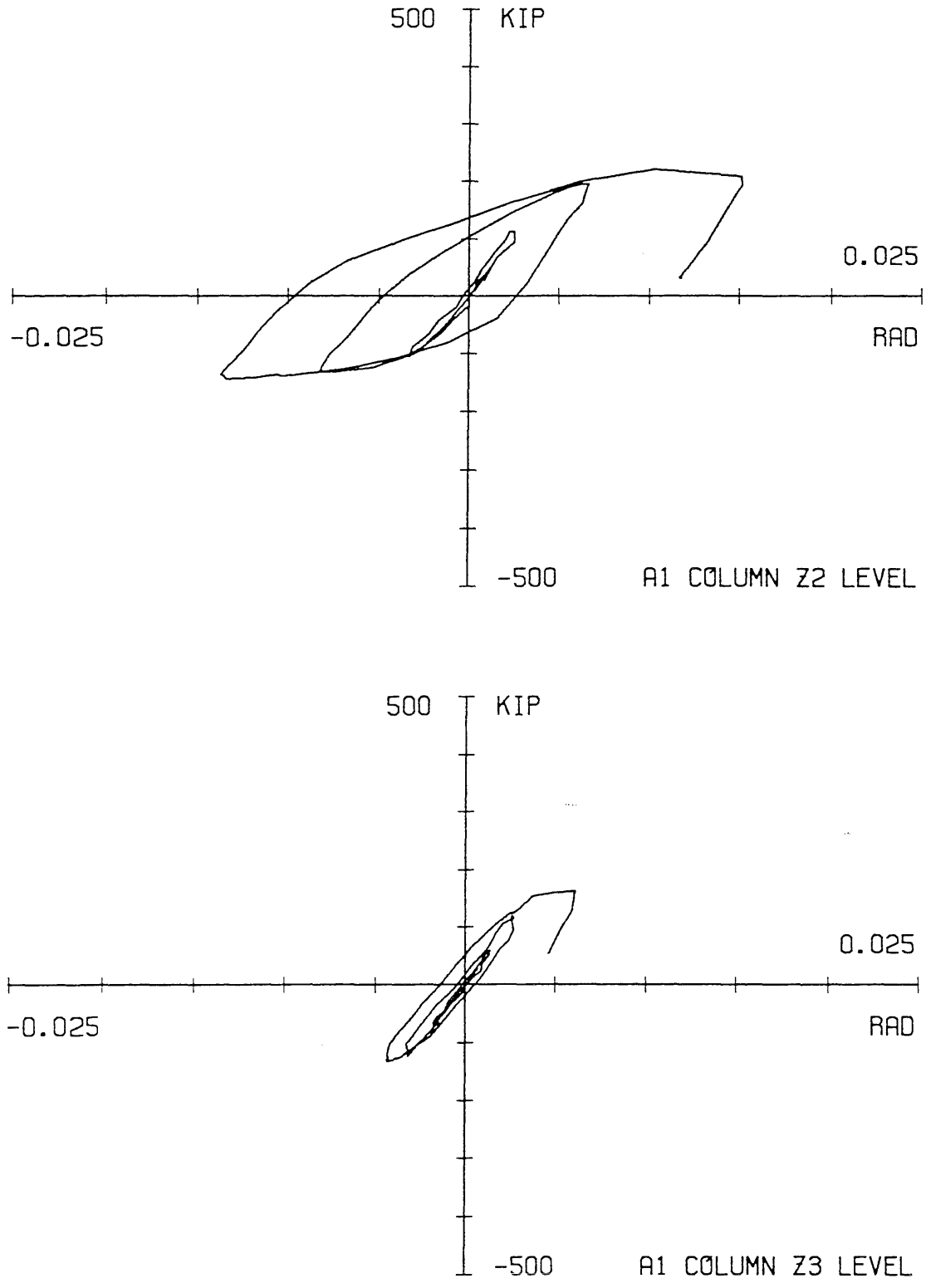

Fig. 5.42 Panel zone response for the A1 column at the Z2 and Z3 levels during the Phase II Sinusoidal tests

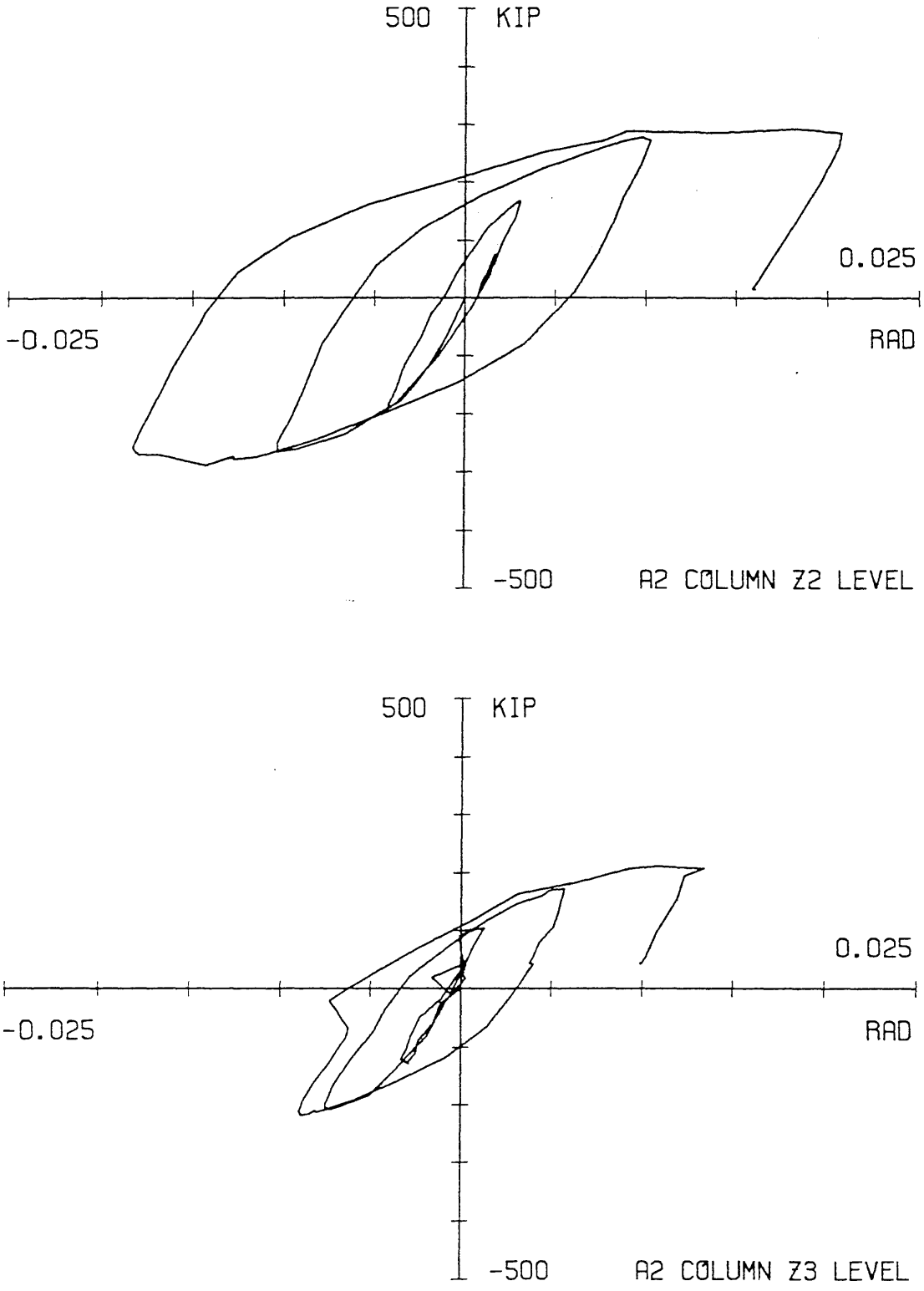

Fig. 5.43 Panel zone response for the A2 column at the Z2 and Z3 levels during the Phase II Sinusoidal tests

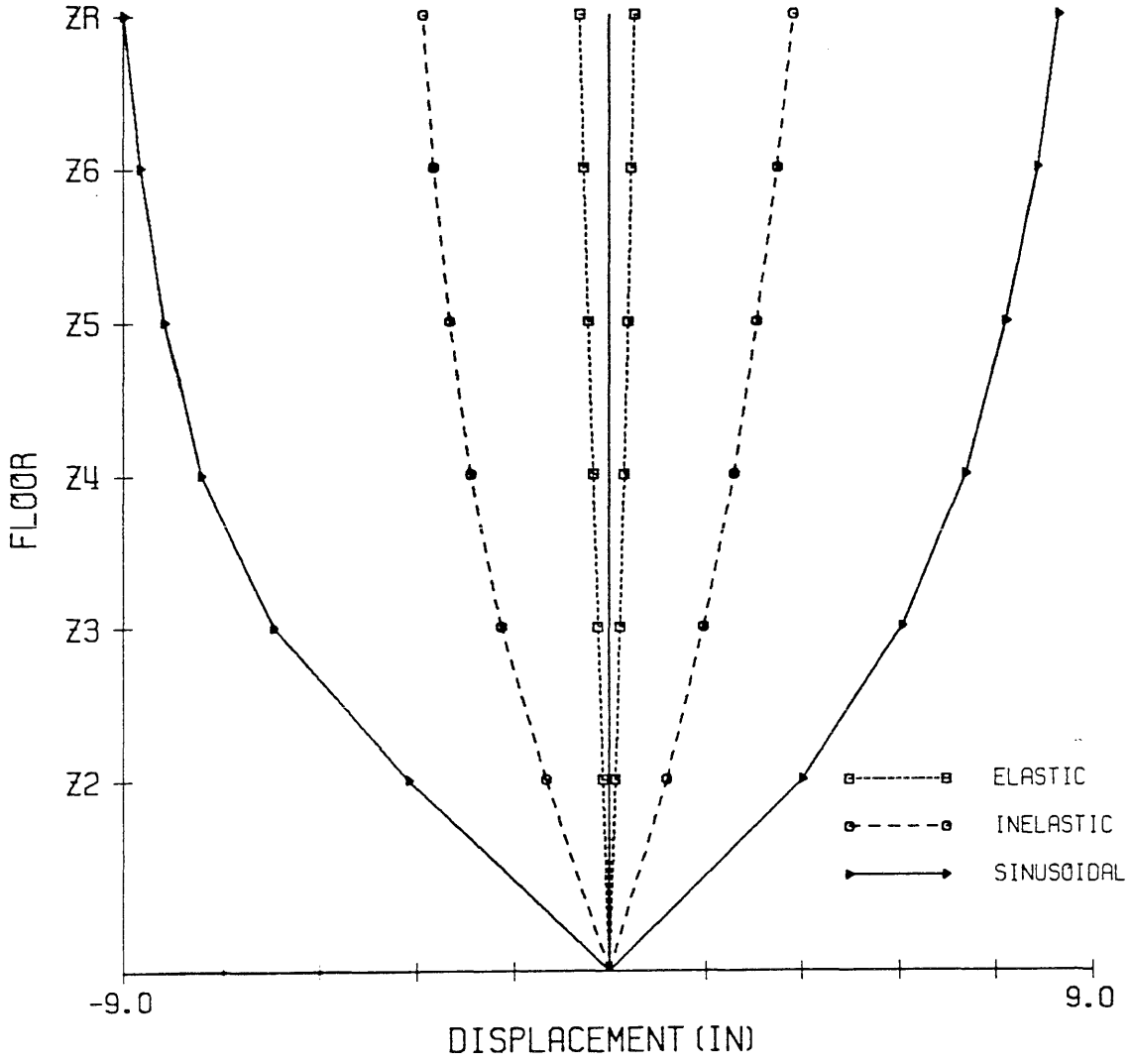

Fig. 5.44 Envelope of maximum story displacements for the Phase II tests

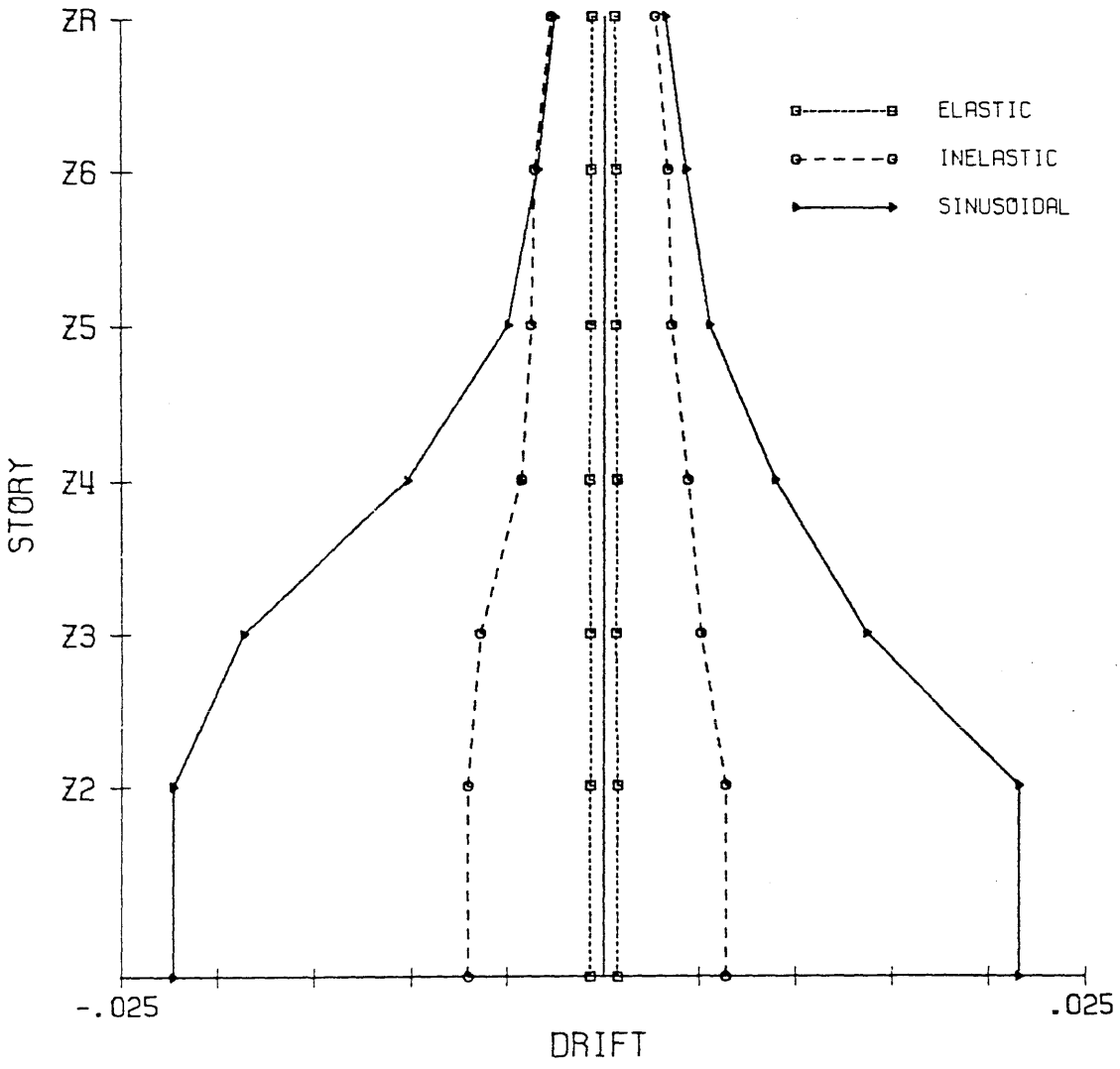

Fig. 5.45 Envelope of maximum story drifts for the Phase II tests

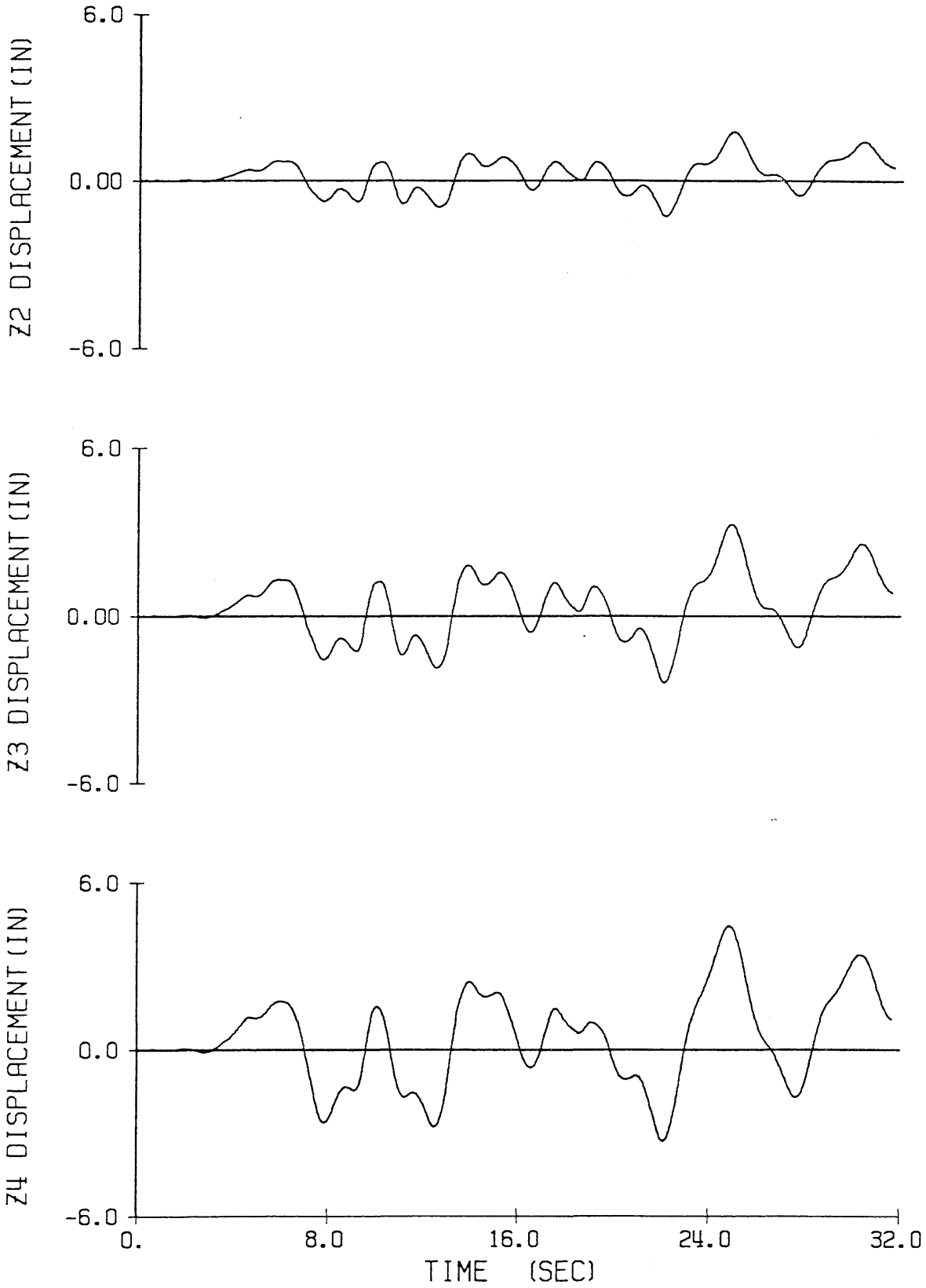

Fig. 6.1 Floor displacements vs. time for the Phase III tests

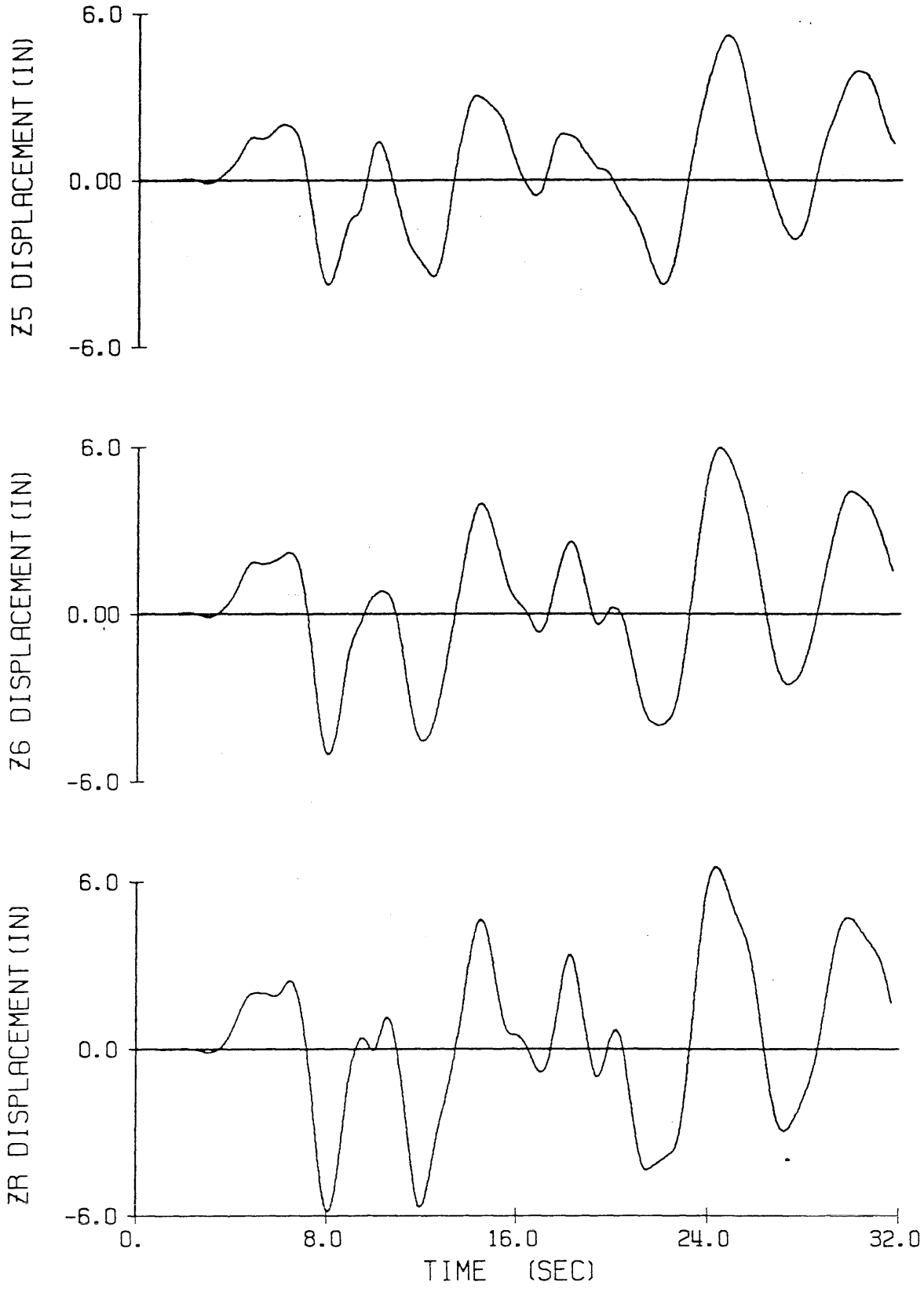

Fig. 6.1 (continued)

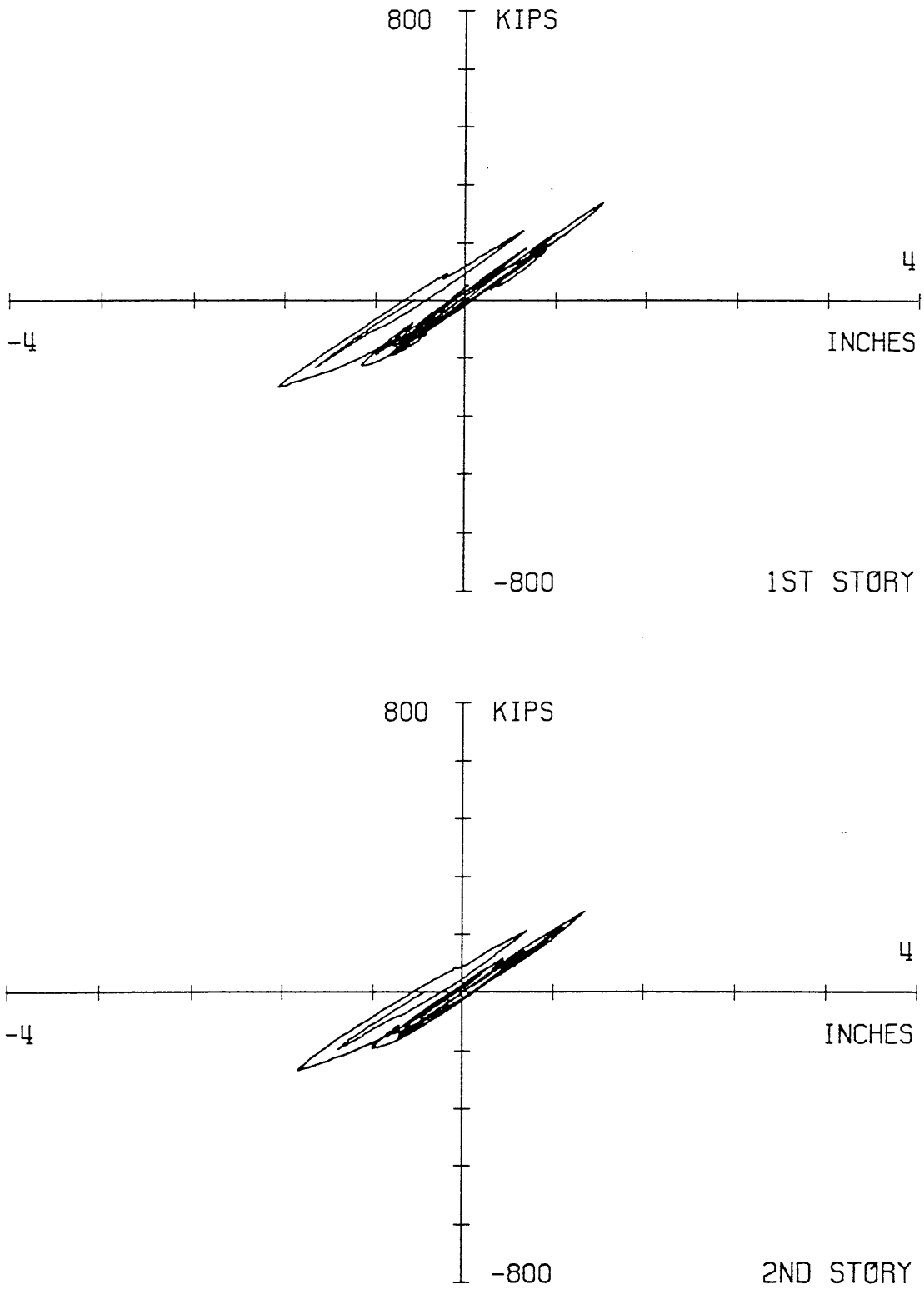

Fig. 6.2 Story shear vs. story displacement for the first and second stories during the Phase III test

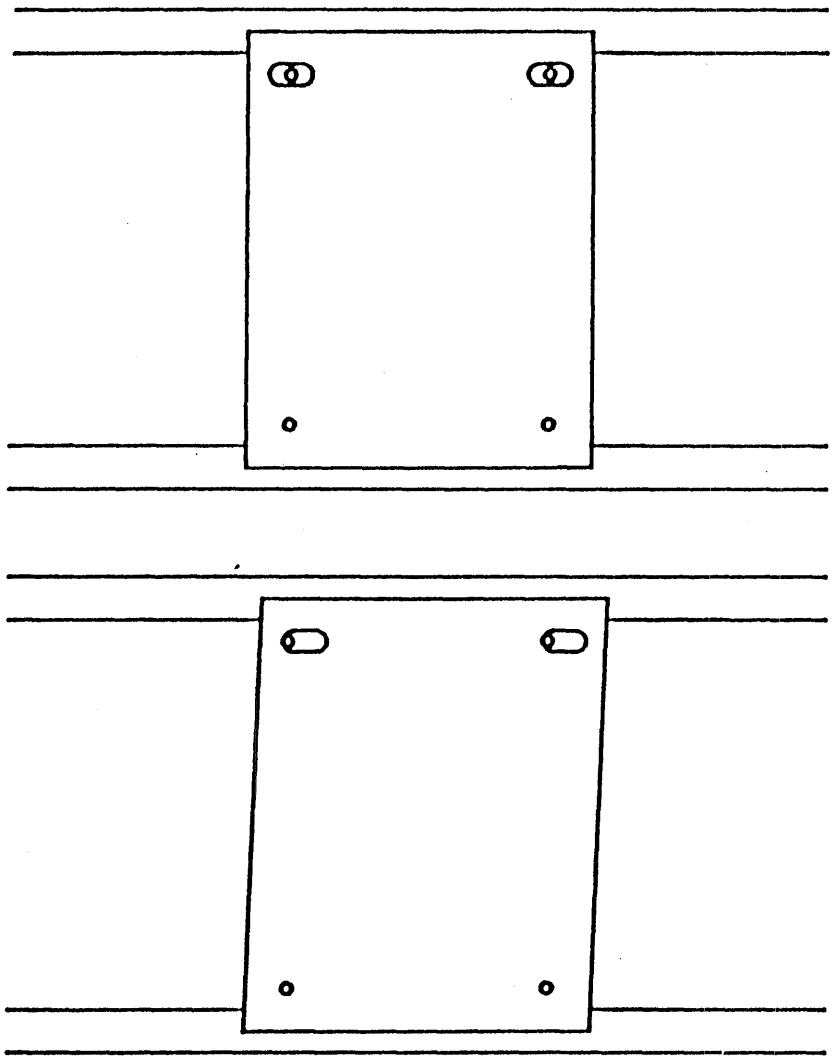

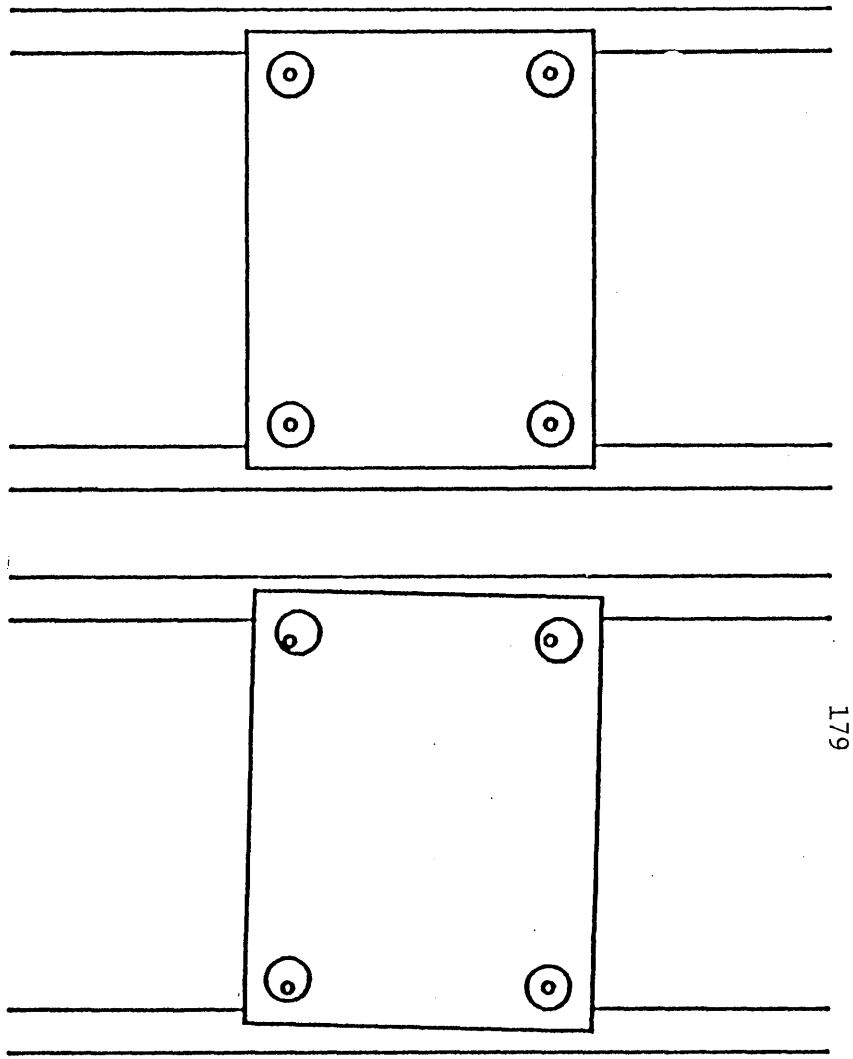

Fig. 6.3 General attachment details for exterior wall panels

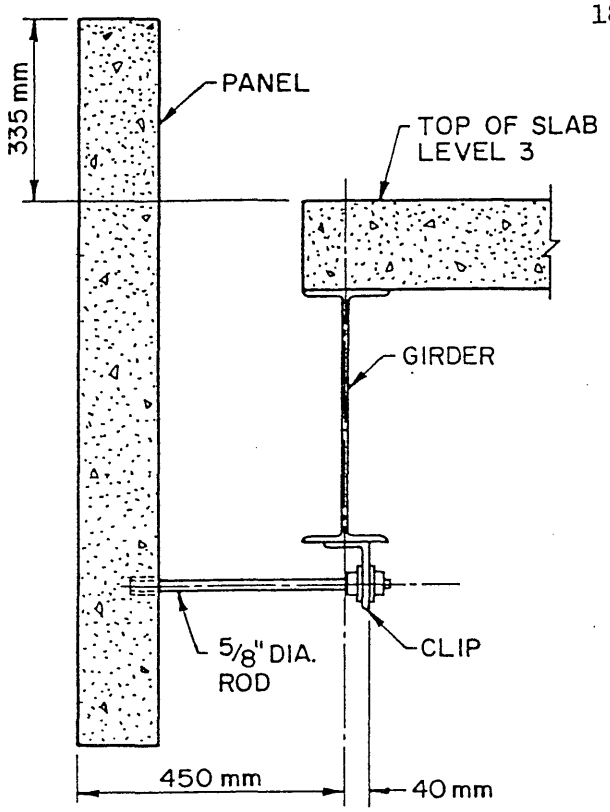

DUCTILE ROD
LATERAL CONNECTION.

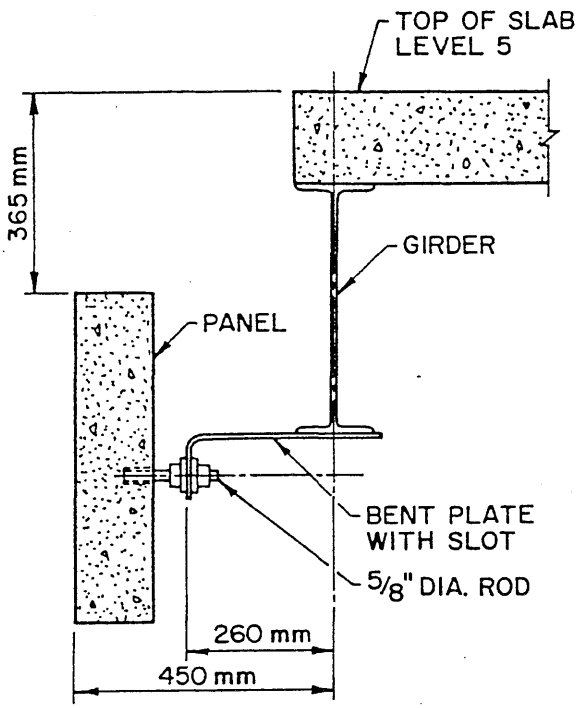

SLOTTED HOLE
LATERAL CONNECTION

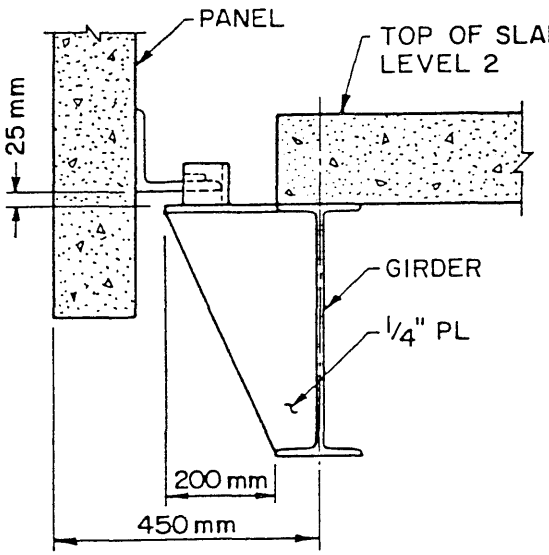

CLIP ANGLE
BEARING CONNECTION

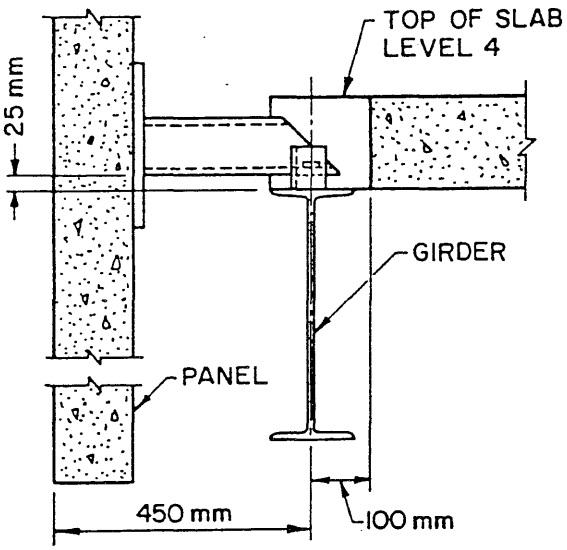

TUBE
BEARING CONNECTION

Fig. 6.4 General attachment details for exterior wall panels (from Ref. 12)